Center for Medical Physics and Biomedical Engineering
Medical University of Vienna

Austrian Society for Biomedical Engineering (ÖGBMT)

13th VIENNA INTERNATIONAL WORKSHOP ON FUNCTIONAL ELECTRICAL STIMULATION

VIENNA
FES

Vienna, Austria, September 23th - 25th, 2019

Belvedere Palace, Vienna

PROCEEDINGS

Proceedings

of the

13th Vienna International Workshop on

Functional Electrical Stimulation

Vienna, Austria
September 23th-25th, 2019

Edited by

Manfred Bijak
Winfried Mayr
Melitta Pichler

Scientific Committee

Gad Alon

Brian Andrews

Christine Azevedo Coste

Manfred Bijak

Radu Ciupa

Mihaela Cretu

Glen Davis

Thordur Helgason

Ursula Hofstoetter

Klaus Peter Koch

Hermann Lanmüller

Johannes Martinek

Karen Minassian

Dejan Popović

Frank Rattay

Martin Reichel

Matthias Krenn

Janez Rozman

Stefan Sauermann

Thomas Schauer

Martin Schmoll

Erika G. Spaich

Thomas Stieglitz

Paul Taylor

José Luis Vargas Luna

Michael Willand

Table of Contents

Session 1: Restoration of movement

ÖGBMT : Stefan-Schuy prize winner

Session 4: Advanced Biosignal Analysis

Session 5: Early Career Panel Discussion

Session6: Parameters and Technology

Session 7: Hybrid systems for exercising cyclic functional movements

Session 1:
Restoration of movement

Sensor based movement detection for functional electrical stimulation during end-effector gait rehabilitation

Schicketmüller A[1,2], Rose G[2], Hofmann M[1]

[1] HASOMED GmbH, Paul-Ecke-Str. 1, 39114 Magdeburg, Germany
[2] Institute for Medical Engineering and Research Campus STIMULATE, University of Magdeburg
Universitaetsplatz 2, 39106 Magdeburg, Germany

Abstract: *The movement of the end-effector based gait rehabilitation system Lyra® was measured during gait training. The movement was recorded using two inertial measurement units. The data was collected during three training sessions of a 39-year-old healthy adult. In order to be able to detect left and right gait cycle, the sensors were located on the feet of the subject. The purpose of these measurements was to test feasibility of a custom-made algorithm which aims to extract main gait events using linear acceleration and angular velocity data with the final goal to trigger functional electrical stimulation during gait rehabilitation. For this purpose, the measurements consisted of three typical velocities used in clinical routine. To check for velocity depended peculiarities of the gait trainer and possible errors of the algorithm the measurements incorporating a specific velocity were analysed independent from each other. The analysis of one velocity period within a measurement consisted of three chunks of data each lasting 2.5 minutes, resulting in 7.5 minutes (225 000 datapoints) of analysed data per inertial measurement unit. Bland-Altman-Diagrams were used to compare the results of the algorithm to manually counted steps which served as a reference. The analysis of the results shows good comparability between gait cycle determined by the algorithm and the reference. Based on these preliminary results a system combining inertial measurement units for triggering functional electrical stimulation with end-effector based gait trainer is feasible and provides promising opportunities for further research.*

Keywords: Lyra, FES, gait rehabilitation

Introduction

End effector gait rehabilitation technologies in combination with conventional physiotherapy have shown to support the rehabilitation process of stroke patients [1]. For chronic stroke patients (6 to 12 months) as well as subacute stroke patients (6 weeks to 6 months) gait trainers with the end-effector principle yielded a superior effect on gait function, balance and activities of daily living compared to conventional gait training [2]. Nevertheless, the passively performed movement induced by the robot can lead to changes in naturally occurring muscle activation patterns [3]. Additionally, the body weight support system partially inhibits muscle activation [4]. By gait event dependent electrical stimulation of the according muscles, this improper muscle activation could be prevented and thereby therapy effects can be improved. Approaches combining exoskeleton type of gait trainer with functional electrical stimulation (FES) were promising [5, 6]. In order to extend the variety of gait trainers which can be equipped with FES, sensors like inertial measurement units can be used to record the movement during the rehabilitation. Gait events can be extracted from this data and can then be used for triggering FES during gait training. This approach reduces the dependencies of information provided by the robot and could result in a flexible and novel setup to equip gait rehabilitation technologies with movement specific FES.

Material and Methods

The movement of the end-effector gait trainer Lyra® (THERA-Trainer, Hochdorf, Germany) was recorded during three training sessions of a 39-year-old healthy adult. The measurements had a duration of 60 minutes including setup time. Two inertial measurement units (MotionSensor, HASOMED GmbH, Magdeburg, Germany) located on the feet of the subject were used for data acquisition (Figure 1). Prior to the first measurement, two specially trained therapists from the NRZ rehabilitation center in Magdeburg supervised the training setup. Furthermore, the therapists checked the adjustment of the footplates and the body weight support system. The amount of body weight support was adjusted to the subject's comfort and was set between 10% and 30%.
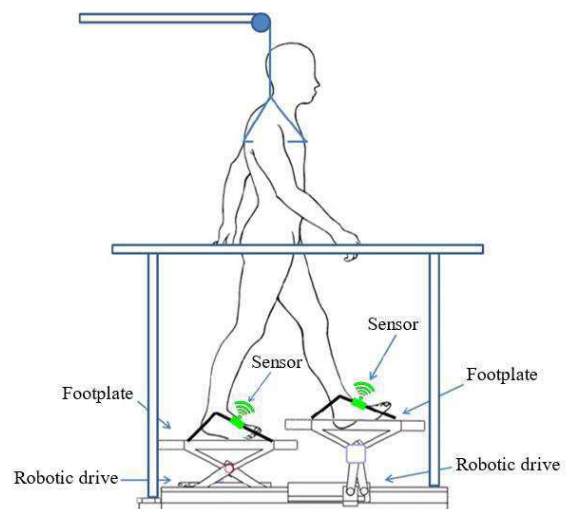
Figure 1: Schematic measurement setup of the end-effector gait training, adapted from [1]

To check the repeatability of the measurements, the setup and the carried-out analysis, the data was recorded on three different days. The measurement was split into three phases in which different velocities were tested (Table 1).

Measurement	Velocity#1 (m/s)	Velocity#2 (m/s)	Velocity#3 (m/s)
1	1.2	1.5	1.7
2	1.2	1.5	1.7
3	1.2	1.5	1.7

Table 1: Tested velocities of the end-effector rehabilitation robot

The velocities were chosen according to a typical training session of the Lyra®. Thus, a broad range of velocities used in clinical routine was covered. The sensors were placed at the subject's feet and were fastened using foot straps. The fixations of the foot plates were wrapped around the foot according to the instruction manual of the Lyra®. The fixation of the sensors and the fixation of the foot plates did not influence each other's functionalities. As in future this setup should enhance the gait training with functional electrical stimulation, it is important that the fixation of the sensor does not hinder the therapist to execute the training. Additionally, it is essential that the sensor position is chosen in a way that four major gait events (Initial Contact, Full-Contact, Heel-Off and Toe-Off) as described in [7] can be detected. Gait event detection was done using a customized algorithm. The algorithm aims to extract the gait events in real time using linear acceleration and angular velocity of the recorded sensor data. Robotic gait specific patterns and the according data sequences served as a basis for the gait event detection. To counteract drift, the sensors were calibrated before usage. Additionally, an initial resting state of the sensors was measured (Figure 2), during this phase the bias of the sensors was calculated. After the calculation of the bias, the training was initiated.

Results

To verify the repeatability of the measurement and the gait event detection, the recorded data was analysed in chunks of 2.5 minutes. In total 7.5 minutes (225 000 datapoints) of each velocity were analysed (Figure 2). This approach enables to check for velocity dependent peculiarities of the gait trainer. As the access/therapy area of the Lyra is optimized for fast setup time and accurate therapy, the space for further equipment (e.g.: optical measurement systems) is limited. Therefore, the chosen way to evaluate the gait detection algorithm was to count the steps manually within the aforementioned chunks. A correctly detected step of the algorithm must fulfil two conditions:

1. All of the four major gait events must be detected in the following sequence: Initial Contact, Full-Contact, Heel-Off and Toe-Off.
2. The detected sequence must be at an adequate time in the data in order to be able to trigger meaningful FES in the future development.

Depending on the velocity of the robot, the number of steps for each chunk were in between 44 and 69 steps per foot. Resulting in a total amount of 2949 analysed steps.
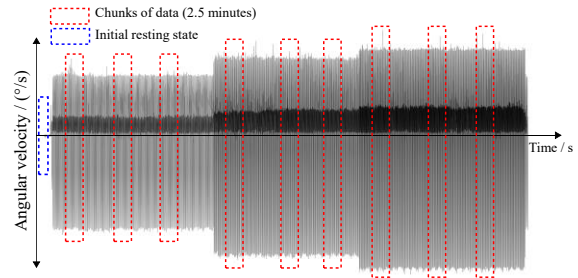
Figure 2: Selection method for analysing data

The detection rate in equation (1) was calculated for each chunk by determining the amount of correctly detected steps of the algorithm ($steps_{algorithm} = steps_{detected} - steps_{false\ detected}$) whereas the manually counted steps served as a reference ($steps_{reference}$). Each chunk was evaluated individually in order to find potential systematic and random errors in the measurement or the algorithm itself.

$$\text{Detection rate } (\%) = \frac{100}{steps_{reference}} * steps_{algorithm} \quad (1)$$

Since not only the difference between the reference detection rate and the detection rate of the algorithm is of importance, but also the variability of data and the possible outliers in one dataset, Bland-Altman-Diagrams were used to compare the results. The reference value was 100% in every comparison. The results of three measurement days of the left sensor can been seen in Figure 3 - Figure 5, the results of the right sensor are depicted in Figure 6 – Figure 8.
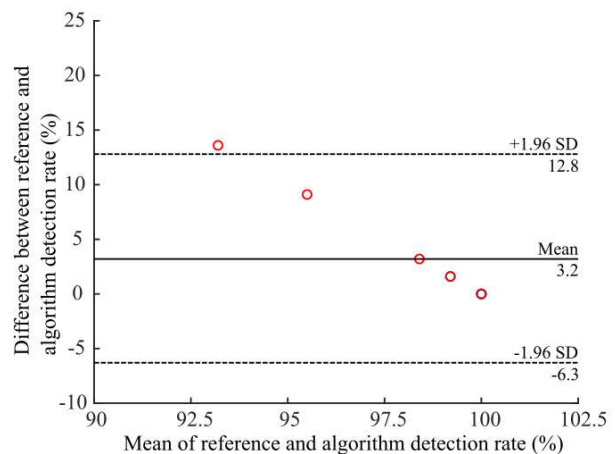
Figure 3: Measurement 1 - Left foot
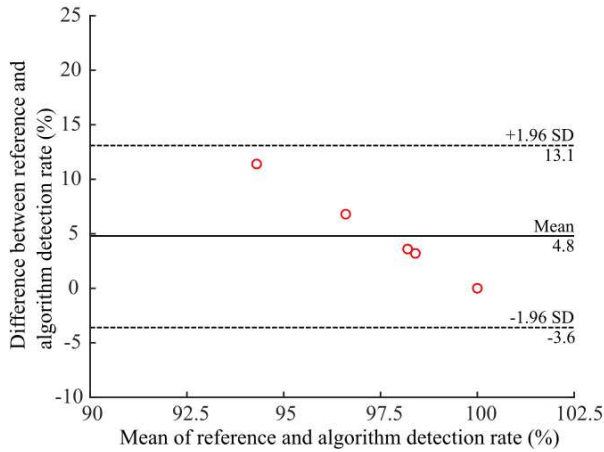
Figure 4: Measurement 2 - Left foot
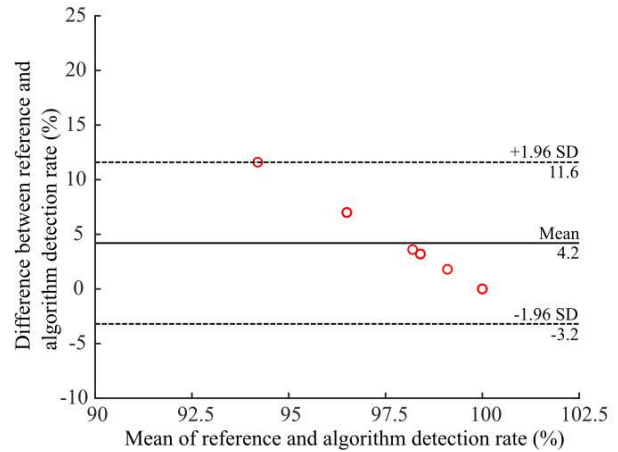
Figure 7: Measurement 2 - Right foot
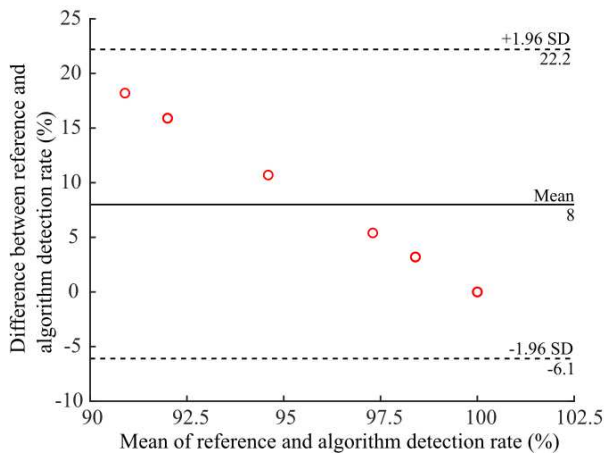
Figure 5: Measurement 3 - Left foot
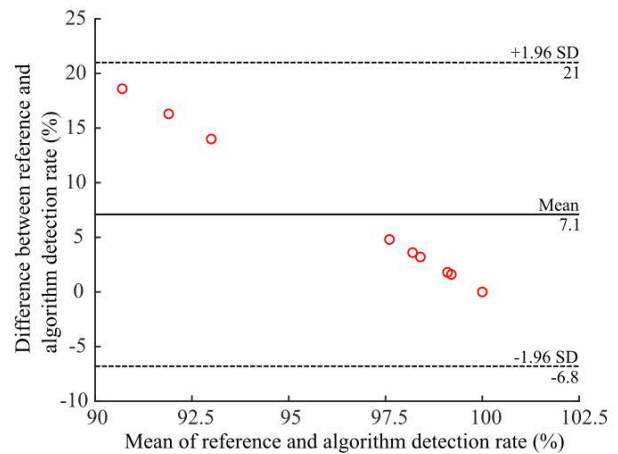
Figure 8: Measurement 3 - Right foot
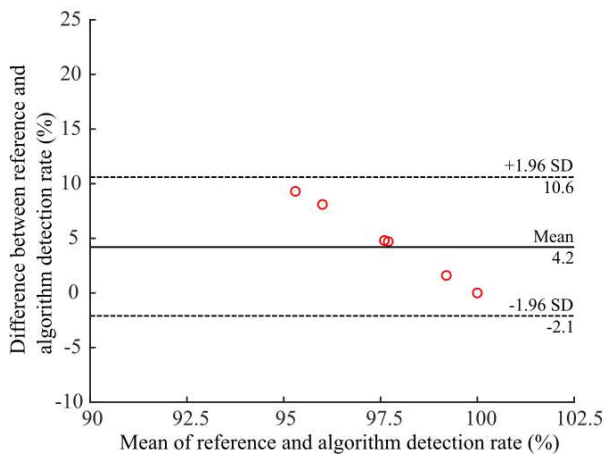
Figure 6: Measurement 1 - Right foot

Discussion

For appropriate interpretation of the Bland-Altman-Diagrams, three main characteristics of the results were taken into consideration:
1) Magnitude of the bias (Mean)
2) Width of the limits of agreement
3) Variability of datapoints and outliers

The first measurement of the left sensor (Figure 3) has a bias of 3.2 and the limits of agreement range from -6.3 to 12.8. The rather small bias is caused by detection rates close to the reference. One datapoint is not within the limits of agreement and is thus considered as an outlier. This outlier has a value of 13.6 which equals a detection rate of 86.4 % for the algorithm. For clinical use, this would mean that for 86.4 % of the steps an electrical stimulation would occur which could still be acceptable if the number of false detected steps is low. Since the aim is to support the gait training with FES, false detected steps (Type 1 errors) are considered as hazardous. Type 1 Errors would trigger an electrical stimulation which is not synchronized with the movement causing unwanted muscle contractions. In contrast to that, Type 2 errors are not considered hazardous as steps which are not detected would not trigger a stimulation. The limits of agreement in Figure 3 have an

acceptable range and the datapoints contained within these limits provide a reasonable result. Comparing Figure 4 to Figure 3 one can see that the bias and the limits of agreement are similar and are thus considered acceptable. The third measurement day and its according Bland-Altman-Diagram of the left sensor is displayed in Figure 5. The upper limit of agreement has a value of 22.2, this rather high value is mainly influenced by three detection rates with a value slightly above 80 %. All three detection rates were calculated for the velocity of 1.2 m/s. Figure 6 and Figure 7 represent the first two measurements of the right foot and provide as good results as the according measurements of the left foot. In Figure 8 an upper limit of agreement with a value of 21 can be seen. Similar to Figure 5, these values are caused by the detection rates measured during the 1.2 m/s training.

Conclusions

Overall the approach to use inertial measurement units to extract gait events during end-effector based gait training is feasible. Furthermore, a setup comprising IMUs to trigger FES during robotic gait training in a clinical setting is realizable. The majority of the results and their according Bland-Altman-Diagrams are satisfying. As mentioned in the discussion, also lower detection rates (e.g.: outlier in Figure 3) could be sufficient as long as false detected gait events are low. False detected steps would trigger a non-physiological stimulation and are thus considered hazardous. Since it is a maxim not to harm patients an analysis regarding Type 1 errors must be considered in future research. Additionally, Type 2 errors which are not considered hazardous for the patient should be investigated in order to improve the overall detection rate. The current analysis was executed in soft real time which means that a separated algorithm to simulate real time conditions was developed. As the Lyra® provides a rigid pre-defined movement with limited influence of the subject executing the training, it can be assumed that the movement data of healthy subjects will be similar to the movement data of patients. To verify whether healthy subjects influence the gait pattern of the system further measurements with patients would be desirable. As the body weight support for the healthy subject was rather low, investigations whether the amount of body weight support influences the gait pattern and further on the algorithm must be performed. First attempts using the stimulator RehaStim (HASOMED GmbH, Magdeburg, Germany) to trigger electrical stimulation based on the extracted events were promising. Using a stimulator like the RehaStim, up to four muscles per leg could be stimulated during the training. Latency of the measurement chain and physiological processes such as muscle contraction have to be taken into consideration for the future design of the system. These preliminary results lead to the conclusion that a system combining end-effector gait training with inertial measurement units to trigger FES is feasible and thus can provide a novel system for future rehabilitation.

References

[1] P.-Y. Cheng and P.-Y. Lai, "Comparison of Exoskeleton Robots and End-Effector Robots on Training Methods and Gait Biomechanics," in *Lecture Notes in Computer Science, Intelligent Robotics and Applications*, D. Hutchison et al., Eds., Berlin, Heidelberg: Springer Berlin Heidelberg, 2013, pp. 258–266.

[2] F. Anaya, P. Thangavel, and H. Yu, "Hybrid FES–robotic gait rehabilitation technologies: a review on mechanical design, actuation, and control strategies," *Int J Intell Robot Appl*, vol. 2, no. 1, pp. 1–28, 2018.

[3] J. M. Hidler and A. E. Wall, "Alterations in muscle activation patterns during robotic-assisted walking," (eng), *Clinical biomechanics (Bristol, Avon)*, vol. 20, no. 2, pp. 184–193, 2005.

[4] S. Hesse, *Lokomotionstherapie: Ein praxisorientierter Überblick*. Bad Honnef: Hippocampus-Verl., 2007.

[5] M. E. Dohring and J. J. Daly, "Automatic synchronization of functional electrical stimulation and robotic assisted treadmill training," (eng), *IEEE transactions on neural systems and rehabilitation engineering : a publication of the IEEE Engineering in Medicine and Biology Society*, vol. 16, no. 3, pp. 310–313, 2008.

[6] C. B. Laursen, J. F. Nielsen, O. K. Andersen, and E. G. Spaich, "Feasibility of Using Lokomat Combined with Functional Electrical Stimulation for the Rehabilitation of Foot Drop," (eng), *European journal of translational myology*, vol. 26, no. 3, p. 6221, 2016.

[7] T. Seel, L. Landgraf, V. C. de Escobar, and T. Schauer, "Online Gait Phase Detection with Automatic Adaption to Gait Velocity Changes Using Accelerometers and Gyroscopes," (eng), *Biomedizinische Technik. Biomedical engineering*, vol. 59 Suppl 1, s758-909, 2014.

Author's Address

Name:
Andreas Schicketmüller

Affiliations:
HASOMED GmbH, Paul-Ecke-Str. 1, 39114 Magdeburg, Germany
Institute for Medical Engineering and Research Campus STIMULATE, University of Magdeburg
Universitaetsplatz 2, 39106 Magdeburg, Germany

Email:
andreas.schicketmueller@hasomed.de

Homepages:
https://www.hasomed.de
https://www.forschungscampus-stimulate.de

The finite state control of stimulation synergy based on data from the instrumented shoe insole

Popović DB[1,2], Popović Maneski L[3]

[1]Serbian Academy of Sciences and Arts, Belgrade, Serbia
[2]Aalbog University, Aalborg, Denmark
[3]Institute of Technical Sciences of the Serbian Academy of Sciences and Arts, Belgrade, Serbia

Abstract: *We describe the method for the generation of stimulation profiles required for the gait assistance in persons with hemiplegia. The technique uses heuristic mapping of the activation profiles for the hip, knee, and ankle joint muscles based on the signals coming from the sensors integrated into an insole. The system design relies on the assumption that there is a multichannel electronic stimulator that can use signals coming from analog and digital sensors to activate up to eight muscle groups. The insole described in the paper comprises five robust, extremely low hysteresis pressure transducers and 3D accelerometer and gyroscope. The heuristic rules are simple and can use non-processed signals for real-time control. The feasibility of the operation was tested only in healthy individuals since the stimulator certification procedure required for clinical tests in persons with hemiplegia is in progress.*

Keywords: *Control of gait, hemiplegia, intelligent sensors, multichannel electrical stimulation*

Introduction

The stable posture and gait are the prerequisites for participating in regular daily life activities. Hemiplegia, which follows in many survivors of a cerebrovascular accident limits the ability for the functional gait. The drop foot is the most prominent handicap, but in reality, the gait abnormalities come from the lack of adequate hip and knee control. Multichannel electrical stimulation can assist the motor output [1 - 3].

We developed and tested the finite state control for the control of the gait in hemiplegics with the UNA SISTEMI stimulators and force sensing resistors built into the insoles and wearable accelerometers [4]. The recent development of a multichannel system MOTIMOVE [5] allows distributed and asynchronous stimulation that enables activation of prime hip, knee and ankle flexors and extensors and can postpone the fatigue [6, 7]. The MOTIMOVE application for the gait restoration requires an appropriate sensors system.

Based on the excellent performance of the sensors system presented by Papas et al. [8] we developed a prototype of a self-contained instrumented insole (Gait Teacher) that comprises robust pressure transducers sensors with no hysteresis [9], one 6D inertial measurement units, circuitry for wireless communication and the rechargeable battery.

The sensors system performance was tested vs. the camera-based systems, and the usual discrepancy was documented. The total force estimated from the measurements which use discrete pressure sensors does not carry information about the full force since the loading also exists in points that are not covered by a sensor. However, the actual ground force reaction size is not relevant for the control. The positioning of the insole is trivial and identical to the procedures used for standard shoe insoles.

Fig. 1: "Gait teacher" with five robust pressure sensors and one 6D inertial measurement unit (left panel) and "MOTIMOVE" eight-channel stimulator to be applied via surface electrodes for the gait assistance in persons with hemiplegia.

The expectation is that the combination of the MOTIMOVE and Gait Teacher can generate synergistic activation of leg muscles in a manner that fits into the preserved motor control of persons with hemiplegia. More precisely, the hypothesis is that the finite state control could mimic the "healthy control"; therefore operate in synchrony with the biological control over the unaffected motor systems in a person with hemiplegia. The sketch of the system components for the gait assistance is shown in Fig. 1
.

Material and Methods

We recorded the signals during various types of gait. The data acquisition software was custom designed in the LabVIEW environment to allow the on-line inspection and storing in time-stamped filed accelerations a_x, a_y and a_z, angular velocities ω_x, ω_y and ω_z and pressures P1, P2, P3, P4 and P5 form both insoles. The sampling rate was

100 samples per second. We show one representative set of recordings that were used for the analysis (Fig. 2).
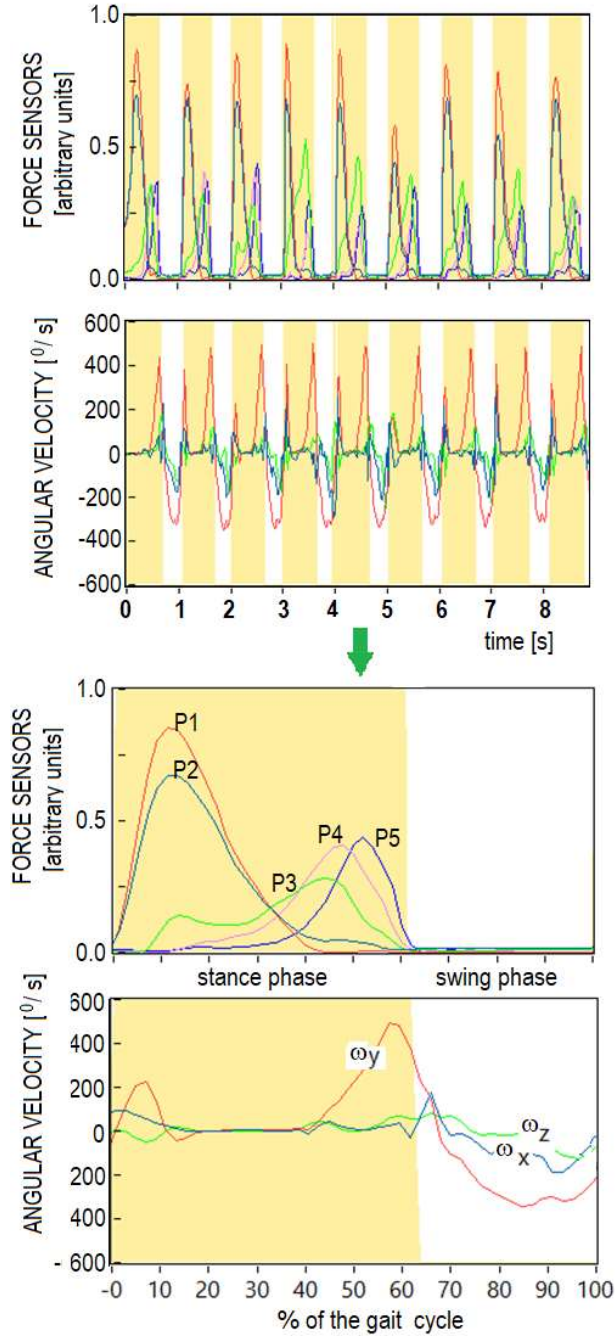
Fig. 2: Signals P1 are P5 are from pressure sensors, and ωx, ωy, and ωz are signals from the gyroscopes of the IMU recorded during the ground level gait. The bottom panels show one characteristic gait cycle

The control method that we propose follows the original work of Tomović et al. [9] where the control of movement was reduced to four states of each joint (Fig. 2): 1) LOCKED, 2) FREE, 3) FLEXION and 4) EXTENSION.
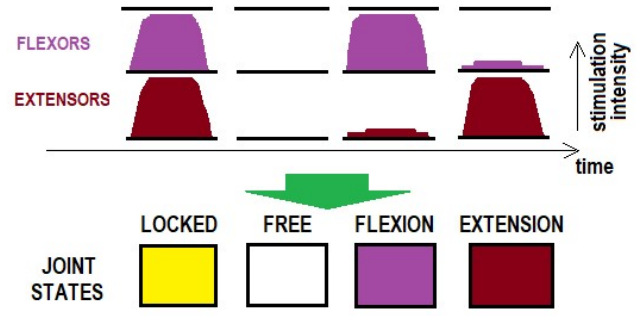
Fig. 3: The sketch of the finite states used for the control of the gait events and phases.

The four states can be realized as the combination of activated agonistic and antagonist's muscles: 1) both muscles stimulated generating net torque zero (co-contraction) and high joint stiffness, 2) both muscles sluggish (no stimulation) resulting with a zero joint stiffness 3) strong flexor activation with no or low-level extensor activation and 4) no or low-level flexor activation and strong extensor activation. The low level of activation of antagonist's muscles is required to minimize the jerky behavior.

The gait can be presented with a sequence of states at joints [11]. The heuristic analysis and minimum entropy analysis generated models of various gait modalities [12 - 14]. The method which serves as the basis for this study is schematically presented in Fig. 3.

Results

The gait events and phases were detected automatically based on the rules shown in Tab. 1. The method for estimation of states can be found in Džepina et al. [15].

Table 1: Rules used for the estimation of the timing of gait phases and gait events. Parameters Ti, i=1,2,3,4,5 are the thresholds, and they were selected at 5% of the maximum.

Gait phase/event	Rules
Heel contact (1)	Max(P1, P2) > T1 AND Max(P3,P4,P5) < T1
Foot flat (2)	Max(P1,P2)> T1 AND Max(P3,P4)> T2 AND $\left\| d\omega_y/dt \right\|$ < T3
Heel off (3)	Max(P1,P2)<T4 AND P5>T5 AND $d\omega_y/dt$ > 0
Toes off (4)	$d\omega_y/dt$<T3 AND Max(P1,P2,P3,P4,P5) > T4
Initial swing (5)	$d\omega_y/dt$<T3 AND Max(P1,P2,P3,P4,P5)< T1
Terminal swing (6)	$d\omega_y/dt$ [k] > 0 AND $d\omega_y/dt$ [k-1] $\leq$ 0

The sketch of the gait cycle with the rules estimated by the machine classification is in Fig 4.
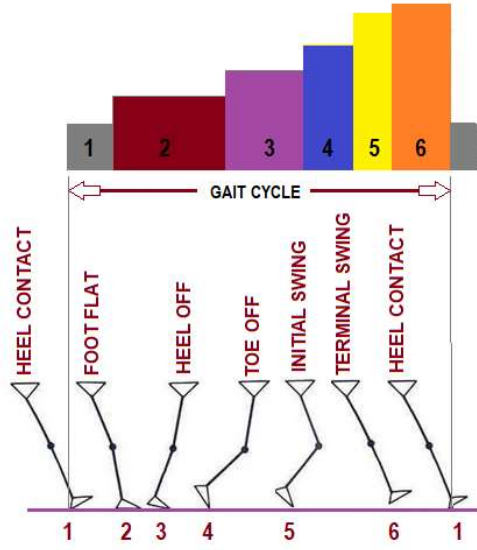
Fig. 4: Sensors signals for the one gait cycle with the gait phases generated from the rules shown in Table 1.

The final phase is the generation of bursts of pulses from the MOTIMOVE. The stimulator allows individual control of the frequency and amplitude of stimulation on each channel and setting of the pulse duration and ramp-up and down in the trapezoidal stimulation profile for all channels.

The stimulator supports the antifatigue unit (AFU) that allows distributed low-frequency activation of large muscles via an array of electrodes. Each AFU connected to one stimulation channel can drive up to four departments of the muscle, and the fused contraction can be generated at the pulse rate as low as 10 to 12 pulses per second.

Fig. 5 shows the whole control paradigm: 1) sensors reading the interaction with the ground and kinematics, 2) application of stored set of thresholds to trigger the selection of the channels to be turned on and off, 3) generation of bursts of current controlled charge pulses where the user sets the intensity and profile of stimulation via a GUI (tablet/computer) operating in Windows environment.

Discussion

We presented an example of signals and rules for the ground level walking. We applied the same methodology to generate sets of rules for walking on stairs, slope, standing up, and sitting down. So far, the tests in persons with no known sensory-motor deficits suggested that the temporal synergies are appropriate and they do not compromise the gait.

The ethics board has approved the protocol for the clinical trials at the University of Belgrade for the previous study, and the only requirement is that the new device has a medical certification.
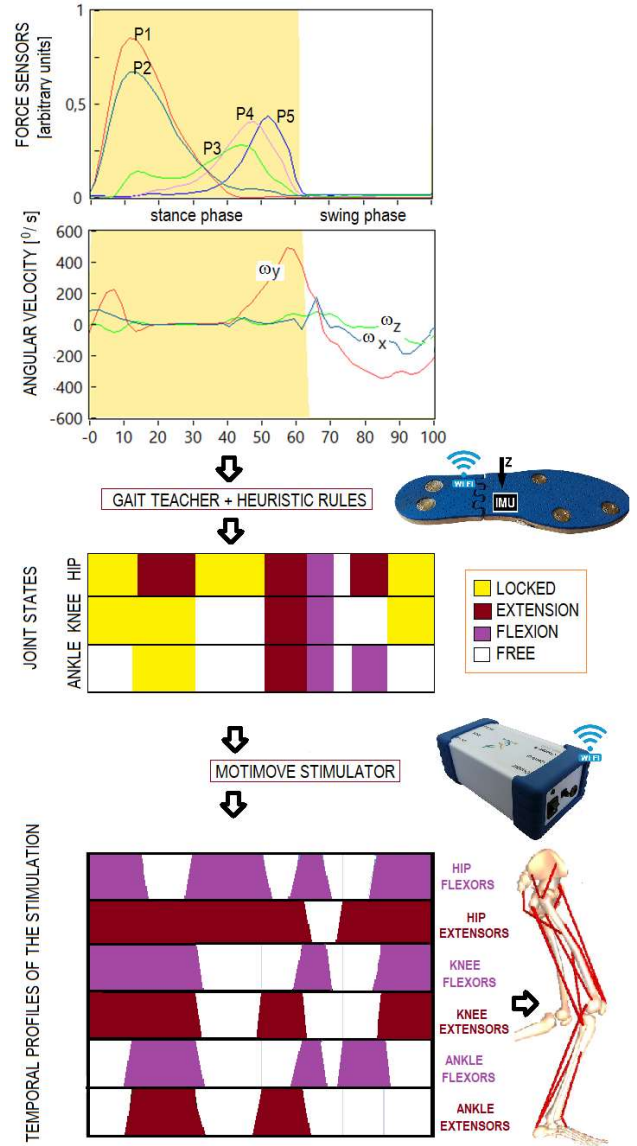
Fig. 5: The graphics model of the finite state control over six muscle groups to support the gait restoration in persons with hemiplegia.

The critical consideration is the practicality of the control when transferred from the research laboratory to real-life usage. The practicality relates to the time needed to start walking and ease of setup.

The prerequisite for the use of the system is the sufficient assisted muscle strength. The contraction achieved in the combination of the voluntary effort and stimulation needs to be strong enough to generate the target movement for all muscle groups that will be stimulated. If this is not the case, then the muscle exercise needs to be initiated (for at least 20 sessions during the four weeks) to strengthen the muscles. Once the muscle strength is achieved, the controlled assistance can be implemented for support during the gait training.

The initial step in applying the system is setting the stimulation parameters and deciding on the positions of the stimulation electrodes. The stimulation parameters (pulse duration, pulse amplitude, pulse rate) determined

the intensity of stimulation. The selection of the appropriate parameters is a compromise between the level of tolerance by the person using the system and the strength of the contraction achieved.

The setup is time consuming (20 minutes or similar) during the initial session, while in the later sessions the setup is short (<5 minutes).

In the system for the gait restoration, the thigh muscles are at the highest risk for being fatigued. The trials of using the antifatigue device for the activation of thigh muscles that require prolong stimulation have been done in an exercise protocol on the exercise bicycle [unpublished data], and the periods where the fatigue does not compromise the application are several times longer compared with the conventional stimulation paradigm [6, 7].

Fine adjustments of the intensity of the stimulation need to be performed during the use to compensate for the muscles fatigue.

Acknowledgment

References

[1] Popović, M.R., Keller, T., Papas, I.P.I., Dietz, V. and Morari, M. Surface-stimulation technology for grasping and walking neuroprostheses. *IEEE Engineering in Medicine and Biology Magazine*, 20(1), pp.82-93. 2001.

[2] Bajd, T., Kralj, A., Štefančič, M. and Lavrač, N. Use of functional electrical stimulation in the lower extremities of incomplete spinal cord injured patients. *Artificial Organs*, 23(5), pp.403-409, 1999.

[3] Kralj, A., Bajd, T. and Turk, R.. Enhancement of gait restoration in spinal injured patients by functional electrical stimulation. *Clinical orthopaedics and related research*, (233), pp.34-43, 1988.

[4] Kojović, J., Djurić-Jovičić, M., Došen, S., Popović, M.B. and Popović, D.B. Sensor-driven four-channel stimulation of paretic leg: functional electrical walking therapy. *Journal of neuroscience methods*, 181(1), pp.100-105, 2009.

[5] https://www.3-x-f.com/, accessed, May 2019

[6] Popović Maneski, L.Z., Malešević, N.M., Savić, A.M., Keller, T. and Popović, D.B. Surface-distributed low-frequency asynchronous stimulation delays fatigue of stimulated muscles. *Muscle & nerve*, 48(6), pp.930-937. 2013.

[7] Malešević, N.M., Popović Maneski, L.Z., Schwirtlich, L. and Popović, D.B. Distributed low-frequency functional electrical stimulation delays muscle fatigue compared to conventional stimulation. *Muscle & nerve*, 42(4), pp.556-562, 2010.

[8] Pappas, I.P., Popović, M.R., Keller, T., Dietz, V., and Morari, M. A reliable gait phase detection system. *IEEE Transactions on neural systems and rehabilitation engineering*, 9(2), pp.113-125. 2001.

[9] https://rehabshop.rs/, accessed, May 2019

[10] Tomović, R., Popović, D. B. and Stein, R.B. *Nonanalytical Methods for Control of Movements*. Singapore, World Science Publishing,1995.

[11] Popović, D.B. Finite state model of locomotion for functional electrical stimulation systems. *Progress in brain research* (97) pp. 397-407, 1993.

[12] Jonić, S., Janković, T., Gajić, V., and Popović, D.B. Three machine learning techniques for automatic determination of rules to control locomotion. *IEEE transactions on biomedical engineering*, 46(3), pp.300-310, 1999.

[13] Kostov, A., Andrews, B.J., Popović, D.B., Stein, R.B. and Armstrong, W.W. Machine learning in control of functional electrical stimulation systems for locomotion. *IEEE Transactions on Biomedical Engineering*, 42(6), pp.541-551, 1995.

[14] Nikolić, Z.M., and Popović, D.B. Predicting quadriceps muscle activity during gait with an automatic rule determination method. *IEEE transactions on biomedical engineering*, *45*(8), pp.1081-1085, 1998.

[15] Džepina, V., Gogić, A., Popović, D.B. "Rules for estimation of gait phases from data acquired by the Gait Teacher insoles." *Proc. 6th IcETRAN Conference*, Srebrno jezero, Serbia. June 3-6 32019, in press.

Author's Address

Dejan B. Popović
Serbian Academy of Sciences and Arts, Belgrade, Serbia and Aalborg University, Aalborg, Denmark
11000 Belgrade, Knez Mihailova 35, Serbia
e-mail:: dbp@etf.rs,
URL: https://vbn.aau.dk/en/persons/100233

An EMG-controlled system combining FES and a soft exoskeleton glove for hand rehabilitation of stroke patients

Grosperrin M[1], Mrachacz-Kersting N[2], Spaich E G[2]

[1]Faculty of Life Sciences, Ecole Polytechnique Fédérale de Lausanne (EPFL), Switzerland
[2]Department of Health Science and Technology, Aalborg University, Denmark

Abstract:

In this paper, we present the development of a hybrid system which supports an active rehabilitation of the closing and the opening of the hand. The particularity of this system is to combine a soft exoskeleton glove, the SEM Glove™, and functional electrical stimulations (FES) to perform both types of hand movements. The created system is also a suggestion of improvement for the SEM Glove™ that is already commercialized by the BIOSERVO company and usable for hand closing rehabilitation only. In our study, a FES system was associated to this glove in order to provide the missing hand opening rehabilitation. To engage the patient in his rehabilitation, our system is electromyogram (EMG)-controlled and is activated according to the patient movement intentions. EMG signals of the muscles involved in the extension and flexion of the fingers were recorded and then processed in order to detect muscle activations. The control of the different elements of the system was then executed based on the results of this detection.
The preliminary results demonstrated that the designed hybrid system shows good performances in detecting correctly the intention of a healthy user. Some improvements could still be made in the signal processing to increase the sensitivity of detection, but we proved that the hybrid system is already operational to assist the hand movements of a healthy user.

Keywords: Hand rehabilitation, EMG signal, Functional Electrical Stimulation (FES), Soft robotics, Signal processing

Introduction

Stroke is one of the most frequent causes of adult disability in the world [1]. Accordingly, numerous researchers have committed themselves to the development of robotic rehabilitation methods that could help stroke patients to recover their motor functions more rapidly. Recently, the importance of the engagement of the patients in their rehabilitation has been discussed and several studies showed that an interactive treatment has better long-term effects than passive therapy [2][3]. This can be achieved e.g. by detecting the intention of the patient to perform different movements from surface electromyographic (EMG) recordings and supporting the production of the desired movement. Similarly to Serpelloni et al. [4], Ho et al. [5], and Mulas et al. [6], we designed an EMG-controlled hand rehabilitation system capable of assisting two movements: hand opening and closing. Our system was implemented with a soft exoskeleton glove supporting the closing of the hand, the SEM Glove™, which is commercialized by the BIOSERVO company [7]. As the glove does not support active opening of the hand, which is a common problem of the hemiparetic hand [8], we added FES to the system to provide hand opening. The FES exploits the residual motor ability by activating the muscles responsible for finger extension. FES, just like robotics, has been commonly used to restore hand function [9]. The HandMaster (BioNESS H300) [10] and the Bionic Glove (Neuromotion) [11] are examples of devices using FES to facilitate the movements of the hand.

In this paper, we describe the development of our hybrid hand rehabilitation system and we present the results of the preliminary test executed on a healthy subject.

Material and Methods

Design of the hybrid system

EMG signals of the extensor digitorum communis and the flexor digitorum superficialis were collected simultaneously on the same arm. Those muscles were selected because they are involved in the extension and flexion of the fingers and are superficial, with their activity being readily detectable using surface electrodes. The control of the whole device corresponded to an open-loop strategy. A detection of muscle activation resulted in the generation of a movement of the fingers by the hybrid system, either activating the glove to close the hand or triggering the stimulations to open the hand, depending on the activated muscle. The acquisition and processing of the data started again as soon as the control system finished classifying the precedent signals.

-EMG

Two surface electrodes (Ambu® Neuroline 720) were placed over each muscle (extensor digitorum communis and flexor digitorum superficialis). A reference electrode was placed at 1/3 on the line between the lateral epicondyle of the humerus and the acromion. The EMG signals were first band-pass filtered, with cut-off frequencies of 5 Hz and 200 Hz and amplified with a gain of 10000 before being digitized.

-Analog to digital converter (ADC)

The EMGs were digitized using an analog to digital converter (NI USB-6221, National Instruments). The input range of the device was set to ±10V and two input channels were used, one for the flexor and one for the extensor muscle. The digital signals were then recorded and processed in the PC.

-FES stimulator

The stimulations promoting the hand opening were delivered with a FES stimulator® for Functional Electrical Therapy developed by UNA consulting (Belgrade). The stimulations were triggered by a rectangular, + 2V pulse, 10 ms long, generated by the DAQ module after detecting activation of the extensor digitorum communis. One active electrode (∅3.2cm, Dura-Stick premium, DJO, Vista, California, USA) was placed over the extensor digitorum communis, on the middle of the forearm, and one reference electrode (5cm x 5cm, Pals, Axelgaard Ltd., Fallbrook, California, USA) was located on the posterior side of the forearm, 2 cm proximal to the wrist (Fig. 1, below).
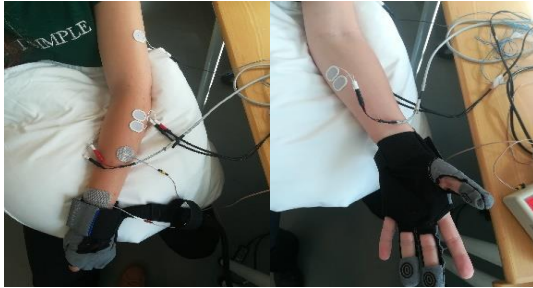
Figure 1: Placement of the different elements of the hybrid system

The stimulator delivered monophasic pulsed currents. The pulse width, stimulation frequency and stimulation duration were respectively set to 200 µs, 30 Hz and 2 seconds. The amplitude of the stimulation was sufficient to generate an extension of the three middle fingers, was specific to each user and, thus, had to be determined before each use. To do so, the amplitude was adjusted progressively and the intensity corresponding to the elicitation of the desired movement was selected.

-Soft exoskeleton glove

The soft exoskeleton glove used in this study was the SEM Glove™ (Soft Extra Muscle Glove) designed by BIOSERVO [7]. The glove covers the thumb, the middle and ring fingers. Hence, in our hybrid system, only the rehabilitation of palmar grasp was targeted as the other more frequent types of grasp could not be supported by the SEM Glove™, indeed it does not cover the index finger [12]. The SEM Glove™'s control system based on fingertip sensors was overridden to be EMG-controlled. Mechanically, the SEM Glove™ is based on an artificial tendons system [6]. Wires are integrated to the glove and linked to the actuators adjusting the tension of the tendons. Thus, the electrical motor powers the actuators which provide the pulling force required for the closing of the hand. The system has a serial port so the desired force values can be logged and communicated directly from a PC. With our new control system, after detecting muscular activation of the flexor digitorum superficialis, the force was modified (from 0N to 5N) to activate the glove closing movement.

Control strategy

The two EMG signals were acquired by the DAQ system at a sampling rate of 1 kHz and in intervals of 150ms. The control of the diverse elements of the device was carried out based on the results of the movement intention detection which was entirely and automatically executed with our Matlab program. An identified activation of the finger flexor led to the activation of the glove closing. While an EMG signal revealing activity of the extensor muscle provoked the triggering of the stimulations and thereby opening of the hand. After every detected opening intention, and during the stimulation, the acquisition was suspended for 2 seconds in order to avoid stimulation artefacts on the EMG recordings.

The algorithm of movement intention detection consisted basically of a signal processing phase and a thresholding phase.
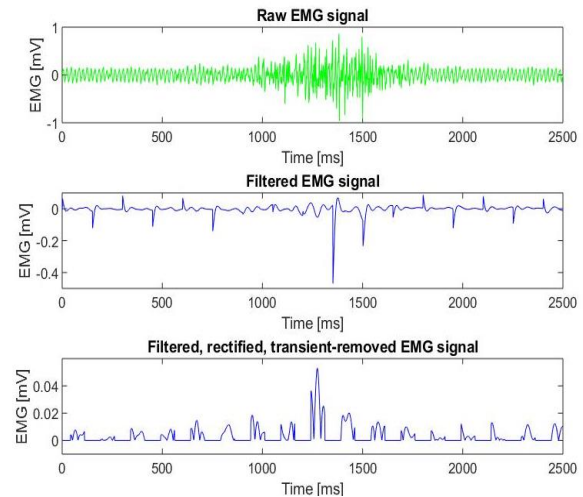
Figure 2: EMG signal of the extensor muscle representing a muscular activation. A 2.5 seconds long signal is shown for better visualisation of the overall EMG activity. The EMG was cut in windows of 150 ms before executing the processing steps. The raw signal is shown in the first panel. The concatenated, 150 ms seconds of filtered and rectified, transient-removed signal are presented in the second and third panels.

A low-pass filter was applied to the 150ms-long signals (Butterworth, 4th order, 20 Hz cut-off frequency) to remove the noise due to the powerline (50 Hz and all its harmonics) and to detect the envelope of the EMG signal [13]. The filter was applied to the signals using the *filtfilt* command of Matlab. This filtering technique enables a zero-phase distortion and filters the signals twice, first in the forward direction and then in the reverse one. Considering this, the order of the final filter was finally doubled (8th). The *filtfilt* command also allows to reduce the startup and ending transients. Even reduced, the transient response due to filtering was still existent. To avoid interpreting them by the thresholding algorithm as a strong muscle activity, the first 40 and last 40 samples were set to 0. Those 80 values presenting the overshooting peaks were thus ignored by the control system during the thresholding phase. Finally, the signals were rectified to visualize more easily the dynamic data (Fig. 2) and their amplitude in relation to the pre-selected activation thresholds.

The activation of the different elements of the system was controlled by a two-steps procedure. Each step involved a thresholds-based detection of EMG activity and a

comparison of the extensor and flexor EMG signals previously normalized by their respective, empirically predefined, thresholds. After acquiring and processing a 150 ms segment of data, the first step, which controlled the activation of the SEM Glove™, was executed. In this step, in this 150 ms window, the amplitude of the processed flexor EMG signal was required to be larger than a predefined flexor threshold and additionally, the peak of the normalized flexor EMG signal was required to be larger than the normalized peak of the extensor EMG signal to activate the SEM Glove™. In the same way, for the second step, the amplitude of the processed extensor EMG signal was required to be larger than a predefined extensor threshold and additionally, the peak of the normalized extensor EMG signal was required to be larger than the normalized peak of the flexor EMG signals to trigger the electrical stimulation. If the conditions of the tests were not fulfilled, the system remained unchanged, and the acquisition and processing of another window of 150 ms of EMG data was undertaken. The control system is presented in Fig. 3.
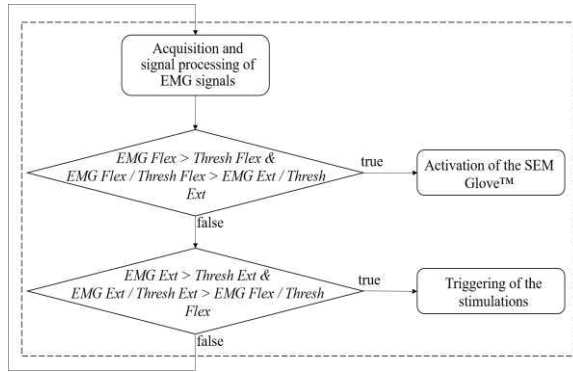
Figure 3: Flow diagram of the detection and classification algorithm. EMG Flex: EMG signal of the flexor muscle; EMG Ext: EMG signal of the extensor muscle; Thresh Flex: threshold defined for the flexor muscle; Thresh Ext: threshold defined for the extensor muscle.

Experimental test

To test the functionality of our hybrid system, a preliminary test with one healthy subject was performed. The goal of the test was to quantify the rate of successful hand openings and closings provided by the system and induced by the movement intention of the user. The participant (female, 24 years old) was asked to perform 100 repetitions of each movement (hand opening and closing), and the response of the hybrid system was noted. The subject sat on a chair and placed the forearm on a pillow placed on her lap to keep the arm resting relaxed.

The test consisted of two phases. First, the thresholds used for detecting muscle activation were determined without using the glove or FES. To this end, the participant was asked to execute extensions and flexions of the fingers, alternatively for 20 seconds, while EMG signals were recorded. The EMG signals were cut into 150 ms long segment that underwent the signal processing steps described earlier. The processed data was visualized (as in Fig.2) and adequate thresholds were set empirically. The second phase corresponded to the actual evaluation of the performance of the system. All the elements of the hybrid system were mounted, activated, and functional. The participant was asked to execute extensions and flexions of the fingers alternating both movements and waiting few seconds in between each. In total, 100 extensions and 100 flexions were executed. For every movement that the subject performed, the response of the hybrid system was classified as being a correctly detected movement, an incorrectly detected movement (if the opening is detected as closing and vice versa) or a non-detected movement. Any additional movements operated by the system and not intended by the subject were also noted.

Results

The number of glove activations, triggered stimulations, and absences of movement were counted for the 100 repetitions of hand closings and openings intended by the subject and are summarized in Table 1.

Table 1: Classification rates of the movement detection

	Correctly detected	Incorrectly detected	Not detected	Sensitivity (%)
	True positive	False negative		
Opening	97	2	1	97
Closing	81	18	1	81

During the test, we totalized 10 additional movements which were not issued from a movement intention of the subject: 7 stimulations and 3 activations of the SEM Glove™ occurred while the subject was waiting to execute the next movement.

Discussion

In this study, we presented the development of a hybrid FES-robotic system with a very good performance of classification and detection of movement intention, especially considering the simplicity of the implemented signal processing. The sensitivity ranged from 97 % for the openings to 81 % for the closings (Tab. 1), reaching comparable performances to the ones reported for a similar system using EMGs recorded on the healthy arm to control the rehabilitation glove worn by the impaired hand [4].The sensitivity for the closing was considerably lower than for the opening movement. This reduction on the sensitivity rate responds to the fact that 18% of the intended closings were detected as openings. We believe that this number could be significantly reduced through a better selection of the thresholds since off-line examination of the EMG signals showed presence of extensor muscle activity during the closing actions. This phenomenon, known as crosstalk, happened because of the anatomy of the forearm, and usually affects the performance of systems based on surface EMG recordings [14]. The EMG electrodes placed over the extensor were close to other strong flexor muscles involved in the finger flexion and their activities were probably involuntarily recorded by the extensor EMG when the subject intended to close the hand, decreasing the sensitivity of our system for closing movement. Most of the actions triggered without movement intention (7

stimulations and 3 glove activations) may be explained by a sudden presence of large amplitude noise in the signal. Our simple filtering allowed to attenuate the noise but did not remove it completely, resulting probably in noise being detected as an intention of movement leading sometimes to an incorrect activation of either the glove or the stimulator.

A limitation of this system is that in every window of 150 ms only 70 ms are used in the thresholding phase. It is possible though that actual muscle activation was present in the remaining, blanked 80 ms. Thus, the technique of removing the values corresponding to the transient period has the advantage of removing the side effects of this simple filtering but also has the drawback of neglecting a part of the signal that could contain important information.

Conclusions

Our study presented the design of a hand rehabilitation hybrid system combining a soft exoskeleton glove and FES, and controlled by EMG to respond to the movement intention of the user. The first preliminary test was performed in one session with a healthy subject. The repeated movements executed by the subject allowed to calculate a sensitivity rate (97% of successful hand opening detections and 81% of hand closing detections) which was satisfying for a first test. The few detection errors or misclassifications were mainly related either to the chosen thresholds or to the signal processing. The robustness of the system could be improved replacing the empirical thresholding by a more automatic and reproducible method - for example an algorithm setting the thresholds according to samples of data - or reducing the sensitivity to noise and eventual crosstalk, by improving the EMG signal processing.

The results obtained are really encouraging and show a promising system. In the future, further tests should be run including healthy and hemiparetic participants to evaluate the robustness of the system.

References

[1] Go, A.S. et al.: Executive summary: heart disease and stroke statistics - 2014 update: a report from the American Heart Association. *Circulation*, vol. 129, no. 3, pp. 399-410, 2014

[2] Hu, X. L., Tong, K. et al.: A Comparison Between Electromyography-Driven Robot and Passive Motion Device on Wrist Rehabilitation for Chronic Stroke, *Neurorehabilitation and Neural Repair*, vol. *23*(8), pp. 837–846, 2009

[3] Blank, A.A. et al.: Current Trends in Robot-Assisted Upper-Limb Stroke Rehabilitation: Promoting Patient Engagement in Therapy, *Curr Phys Med Rehabil Rep,* vol. 2, pp.184-195, 2014

[4] Serpelloni, M. et al.: Preliminary study of a robotic rehabilitation system driven by EMG for hand mirroring, *2016 IEEE International Symposium on Medical Measurements and Applications (MeMeA)*, Benevento, pp. 1-6, 2016

[5] Ho, N.S.K. et al.: An EMG-driven exoskeleton hand robotic training device on chronic stroke subjects: Task training system for stroke rehabilitation. *IEEE International Conference on Rehabilitation Robotics*., 2011

[6] Mulas, M. et al.: An EMG-controlled exoskeleton for hand rehabilitation. *Proceedings of the 2005 IEEE 9th International Conference on Rehabilitation Robotics*, *2005*, pp. 371-374, 2005

[7] Nilsson, M. et al.: The Soft Extra Muscle system for improving the grasping capability in neurological rehabilitation. *2012 IEEE-EMBS Conference on Biomedical Engineering and Sciences, IECBES 2012*, pp. 412-417, 2012

[8] Lang, C.E. et al.: Recovery of Thumb and Finger Extension and Its Relation to Grasp Performance After Stroke. *Journal of neurophysiology*, vol. 102, no. 1, pp. 451-45, 2009

[9] Crema, A., et al.: A Wearable Multi-Site System for NMES-Based Hand Function Restoration. *IEEE Transactions on Neural Systems and Rehabilitation Engineering*, vol. 26, no. 2, pp. 428–440, 2018

[10] Snoek, G.J. et al.: Use of the NESS Handmaster to restore handfunction in tetraplegia: Clinical experiences in ten patients. *Spinal Cord*, vol. *38*, no. 4, pp. 244–249, 2000

[11] Popovic, D. et al.: Clinical evaluation of the bionic glove. *Archives of Physical Medicine and Rehabilitation*, vol. 80, no. 3, pp. 299-304, 1999

[12] Radder, B. et al.: User-centred input for a wearable soft-robotic glove supporting hand function in daily life. *IEEE International Conference on Rehabilitation Robotics*, pp. 502–507, 2005

[13] Qizhu, S. et al.: Onset determination of muscle contraction in surface electromyography signals analysis. *2005 IEEE International Conference on Information Acquisition*, 2005

[14] Farina, D. et al.: Surface EMG crosstalk evaluated from experimental recordings and simulated signals. *Methods of information in medicine,* vol. 43, no. 1, pp. 30-35, 2004

Author's Address

Grosperrin Marion
Faculty of Life Sciences, Ecole Polytechnique Fédérale de Lausanne (EPFL), Switzerland
grosperrin.marion@gmail.com

Mrachacz-Kersting Natalie
Department of Health Science and Technology, Aalborg University, Denmark
nm@hst.aau.dk
https://vbn.aau.dk/da/persons/104836

Spaich Erika G.
Department of Health Science and Technology, Aalborg University, Denmark
espaich@hst.aau.dk
https://vbn.aau.dk/da/persons/104344

Noninvasive spinal cord stimulation improves walking performance in an individual with multiple sclerosis

Hofstoetter US[1], Freundl B[2], Binder H[2]

[1]Center for Medical Physics and Biomedical Engineering, Medical University of Vienna, Austria
[2]Neurological Center, SMZ Baumgartner Hoehe, Otto-Wagner-Hospital, Vienna, Austria

Abstract: Epidural spinal cord stimulation (SCS) is currently regarded as one of the most promising intervention methods to improve motor function in individuals with severe spinal cord injury. In parallel, an increasing number of studies is suggesting that noninvasive SCS can improve spasticity and residual motor control in the same subject population. This case study explores for the first time whether noninvasive SCS would improve walking performance of an individual with multiple sclerosis. For reproducibility, the participant was tested on two days. Noninvasive SCS was applied to target the lumbar posterior roots at 50 Hz and sensory level for the lower extremities. Walking function was assessed clinically before and after a 30-minute session of stimulation that was applied in a supine position. Walking speed assessed by the 10-meter walk test and walking endurance assessed by the 2-minute walk test were improved in both sessions with carry-over effects lasting for two hours. Improvements in walking function were complementarily suggested by the timed-up-and-go test. This case study motivates to test noninvasive SCS in upper motor neuron disorders not limited to spinal cord injury.

Keywords: human, noninvasive, multiple sclerosis, spinal cord stimulation, walking function

Introduction

Epidural spinal cord stimulation (SCS) is regarded a breakthrough intervention for the recovery of locomotor function after spinal cord injury (SCI) [1–4]. Interestingly, its first application in motor disorders was in multiple sclerosis (MS) and the improvements produced in this patient population surpassed that of any other intervention available at that time [5, 6]. Meanwhile, a noninvasive, surface-electrode based method of SCS [7,8] has been successfully applied in SCI to enhance motor function by several independent groups [9–12]. These results prompted us to test, for the first time, whether noninvasive SCS would augment the walking performance of an individual with MS.

Material and Methods

The effect of noninvasive SCS on locomotor function was tested in a 58-year-old woman with a 30-year history of MS (EDSS score: 6.5; requires a walker). The study was approved by the Ethics Committee of the City of Vienna. Written informed consent was obtained. The protocol (Fig. 1A) was conducted twice to test the reproducibility of the stimulation-induced effects. On the first experimental day (session 1), walking performance was assessed using the 10-meter and the 2-minute walk tests (2minWT, 10MWT) before and immediately after the application of SCS. In session 2 (two weeks later), the same protocol was repeated, yet complemented by the timed-up-and-go test (TUG) as well as additional post-SCS assessments two and 24 hours after the intervention, to monitor potential prolonged carry-over effects. SCS was delivered through self-adhesive hydrogel surface electrodes (Schwamedico GmbH, Germany) placed over the T11/T12 vertebral processes and the lower abdomen (Fig. 1B) [7, 10]. The Stimulette r2x+ (Dr. Schuhfried Medizintechnik GmbH, Austria) produced charge-balanced, symmetric, biphasic rectangular pulses (1 ms/phase) [7]. The effects of SCS were hypothesized to be conveyed through the stimulation of lumbosacral posterior-root afferents [1]. The elicitation of posterior root-muscle (PRM) reflexes in the legs [7] (Fig. 1C) and the generation of paraesthesias in lower-limb dermatomes [10] (Fig. 1D) warranted the stimulation of these target neural structures. For the neuromodulatory intervention, stimulation was applied at 50 Hz for 30 minutes with the subject lying comfortably supine. The amplitude was set to a level that produced distant paraesthesias, without generating leg-muscle contractions [6, 10].

Results

SCS reproducibly improved walking performance considerably beyond the subject's normal ability. Gait speed (calculated from the 10MWT) increased in session 1 from 0.9 km/h pre-SCS to 2.3 km/h post-SCS, and in session 2 from 1.1 km/h to 1.8 km/h immediately post-SCS and 2.0 km/h two hours later (Fig. 2A). The distance covered during the 2minWT increased in session 1 from 26 m to 46 m and in session 2 from 37 m to 61 m and 60 m, respectively (Fig. 2B). Likewise, the time to complete the TUG (session 2) decreased from 31.4 s pre-SCS to 20.4 s and 18.3 s in the two post-SCS assessments (Fig. 2C). Following SCS, there was an enhanced left-right symmetry of the gait pattern with reduced foot supination during stance and improved stance-to-swing transitions. After 24 hours (session 2), the gait speed was 1.4 km/h and the distance covered during the 2minWT 35 m.

Figure 1: Study protocol and noninvasive spinal cord stimulation. (A) Two experimental sessions were conducted to test for carry-over effects of 30 minutes of noninvasive spinal cord stimulation (SCS) [10] on walking performance. In session 1, the 10-meter and the 2-minute walk tests (10MWT, 2minWT) were conducted before as well as immediately after SCS. In session 2, the same protocol, complemented by the timed-up-and-go test (TUG), was repeated, and two additional post-SCS assessments were conducted after two and 24 hours. (B) Electrode set-up used for SCS, with a self-adhesive hydrogel surface electrode (5 x 9 cm) placed longitudinally over the T11/T12 vertebral processes and a pair of interconnected electrodes (8 x 13 cm each) over the lower abdomen [7, 10]. (C) *(i)* Lumbar SCS was verified by the elicitation of posterior root-muscle (PRM) reflexes [7] by single stimuli (black arrow heads), recorded via surface-electromyography from L2–S2 innervated rectus femoris (RF), biceps femoris (BF), tibialis anterior (TA), and soleus (Sol) of right (R) and left (L) leg. No responses were obtained in RRF. *(ii)* Double stimuli revealed post-activation depression of the responses, confirming their reflex nature [7]. Shown are exemplary results of LSol, three repetitions superimposed. (D) 50-Hz SCS with an intensity of 90% of the lowest PRM-reflex threshold reproducibly elicited paraesthesias in distant dermatomes innervated by lumbosacral spinal cord segments (shaded areas) [7, 10].

Discussion

This study is the first to demonstrate temporarily lasting improvements of walking performance by noninvasive lumbar SCS in an individual with MS. The positive effects were reproducibly obtained on separate experimental days, coincided with the stimulation application, and were clearly beyond the subject's day-to-day variability, strongly hinting at a causal relationship. Likely, they were caused by the widespread, bilateral afferent input to the lumbar spinal cord provided by the noninvasive SCS [7] that in turn transsynaptically engaged and rebalanced the operation of dysregulated spinal locomotor circuits, *i.a.*, by altering the central excitatory state and neurotransmitter release for several hours [6]. In addition, an antispasticity effect of the stimulation [10, 13] may have further contributed through the unmasking of residual motor function. The present results suggest the high potential of noninvasive SCS, when repetitively administered, to bring immediate therapeutic benefits by enhancing motor function and improving quality of life of individuals living with MS.

Acknowledgements
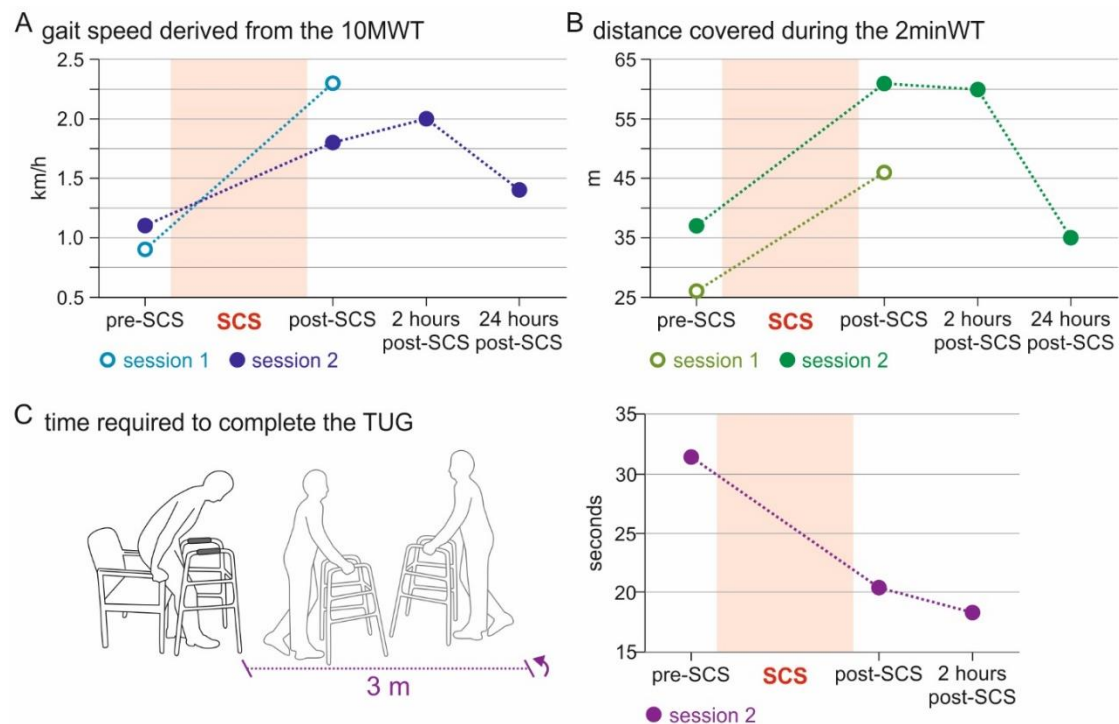
Figure 2. Augmentation of walking performance by noninvasive spinal cord stimulation. (A) Gait speed calculated from the 10-meter walk test (10MWT), (B) distance covered during the 2-minute walk test (2minWT), and (C) times required to complete the timed-up-and-go test (TUG) in sessions 1 and 2 and at different time points before and after 30 minutes of 50-Hz spinal cord stimulation (SCS) as indicated. All measures were markedly improved immediately as well as two hours after the stimulation.

References

[1] Minassian, K. et al.: Targeting Lumbar Spinal Neural Circuitry by Epidural Stimulation to Restore Motor Function After Spinal Cord Injury, *Neurotherapeutics*, vol. 13, pp. 284–94, Apr. 2016.

[2] Angeli, CA. et al.: Recovery of Over-Ground Walking after Chronic Motor Complete Spinal Cord Injury, *N. Engl. J. Med.*, vol. 379, pp. 1244–1250, Sep. 2018.

[3] Gill, ML. et al.: Neuromodulation of lumbosacral spinal networks enables independent stepping after complete paraplegia, *Nat. Med.*, vol. 24, pp. 1677–1682, Nov. 2018.

[4] Wagner, FB. et al.: Targeted neurotechnology restores walking in humans with spinal cord injury, *Nature*, vol. 563, pp. 65–71, Nov. 2018.

[5] Cook, AW, Weinstein, SP: Chronic dorsal column stimulation in multiple sclerosis. Preliminary report, *N. Y. State J. Med.*, vol. 73, pp. 2868–72, Dec. 1973.

[6] Illis, LS. et al.: Spinal cord stimulation in multiple sclerosis: clinical results, *J. Neurol. Neurosurg. Psychiatry*, vol. 43, pp. 1–14, Jan. 1980.

[7] Hofstoetter, UH. et al.: Common neural structures activated by epidural and transcutaneous lumbar spinal cord stimulation: Elicitation of posterior root-muscle reflexes," *PLoS One*, vol. 13, Jan. 2018.

[8] Minassian, K. et al.: Posterior root-muscle reflexes elicited by transcutaneous stimulation of the human lumbosacral cord, *Muscle Nerve*, vol. 35, pp. 327–36, Mar. 2007.

[9] Minassian, K. et al.: Spinal Rhythm Generation by Step-Induced Feedback and Transcutaneous Posterior Root Stimulation in Complete Spinal Cord-Injured Individuals, *Neurorehabil. Neural Repair*, vol. 30, pp. 233–43, Mar. 2016.

[10] Hofstoetter, US. et al.: Modification of spasticity by transcutaneous spinal cord stimulation in individuals with incomplete spinal cord injury, *J. Spinal Cord Med.*, vol. 37, pp. 202–11, 2014.

[11] Estes, SP. et al.: Priming Neural Circuits to Modulate Spinal Reflex Excitability, *Front. Neurol.*, vol. 8, p. 17, Feb. 2017.

[12] Gad, P. et al.: Weight Bearing Over-ground Stepping in an Exoskeleton with Non-invasive Spinal Cord Neuromodulation after Motor Complete Paraplegia, *Front. Neurosci.*, vol. 11, p. 33, Jun. 2017.

[13] Elbasiouny, SM. et al: Management of spasticity after spinal cord injury: current techniques and future directions, *Neurorehabil. Neural Repair*, vol. 24, pp. 23–33, Jan. 2010.

Author's Address

Ursula S. Hofstoetter
Center for Medical Physics and Biomedical Engineering
Medical University of Vienna
Waehringer Guertel 18-20/4L
1090 Vienna, Austria
ursula.hofstoetter@meduniwien.ac.at
https://zmpbmt.meduniwien.ac.at

Investigation on the Interaction of Monosynaptic and Polysynaptic Activity Underlying Posterior Root Reflexes

Haberbusch M[1], Vargas Luna JL [1], Mayr W[1,2]

[1]Center for Medical Physics and Biomedical Engineering, Medical University of Vienna, Austria
[2]Vienna University of Technology, Austria

Abstract: *A preliminary spinal cord stimulation study with a sample of two healthy participants was carried out to investigate the reciprocal interaction of monosynaptic and polysynaptic activity underlying posterior root reflexes. For this purpose, single pulses of transcutaneous electrical spinal cord stimulation were applied at T12-L3 vertebral level, while monitoring the EMG activity from quadriceps, hamstrings, tibialis anterior and triceps surae in both legs. To examine the interaction between monosynaptic and polysynaptic activity, a second pulse was introduced to elicit a conditioning monosynaptic response, which was shifted from 10 to 300 ms. It was found that moving the conditioning monosynaptic response towards the polysynaptic activity, effectively reduces its RMS voltage. On the other hand, the PTP voltage of the conditioning monosynaptic response was significantly increased when entering the timeframe of polysynaptic activity.*

Keywords: Spinal Cord Stimulation, Posterior Root Reflexes, Trans-synaptic Activity

Introduction

The research on spinal cord stimulation (SCS) has a long tradition and in practice was initially used for the treatment of symptoms as neuropathic pain or spasticity in persons suffering from multiple sclerosis. However, nowadays, SCS is also frequently applied for the treatment of non-progressive diseases such as spinal cord injury (SCI), providing artificial input to neuronal premotor circuitries below the injury site. SCS allows to effectively modify spasticity and motor control, thus improving the patient's quality of life, and helping to maintain the neuromuscular substrate for a potential later biological repair. In order to further improve this treatment modality, it is necessary to gain a better understanding of the neuronal pathways and interactions underlying posterior root reflexes (PRR).

Previous research has shown that not only stimulation rate, -site and -intensity, but also the interaction of neuronal activity elicited by consecutive stimuli may have an influence on the final motor output. Earlier studies have already examined the interaction of sequentially elicited monosynaptic PRR reflexes [1-3]; however, to our knowledge, no previous research has been conducted on the reciprocal influence of monosynaptic and polysynaptic activities underlying PRRs. For this purpose, paired stimuli of transcutaneous spinal cord stimulation (tSCS) were applied along the T12 and L3 vertebral segments, while monitoring the electromyographic (EMG) activity in both legs.

Material and Methods

Subjects: The assessments were performed in two male volunteers with no known neurological diseases. The corresponding subject information is listed in Table 1.

Table 1: Subject Data

Subject	Age	Height (cm)	Weight (kg)
M03	32	184	88
M04	28	178	72

In one volunteer (M03), the measurement was divided into two sessions with 22 days in between. The study was approved by the local ethics committee. All subjects gave their informed consent.

Measurement setup: The SCS was applied via self-adhesive, rectangular (5x5 cm) surface TENS electrodes (FITOP®, USA) placed in a bipolar array. The cathode was placed between the intervertebral space T11-L1 and individually adjusted on all sessions to optimize the response size in amplitude and symmetry, in relation with the contralateral leg. The anode was placed over the L3 vertebrae. The stimulation pulses were produced by two linear isolated stimulators (STMISOLA, Biopac Systems, Inc., USA) connected in parallel. This allows us to reach current intensities of up to 200 mA, required to elicit polysynaptic responses. The stimulation sequences were digitally generated by a custom LabVIEW™ application, previously developed at the Medical University of Vienna [4].

The stimulation effect on the spinal cord circuitry was indirectly monitored via bilateral EMG of the lower limb muscles. Specifically, we monitored the EMG activity of quadriceps (Q), hamstrings (H), tibialis anterior (TA), and triceps surae (TS) muscle groups by applying pairs of pre-gelled Ag/AgCl surface electrodes (Ambu® BlueSensor N ECG Electrode) with an inter-electrode distance of 1.5 cm. A reference electrode was placed at the proximal head of the fibula bone of each leg. Prior to electrode application, the skin was cleaned and roughened with abrasive skin gel (Nuprep®, Weaver and Company Aurora CO, USA) to reduce the skin impedance. Finally, to maintain the position through the whole measurement, the electrodes

were taped to prevent detachment during the contractions. In addition to the EMG, a second device was used to record the stimulation current for further post-processing purposes. All the signals were acquired through custom measurement devices [5] and a custom LabVIEW™ application that was developed at the Medical University of Vienna.

Measurement Protocol: The measurement protocol was designed to investigate the reciprocal interaction of monosynaptic and polysynaptic activity underlying PRRs. Paired pulses were used, as they are proven to be an effective approach for the examination of transsynaptic mechanisms underlying PRRs [1-3].

Two different stimulation intensities were used. Both intensities comply with two conditions: (1) be strong enough to effectively depolarize small diameter nerves in the dorsal roots (afferent fibres) and produce a stable polysynaptic response in at least one channel and; (2) if possible, be low enough to avoid direct activation of the motoneurons in ventral roots (efferent fibres). To do this, an initial screening of the responses to single pulses was performed from monosynaptic thresholds up to 200 mA or the maximum tolerable intensity. From such recording, the intensities for the test were defined.

Single cathodic-anodic biphasic stimulation pulses with a duration of 1 ms per phase were applied. The assessment of the interaction between monosynaptic and polysynaptic responses was done using pairs of identical stimuli. The first pulse (test) was applied at the previously defined intensity to elicit a monosynaptic and a polysynaptic response. The second pulse (conditioning) was introduced with an interstimulus interval (ISI) between 10 and 300 ms to produce a second monosynaptic response which approaches the polysynaptic test response with increasing ISI.

Data Processing: The recorded data was post-processed using MATLAB® and included the following steps: (1) All recorded channels have been filtered by application of a twelfth-order high-pass Butterworth filter at a cut-off frequency of 10 Hz, removing noise such as movement artefacts. (2) Stimulation artefacts have been identified by the use of the stimulation channel data. Therefore, a threshold of 1 mA was used to identify the artefact onset. We considered the artefact onset to be 0.5 ms prior to the first exceedance of the threshold, whereas the end of the artefact was assumed to be 5 ms after the identified artefact onset. (3) PRR responses were quantified, considering monosynaptic response intervals to begin 6 ms after stimulus onset and to last for 35 ms. Polysynaptic responses were assumed to occur between 100 and 200 ms after stimulus onset, which was consistent with the ranges observed by visual inspection of the signals. (4) Monosynaptic PRR responses were quantified by their PTP voltages, whereas polysynaptic PRR responses were quantified by their respective RMS voltages. Because of the monosynaptic test and conditioning responses overlapped for ISIs below 30ms, they could not be independently identified, thus the corresponding values were discarded. Unlike the short-latency monosynaptic reflexes, the polysynaptic reflexes tend to be less

synchronized, and their responses are less distinct, thus lower in amplitude but rather long in duration. Because of this, RMS voltages provide a more representative metric to quantify the polysynaptic activity. In order to avoid bias in the quantification of the polysynaptic responses, the monosynaptic conditioning responses were removed for ISIs of 70 to 190 ms, since they overlap the polysynaptic activity, evoked by the test stimulus.

In order to analyze the overall results, the PTP and RMS voltages of the monosynaptic and polysynaptic responses of all measurements have been normalized, and the mean values were calculated. The PRR responses were normalized to the mean PTP voltage of the monosynaptic test responses. The polysynaptic PRR responses were normalized to the mean RMS voltage of the second polysynaptic response for ISIs between 250 and 300 ms.

Results

The reciprocal interactions of monosynaptic and polysynaptic PRR were analyzed using paired pulses with gradually increasing ISIs at constant stimulation intensities. In subject M04, stable polysynaptic PRR responses could be elicited in the right quadriceps (RQ) and left quadriceps (LQ), however in subject M03 stable responses could only be achieved in RQ, hence, exclusively the data of RQ was used for the analysis.

Figure 1 shows representative PRR responses to paired stimuli with an intensity of 140 mA recorded in RQ of subject M03 for different ISIs, whereas Figure 2 depicts the summary of the behavior observed along the four datasets, showing the P2P — for monosynaptic — and the RMS — for polysynaptic — values at the different ISIs.
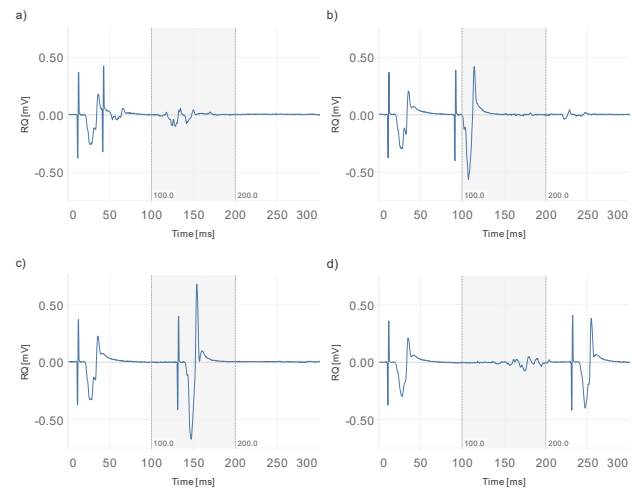
Figure 1: PRR responses to paired stimuli with an intensity of 140 mA recorded in RQ of subject M03 for ISIs of (a) 30 ms, (b) 80 ms, (c) 120 ms and (d) 220 ms, including stimulation artefacts.

Monosynaptic Responses: As depicted in Figure 2a, the short latency responses to the test stimulus were similar along the whole stimulation sequence with a normalized standard deviation of 0.2, which is expected from this kind of monosynaptic responses. The second response,

however, shows distinct trends of the PTP voltage as the ISI is increased.

At a short ISI of 30 ms, there is a substantial suppression of the conditioning monosynaptic response. This is consistent with the refractory behavior identified by [2,3], indicating that the recorded PRR responses were of reflex nature, rather than direct motor responses.

Nevertheless, this behavior is less distinct in subject M03 (Figure 2c), suggesting activation of a subset of ventral root axons at one of the intensities tested. Unlike the data reported in previous work [2,3], the second response not only recovered after 100 ms but reached values as high as twice the amplitude of the monosynaptic test response.
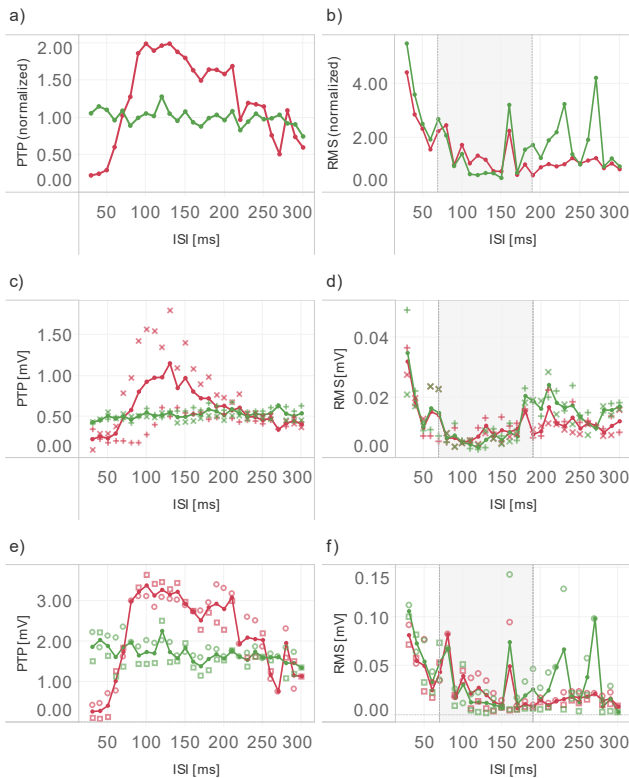
Figure 2: Total (a) Normalized PTP voltage of monosynaptic response to test (green) and conditioning (red) stimulus, (b) normalized RMS voltage of first (green) and second (red) polysynaptic response. (c) and (d) shows the same data for subject M03 without normalization, whereas (e) and (f) shows the data for subject M04: + M03 (140 mA), x M03 (160 mA), o M04 (120 mA) and □ M04 (140 mA). In the highlighted area, the second monosynaptic response was removed for RMS voltage calculation of the first polysynaptic response.

This elevation was observed on ISIs between 70 to 130 ms on subject M03 (Figure 2c), and 70 to 100 ms on M04 (Figure 2e). For subject M03 this behavior is rather transient, starting to decrease immediately after reaching its peak, and eventually settling down to the level of the monosynaptic control response at an ISI of 210 ms (Figure 2c). In contrast, for subject M04, the conditioning monosynaptic response remains at a significantly high level, until it steeply decreases between ISIs of 210 to 220 ms, eventually reaching the level of the monosynaptic test response (Figure 2e). The significant increase of the conditioning monosynaptic response in comparison to the control response in both subjects suggests either excitatory influence of polysynaptic onto monosynaptic reflex arcs, or the summation of the recorded EMG signals of monosynaptic and polysynaptic responses due to constructive interference. After such period, both monosynaptic responses were of similar size (Figure 2a).

Polysynaptic Responses: In general, the highest polysynaptic activity is observed at the shortest ISIs, which might be due to the summation of the activity produced by each pulse when they are close together. The initial amplitudes rapidly decline as the conditioning monosynaptic response gets closer to the timeframe of the first polysynaptic activity (Figure 2b). Once the conditioning pulse comes after the onset of the first polysynaptic response, its RMS voltage starts to increase again, until reaching a plateau, as soon as the conditioning pulse completely exceeds the timeframe of polysynaptic activity (Figure 2b). It is important to notice that this plateau is smaller than the polysynaptic activity detected at the shortest ISIs. The second polysynaptic response resembles a similar behavior, reaching a plateau at an ISI of 200 ms (Figure 2b).

Both polysynaptic responses show low scattering in subject M03 (Figure 2d), whereas for subject M04 especially the first polysynaptic response exhibits rather strong fluctuations (Figure 2f), nevertheless, overall trends can still be identified. In subject M03 for ISIs of 30 to 50 ms (Figure 2d), and in subject M04 for values from 30 to 60 ms (Figure 2f), the polysynaptic activity, elicited by the test and conditioning stimulus, show a significant attenuation.

In subject M03, both polysynaptic responses decrease further until an ISI of 100 ms is reached (Figure 2d). From this point on, both responses start to increase up to an ISI of 180 ms, where they eventually level off (Figure 2d). From this ISI on, the first polysynaptic response has a slightly higher RMS voltage than the second one. The described behavior might indicate a suppressive influence of monosynaptic onto polysynaptic PRR. In contrast, for subject M04, the decrease persists for ISIs of up to 150 ms, while the first polysynaptic response shows a slightly stronger decline than the second response (Figure 2f). From this point on, the second polysynaptic response remains rather stable, whereas, for the first polysynaptic response, it is hard to make any assumptions due to its strong fluctuations in RMS voltage. However, as the results of subject M03 show, the magnitude of the first polysynaptic response is also higher than of the second one.

Discussion

Monosynaptic Responses: The monosynaptic responses to the test stimulus remain stable in all measurements, since they are not subject to influences of preceding conditioning neural activity. However, the monosynaptic responses to the conditioning stimulus and the polysynaptic activities exhibit distinct trends which may be explained by different mechanisms.

For subject M04, both stimulation intensities were below the activation threshold of ventral roots, which is depicted by the attenuation of the monosynaptic conditioning response for ISIs below 60 ms, eventually reaching the same level as the monosynaptic test response (Figure 2d), which most likely results from post-activation, or homosynaptic depression [1-3]. However, this effect was less significant in subject M03 (Figure 2c) which suggests that the stimulation intensities needed to elicit the desired polysynaptic activity exceeded the activation threshold of a subset of ventral root axons, also leading to direct motor responses.

As the conditioning monosynaptic response starts to enter the timeframe of polysynaptic activity elicited by the test stimulus at an ISI of 70 ms, its PTP voltage is significantly increased compared to the monosynaptic control response (Figure 2a). The substantial increase of the PTP voltage of the conditioning monosynaptic response may be explained by an overlap and thus summation of the monosynaptic and polysynaptic PRR responses, elicited by the test and the conditioning stimulus.

Finally, another possible mechanism that might be responsible for the strong elevation of the monosynaptic control response maybe the increase of alpha motoneuron excitability due to the concurrent polysynaptic activity of excitatory last-order interneurons elicited by the test stimulus [6].

Polysynaptic Responses: Possible mechanisms for the significant attenuation of both polysynaptic responses (Figure 2b) may include the concurrent activity of inhibitory last-order interneurons lowering the alpha motoneuron excitability [6], postsynaptic receptor desensitisation [7], the refractory behaviour of alpha motoneurons shared by monosynaptic and polysynaptic pathways, and the decreasing interference of both polysynaptic responses due to increasing ISIs. With further increase of the ISI, the conditioning monosynaptic response starts to leave the timeframe of the first polysynaptic PRR response, and, consequently the polysynaptic activity starts to recover, eventually reaching a plateau at a higher magnitude, which further supports our assumptions on the suppressive behavior of monosynaptic onto polysynaptic activity. However, the mentioned possible mechanisms that might be involved are not mutually exclusive, and all of them may account to this phenomenon to a certain extent.

Conclusions

Although the data exhibited uncertainties due to fluctuations of polysynaptic response RMS voltages, the conducted measurements were able to provide possible information on the reciprocal interactions of monosynaptic and polysynaptic activities underlying PRRs.

First, the refractory behavior of PRRs could be identified, which indicates, that the elicited PRR responses were indeed of reflex nature, rather than direct motor responses. On the one hand, it was found that moving the conditioning monosynaptic response towards the polysynaptic activity effectively reduces its RMS voltage. The data suggest an inhibitory effect of monosynaptic onto polysynaptic

pathways. On the other hand, the PTP voltage of the conditioning monosynaptic response was significantly increased when entering the timeframe of polysynaptic activity. As the data indicates, concurrent polysynaptic activity may tend to elevate monosynaptic PRR responses. Ultimately, the findings suggest a further investigation of the reciprocal interactions of monosynaptic and polysynaptic activities using the proposed protocol, which may help to gain a deeper insight into the involved transsynaptic mechanisms underlying PRRs.

References

[1] M. Milosevic, Y. Masugi, A. Sasaki, D. G. Sayenko, and K. Nakazawa, "On the reflex mechanisms of cervical transcutaneous spinal cord stimulation in human subjects," Journal of neurophysiology, 2019

[2] K. Minassian, B. Jilge, F. Rattay, M. Pinter, H. Binder, F. Gerstenbrand, and M. R. Dimitrijevic, "Stepping-like movements in humans with complete spinal cord injury induced by epidural stimulation of the lumbar cord: electromyographic study of compound muscle action potentials," Spinal cord, vol. 42, no. 7, p. 401, 2004

[3] K. Minassian, I. Persy, F. Rattay, M. R. Dimitrijevic, C. Hofer, and H. Kern, "Posterior root–muscle reflexes elicited by transcutaneous stimulation of the human lumbosacral cord," Muscle & Nerve, vol. 35, no. 3, pp. 327–336, 2007

[4] S. Eickhoff, "Development of a computer controlled stimulation and recording system for trans-spinal electrical stimulation," Master's thesis, Vienna University of Technology, 2017

[5] C. Kast, M. Krenn, W. Aramphianlert, C. Hofer, O. C. Aszmann, and W. Mayr, "Modular Multi-channel Real-time Bio-signal Acquisition System," International Conference on Advancements of Medicine and Health Care through Technology; 12th-15th October 2016, Cluj-Napoca, Romania. Springer, Cham, 2017

[6] R. M. Brownstone and T. V. Bui, "Spinal interneurons providing input to the final common path during locomotion," Progress in brain research, vol. 187, pp. 81–95, Elsevier, 2010

[7] M. V. Jones, and G. L. Westbrook, "The impact of receptor desensitization on fast synaptic transmission," Trends in neuroscience, vol 19, no. 3, pp. 96-101, Elsevier, 1996

Author's Address

Max Haberbusch
Medical University of Vienna, Austria
max.haberbusch@gmail.com

Comparison of Results from a Spasticity Assessment of the Ankle Joint using the Tardieu Scale and EMG Activity Recorded Simultaneously in Stroke Patients

Magnusdottir G[1], Karason H[2], Chenery B[2], Gudmundsdottir V[1], Kristinsdottir K[2], Ludvigsdottir G K[1], Mayr W[3], Helgason T[1,2]

[1]Rehabilitation department at Grensas, Landspitali-Uni.Hospital, Reykjavík, Iceland
[2]Health Technology Center, Reykjavik University – Landspitali-Uni.Hospital, Reykjavik, Iceland
[3]Medical University of Vienna, Vienna, Austria

Abstract: Efficient treatments for the abatement of spasticity are scarce but the technique of transcutaneous Spinal Cord Stimulation (tSCS) has proven useful. In this research, the effects of tSCS on four post-stroke patients were investigated and the passive range of motion (PROM) and the quality of muscle reaction of the ankle joint were evaluated before and after treatment. The quality of muscle reaction and the PROM were also compared to the electromyography (EMG) muscle activity in order to reveal a correlation. The results indicated an increased ankle joint flexibility and a slight increase in the quality of muscle reaction after treatment in all cases apart from one. The results also suggested a decrease in EMG activity following an increase in the passive range of motion.

Keywords: Tardieu Scale, EMG, Stroke, Spasticity, Transcutaneous Spinal Cord Stimulation

Introduction

Spasticity is a motor disorder that it arises in over 30% of stroke patients and is characterized by hypersensitivity of the stretch reflexes. It can lead to muscle contracture, impediment of mobility and commonly induces pain [1]. Spasticity is defined as disordered sensorimotor control, resulting from an upper motor neuron lesion, presenting as intermittent or sustained involuntary activation of muscle [2]. Motor impairments are the most widely recognized impairments caused by stroke, including symptoms such as paralysis, loss of dexterity, hyperreflexia, spasticity and muscle stiffness [3].

The Tardieu scale is commonly used by clinicians to quantify spasticity. The spastic muscle is evaluated by grading the resistance to a passive stretch carried out at a very slow speed and a high speed, respectively. [4] The resistance could be caused by both neurogenic and mechanical components of the spasticity making measurements based on resistance insensitive. Since the Tardieu scale makes use of various velocities it evades the presence of contracture and is therefore able to differentiate between spasticity and contracture [5].

Transcutaneous Spinal Cord Stimulation (tSCS) has already been proven to alleviate spasticity in SCI patients and have a positive effect on motor function [6,7]. In tSCS bipolar short latency rectangular pulses are used to depolarize lumbosacral posterior roots [8] but the complete influence of tSCS on the spinal cord neural circuitry is still unknown.

The presented work is a part of a bigger study in which the aim is to assess the effect of tSCS in community dwelling individuals post-stroke. Here we explore the results from the use of the Tardieu scale in the assessment of spasticity and compare it to electromyography (EMG) results that were obtained simultaneously. Firstly, we

explore the correlation of the passive range of motion (PROM) of the ankle joint and muscle activity in the lower limb muscles and secondly, the effects of tSCS on the PROM of the ankle joint in stroke patients. The relationship between the quality of muscle reaction (i.e. spasticity) and the muscle activity recorded simultaneously was also examined.

Material and Methods

Data was collected on four stroke patients (mean age 65.5 ± 7.6 years) with spastic hemiplegia. One female who had haemorrhagic stroke and three males who had ischemic stroke. Tab. 1 summarizes the participant characteristics.

The study used four phases (A1, B1, A2, B2) of alternating baseline (A) and intervention (B) with an 18 to 24 weeks washout period in between. Included in each phase were three sessions of measurements performed on separate days but at the same time of the day. Measurements were performed at the Medical Technology Centre of Landspitali University Hospital and Reykjavik University.

Table 1: Participant Characteristics

	Gender	Age (yrs)	Ischemic (I) / Haemorrhagic (H) stroke	Years since onset
S3	Female	58	H	12
S4	Male	60	I	2
S5	Male	71	I	2
S6	Male	73	I	5

The intervention consisted of a 30-minute home

application of transcutaneous Spinal Cord Stimulation (tSCS) daily for three weeks. Self-adhesive electrodes were used, one circle electrode (5 cm diameter) positioned centrally to the back, at the level between the T11-T12 spinous processes, interconnected with a pair of rectangular reference electrodes (8x13 cm) placed over the lower anterior abdomen, symmetrical to the navel. The vertebral electrode on the back acted as the cathode and the two abdominal electrodes functioned as a single anode electrode. The placement of the electrodes can be seen in Fig. 1. Participants received electrical stimulation with a frequency of 60 Hz, constant current, 360 µs width and asymmetrical biphasic charge balanced pulses at an intensity of 90% of the threshold for eliciting muscle reaction as recorded by EMG in the lower limb muscles.

Figure 1: Position of the electrodes for the transcutaneous spinal cord stimulation. The electrode on the back has a diameter of 5 cm and is placed between the T11 and T12 vertebrae. The electrodes on the lower abdomen are 8x13 cm each, connected as a single electrode and located symmetrically on each side of the navel.

Electrophysiological and biomechanical assessment methods for spasticity were applied and have been described in our earlier work [7]. Here we firstly look at the root mean square (RMS) of the electromyography (EMG) recorded during a spasticity assessment using the Tardieu scale to determine the passive range of motion (PROM) of the ankle joint at a slow speed (V1).

The Tardieu scale is a clinical measure of muscle spasticity that involves assessing resistance to passive movement thereby addressing the velocity-dependent aspect of spasticity [4]. The test is performed by a physical therapist who initiates a brisk dorsiflexion movement of the relaxed ankle, activating the monosynaptic stretch reflex pathway. The spastic characteristics of the reflex pathway are then monitored by recording activity from the tibialis anterior (TA) and triceps surae (TS) muscles with EMG. The measurements were carried out in a supine position using goniometers to record joint movement for the ankle plantar flexors.

In addition to examining the PROM, the quality of muscle reaction was also considered using the Tardieu scale at a fast speed (V3). The quality of muscle reaction was evaluated during the passive movement of the ankle and graded on a scale from 1 to 5 where 1 represented no increase in muscle tone and 5 represented rigid flexion.

The EMG data was processed with Matlab R2014b (The MathWorks, Inc.) using the open-source toolbox EEGLab. A 4th order Butterworth high-pass filter with cutoff frequency at 15 Hz and a low-pass filter at 500 Hz was applied along with notch filters at 50 Hz, 100 Hz, 150 Hz and so forth. The RMS of the signal was calculated over an interval covering the first 10 seconds after the initiation of the movement for the PROM but only the first 3 seconds for the quality of muscle reaction.

Results

The graph in Fig. 2 illustrates the relationship between ankle joint flexibility in degrees and the RMS value of the EMG signal. An evident correlation between the flexibility of the ankle joint and the EMG muscle activity is observed. A decrease in EMG activity follows an increase in flexibility.
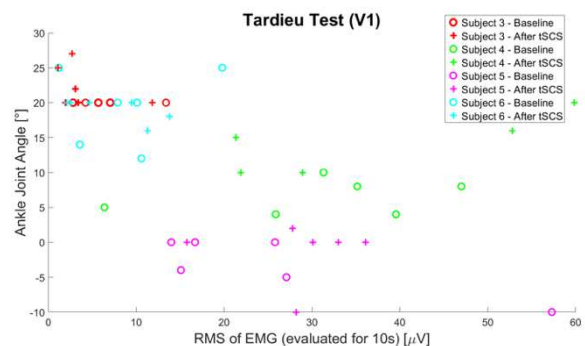
Figure 2: Shows the relationship between ankle joint flexibility (degrees) and the root-mean-square (RMS) value of the EMG signal obtained during involuntary stretch of the plantar flexors. The graph shows that with increasing flexibility of the ankle joint the EMG activity tends to decrease correspondingly.
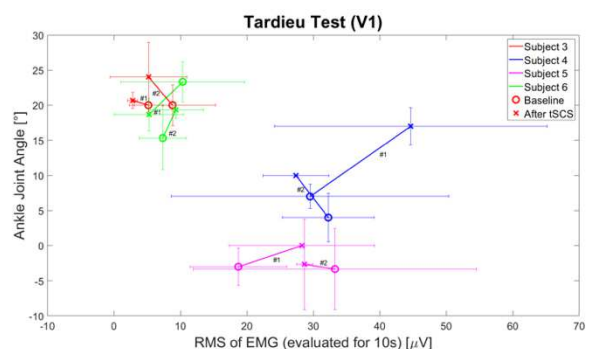
Figure 3: Depicts the progress of each subject. The mean value of each measurement (A1, B1, A2 and B2) is plotted along with its standard deviation. The baseline value (A) is depicted with a circle whereas the value obtained after the tSCS treatment (B) is depicted with a x. The graph shows increased flexibility after treatment for all measurements except phase 1 for subject 6, but does not show a decrease in EMG activity after treatment for all subjects.

The graph in Fig. 3 outlines the progress of each subject. An increase in flexibility after the treatment was consistently experienced, with the exception of phase 1 for subject 6. The graph does not
show a direct correlation between increase in flexibility and decrease in EMG activity. Only 4 measurements
depict a decrease in EMG activity alongside with increased flexibility.

The quality of muscle reaction of the subjects before and after treatment was relatively constant and only yielded scores between 2 and 3. The graph in Fig. 4 depicts the quality of muscle reaction for each subject before and after treatment. A slight decrease in the Tardieu score after the tSCS treatment can be observed for subjects 3, 4 and 5. The RMS of the EMG activity recorded during the experiment is evenly distributed and does not show any tendency to increase or decrease after treatment.
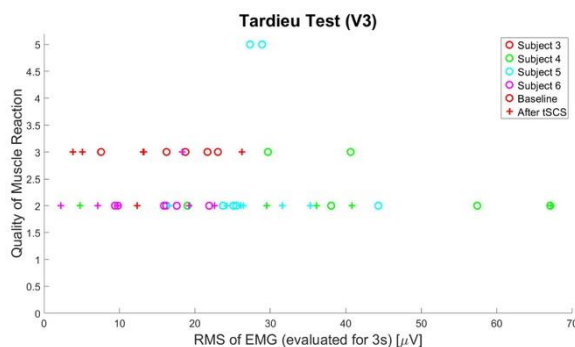
Figure 4: Depicts the relationship between the quality of muscle reaction (i.e. spasticity) obtained with the Tardieu scale and the RMS value of the EMG obtained simultaneously. The baseline values (A) are illustrated with a circle but the values obtained after the tSCS treatment (B) are depicted with a +. A drift downward and to the left was expected but is not distinctive. Subjects 3, 4 and 5 show a minor improvement in the quality of muscle reaction after the tSCS treatment.

The progress of the quality of muscle reaction for each subject before and after the tSCS treatment can be observed in Fig. 5. The average values for the baseline measurements and the measurements obtained after the treatment are plotted along with their corresponding standard deviation. A slight improvement can be seen for subjects 3, 4 and 5 but a minor decrease in the quality of muscle reaction can be seen for subject 6. The baseline measurements for subjects 3 and 6 and the measurements after the treatment for subjects 4 and 5 presented identical results, leading to a standard deviation of 0.
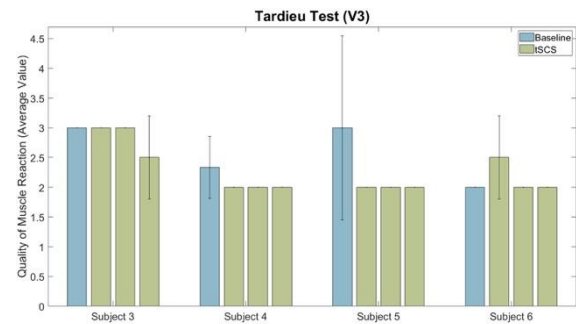
Figure 5: Illustrates the results of the quality of muscle reaction before and after tSCS treatment acquired using the Tardieu scale. The blue bars show the average of baseline measurements for each subject. The green bars depict the average of the measurements from both phases taken each week after the tSCS treatment. The first green bar represents the average value of the measurements taken in the first week of the treatment phase and so forth. The error bars illustrate the standard deviation. A lower score for the quality of muscle reaction is observed for all individuals except subject 6.

Discussion and Conclusion

In the presented work two parameters of the Tardieu scale (passive range of motion and quality of muscle reaction) were compared to EMG results recorded simultaneously in stroke patients before and after tSCS treatment.

The results show a correlation between the passive range of motion (PROM) of the ankle joint and the RMS of an EMG signal recorded simultaneously from the TA and TS muscles. They also show a positive increase in the passive range of motion of the ankle joint after tSCS treatment for all measurements except phase 1 for subject 6.

A slight increase in the quality of muscle reaction after the treatment can be observed for subjects 3, 4 and 5. On the other hand, the results do not depict a clear trend towards decreased EMG muscle activity after tSCS treatment, as was expected.

Since the results for the quality of muscle reaction (V3) suggest an increase for 3 out of 4 subjects after the treatment but do not show a definite decrease in EMG muscle activity, it can be concluded that the tSCS treatment does improve the quality of muscle reaction but does not necessarily decrease the EMG muscle activity concurrently. However, the results are to some extent inconclusive whereas the standard deviation in the bars that represent changes is high.

From the results for the passive range of motion (V1) it can be concluded that there is a substantial correlation between muscle activity and flexibility and that tSCS can be helpful in improving the range of motion of joints in individuals with spasticity.

The results for the passive range of motion and quality of muscle reaction are unanimous in that they show a slight improvement after the tSCS treatment for subjects 3, 4 and 5. In that way, the results exhibit a consistency between the different parameters of the Tardieu scale.

However, the subject pool was relatively small with only four subjects participating in the study. Therefore, in order to make a clear conclusion this topic has to be further investigated with more participants.

The validity of the Tardieu scale has been disputed since there are many external factors that may influence the outcome. One of those factors is the interpretation and experience of the clinician performing the test. Consequently, there is a rising demand for a more convenient and reliable way to quantify spasticity.

References

[1] Bhakta, B. B. (2000). Management of spasticity in stroke. Br Med Bull, 56(2), 476-485.

[2] Pandyan A, Gregoric M, Barnes M, Wood D, van W, Burridge J et al. Spasticity: Clinical perceptions, neurological realities and meaningful measurement. Disabil Rehabil 2005;27:2-6.

[3] Langhorne, P., Coupar, F., & Pollock, A. (2009). Motor recovery after stroke: a systematic review. The Lancet Neurology, 8(8), 741-754. doi:https://doi.org/10.1016/S1474-4422(09)70150-4

[4] Boyd, R. N., & Graham, H. K. (1999). Objective measurement of clinical findings in the use of botulinum toxin type A for the management of children with cerebral palsy. *European Journal of Neurology, 6*(S4), s23-s35. doi:doi:10.1111/j.1468-1331.1999.tb00031.x

[5] Patrick E, Ada L. The Tardieu Scale differentiates contracture from spasticity whereas the Ashworth Scale is confounded by it. *Clin Rehabil.* (2006) 20:173– 82. doi: 10.1191/0269215506cr922oa

[6] Hofstoetter, U.; McKay, W.; Tansey, K.; Mayr, W; Kern, H Minassian, Karen: ,,Modification of Spasticity by Transcutaneous Spinal Cord Stimulation in Individuals with Incomplete Spinal Cord Injury". In: *The Journal of Spinal Cord Medicine,* 37, M b arz, Nr.2, S. 202-211**,** 2014

[7] Vargas Luna, J L.; Gudfinnsdottir, H K.; Magnusdottir, G; Gudmundsdottir, V; Krenn, M; Mayr, W; Ludvigsdottir, Gudbjorg; Helgason, Thordur: ,,Effects of Sustained Electrical Stimulation on Spasticity Assessed by the Pendulum Test". In: Current Directions in Biomedical Engineering 2, Nr. 1. S. 405-407, 2016

[8] Minassian, K., Persy, I., Rattay, F., Dimitrijevic, M. R., Hofer, C., & Kern, H. (2007). Posterior root-muscle reflexes elicited by transcutaneous stimulation of the human lumbosacral cord. *Muscle and Nerve, 35*(3), 327-336. doi:10.1002/mus.20700

SPINAL CORD STIMULATION FOR ENHANCING MOTOR RECOVERY AFTER STROKE AND IMPROVING CHRONIC PAIN: IDENTIFYING RESPONDERS USING KETAMINE AND MAGNETIC STIMULATION

Nishino K[1], Yamaguchi S[1], Hirayama T[2], Imamura K[3]

[1]Department of Neurosurgery, Kakunodate General Hospital, Akita, Japan
[2]Deptartment of Neurosurgery, Nihon Univiversity Tokyo, Japan
[3]Department of Systems Life Engineering, Maebashi Institute of Technology, Maebashi, Japan

Abstract: The spinal premotor centre is a group of interneurons located in the dorsal columns, supposed to regulate the output of the alpha-motoneuron system. Recently, epidural spinal cord stimulation (SCS) was applied to target the spinal premotor centre. Here, we report that magnetic stimulation applied over Th11 and L1 vertebral levels induced dramatically rapid motor recovery in 13 out of 17 patients with stroke, assessed by neurological evaluations of actives of daily living and the 10-m walk test. Evaluations were conducted immediately after, 10 minutes after as well as one day after magnetic stimulation had been applied. The improvements outlasted the stimulation for 24 hours. Additionally, we tested the effects of SCS on pain and locomotor function in six patients with chronic pain. We found that the effects induced by magnetic stimulation and a low dose of ketamine infusion, a NMDA receptor antagonist, correlate with the degree of motor recovery obtained by SCS. We hence suggest that these methods could be used to preoperatively identify responders to SCS, both in patients with stroke and patients with neuropathic pain with or without locomotor dysfunction.

Introduction

The spinal premotor centre is a group of interneurons located in the dorsal column and is supposed to regulate the output of the alpha-motoneuron system. Its importance for motor recovery and controlling spinal spasticity has been repeatedly shown [1–3]. Epidural spinal cord stimulation (SCS) was introduced as a tool to target the spinal central pattern generator by Dimitrijevic et al. [4] and other scientists [5–7], and as a tool to target propriospinal neurons [8]. Further, Yamamoto et al. indicated that pharmacological examination prior to the implantation of an epidural SCS system could predict whether SCS would reduce neuropathic pain or spinal spasticity [1–3]. Recently, it was found that certain conditions of peripheral neuropathic pain also respond to treatment with SCS [9,10]. Our preliminary clinical observations suggest that low-dose infusion of ketamine and magnetic stimulation can be used as predictors of the degree of motor recovery and pain reduction later induced by epidural SCS, both in patients with stroke as well as chronic pain conditions.

Material and Methods

All trials were done in a single-arm trial.

Magnetic stimulation

Seventeen patients with chronic stroke (13 brain infarcts, 4 cases of intracerebral hematoma, 3 males) were included between 2015 and 2016. Times post-stroke inter-individually varied between three weeks and 15 years. Magnetic stimulation was applied over the Th11 and L1 vertebrae using the Magstim 200 (Magstim Co Ltd., UK) with 60-80% of the full energy level, 3-5 times single stimulation. Neurological evaluations, assessments of activities of daily living and the 10-m walk test were done immediately after, 10 minutes after as well as one day after the stimulation.

SCS in patients with stroke

Ten patients with stroke with locomotor dysfunction (9 males, age: 28–82 years) were studied. Times post-stroke varied between one month (one case) and five years. Five patients showed mild conscious impairment and spastic motor deficits with grades 2-3 on the Modified Ashworth Scale, while the rest showed motor deficits only. Initially, two SCS arrays were implanted in six patients, one at the level of the cervical spinal cord and the other one at Th11–L1 vertebral levels. In these patients, the treatment started with cervical SCS. If the neurological outcome was inadequate after three months, SCS over the lumbar spinal cord (Th11–L1 vertebral levels) was added. In the remaining patients, a single SCS electrode array was implanted at Th11–L1 vertebral levels.

SCS in patients with chronic pain

Six patients (3 males, age: 39–87 years, all without CNS lesion) were included. Two patients suffered from osteoarthritis of the knee, two from fibromyalgia, one from herpes zoster lesion, and one from spondylosis. SCS was applied to test its effect on pain, locomotor dysfunction, and spasticity. Stimulation parameters were: pulse width, 210 μsec, stimulation frequency, 30–60 Hz, stimulation amplitude, 1–2 V. In four patients, low-dose ketamine

infusions (15 mg) for four hours and magnetic stimulation were applied prior to implanting the epidural SCS system.

Results

Magnetic stimulation
Thirteen of the seventeen patients with stroke improved their modified Ranking Scale (mRS). Specifically, out of eight patients with mRS scores > 4, five had mRS scores of 3 and two patients had mRS scores < 2 after the stimulation. These improvements outlasted the stimulation application for 24 hours. No observations beyond 24 hours are available. After the stimulation, six of the patients otherwise unable to stand and ambulate showed improvements in their walking ability that persisted for at least 24 hours.

SCS in patients with stroke
Of the six patients with cervical SCS, five showed neurological improvements. Two cases with hemiplegia and tetraplegia showed full motor recovery of the upper limbs within the first 24 hours, yet no patient showed full recovery of normal gait. With SCS at Th11–L2 vertebral levels applied at 1–1.2 kHz, all four patients in whom the ketamine test conducted prior to the implantation revealed positive results, restored their ability to walk within the first week of stimulation. High-frequency SCS hence appears as a promising tool to restore gait after stroke. Further, SCS at Th11–L2 vertebral levels reduced pain in two patients, improved the range of motion and the ability to stand in four patients, and increased the walking speed in one patient. No effects were observed in four patients.

SCS in patients with chronic pain
All four patients in whom the ketamine test was performed, positive results were obtained shortly after the infusions, lasting for 6–12 hours. Further, magnetic stimulation improved the ability to stand up from sitting and to remain in an upright position in the four patients, yet did not result in pain relief. Epidural SCS at Th11–L2 vertebral levels restored walking function within one to two weeks, and these improvements lasted for 18 months after SCS.

Discussion

SCS is widely used as a reliable modality to reduce neuropathic pain. Regarding SCS for motor recovery, Nakamura et al. showed reduced muscle spasticity in patients with stroke, without further motor improvement [11]. Dimitrijevic et al. analysed six clinical cases of spinal cord injury between C5 and Th8 and demonstrated firstly the existence of the human central pattern generator in 1998 [4]. Further clinical trials of SCS were performed in spinal cord injury and stroke [12, 4–6, 16–19] and pointed out that in humans the stimulating condition is a key to restore motor functions. Our studies with SCS applied at Th11–L2 vertebral levels using frequencies of 30–90 Hz did not show motor recovery in general, but transient recovery of motor function in those patients in whom the ketamine test and magnetic stimulation produced positive

results. On the other hand, cervical SCS induced prompt full recovery of upper-limb motor function in chronic stroke patients with hemiplegia or tetraplegia. Dr. Isa previously showed that propriospinal interneurons of the cervical spinal cord are involved in rapid motor recovery of the upper limb in spinal cord injury [20]. SCS at 1–1.2 kHz showed promising effects on the locomotor ability of four patients. It therapeutic efficacy in hemiplegia and locomotor dysfunction in patients with stroke and chronic pain will be further investigated.

Conclusions

In patients with stroke and chronic neuropathic pain with locomotor dysfunctions, magnetic stimulation and ketamine tests may be useful to identify responders to SCS.

References

[1] Yamamoto T, Hirayama T, Katayama Y, Tsubokawa T, et al.: Usefulness of the morphine/thiamylal test for the treatment of deafferentation pain. Pain Research, 6: 143-146, 1991.

[2] Yamamoto T., Katayama Y., Hirayama T, Tsubokawa T: Pharmacological classification of central post-stroke pain: comparison with the results of chronic motor cortex stimulation therapy. Pain, 72:1-2, 5-12, 1997.

[3] Yamamoto T., Katayama Y., Maejima S., Hirayama T.: 5-HT3 antagonist for the treatment of central pain: comparison with the results of pharmacological test. Pain Research 12:109-114, 1997.

[4] Dimitrijevic MR, Gerasimenko Y, Pinter MM: Evidence for a spinal central pattern generator. Ann NY Acad Sci. 860:360-76, 1998

[5] Milan R. Dimitrijevic, Simon M. Danner, Winfried Mayr: Neurocontrol of Movement in Humans With Spinal CordInjury, Artificial Organ: 39(10):823-833, 2015

[6] Minassian K, McKay BW et al: Targeting Lumbar Spinal Neural Circuitry by Epidural Stimulation to Restore Motor Function After Spinal Cord Injury, Neurotherapeutics. 13(2): 284–294, 2016

[7] MinassianK, Jilge B, RattayF, PinterMMH, et al: Stepping-like movements in humans with complete spinal cord injury induced by epidural stimulation of the lumbar cord: electromyographic study of compound muscle action potentials, Spinal cord 42, 401-416, 2004

[8] E Formento, K Minassian, F Wagner et al: Electrical spinal cord stimulation must preserve proprioception to enable locomotion in humans with spinal cord injury, Nature Neuroscience 21 1728-1741, 2018

[9] Lowry AM, Simopoulos TT: spinal cord stimulation for the treatment of chronic pain following total knee replacement, Pain Physician 13:251-256, 2010

[10] Kim SJ, Lee G, Bae H, et al: Cortical astrocytes rewire somatosensory cortical circuits for peripheral neuropathic pain. J Clin Invest. 126(5):1983-97, 2016

[11] Nakamura. S, Tsubokawa T, Y Sugano Y:Dorsal Column stimulation for post-apoplectic spastic hemiplegia: report of three cases, Neurologia medico-chirurgica, 24,180-186,1984.

[12] Lowry AM, Simopoulos TT: Spinal cord stimulation for the treatment of chronic pain following total knee replacement, Pain Physician 13:251-256, 2010

[13] Yamamoto T, Hirayama T, Katayama Y, Tsubokawa T, et al.: Usefulness of the morphine/thiamylal test for the treatment of deafferentation pain. Pain Research, 6: 143-146, 1991.

[14] Yamamoto T., Katayama Y., Hirayama T, Tsubokawa T: Pharmacological classification of central post-stroke pain: comparison with the results of chronic motor cortex stimulation therapy. Pain, 72:1-2, 5-12, 1997.

[15] Yamamoto T., Katayama Y., Maejima S., Hirayama T.: 5-HT3 antagonist for the treatment of central pain: comparison with the results of pharmacological test. Pain Research 12:109-114, 1997.

[16] Minassian K, Hofstoetter U, Dzeladini F, et al: The Human Central Pattern Generator for Locomotion, Neuroscientist.; 23(6):649-663, 2017.

[17] Hostoetter U, McKay B W et al: Modification of spasticity by transcutaneous spinal cord stimulation in individuals with incomplete spinal cord injury, J Spinal Cord Med. 37(2):202–211,2014

[18] Flynn JR, Graham BA, Galea MP, et al: The role of propriospinal interneuron in recovery from spinal cord injury. Neuropharmacology. 60(5):809-22. 2019

[19] Tohyama T, Kinoshita M, Isa K et al: Contribution of propriospinal neurons to recovery of hand dexterity after corticospinal tract lesions in monkeys, Proc Natl Acad Sci USA 17;114(3):604-609, 2017

[20] Tohyama T, Kinoshita M, Isa K et al: Contribution of propriospinal neurons to recovery of hand dexterity after corticospinal tract lesions in monkeys, Proc Natl Acad Sci USA 17;114(3):604-609, 2017

Author's Address

Katsuhiro Nishino
Department of Neurosurgery, Kakunodate General Hospital, Kakunodate, Senboku City, Akita, Japan
knishino.ns@kakunodate-hp.com

Reconstructive Neurosurgery

Brown JM[1][2]

[1]Massachusetts General Hospital, Boston, USA
[2]Harvard Medical School, Boston, USA

Abstract: *Reconstructive Neurosurgery is the practice of applying procedures to the central or peripheral nervous system that corrects deficits by augmenting neural control, restoring neural connectivity, and redistributing intact residual functions. We will review nerve reconstruction, nerve transfers, tendon transfers, selective peripheral neurotomy and correcting lower motor neuron deficits in order to allow for application of FES systems*

Keywords: *Reconstructive neurosurgery, nerve transfer, selective peripheral neurotomy*

Author's Address

Justin M. Brown, MD
Massachusetts General Hospital
Harvard Medical School
jmbrown@mgh.harvard.edu
paralysis.mgh.harvard.edu

Session 2:
WEARPLEX:
European multidisciplinary Research and
Innovation Action on WEARable
multiPLEXed biomedical electrodes

Introduction of EU-H2020 project WEARPLEX - Wearable multiplexed biomedical electrodes

Milos Kostic[2,10], Russel Torah[1], Steve Beeby[1], Matija Strbac[10], Thierry Keller[2], Senentxu Lanceros-Mendez[3], Peter Andersson Ersman[4], Maxim Polomoshnov [5], Strahinja Dosen[6], Rune Wendelbo[7], Séverine Chardonnens[8], Antti Tauriainen[9]

[1]University of Southampton, United Kingdom
[2] Fundacion TECNALIA Research and Innovation, Spain
[3] Fundacion Bcmaterials - Basque Centre for Materials, Applications & Nanostructures, Spain
[4] RISE Acreo AB, Sweden
[5]Chemnitz University of Technology, Germany
[6]Aalborg University, Denmark
[7]Abalonyx AS, Norway
[8]IDUN Technologies AG, Switzerland
[9]Screentec OY, Finland
[10]Tecnalia Serbia Ltd, Serbia

Abstract: *We intend to present the WEARPLEX project to the broader scientific community, which is well represented in the Vienna international workshop on FES. This three-year research and innovation action is funded by the H2020 program. The project aim is to develop multiplexed biomedical electrodes that can be applied either in the field of electrical stimulation or for recording of electrophysiological signals. We will shorty describe the WEARPLEX objectives, concept, approach and research team. One of the post-conference workshops will be dedicated to presenting first results and early prototype of a WEARPLEX electrode for recording and for electrical stimulation.*

Keywords: *multipad electrode, flexible electronics, printed electronics, post-conference workshop, H2020*

Introduction

Electrodes that allow controlled propagation and delivery of electrical pulses play a key role in a variety of applications such as neuromotor rehabilitation [1–3], neuromodulation for tremor suppression and electro-analgesia [4], sports [5,7], wound healing [6,8], drug delivery [9] and more. Even more widespread application of the same basic technology is in the recording of electrophysiological signals. Recent advances in signal processing and control algorithms have opened the possibility for the broad use of these signals in human-machine interfacing, most notably the use of EMG for controlling various devices, from multi DoF prosthetic limbs [10, 11], through to consumer devices such as computers, home appliances, drones [12] and video games [13].

Key variables in the applications of biomedical electrodes are their shape and placement, as these determine the detection points during recording, as well as the current flow during stimulation and thereby, muscle activation characteristics. Muscle selectivity and recruitment, be it in recording or stimulation, and/or ion propagation of active agents i.e. medicaments in iontophoretic applications, is of fundamental importance. The optimal electrode configuration is dependent on the electrode-skin interface as well as skin impedance and physical characteristics and is therefore person-specific and change on a daily basis [14].

Multi-pad electrodes have shown great potential in addressing these problems by allowing a programmable interface to alter the active electrode surface [1]. By having a larger number of independent pads that can be programmably activated in a sequence [15] or selected to form a single electrode, in a manner that can be personalized for each patient, the multi-pad approach provides a powerful platform for control of current propagation [16].

There are two main limiting factors of the existing technology: 1) multi-pad electrodes need to connect to the stimulator/recording device with as many leads as there are pads, leading to a linear correlation between the system size and resolution, and 2) electrodes are printed on rigid substrates limiting their adherence to curved or moving body parts.

In the WARPLEX project we propose a paradigm shift in designing of the recording and stimulation systems, as the switching electronics is shifted from the custom-made stimulator/recording device to the electrode, leading to a universal solution compatible with any stimulation or recording system.

WEARPLEX objectives

WEARPLEX is a multidisciplinary research and innovation action with the overall aim to develop cost-effective flexible and wearable textile based configurable biomedical electrodes for recording of electrophysiological signals or delivering targeted electric charge in applications that require high resolution over large areas of the body. This includes development of technologies and manufacturing processes for multi-pad electrodes with integrated logic circuits that enable flexible configuration

of electrodes connected to a recording or stimulation channel, all on the same textile substrate.

The project will involve fundamental research into the underpinning technologies and developing large-scale printing processes in combination with complementary manufacturing technologies.

The project aims to demonstrate the technology through fabrication of three versions of demonstrators, which are increasingly sophisticated as the project progresses.

WEARPLEX concept

This project focuses on developing materials and processes that enable organic electronics and flexible electrodes to be incorporated into textiles with the clear aim of developing highly usable biomedical electrodes that can be applied across range of scenarios with currently unmet needs. This research will push innovations in electronic textiles and demonstrate the benefits and opportunities in the medical electronics sector. The project is focused on this sector but the technologies that will be developed are key for all areas of wearable electronic textiles and even beyond this to other textile markets such as automotive, aerospace, furnishings and technical textiles.

In the state of the art multi-pad systems all of the logic circuits are located in the driving device i.e. outside of the electrode. This means that each pad needs to be connected to the stimulator through a direct lead and an increase in the number of pads reflects exponentially on the cost and complexity of the system. Migration of active electronic components to the electrode will enable a much greater number of electrodes and unlock the full potential of this technology.

The printed electronics implemented in a switching matrix will allow the individual pads to be connected in arbitrary configurations to the output leads of the electrode. Therefore, the pads will be flexibly organized into several virtual electrodes of arbitrary position, shape and size which then can be connected to any standard multichannel recording and stimulation system. In addition, the methods will be developed for automatic calibration of the virtual electrodes. The pads will be used for spatial scanning to detect stimulation/recording hotspots and adjust the virtual electrodes accordingly.

Therefore, the WEARPLEX project will lead to a new generation of smart electrodes that will be able to adapt simultaneously to the user (wearable and flexible garment), recording/stimulation scenario (movement type and target muscles) and recording/stimulation system (number of channels).

Two parallel approaches will be explored for the realisation of the electronic functionalisation. Printable active organic materials will be used to realise components with the required performance and bare die inorganic electronic components will be packaged in a manner that enables reliable integration into the textile substrates. This combination of approaches will enable the full integration of the required electronic functionality, establish the comparative merits of each approach, advance the state of the art across a broader range of technologies and provide inherent mitigation against technical risks.

WEARPLEX approach

To achieve its ambitious goals, the WEARPLEX project is based on a highly transdisciplinary approach. Experts from different fields such as materials development, printed electronics and e-textiles, process engineering and production technology, system control and health technologies will work together, contribute and integrate their respective know-how (Figure 1). The combined expertise will allow developing the novel system and validating the innovative WEARPLEX technology in relevant environment and enable the successful production of the two selected applications.
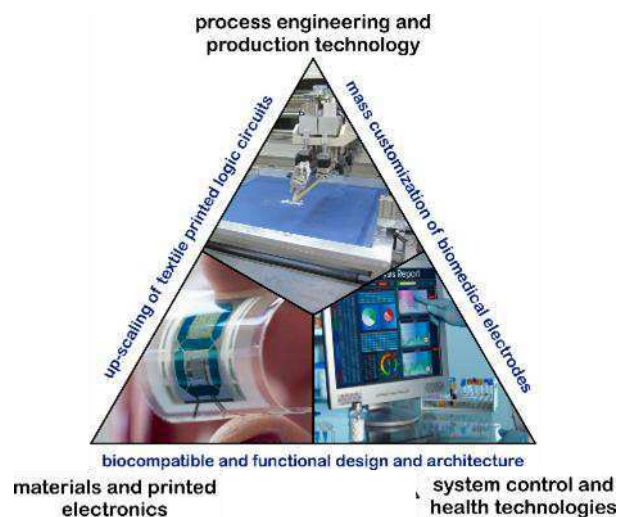
Figure 1. Multidisciplinary approach of the WEARPLEX project

The overall approach of the project (Figure 2) is characterized by several interrelated tasks (materials development, printed electronics designs, e-textiles and process engineering) feeding into a production process that integrates these tasks in order to realise the wearable multiplexed biomedical electrode. The final fabrication processes and parameters are then used to realise the demonstrators for selected applications.
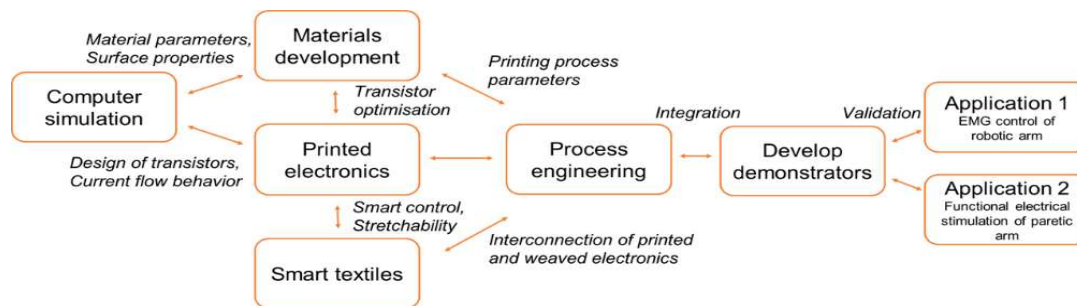
Figure 2. Overall approach of the project

WEARPLEX Team

The WEARPLEX consortium consists of a set of carefully chosen partners with expertise and background in the different areas of the multidisciplinary endeavour that is the WEARPLEX project. There is a total of 9 partners from 8 different countries in Europe (United Kingdom, Spain, Germany, Sweden, Denmark, Finland, Switzerland and Norway) as shown in Figure 3. Each partner was selected based on its specific and unique expertise and market position. Hence, a highly interdisciplinary and complementary consortium could be formed.

The consortium represents technical experts and researchers form the areas of chemistry, biomaterials, electronics, automated control, process engineering, smart textiles and health technologies, as well as the industrial partners who bring complementary expertise and resources, which are essential to realize the scientific, technological and exploitation/dissemination objectives of the project.

The consortium consists of three universities (UoS, TUC, AAU), three European Research and Technology Organisations (TEC, BCM, ACR) and three SME (SCT, ABL, IDT) with different areas of expertise. Most of the consortium partners have been or are involved in EU funded projects with an excellent track record.

The different WEARPLEX partners were selected based on their expertise (technical and industrial) and resources (materials, processes, laboratory systems) that they brought to the development and testing of the WEARPLEX technology. This has resulted in a consortium that consists of a rich mixture of complementary expertise, which will lead to cross-fertilisation between different areas that have not been (properly) explored previously.

Conclusions

The WEARPLEX project present one of the most comprehensive research and innovation actions directed towards improvement of the biomedical electrodes in Europe today. In order for it to succeed significant involvement from the scientific community and other stakeholders is needed. Therefore, the participants of the 13th Vienna Int. Workshop on FES are most welcome to join the stakeholder workshop organised in the post-conference program and provide their feedback.
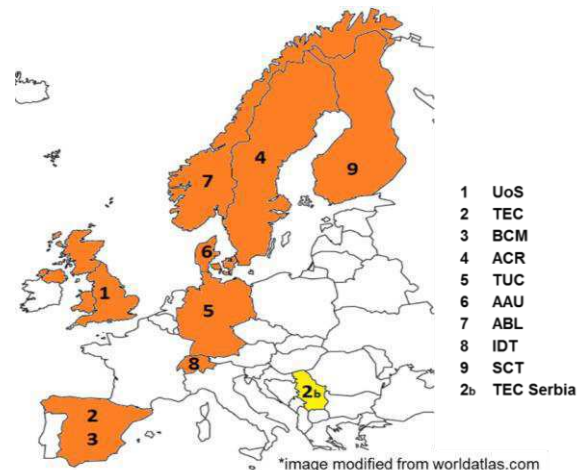
Figure 3. European approach in the WEARPLEX consortium

Acknowledgement

References

[1] Malešević, J. et al. A decision support system for electrode shaping in multi-pad FES foot drop correction. J. Neuroeng. Rehabil. 14, (2017).

[2] Malešević, N. M. et al. A multi-pad electrode based functional electrical stimulation system for restoration of grasp. J. Neuroeng. Rehabil. 9, 66 (2012).

[3] Howlett, O., et al. Functional electrical stimulation improves activity after stroke: A systematic review with meta- analysis. Arch. Phys. Med. Rehabil. 96, 934–943 (2015).

[4] White, P. F., Li, S. & Chiu, J. W. Electroanalgesia: its role in acute and chronic pain management. Anesth. Analg. 92, 505–513 (2001).

[5] Babault, N., et al. Does electrical stimulation enhance post-exercise performance recovery? European Journal of Applied Physiology 111, 2501–2507 (2011).

[6] Ennis, W. J., et al. Advanced technologies to improve wound healing: Electrical stimulation, vibration therapy, and ultrasound-what is the evidence? Plast. Reconstr. Surg. 138, 94S–104S (2016).

[7] Taradaj, J. et al. The effect of neuromuscular electrical stimulation on quadriceps strength and knee function in

professional soccer players: Return to sport after ACL reconstruction. Biomed Res. Int. 2013, (2013).

[8] Thakral, G. et al. Electrical stimulation to accelerate wound healing. Diabetic Foot and Ankle 4, (2013).

[9] Filipovic, N., et al. Computational and experimental model of transdermal iontophorethic drug delivery system. Int. J. Pharm. 533, 383–388 (2017).

[10] Dosen, S., et al. EMG Biofeedback for online predictive control of grasping force in a myoelectric prosthesis. J. Neuroeng. Rehabil. 12, (2015).

[11] Isaković, M., et al. "Optimization of Semiautomated Calibration Algorithm of Multichannel Electrotactile Feedback for Myoelectric Hand Prosthesis." Applied Bionics and Biomechanics 2019 (2019).

[12] Cacace, J. et al. A control architecture for multiple drones operated via multimodal interaction in search & rescue mission. in SSRR 2016 - International Symposium on Safety, Security and Rescue Robotics 233–239 (2016). doi:10.1109/SSRR.2016.7784304

[13] Armiger, R. S., et al. A real-time video game interface for training and evaluation of dexterous upper-extremity neuroprosthetic control algorithms. in 2008 IEEE-BIOCAS Biomedical Circuits and Systems Conference, BIOCAS 2008 121–124 (2008). doi:10.1109/BIOCAS.2008.4696889

[14] Malesevic, J. et al. Evolution of Surface Motor Activation Zones in Hemiplegic Patients During 20 Sessions of FES Therapy with Multi-pad Electrodes. Eur. J. Transl. Myol. 26, 6059 (2016).

Author's Address

Name: Miloš Kostić

Affiliation: Fundacion TECNALIA Research and Innovation, Spain; Tecnalia Serbia Ltd, Serbia

eMail: milos.kostic@tecnalia.com

Session 3:
Aging, dystrophic and denervated Muscle

Home based Functional Electrical Stimulation for early-aging and aging, a narrative review

Carraro U[1,2,3], Hofer C[4], Taylor MJ[5], Albertin G[2,6], Gargiulo P[7], Marcante A[3], Loefler S[4,8], Jarvis JC[9], Ravara B[1,2,6], Mayr W[10], Zampieri S[1,2,4], Kern H[8]

[1]A&C M-C Foundation for Translational Myology, Padova, Italy
[2]Interdepartmental Research Centre of Myology, Dept. Biomedical Sciences, University of Padova, Italy
[3]Fondazione Ospedale San Camillo IRCCS, Venezia, Italia
[4]Ludwig Boltzmann Institute for Rehabilitation Research, St. Pölten, Austria
[5]Faculty of Engineering and IT, The University of Sydney, Camperdown, Australia
[6]Department of Neuroscience, Section of Human Anatomy, University of Padova, Italy
[7]Reykjavik University, Reykjavik, Iceland
[8]Physiko und Rheumatherapie – Institut für Physikalische Medizin, St. Pölten, Austria
[9]School of Sport and Exercise Science, Liverpool John Moores University, UK
[10]Center for Medical Physics and Biomedical Engineering, Medical University of Vienna, Austria

Abstract: Functional electrical stimulation (FES) is used in diverse populations to allow persons who are unable or reluctant to move their limbs to exercise, usually by surface neuromuscular electrical stimulation (NMES), also known as transcutaneous electrical nerve stimulation (TENS), in hospital settings or outpatient services. If properly instructed, many of the persons-in-need may continue at home with FES-induced training with a daily frequency and for the long duration of time needed to achieve clinically-relevant outcomes. Standing on the experience of the EU Project RISE, of our studies in aging persons, and of more recent published data, we are confident that FES may contribute to a better life for an expanding population of aged persons and of early aged patients suffering with mobility impairments due to neuromuscular disorders or systemic diseases. This narrative review will cover results of surface NMES/TENS and of FES for denervated degenerated muscles (DDM) delivered, in the last case extending the report to the benefits of costimulation of agonist and antagonist leg muscles, and including results at the level of the stimulated skin. While used to enable SCI patients to train muscles and the cardiovascular system, home based FES (h-bFES) has been extended to persons suffering with chronic failure of heart, lung, kidney, and to the elderly. Limb NMES have been shown to resolve subcutaneous edema, while recent data support h-bFES for DDM to recover skin from SCI-induced atrophy and flattening. In conclusion, h-bFES is a safe and effective therapy for an expanding population of aged persons and of early aged patients with mobility impairments due to neuromuscular disorders or systemic diseases.

Keywords: home based functional electrical stimulation (h-bFES), muscle weakness, skin atrophy, early aging, aging

Introduction

Functional electrical stimulation (FES) is used in diverse populations to allow who is unable or reluctant to move limbs to exercise, usually by surface neuromuscular electrical stimulation (NMES), also known as transcutaneous electrical nerve stimulation (TENS), in hospital settings or outpatient services [1]. If properly instructed, many of the persons-in-need may continue at home with FES-induced training (h-bFES) at the daily frequency and for the appropriate duration needed to achieve clinically relevant outcomes [2]. In this narrative review, we have scanned the available published literature, summarizing pertinent findings, in particular, the clinical data from the EU Project – RISE [3,4], but extending the report to benefit of co-stimulation of agonist and antagonist leg muscles [5]. Stressing the potential for FES as a home therapy in several different populations of early aging persons, i. e., suffering with chronic organ failures [1,6-10], and the elderly [11-23], we will show that the positive effects of surface electrical stimulation by large electrodes and purpose-designed stimulators, now commercially available [21], usually observed as improvements of function and structure of skeletal muscles, are extended to skin [24-27].

State of the art of h-b FES

Neuromuscular Diseases: FES was implemented in individuals with CNS diseases, such as spinal cord injury and cerebral palsy [28,29], starting more than 60 years ago [30]. Much more recent applications are those at the home [31-33], including a recent series of reports related to the 2016 First Cybathlon [34]. Functional electrical stimulation exercise usually involves stimulation of intramuscular nerves. This may be carried out in a variety of modalities such as, cycling [35], rowing [36], or walking [37]. Recently there was great interest in motivating SCI patients to perform FES cycling by organising competitions among FES Cycling SCI athletes. This was achieved after many months of training performed also at home after careful instructions in clinics or outpatient services [38-43]. Although there is still debate concerning the balance between cost (time, capital, investment,

interference with daily living) and long-term benefit, many practitioners and institutions recognize the value of FES in their clinical practice [44]. We are confident that the results of the EU Project RISE [2-4,45], of the studies performed in Vienna and elsewhere on skeletal muscle of lifelong active seniors [46,47] and of sedentary seniors before and after months of h-bFES [12-21] will demonstrate its clinical value. We certify that all applicable rules concerning the ethical use of human volunteers were followed during the course of those researches (approval of ethical committee, Vienna, Austria: EK-02-068-0702).

Myokines in h-bFES Recovery of Muscle in Permanent Denervation and Aging: Since sub-clinical denervation events contribute to both atrophy and the decreased contractile speed of aged muscle, we saw a parallel to spinal cord injury and decided to look at both groups together [48]. The muscles from lifelong active seniors have more muscle bulk and more slow fiber-type groupings than those of sedentary seniors, demonstrating that physical activity maintains slow motoneurons that reinnervate the transiently denervated muscle fibers. On the other hand, muscle degeneration occurs with irreversible *Conus* and *Cauda Equina* syndrome, a spinal cord injury in which the human leg muscles could be permanently disconnected from the peripheral nervous system [2,49]. In these patients a complete loss of muscle fibers occurs within five to ten years after injury [45]. Their recovered tetanic contractility, induced by h-bFES [2], can restore the muscle size and function in compliant Spinal Cord Injury patients, allowing them to perform electrical stimulation-supported stand-up and step-in place training [3,4], when a purpose developed electrical stimulator provides the necessary high currents to large surface electrodes covering the Quadriceps muscles (now commercially available: "Stimulette den2x" of the Schuhfried Medizintechnik GmbH, Vienna, Austria) [50]. It is here worthwhile to stress that the use of the pairs of very large surface electrodes (needed to reach almost all the denervated muscle fibers of the quadriceps muscle) induces considerable co-contraction of the hamstrings, that are therefore also substantially recovered from atrophy and degeneration (5). Thus, the cushioning effect due to co-contraction of agonist and antagonist thigh muscles, a validated model of muscle recovery/hypertrophy in animal models [51,52], is obtained, saving h-bFES training time. This peculiarity of h-bFES for DDM, together with the evidence provided by Muscle Color Computed Tomography of thigh muscles [3-5,53], a mode of clinical imaging that SCI persons may easily appreciate, contributes to maintain compliance of patients. Recent observations of the impact of h-bFES on stimulated skin add to those positive evidence. The data indeed provide evidence that epidermal atrophy and flattening worsen with years of SCI and that h-bFES by large surface electrodes reverses SCI-induced skin changes, producing a statistically significant recovery of epidermis thickness and number/morphology of dermal papillae, with minor changes of Langerhans Cells. Thus, in SCI patients, the impressive beneficial effects of two years of electrical stimulation on strength, bulk, and myofiber size of thigh muscles are extended to the skin, suggesting that h-bFES by large electrodes would be also clinically relevant for dermatological complications in SCI and beyond [25-28, and Albertin et al., personal communication].

Whether the effects of electrical stimulation on skin is direct and local or is the consequence of systemic circulating factors released by muscle cells (myokines) remains to be determined. Myokines are indeed produced and released by muscle fibers under contraction and exert both local and systemic effects. Changes in patterns of myokine secretion, particularly of IGF-1 isoforms, occur in long-term Spinal Cord Injury and in aging [19]. Their modulation is a documented key factor in h-bFES - mediated muscle recovery (see for a review [48]).

h-bFES and chronic organ failures. Evaluation of a new risk in cardiac disorders: While conventionally used in neuromuscular disorders to train muscles and cardiovascular system, h-bFES has been extended to persons suffering with chronic failure of heart, lung, and kidney, often producing positive metabolic and functional outcomes [1,6,7,8, 9,10]. Since persons in cardiac failure commonly wear implanted cardiac pace-makers (PM) or defibrillators, there is some concern regarding the potential risks of performing surface electrical stimulation, usually TENS, NMES or FES, in this potentially very large population of patients [54]. Recently, however safety measures were conclusively identified on an *in vitro* full size model mimicking the electrical characteristics of the human body to evaluate the application of electrical stimulation (ES) on permanent PM devices [55]. Various configurations with respect to energy modality, position of the stimulation electrodes and PM device models were tested. Unilateral ES application did not cause interference with PM function. However, bilateral stimulation caused switching to V00 back-up pacing due to electrical interference. In conclusion, the use of ES potentially interferes with PM therapy, especially if the electrodes are positioned bilaterally; however, unilateral ES application is safe in all tested configurations [55].

Conclusions

In conclusion, Home-based Functional Electrical Stimulation (i.e., ES, TENS, NMES and FES for DDM) is a safe and effective therapy for an expanding population of aged persons and of early aged patients with mobility impairments due to neuromuscular disorders and systemic diseases.

Acknowledgement

and by the A&C M-C Foundation for Translational Myology, Padova, Italy.

References

[1] Jones S, Man WD, et al. Neuromuscular electrical stimulation for muscle weakness in adults with advanced disease. Cochrane Database Syst Rev. 2016;10:CD009419

[2] Kern H, Carraro U. Home-based Functional Electrical Stimulation for long-term denervated human muscle: History, basics, results and perspectives of the Vienna Rehabilitation Strategy. Eur J Transl Myol. 2014b;24(1): 27-40.

[3] Kern H, Carraro U, et al. One year of home-based daily FES in complete lower motor neuron paraplegia: recovery of tetanic contractility drives the structural improvements of denervated muscle. Neurol Res. 2010;32:26-3.

[4] Kern H, Carraro U, et al. Home-based functional electrical stimulation rescues permanently denervated muscles in paraplegic patients with complete lower motor neuron lesion. Neurorehabil Neural Repair. 2010;24:709-21.

[5] Kern H, Gargiulo P, et al. To Reverse Atrophy of Human Muscles in Complete SCI Lower Motor Neuron Denervation by Home-Based Functional Electrical Stimulation. Adv Exp Med Biol. 2018;1088:585-591. doi: 10.1007/978-981-13-1435-3_27.

[6] Harris S, LeMaitre JP, et al. A randomised study of home-based electrical stimulation of the legs and conventional bicycle exercise training for patients with chronic heart failure. Eur Heart J. 2003;24: 871-878.

[7] Soska V, Dobsak P, et al. Exercise training combined with electromyostimulation in the rehabilitation of patients with chronic heart failure: A randomized trial. Biomed Pap Med Fac Univ Palacky Olomouc Czech Repub. 2014;158: 98-106.

[8] Neder JA, Sword D, et al. Home based neuromuscular electrical stimulation as a new rehabilitative strategy for severely disabled patients with chronic obstructive pulmonary disease (COPD). Thorax. 2002;57:333-337.

[9] Brüggemann AK, Mello CL, et al. Effects of Neuromuscular Electrical Stimulation During Hemodialysis on Peripheral Muscle Strength and Exercise Capacity: A Randomized Clinical Trial. Arch Phys Med Rehabil. 2017;98(5):822-831.e1.

[10] McGregor G, Ennis S, et al. Feasibility and effects of intra-dialytic low-frequency electrical muscle stimulation and cycle training: A pilot randomized controlled trial. PLoS One. 2018;13(7):e0200354. doi: 10.1371/journal.pone.0200354. eCollection 2018.

[11] Caulfield B, Prendergast A, et al. Self directed home based electrical muscle stimulation training improves exercise tolerance and strength in healthy elderly. 35th Annual International Conference of the IEEE EMBS, Osaka, Japan, 3-7 July 2013.

[12] Kern H, Barberi L, et al. Electrical stimulation counteracts muscle decline in seniors. Front Aging Neurosci. 2014 Jul 24;6:189.

[13] Zampieri S, Pietrangelo L, et al. Lifelong physical exercise delays age-associated skeletal muscle decline. J Gerontol A Biol Sci Med Sci. 2015;70: 163-173.

[14] Mayr W. Neuromuscular Electrical Stimulation for Mobility Support of Elderly. Eur J Transl Myol. 2015;25(4):263-8..

[15] Protasi F. Mitochondria Association to Calcium Release Units is Controlled by Age and Muscle Activity. Eur J Transl Myol. 2015;25(4):257-62.

[16] Sarabon N, Löfler S, et al. Mobility Test Protocols for the Elderly: A Methodological Note. Eur J Transl Myol. 2015;25(4):253-6.

[17] Cvecka J, Tirpakova V, et al. Physical Activity in Elderly. Eur J Transl Myol. 2015 Aug 25;25(4):249-52.

[18] Zampieri S, Mosole S, et al. Physical Exercise in Aging: Nine Weeks of Leg Press or Electrical Stimulation Training in 70 Years Old Sedentary Elderly People. Eur J Transl Myol 2015b;25(4):237-42.

[19] Barberi L, Scicchitano BM, Musaro A. Molecular and Cellular Mechanisms of Muscle Aging and Sarcopenia and Effects of Electrical Stimulation in Seniors. Eur J Transl Myol. 2015;25(4):231-6.

[20] Hamar D. Universal Linear Motor Driven Leg Press Dynamometer and Concept of Serial Stretch Loading. Eur J Transl Myol. 2015;25(4):215-9.

[21] Zampieri S, Mammucari C, et al. Physical exercise in aging human skeletal muscle increases mitochondrial calcium uniporter expression levels and affects mitochondria dynamics. Physiol Rep. 2016;4(24). pii: e13005.

[22] Carraro U, Kern H, et al. Recovery from muscle weakness by exercise and FES: lessons from Masters, active or sedentary seniors and SCI patients. Aging Clin Exp Res. 2017;29(4):579-90.

[23] Carraro U, Gava K, et al. Safe Antiaging Full-Body In-Bed Gym and FES for Lazy Persons: Home In-Bed Exercises for Fighting Muscle Weakness in Advanced Age. In: Rehabilitation Medicine for Elderly Patients, Masiero S, Carraro U, Eds., 2018a, pag. 43-52. ISBN 978-3-319-57405-9 ISBN 978-3-319-57406-6 (eBook).

[24] Albertin G, Kern H, et al. Two years of Functional Electrical Stimulation by large surface electrodes for denervated muscles improve skin epidermis in SCI. Eur J Transl Myol. 2018a;28(1):7373.

[25] Albertin G, Hofer C, et al. In complete SCI patients, long-term functional electrical stimulation of permanent denervated muscles increases epidermis thickness. Neurol Res. 2018b;40(4):277-282.

[26] Ravara B, Hofer C, et al. Dermal papillae flattening of thigh skin in Conus Cauda Syndrome. Eur J Transl Myol 2018 Dec 13;28(4):7914.

[27] Burgess LC, Immins T, et al. Effectiveness of neuromuscular electrical stimulation for reducing oedema: A systematic review. J Rehabil Med 2019;51:237–243.

[28] Kralj A, Bajd T. Functional Electrical Stimulation: Standing and Walking after Spinal Cord Injury. CRC Press, Inc., Boca Raton, Florida, United States of America, 1989.

[29] Andrews BJ. History of Motor FES: who were the pioneers? Proceedings of the 16thAnnual International FES Society Conference, São Paulo, Brazil, South America, 8-11 September 2011.

[30] Giaimo, CV. Electrical control of partially denervated muscles. US Patent2737183. 1956. Patents: https://patents.google.com/patent/US2737183, 7/3/18.

[31] Alon G, Sunnerhagen KS, et al. A home-based, self-administered stimulation program to improve selected hand functions of chronic stroke. NeuroRehabilitation. 2003;18:215-225.

[32] Johnston TE, Smith BT, et al. Outcomes of a home cycling program using Functional Electrical Stimulation or passive motion for children with spinal cord injury: A case series. J Spinal Cord Med. 2008;31(2):215-221.

[33] Dolbow DR, Gorgey AS, Cifu DX, et al. Feasibility of home-based functional electrical stimulation cycling: case report. Spinal Cord. 2012;50:170-171.

[34] Coste CA, Bergeron V, et al. Comparison of strategies and performance of functional electrical stimulation cycling in spinal cord injury pilots for competition in the first ever CYBATHLON. Eur J Transl Myol. 2017;27(4):7219.

[35] Fornusek C. An isokinetic functional electrical stimulation leg cycle ergometer for individuals with spinal cord injury. Doctor of Philosophy (PhD) thesis, The University of Sydney, 2005.

[36] Downey RJ, Cheng TH, et al. Switched Tracking Control of the Lower Limb During Asynchronous Neuromuscular Electrical Stimulation: Theory and Experiments. IEEE Trans Cybern. 2017;47(5):1251-1262. doi: 10.1109/TCYB.2016.2543699.

[37] Pieber K, Herceg M, et al. Optimizing stimulation parameters in functional electrical stimulation of denervated muscles: a cross-sectional study. J Neuroeng Rehabil. 2015;12:51. doi: 10.1186/s12984-015-0046-0.

[38] Metani A, Popović-Maneski L, et al. Functional electrical stimulation cycling strategies tested during preparation for the First Cybathlon Competition – a practical report from team ENS de Lyon. Eur J Transl Myol. 2017;27(4):7110.

[39] Leung KW, Tong RK, et al. The Effectiveness of Functional Electrical Stimulation (FES) in On-Off Mode for Enhancing the Cycling Performance of Team Phoenix at 2016 Cybathlon. Eur J Transl Myol. 2017;27(4):7132.

[40] Arnin J, Yamsa-Ard T, et al. Development of practical functional electrical stimulation cycling systems based on an electromyography study of the Cybathlon 2016. Eur J Transl Myol. 2017;27(4):7111.

[41] Guimarães JA, da Fonseca LO, et al. FES Bike Race preparation to Cybathlon 2016 by EMA team: a short case report. Eur J Transl Myol. 2017;27(4):7169.

[42] Berkelmans R, Woods B. Strategies and performances of Functional Electrical Stimulation Cycling using the BerkelBike with Spinal Cord Injury in a competition context (CYBATHLON). Eur J Transl Myol. 2017;27(4):7189.

[43] McDaniel J, Lombardo LM, et al. Cycle Training Using Implanted Neural Prostheses: Team Cleveland. Eur J Transl Myol. 2017;27(4):7087.

[44] Bersch I, Tesini S, et al. Functional electrical stimulation in spinal cord injury: clinical evidence versus daily practice. Artif Organs 2015;39:849–854.

[45] Kern H, Hofer C, et al. Atrophy, ultrastructural disorders, severe atrophy and degeneration of denervated human muscle in SCI and Aging. Implications for their recovery by Functional Electrical Stimulation, updated 2017. Neurol Res 39:660-666.

[46] Zampieri S, Pietrangelo L, et al. (2015) Lifelong physical exercise delays age-associated skeletal muscle decline. J Gerontol A Biol Sci Med Sci. 2015 Feb;70(2):163-73.

[47] Mosole S, Carraro U, et al. Use it or Lose It: Tonic Activity of Slow Motoneurons Promotes Their Survival and Preferentially Increases Slow Fiber-Type Groupings in Muscles of Old Lifelong Recreational Sportsmen. Eur J Transl Myol. 2016;26(4):5972.

[48] Sajer S, Guardiero GS, Scicchitano BM. Myokines in Home-Based Functional Electrical Stimulation-Induced Recovery of Skeletal Muscle in Elderly and Permanent Denervation. Eur J Transl Myol. 2018;28(4):7905.

[49] Boncompagni S, Kern H, et al. Structural differentiation of skeletal muscle fibers in the absence of innervation in humans. Proc Natl Acad Sci U S A. 104: 19339-19344.

[50] https://www.schuhfried.com/umbraco/Surface/Authent icationSurface/Login?return Url=%2Fportal

[51] Bijak M, Unger E, et al. "Abstract: MiniVStim18B: A highly configurable battery powered FES implant for long-term implantation in small animals" in "Abstracts of the 2016 Spring Padua Muscle Days, Terme Euganee, Padua, Italy, April 13–16, 2016". Eur J Transl Myol 2016;26. doi: 10.4081/ejtm.2016.5904

[52] Schmoll M, Unger E, et al. SpillOver stimulation: A novel hypertrophy model using co-contraction of the plantar-flexors to load the tibial anterior muscle in rats. PLoS One. 2018 Nov 20;13(11):e0207886.

[53] Edmunds K, Gíslason M, et al. Advanced quantitative methods in correlating sarcopenic muscle degeneration with lower extremity function biometrics and comorbidities. PLoS One (2018) 13: e0193241.

[54] Gozani SN. Fixed-site high-frequency transcutaneous electrical nerve stimulation for treatment of chronic low back and lower extremity pain. J Pain Res. 2016;9:469-479.

[55] Egger F, Hofer C, Hammerle FP, Löfler S, Nürnberg M, Fiedler L, Kriz R, Kern H, Huber K. Influence of electrical stimulation therapy on permanent pacemaker function. Wien Klin Wochenschr. 2019 Apr 25. doi: 10.1007/s00508-019-1494-5

Author's Address

Ugo Carraro
Interdepartmental Research Centre of Myology, Dept. Biomedical Sciences, University of Padova, Italy
eMail: ugo.carraro@unipd.it

FES for treatment of age related laryngeal muscle atrophy

Gugatschka M[1], Mayr W[2], Hortobagyi D[1], Jarvis J[3], Feiner M, Gerstenberger C[1]

[1]Division of Phoniatrics, ENT University Hospital Graz, Medical University Graz, Austria
[2] Center for Medical Physics and Biomedical Engineering, Medical University of Vienna, Austria
[3] School of Sport and Exercise Sciences, Liverpool John Moores University, Liverpool, United Kingdom

Abstract: *Age related atrophy of the laryngeal muscles leads a glottal gap and subsequently to a hoarse and little sustainable voice. In the present study we evaluated the effects of FES in an ovine model with a fully implantable stimulation system. Animals received training over several weeks (4 to 11 weeks). Subsequently we performed the first prospective human study applying FES superficially via electrodes attached bilaterally to the larynx. Direct stimulation of different parts of the recurrent laryngeal nerve in animals lead to significant increases of the muscle fibre diameters and muscle volumes. In contrast to this, we could not identify significant parameters regarding objective vocal parameters in group of elderly women.*

Keywords: *aged voice, laryngeal sarcopenia, FES*

Introduction

Like all muscles in the human body, also the laryngeal muscles undergo age related changes, such as atrophy. This process diminishes the volume of the muscle that builds up the vocal fold (VF), leading to an incomplete closure during voice production (aka. phonation). This leads to a hoarse and little sustainable voice and separates affected individuals from social life.

In the reported study, we investigated the effects of FES in animal studies, as well as in the first prospective human trial in aged women. Our approach is based on the 'bodybuilder approach', which means that we wanted to rejuvenate age related VF atrophy by muscular hypertrophy triggered by resistance training.

Material and Methods

(a) For the animal trials aged sheep were employed as a model, as their larynx is similar in size and dimensions to the human larynx. During several trials we changed position of the stimulation electrode, as well as different stimulation patterns. Radio-controlled implants were sutured under the skin and operated via infrared control. Training periods reached from 4 to eleven weeks.(1,2) Outcome parameters were manifold and included changes of the molecular (by qPCR), cellular (immune-histology) and macroscopic level (3D reconstructions based on micro CT-scans(3)).

(b) For the human trial volunteers were gathered by a newspaper announcement. More than hundred women reporting age related vocal symptoms entered the screening phase of the study. After applying inclusion criteria, no more than 17 were left and concluded all study procedures. These consisted of superficial FES over the course of eight weeks. Outcome parameters comprised voice related parameters (loudness, clarity of voice, duration of maximum phonation) as well as endoscopical features (shape of VF, size of glottal gap).

Results

(a) animal trials: In a first trial the tip of the electrode was fixed to the recurrent laryngeal nerve which supplies opening and closing fibres to the laryngeal muscles. After one daily training session (tetanic stimulation for two minutes) we identified a significant increase of mean fibre diameter when comparing stimulated to unstimulated side. No signs of damage (fibrosis) were noticed.(2) In a subsequent trail only closing fibres were stimulated over a prolonged time of eleven weeks. Outcome parameters comprised 3D reconstructions of the muscles based on micro-CT scans. We found significantly upregulated volumes when comparing right (stimulated) and left (unstimulated) VF. Again, no signs of muscle fibre damage or fibre type shifts were noticed.(1)

(b) Patients were allocated to two different groups, where group A received full effective training over eight weeks and group B received four weeks of subthreshold stimulation, followed by four weeks of effective training just like group A. All participants performed homebased training five days a week.

Interestingly both groups improved over the course of the eight weeks when measured by subjective (self-evaluated) voice parameters (VHI-12). However, neither group was superior. When regarding the objective parameters no statistically significant differences (inter-/ as well as intragroup differences) were observed over the course of time.

Discussion

The percentage of elderly people has been steadily increasing during the last decades in most Western societies and large parts of Asia. This is accompanied by a steady increase of age-related diseases. These changes do not spare the larynx. Although the term presbylarynx denotes the typical age-related morphological changes observed, presbyphonia delineates age-related voice changes that comprise a hoarse and breathy voice and significantly reduced vocal capacity. Implications of these

vocal changes may lead to a reduced quality of life with social withdrawal. Up to 30% of elderly people complain about some disorder of the voice, and most of these individuals have a chronic problem.

FES has proven to be a possible upcoming treatment option for a number of laryngeal disorders, such as VF paralysis and spasmodic dysphonia. In this presentation we examined possible effects on age related laryngeal sarcopenia. We found significant increases of both muscle fibre diameters and muscle volume in an ovine model using a fully implantable stimulation device. Notably we did not detect a significant fibre type switch, nor signs of muscle fibre damage. There are, however, shortcomings of our study. The volumetric findings need to be tested functionally to study the effects on vibration characteristics and vocal outcome by ex vivo phonation models.

Superficial FES in humans did not reveal significant changes when it comes to vocal parameters. Our study was the first to investigate the effects of FES in aged laryngeal muscles, whereas there is a smaller amount of literature studying the effects of FES in laryngeal palsy reporting insecure results.

Conclusions

While a direct stimulation of the recurrent laryngeal nerve lead to significant increases of the vocalis muscle in the ovine model, we could not observe vocal changes following an eight weeks trails pursued in aged women. Further studies need to be employed to identify optimized training patterns.

References

(1) Gugatschka M, Jarvis JC, Perkins JD, Bubalo V, Wiederstein-Grasser I, Lanmuller H, et al. Functional Electrical Stimulation Leads to Increased Volume of the Aged Thyroarytenoid Muscle. Laryngoscope 2018 Dec;128(12):2852-2857.

(2) Karbiener M, Jarvis JC, Perkins JD, Lanmuller H, Schmoll M, Rode HS, et al. Reversing Age Related Changes of the Laryngeal Muscles by Chronic Electrostimulation of the Recurrent Laryngeal Nerve. PLoS One 2016 Nov 28;11(11):e0167367.

(3) Gerstenberger C, Dollinger M, Kniesburges S, Bubalo V, Karbiener M, Schlager H, et al. Phonation Analysis Combined with 3D Reconstruction of the Thyroarytenoid Muscle in Aged Ovine Ex Vivo Larynx Models. J Voice 2017 Sep 27.

Author's Address

Assoc. Prof. Dr. Markus Gugatschka
Division of Phoniatrics, ENT University hospital Graz, Medical University Graz, Austria
e-mail: markus.gugatschka@medunigraz.at
https://forschung.medunigraz.at/fodok/suchen.person_ueb ersicht?sprache_in=de&menue_id_in=101&id_in=11346 59

Treatment of Central Core Disease with Functional Electrical Stimulation: a Case Report.

Iodice P[1,2], Boncompagni S[1], Pietrangelo L[1], Galli L[3], Pierantozzi E[3], Rossi D[3], Fusella A[1], Caulo M[4], Kern H[5], Sorrentino V[3], Protasi F[1,6]

[1]CeSI-Met - Center for Research on Ageing and Translational Medicine, University G. d'Annunzio of Chieti, Italy

[2]CETAPS - EA3832, University of Rouen Normandy, France

[3]Department of Molecular and Developmental Medicine, University of Siena & Azienda Ospedaliera Universitaria Senese, Italy

[4]DNICS, Department of Neuroscience, Imaging, and Clinical Sciences, University G. d'Annunzio of Chieti, Italy

[5]Ludwig Boltzmann Institute of Electrical Stimulation and Physical Rehabilitation, Vienna, Austria.

[6]Department of Medicine and Aging Science, University G. d'Annunzio of Chieti, Italy.

Abstract: Central Core Disease (CCD) is a congenital myopathy characterized by presence of amorphous central areas (or cores) lacking glycolytic/oxidative enzymes and mitochondria in skeletal muscle fibers. As no treatments are available for CCD, currently management of patients is essentially based on physiotherapy approaches. Here we tested the efficacy of Functional electrical stimulation (FES) in counteracting muscle loss and improve function in the lower extremities of a 55-year-old female patient which was diagnosed with CCD at the age of 44. The patient was treated with FES for 26 months and subjected before, during, and after training to a series of functional and structural assessments: measurement of maximum isometric force of leg extensor muscles, magnetic resonance imaging, a complete set of functional tests to assess mobility in activities of daily living, and analysis of muscle biopsies by histology electron microscopy. All results point to an improvement of muscle structure and function induced by FES suggesting that this approach could be considered as an additional supportive measure to maintain/improve muscle function and reduce muscle loss in CCD patients.

Introduction

Central core disease (CCD), first described in 1956 [1], is one of the most common human congenital myopathies characterized by hypotonia and proximal muscle weakness [2]. The typical form of dominantly inherited CCD is usually associated with a moderate degree of disability and carries an overall favorable prognosis, although clinical variability is often observed even within the same family [3-5]. Orthopedic complications are frequent in CCD and comprise congenital dislocation of the hips [6], scoliosis [7], and foot deformities [8].

An accurate incidence and prevalence of CCD are unknown [9]. By definition, CCD is considered a rare disease by the Office of Rare Disease, implying that it affects fewer than 5 people in 10,000 in the EU. Diagnosis of CCD is confirmed by histological examination of muscle biopsies showing amorphous central areas (or *cores*) lacking glycolytic/oxidative enzymes and mitochondria [3]. About 90% of CCD cases are linked to mutations in the RYR1 gene [10], encoding for a protein of about 550 KDa that forms the sarcoplasmic reticulum (SR) Ca^{2+} release channel of skeletal muscle, i.e. the

ryanodine receptor type-1 (RyR1). No treatment is currently available for CCD and management of patients is essentially supportive based on a multidisciplinary approach. Usually, orthopedic complications limit the ability of CCD adult patient to perform physical exercise [2].

Material and Methods

In the present study, we tested the efficacy of 26 months of FES training in counteracting muscle loss and improving structure and function in the lower extremities of a 55-year-old female patient diagnosed with CCD at the age of 44.

- *Genetic Screening.* Mutation screening by conventional Sanger sequencing on specific regions of the RYR1 gene was performed in all family members for whom DNA was available (Fig. 1). In detail, primers were designed using Primer3software (http://frodo.wi.mit.edu/primer3) to amplify all RYR1 exons. Genomic DNA was extracted from peripheral blood leucocytes by standard procedures. Amplified DNA fragments were directly sequenced on an ABI3500 Genetic Analyzer (Applied Biosystems), using the Big-Dye Terminator v3.1 kit and analyzed with Sequencer 5.0 software (Gene Codes

Corporation). DNA mutation numbering was based on cDNA reference sequence (NM_000540.2), taking nucleotide +1 as the A of the ATG translation initiation codon.

- *FES protocol.* Stimulators and electrodes used in this study derives from devises developed in the EU project RISE [11-12]. The patient was provided with stimulators and electrodes, and after appropriate training and instructions, was able to perform FES at home. Two pairs of large electrodes, each having an area of 200 cm^2, were strapped to the anterior surface of the thighs in proximal and distal positions. Twitch contractions were elicited by biphasic rectangular current pulses lasting 100 to 150 ms and up to ±200 mA amplitude, representing an impulse energy up to ~2 Joules, to recruit fibers throughout the Quadriceps Femoris muscles. The long duration of the impulses needed for stimulation precluded the use of frequencies that would elicit tetanic contractions: training was initiated at 2 Hz, delivered for 15 min/day (series of 4 s on, 2 s off), 3 days/week. During the first/second month, muscle excitability progressively increased allowing an increase of 2 Hz stimulation, 2 × 10 min stimulation (2 min rest). As training proceeded, excitability of the muscle continued to increase, and from the third month onwards, training time stimulation were increased to 3 × 10 min (2 min rest).

- *Muscle structure and function.* Muscle structure and ultra-structure was assessed by Magnetic Resonance Imaging (MRI), histology, and Electron Microscopy (EM), whereas muscle function was assessed by measurements of maximum isometric force (MIF) and activities of daily living (ADL). The effect of FES on muscle structure and function before the beginning of the 26 months of FES stimulation (T0), and at 3 different time points: T1, 5 months; T2, 14 months; T3, 26 months.

Results

- *Genetic Screening.* Sequence analysis of the RYR1 gene identified a missense mutation (c.7354C>T) in exon 46 resulting in the substitution of the Arg in position 2452 with a Trp (p.R2452W) and a duplication (c.12853_12864dup12, p.Thr4285_Thr4288dup) in exon 91, involving 4 amino acid residues (Thr,

Ala, Ala, Thr, p.Thr4285_Thr4288dup) in exon 91 was also observed (Fig. 1).
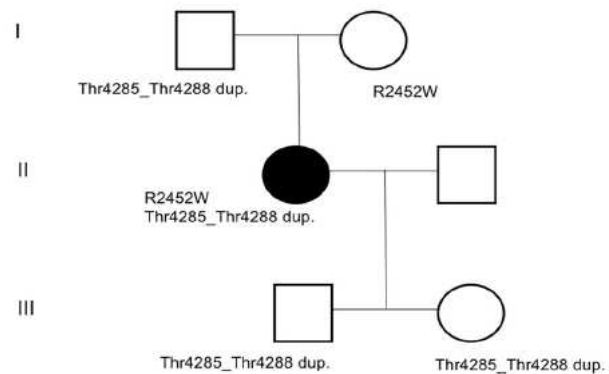
Figure 1. Gentetic family pedigree. The black filled symbol represents the affected proband. Sequence analysis of the proband RYR1 gene identified a missense mutation (c.7354C>T) in exon 46, resulting in the substitution of an Arg in position 2452 with a Trp (p.R2452W), and a duplication c.12853_12864dupACGGCGGCCACG involving 4 amino acid residues (Thr, Ala, Ala, Thr, p.Thr4285_Thr4288dup) in exon 91. The genotype of family members tested is reported below each symbol.

- *Effect of FES on muscle structure.* At the EM level 11 to 15 fibers were analysed (Fig. 2). Fibers presented with different appearances: a) *apparently normal fibers,* which displayed a normal cross striation pattern of the skeletal muscle fibers (Fig. 2 A); b) fibers with *unstructured cores* (Fig. 2 B), extended areas in which myofibrils were disrupted and replaced by amorphous cytoplasmic material; and c) fibers with *contracture cores* (Fig. 2 C), regions with laterally-packed and/or over-contracted myofibrils. In *unstructured cores,* mitochondria were often damaged (Fig. 2 B), while in *contracture cores* both mitochondria and SR were scarce or completely missing (Fig. 2 C).

Before FES training (T0), only 18% of total skeletal fibers analysed (n=11) displayed the normal cross striation pattern, with the remaining 82% presenting structural abnormalities, i.e. either *unstructured* or *contracture cores* (Table in Fig. 2). In fibers analysed after FES training (n=15), while recovery was definitely not complete, the percentage of cores was significantly reduced from 82 to 53% (Table in Fig. 2), accompanied by a parallel increase (from 18 to 47%) in the percentage of fibers with a fairly normal appearance (Table in Fig. 2).

- *Effect of FES on muscle function.* Measurements of MIF in leg extensor muscles was measured before (T0), and after 5 (T1), 14 (T2), and 26 (T3) months of FES treatment (Fig. 3 A and B): MIF

increased in both legs (Fig. 3 B), beginning at 5 months (T1, 8%) of treatment and continuing during the entire length of the study (9% at T2, and 11% at T3).

- Effect of FES on Activities of Daily Living (ADL). A complete set of functional tests was used to assess mobility in activities of daily living (ADL): Timed Up and Go Test (TUGT), 10m Self Paced Walk Test (SPWT) and Short Physical Performance Battery (SPPB) as in Kern et al. [12]. The results of these tests were slightly contradictory, as at T1 and T2 the results collected point to a worsening of the patient's performance, while a possible improvement was detected at T3: a) shorter total times in TUGT test (-3.2%); b) an improvement in 10m walking performance, time needed to cover 10 m (speed) and number of steps during SPWT decreased (-5.1% and -4.2%, respectively); c) higher score obtained in the SPPB (6 vs. 8 points). Taken together, these data suggest a slight improvement of the patient's ADL at T3, but the reason for the partially negative

outcome at T1 and T2 is unclear, and will be further discussed below.

	A	B	C
	Apparently normal fibers	**Fibers with** *unstructured cores*	**Fibers with** *contracture cores*
T0 (11 fibers)	18%	46%	36%
T2 (15 fibers)	47%*	27%	26%
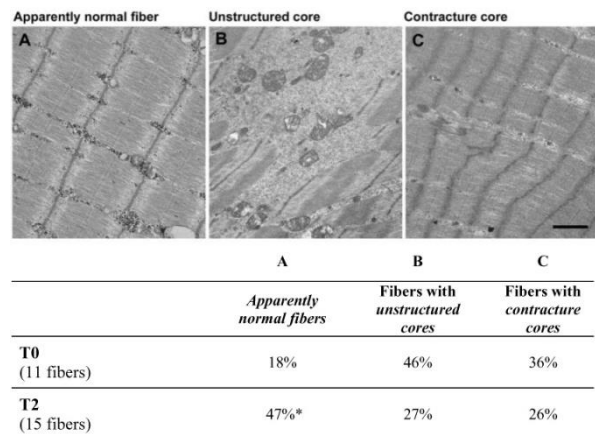
Figure 2. Appearance of skeletal fibers in electron microscopy (EM). Fibers were classified for the quantitative analysis in different categories: A) *apparently normal fibers* (panel A) with a typical pale-dark striation; B) fibers with *unstructured cores* (panel B), presenting extended areas in which myofibrils were disrupted and replaced by amorphous cytoplasmic material; C) fibers with *contracture cores* (panel C) with extended regions with laterally-packed and over-contracted myofibrils. Scale bar: 1 µm. Percentage, before (T0) and after 14 months (T2) were respectively reported in column A, B and C. Data are expressed as % of total fibers analyzed.
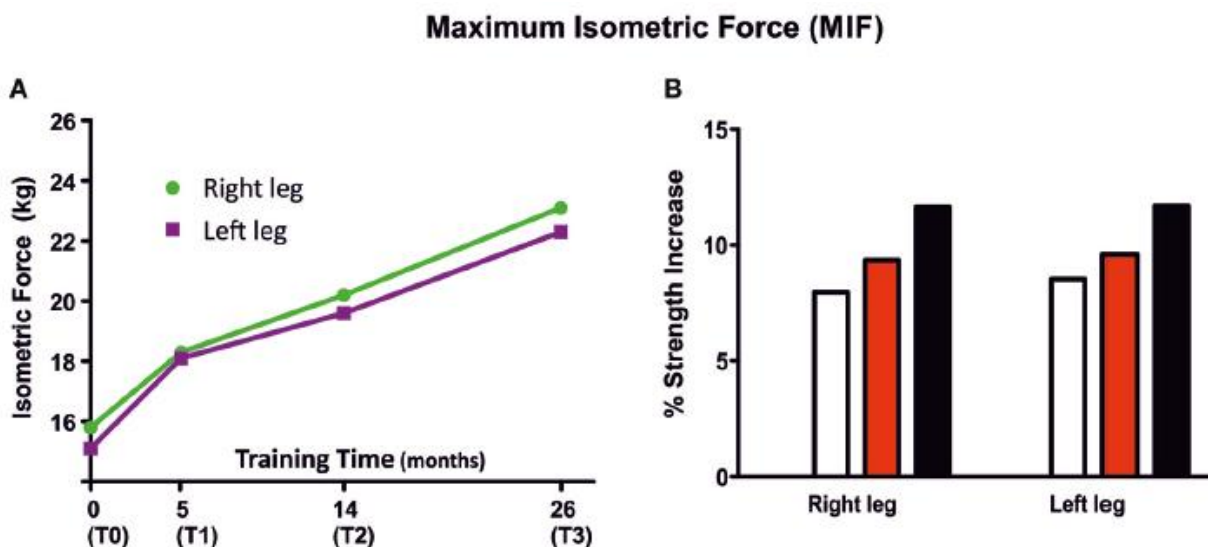
Figure 3. Maximum Isometric Force (MRI). A) Measurements of MIF based on leg extension movement before (T0) and after 5 (T1), 14 (T2), and 26 (T3) months of FES training. B) Variations in MIF expressed as percentage, where values from T0 were taken as 0%.

Discussion

The case report presented in this study represents an attempt to find possible strategies for CCD patients to exercise muscles in the lower extremities. We tested the possibility of using FES to improve muscle function in a 55-year-old female patient diagnosed with CCD at the age of

44 by providing stimulators and electrodes to the patient at home (home-based FES)[13]. Results of this study are moderately encouraging, even if we should point out that there was no real evidence of improvement at T1 and T2, but rather a general worsening of performance in the various tasks. The reason for this partial negative outcome is unclear. One of the possible explanations is the

low back-pain lamented by the patient for several months during the trial, a problem that had temporally caused a significant reduction in her daily walking activities. Though, the slight improvement of the patient's ADL at T3 was encouraging, as ADL tests are considered in literature as a parameter to score the degree of independence and an indirect index of muscle strength [12-15].

Overall, the study suggests that FES could be considered as an additional supportive measure to maintain/improve muscle function in CCD patients.

References

[1] Magee, K.R., Shy, G.M. A new congenital non-progressive myopathy. *Brain,* vol. 79, pp. 610–621, 1956.
[2] Jungbluth, H. Multi-minicore Disease. *Orphanet J Rare Dis*, vol. 2, p. 31, 2007.
[3] Dubowitz, V., Roy, S: Central core disease of muscle: clinical, histochemical and electron microscopic studies of an affected mother and child. *Brain,* vol. 93, pp.133–146, 1970.
[4] Bethlem, J., van Wijngaarden, G.K., et al: Observations on central core disease. *J Neurol Sci*, vol. 14, pp. 293-299, 1971.
[5] Patterson, V.H., Hill, T.R., et al: Central core disease: clinical and pathological evidence of progression within a family. *Brain,* vol. 102, pp. 81–94, 1979.
[6] Ramsey, P.L., Hensinger, R.N: Congenital dislocation of the hip associated with central core disease. *J Bone Joint Surg Am*, vol. 57, pp. 648–651, 1975.
[7] Merlini, L., Mattutini, et al: Non-progressive central core disease with severe congenital scoliosis: a case report. *Dev Med Child Neurol,* vol. 29, pp.106–9, 1987.
[8] Gamble, J.G., Rinsky, L.A., et al: Orthopaedic aspects of central core disease. *J Bone Joint Surg Am*, vol. 70, pp. 1061–1066, 1988.
[9] Jungbluth, H: Central core disease. *Orphanet J Rare Dis.,* vol. 15, pp 2-25, 2007.
[10] Robinson, R., Carpenter, D., et al.: Mutations in *RYR1* in malignant hyperthermia and central core disease. *Hum Mutat*, vol. 27, pp. 977–989, 2006.
[11] Modlin, M., Forstner, C., et al.: Electrical Stimulation of Denervated Muscles: First Results of a Clinical Study. *Artif Organs,* vol. 29, pp. 203–206, 2005.
[12] Kern, H., Carraro, U., et al.: Home-Based Functional Electrical Stimulation Rescues Permanently Denervated Muscles in Paraplegic Patients With Complete Lower Motor Neuron Lesion. *Neurorehabil Neural Repair*, vol. 24, pp. 709–721, 2010.
[13] Kern, H., Barberi, L., et al.: Electrical stimulation counteracts muscle decline in seniors. *Front Aging Neurosci,* vol. 6, p.189. 2014.
[14] Corrigan, D., Bohannon, R.W: Relationship between knee extension force and stand-upper formance in community-dwelling elderly women. *Arch Phys Med Rehabil,* vol. 82, pp.1666–1672, 2001.
[15] Freiberger, E., Blank, W.A, et al: Effects of a complex intervention on fall risk in the general practitioner setting:a Cluster randomized controlled trial. *Clin Interv Aging,* vol. 8, pp.1079–1088, 2013.

Author's Address

Iodice Pierpaolo
CeSI-Met - Center for Research on Ageing and Translational Medicine, University G. d'Annunzio of Chieti, Italy, CETAPS - EA 3832, University of Rouen Normandy, France.
pierpaolo.iodice@univ-rouen.fr

Boncompagni Simona
CeSI-Met - Center for Research on Ageing and Translational Medicine, University G. d'Annunzio of Chieti, Italy.
simona.boncompagni@unich.it

Pietrangelo Laura
CeSI-Met - Center for Research on Ageing and Translational Medicine, University G. d'Annunzio of Chieti, Italy.
laura.pietrangelo@unich.it

Galli Lucia
Department of Molecular and Developmental Medicine, University of Siena & Azienda Ospedaliera Universitaria Senese, Italy.
lucia.galli@unisi.it
Pierantozzi Enrico

Selective surface stimulation in unilateral vocal fold paralysis (UVFP)

Schneider-Stickler B[1], Leonhard M[1], Krenn M[2,3], Mayr W[2]

[1]Department of Otorhinolaryngology, Medical University of Vienna, Austria
[2]Center for Medical Physics and Biomedical Engineering, Medical University of Vienna, Austria
[3]Center for Neuroscience and Neurological Recovery, University of Mississippi, Jackson, MS, USA

Abstract: *Unilateral vocal fold paralysis (UVFP) is a rare disease and as such its diagnosis and treatment procedures are little or not standardized. Until now, surface electrical stimulation of the neck region corresponding to the thyroarytenoid (TA) muscle position has been evaluated in preliminary studies with a small sample size. It is the aim of our trial to provide systematic data on this approach.*

Evaluation under videolaryngoscopy of the stimulation parameters causing visually detectable medialization of the ailing vocal fold (VF) at rest and during phonation in patients suffering from UVFP for less than 3 months at time of examination.

So far, we enrolled 16 patients diagnosed with UVFP. Medialization of both the ailing and the healthy VF was observed with stimulations elicited at 1 Hz, with pulse duration between 50 and 250 msec, and amplitude between 3 and 7 mA. In this parameter range no adverse event such as increased swallowing reflex, platysma, or coughing was observed.

Surface electrostimulation of the neck region corresponding to the thyroarytenoid (TA) muscle position showed promising results. Our study aims to reach a minimum sample size of 30 subjects in order to confirm these preliminary data.

Keywords: *Vocal fold paralysis, muscle denervation, direct muscle stimulation, functional electrical stimulation, FES*

Author's Address

Berit Schneider-Stickler
Medical University of Vienna
berit.schneider-stickler@meduniwien.ac.at
https://www.meduniwien.ac.at/web/en/

Long-term home-based Surface Electrostimulation is useful to prevent atrophy in denervated Facial Muscles

Volk GF[1,2], Thümmel M[3], Mothes O[1,3], Arnold D[4], Thielker J[1,2], Denzler J[3], Mastryukova, V[1,2], Mayr W[5], Guntinas-Lichius O[1,2]

[1]ENT-Department, Jena University Hospital, Jena, Germany
[2]Facial Nerve Center Jena, Jena University Hospital, Jena, Germany
[3]Computer Vision Group, Friedrich-Schiller-University Jena, Germany
[4]Institute of Systematic Zoology and Evolutionary Biology with Phyletic Museum, Friedrich-Schiller-University Jena, Jena, Germany
[5]Medical University Vienna, Center for Medical Physics and Biomedical Engineering, General Hospital Vienna, Vienna, Austria.

*Abstract: 5 patients with facial paralysis received a home-based electrostimulation (ES) with charge-balanced biphasic triangular impulses 3x5min twice a day. Before the first ES, and every 4 weeks during the ES, all patients underwent regular needle electromyography (EMG), ultrasound and 3D-video measurements. Additionally, stimulation settings, patients' home-stimulation diaries and parameters were recorded. No patient reported relevant adverse events linked to ES. Training with optimized electrode positioning was associated with stable and specific zygomaticus muscle activation, accompanied by a reduction of the necessary minimum pulse duration from 250 to 70ms per phase within 16 weeks. Even before reinnervation, objective 3D-videos, sonography, MRI, and patient-related parameters (FDI, FaCE) improved significantly compared to the pre-stimulation situation. Preliminary results suggest that ES home-based training is beneficial for patients with denervated facial muscles in reducing muscle atrophy, maintaining muscle function and improving facial symmetry. A lack of relevant adverse events shows that such ES is safe. The patients showed excellent compliance with the protocol and rated the stimulation easy and effective.
Ach*

Introduction

Often, skull base or petrosal bone tumors and surgeries cause facial nerve paralysis and consequently result in neuromuscular atrophy of facial muscles. Because of the distance between the lesion site and the denervated muscles, reinnervating axons need several months to reach the muscles. To reduce or even prevent the muscle atrophy, electrostimulation (ES) could have a beneficial effect for facial muscles (1, 2) similar to limb muscles (3). The aim of the present study is to evaluate the effects of transcutaneous facial muscle stimulation on the denervated zygomaticus muscle.

Material and Methods

As far as May 2019, we enrolled 5 patients (4 female) with facial paralysis (duration between 1 month and 16 years). The affected hemiface was the right side in 3 and the left side in 2 cases. The etiology of the facial paralysis, confirmed by needle electromyography (EMG), was in all cases iatrogenic, i.e. following vestibular schwannoma surgery. Before the first ES, and every 4 weeks during the ES, all patients underwent regular needle EMG, ultrasound (4), MRI (5) and 3D-video measurements (6). The stimulation parameters and patients home-stimulation diaries were recorded. Additionally, all patients completed the forms for Facial Disability Index (FDI) and the Facial clinometric evaluation scale (FaCE). Stimulation settings and parameters were recorded and both objective and subjective outcome measures ware used for the result analysis.

The test stimulation was performed every four weeks with the STMISOLA; BIOPAC Systems Inc. Two surface electrodes (60x40mm Flextrode Plus; Krauth+Timmermann) were placed as close as possible to the lip corner on the ailing hemiface. The amplitude required to elicit a selective zygomaticus muscle contraction on the ailing hemiface was investigated at the following pulse durations: 1000, 500, 250, 100, 50, 25, 15, 10, 5 and 1ms both with triangular and rectangular waveform. Burst frequency was constantly kept at 1Hz.

The most effective combination of pulse duration and intensity was chosen based on the results obtained with the STMISOLA and the visual evaluation of the patient's response. Once the parameters were selected and programmed on the Stimulette r2x (Dr. Schuhfried GmbH, Vienna), the patient was asked to perform 5 min stimulation in order to exclude potential muscle fatigue. The stimulation was given in charge-balanced biphasic triangular impulses with fixed build-up time (5s); build-up pause (1s); and training duration of 5 min.

To quantify the effect of such a 5 min training, at some follow-up days, 3D-videos were not only recorded before, but also after this 5 min of ES training. After fine-registration between the 3D scan before and after the ES, the point-wise distances to the closest points between both 3D scans are calculated and coloured (Figure 1).

Blue means 0 mm distance and red means 3 mm distance. White and black squares indicate facial landmarks (black = before ES; white = after ES).

At home, the training was performed 3x5min with 5 min pause between in the morning and in the evening every day till the next follow-up after 4 weeks. All patients recorded every stimulation in a dairy.
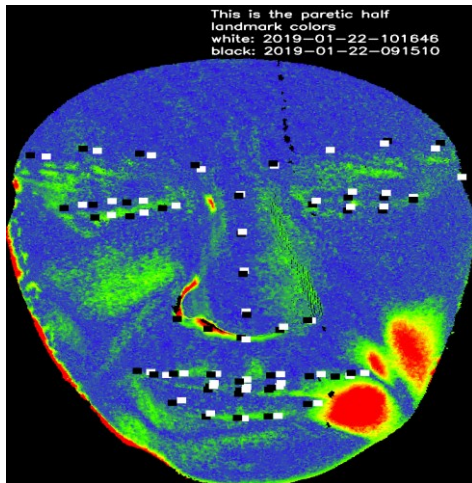
Figure 1: The changes of the surface of the face due to 5 minutes of electrostimulation are visualised as "Heatmap". Example of one patient with denervated facial muscles on the left side. After fine-registration between the 3D scan before and after the ES, the point-wise distances to the closest points between both 3D scans are calculated and colored. Blue means 0 mm distance and red means 3 mm distance. White and black squares indicate facial landmarks (black = before ES; white = after ES). The red area corresponds to the activated zygomatic muscle. So a positive increase of muscle tension even after the ES can be detected.

Results

No patient reported relevant adverse events linked to ES home-based-training. Training with optimized electrode positioning associated with stable and specific zygomaticus muscle activation, accompanied by a reduction of the necessary minimum pulse duration from 250 to 70ms per phase within 16 weeks (Figure 2). Even before reinnervation, objective parameters (3D-videos (Figure 1), sonography, MRI) and subjective parameters (FDI, FaCE) improved significantly compared to the pre-stimulation situation.

The changes of the surface of the face recorded by 3D-videoas were visualised by this "Heatmap". In Figure 1, the example of one patient is provided: The Patient had denervated facial muscles on the left side. After fine registration of the 3D scans before and after ES, the corner of the paralytic left corner of the mouth moved 5.3 mm latero-cranial. The red area with changes from at least 3 mm corresponds to the activated zygomatic muscle. So a positive increase of muscle tension even after the ES can be detected.

Conclusions

ES home-based training is beneficial for patients with denervated facial muscles in reducing muscle atrophy, maintaining muscle function and improving facial symmetry. The accurate selection of the stimulation parameters and positioning of the electrode is necessary to ensure the training specifically for the selected facial muscle. A lack of relevant adverse events shows that such ES is safe. The patients showed excellent compliance with the protocol and rated the stimulation easy and effective.
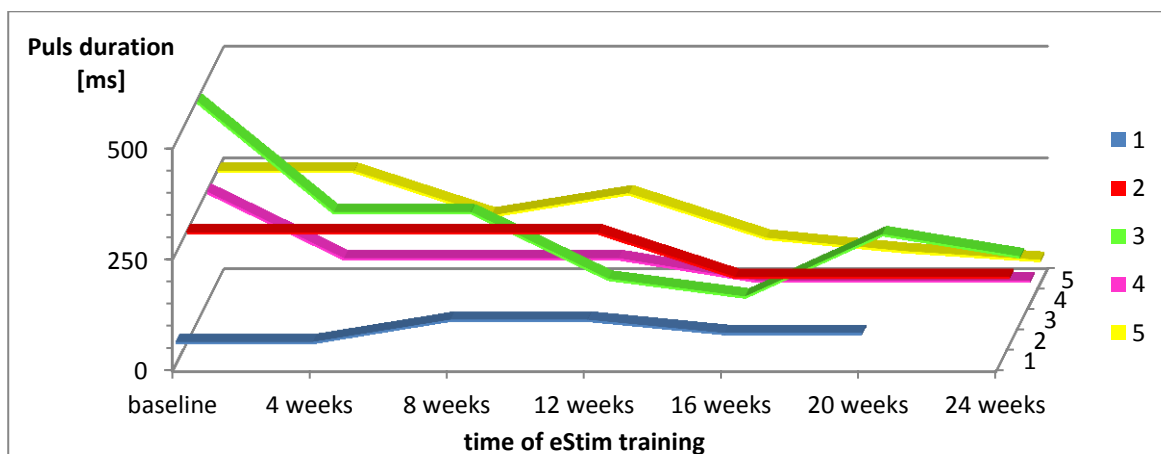
Figure 2: Change of pulse duration used for daily electrostimulation (ES) home training over the first 24 weeks. The different colour coded graphs show the values of each single patient. A reduction of the pulse duration needed is seen over time in most patients.

Funding and Acknowledgement

References

[1] J. Gittins, K. Martin, J. Sheldrick, A. Reddy, and L. Thean, "Electrical stimulation as a therapeutic option to improve eyelid function in chronic facial nerve disorders," Investig. Ophthalmol. Vis. Sci., vol. 40, no. 3, pp. 547–554, 1999.

[2] A.K. Fargher & S.E. Coulson, "Effectiveness of electrical stimulation for rehabilitation of facial nerve paralysis" Physical Therapy Reviews, DOI: 10.1080/10833196.2017.1368967, 2017

[3] W. Mayr, C. Hofer, M. Bijak, D. Rafolt, E. Unger, M. Reichel, S. Sauermann, H. Lanmueller, and H. Kern, "Functional Electrical Stimulation (FES) of Denervated Muscles : Existing and Prospective Technological Solutions," Eur. J. Transl. Myol., vol. 12, no. 1, pp. 1–4, 2002.

[4] G.F. Volk, M. Sauer, M. Pohlmann, O. Guntinas-Lichius, "Reference values for dynamic facial muscle ultrasonography in adults" Muscle Nerve. 2014 Sep;50(3):348-57. doi: 10.1002/mus.24204

[5] G.F. Volk, I. Karamyan, C.M. Klingner, J.R. Reichenbach, O. Guntinas-Lichius O. „Quantitative magnetic resonance imaging volumetry of facial muscles in healthy patients with facial palsy" Plast Reconstr Surg Glob Open. 2014 Jul 9;2(6):e173.

[6] M. Thümmel, O. Mothes, G F. Volk, O. Guntinas-Lichius, J. Denzler. (2019). Analyzing the Progress in Therapy of Facial Paralysis using 3D Face Scans. Manuscript in preparation.

Author's Address

Priv.-Doz. Dr. med. habil. Gerd Fabian Volk
Klinik und Poliklinik für Hals-, Nasen- und Ohrenheilkunde, Institut für Phoniatrie und Pädaudiologie
Universitätsklinikum Jena
Haus A, Am Klinikum 1
D-07747 Jena
Tel. +49-3641 9 329396, Telefax: +49-3641 9 329306
Email: fabian.volk@med.uni-jena.de

Obstetric brachial plexus injury (OBPI): Is functional electrical stimulation (FES) a viable intervention option?

Alon G,

University of Maryland, School of Medicine, USA

Abstract: *An estimated 35,000 newborns will acquire obstetric brachial plexus injury (OBPI) each year in the USA. Despite major advancements in early neurosurgical procedures resulting in peripheral re-innervation, the recovery process typically takes several years. The inability to activate the upper extremity (UE) muscles during this period results in severe atrophy, joints contracture, diminished peripheral blood flow, limbs length discrepancy, all contributing to impaired development of UE use during uni-and bilateral daily functions. Functional electrical stimulation (FES) augmentation of recovery after damage to the brain is document extensively in peer-reviewed rehabilitation literature. In contrast, FES is seldomly considered a treatment option in OBPI. The primary reason is that in the absence of peripheral innervation, the efficacy of FES has been traditionally questioned. However, knowing that the majority of toddlers who underwent neurosurgical procedures will recover varying degrees of innervation, raise the question can FES help recover muscle strength of the re-innervated yet very weak muscles? This presentation focus on determining who is a candidate for FES training and how to utilize FES to enhance the recovery and functional use of the paretic UE of children with OBPI.*

Keywords: *OBPI, FES, Upper extremity*

Introduction

Among newborns in the USA, the annual incidence of obstetric brachial plexus injury (OBPI) is about 0.9% resulting in estimated 35,000 newborns with paralysis/paresis on the upper extremity (UE) [1]. For some babies full or almost full recovery of UE function is expected [2]. But for 20-30%, the normal development is impaired as the paretic UE undergo varying degrees of muscle atrophy, loss of joint range of motion in the gleno-humeral, "scapula-thoracic", elbow, and wrist joints, and limited use of the UE in daily functions [3]. Functional electrical stimulation (FES) is seldomly considered in the management of OBPI [5]. One reason for not considering FES is the uncertainty of sufficient innervation of the atrophied, paretic muscles. This paper presents a novel clinical approach to screen babies and children with OBPI and develop a treatment plan for those who are candidate for FES intervention.

Material and Methods

Screening:

The stimulation parameters needed for screening include symmetric biphasic waveform pulse generator (FES); phase/pulse duration of 300-400 microsec; 1-2 pulses per sec; and peak current intensity of no less than 100 mA. The electrodes are placed on each target muscle group. An example for the wrist-finger extensors is illustrated in figure 1.)

Figure 1: Placement of electrodes to activate wrist extensors

Testing of UE joints mobility:

Limited active and particularly passive range of motion (PROM) are the primary impairments that prevent children with OBPI from using the UE [5][6]. Specifically, the limited PROM of the gleno-humeral, elbow, and wrist joints must be documented at initial screening. One exception to hypomobility is the hypermobility of the "scapula-thoracic" joint resulting in the typical "winging scapula" (figure 2)

Figure 2: "Winging Scapula"

Specifically, the unstable scapula protrudes, elevates, and internally rotates. The cause is damage to the subscapular

and/or long thoracic nerves. The more unstable the scapula the less the chance of using the UE during reaching and over-head daily functions.

Intervention:

Once the determination is made that the child is likely to benefit from FES, it is incorporated to enhance the recovery of muscle strength and motor control within the framework of normal development. For treatment purposes, the pulse rate is increased to induce tetanic contraction. Clinical experience suggests that unlike adults, in very young children (1-6 years) only 5-10 pulses per sec may induce tetanic contraction. Accordingly, it is the clinical observation that determine the specific pulse rate needed to induce tetanic contraction in each muscle. In general, the pulse rate should be kept low to minimize the chance of muscle fatigue. Example of activities can be seen in figure 3.

Figure 3: Examples of activities

However, without restoring joints range of motion, FES is not likely to benefit children with OBPI. A critical component of the intervention is therefore to provide specific physical exercises to restore or maintain mobility of the gleno-humeral, elbow and if needed wrist joints' range of motion. The hyper mobility of the "scapula-thoracic" joint as seen in figure 2, cannot be improved by exercises or FES. FES cannot induce contraction of the subscapularis and serratus anterior because they are covered by the scapula. At best, FES can activate the rhomboids and middle-lower trapezius (figure 2.) and minimize scapular upward rotation/elevation during reaching activities. Firm stabilization of the markedly unstable scapula will most likely require surgery [7].

Documented Results

The first and only reported clinical data using FES to manage OBPI was published in 2016 [4]. The author compared a group that received 3 months of structured weight bearing exercise program to a group that received the same program combined with neuromuscular electrical stimulation. Mallet grading system and dual-energy x-ray absorptiometry were used to evaluate shoulder function and bone mineral density (BMD) respectively. Adding the stimulation program resulted in significantly better outcomes.

Summary

Babies and children with neuromuscular and functional deficits resulting from OBPI should be screened to determine candidacy for FES. If the testing indicates sufficient innervation, FES if combined with other interventions, may enhance the recovery of muscle strength, motor control and functional use of the upper extremity.

References

[1] DeFrancesco CJ, Shah DK, Rogers BH, Shah AS. The Epidemiology of Brachial Plexus Birth Palsy in the United States: Declining Incidence and Evolving Risk Factors. *J Pediatr Orthop.* 2019;39(2):e134-e140.

[2] Zuarez-Easton S, Zafran N, Garmi G, Hasanein J, Edelstein S, Salim R. Risk factors for persistent disability in children with obstetric brachial plexus palsy. *J Perinatol.* 2017;37(2):168-171.

[3] Sjoberg I, Erichs K, Bjerre I. Cause and effect of obstetric (neonatal) brachial plexus palsy. *Acta Paediatr Scand.* 1988;77(3):357-364.

[4] Elnaggar RK. Shoulder Function and Bone Mineralization in Children with Obstetric Brachial Plexus Injury After Neuromuscular Electrical Stimulation During Weight-Bearing Exercises. *Am J Phys Med Rehabil.* 2016;95(4):239-247.

[5] Ruyer J, Grosclaude S, Lacroix P, Jardel S, Gazarian A. Arthroscopic isolated capsular release for shoulder contracture after brachial plexus birth palsy: clinical outcomes in a prospective cohort of 28 children with 2 years' follow-up. *J Shoulder Elbow Surg.* 2018;27(8):e243-e251.

[6] Luszawski J, Marcol W, Mandera M. The components of shoulder and elbow movements as goals of primary reconstructive operation in obstetric brachial plexus lesions. *Neurol Neurochir Pol.* 2017;51(5):366-371.

[7] Mackenzie WG, Riddle EC, Earley JL, Sawatzky BJ. A neurovascular complication after scapulothoracic arthrodesis. *Clin Orthop Relat Res.* 2003(408):157-161.

Author's Address

Gad Alon
University of Maryland, School of Medicine, USA
GAlon@som.umaryland.edu
https://www.medschool.umaryland.edu/profiles/Alon-Gad/

DEVELOPMENT OF A SINGLE-SITE DEVICE FOR CONJOINED GLUCOSE SENSING AND INSULIN DELIVERY IN TYPE 1 DIABETES PATIENTS

Tschaikner M

Department of Internal Medicine, Division of Endocrinology and Diabetology,
Medical University of Graz, Austria

Abstract: *Goal: Diabetes patients are increasingly using a continuous glucose sensor to monitor blood glucose and an insulin pump connected to an infusion cannula to administer insulin. Applying these devices requires two separate insertion*
sites, one for the sensor and one for the cannula. Integrating sensor with cannula to perform glucose sensing and insulin infusion through a single insertion site would significantly simplify and improve diabetes treatment by reducing the overall system size and the number of necessary needle pricks. Presently, several research groups are pursuing the development of combined glucose sensing and insulin infusion devices, termed single-port devices, by integrating sensing and infusion technologies created from scratch. Methods: Instead of creating the device from scratch, we utilized already existing technologies and introduced three design concepts of integrating commercial glucose sensors and infusion cannulas. We prototyped and evaluated each concept according to design simplicity, ease of insertion, and sensing accuracy. Results: We found that the best single-port device is the one in which a Dexcom sensor is housed inside a Medtronic cannula so that its glucose sensitive part protrudes from the cannula tip. The low degree of component modification required to arrive at this configuration allowed us to test the efficiency and safety of the device in humans. Conclusion: Results from these studies indicate the feasibility of combining commercial glucose sensing and insulin delivery technologies to realize a functional single-port device. Significance: Our development approach may be generally useful to provide patients with innovative medical devices faster and at reduced costs.

Keywords: *artificial pancreas, electrochemical glucose sensor, insulin infusion set, insulin pump, medical device development, single-port device*

Author's Address

Mathias Tschaikner
Department of Internal Medicine,
Division of Endocrinology and Diabetology
Medical University of Graz
mathias.tschaikner@medunigraz.at

Session 4:
Advanced Biosignal Analysis

Decomposition of hdEMG data of a child with spastic Cerebral Palsy: A case study pre and post BoNT-A treatment

Wiedemann L[1], McDaid A[1], Holobar A[2]

[1]Department of Mechanical Engineering, The University of Auckland, 1010, New Zealand
[2]Faculty of Electrical Engineering and Computer Science, University of Maribor, Maribor, 2000, Slovenia

Abstract: *Cerebral Palsy (CP) affects voluntary control of movement which leads to ongoing structural changes of the muscle. Extracting motor unit firing characteristics from high-density electromyographic (hdEMG) signals in children with CP might improve our understanding of the neural drive in this condition. This pilot study investigates the feasibility of hdEMG decomposition in one child with spastic Cerebral Palsy pre and post Botulinum Neurotoxin-A (BoNT-A) treatment. HdEMG data of the Gastrocnemius medialis during voluntary isometric force ramps of one individual with spastic Cerebral Palsy were decomposed. The performance of the decomposition was evaluated by the number of MUs identified, total number of discharges, MU firing rate and pulse-noise-ratio (PNR). A maximum number of five MUs were identified from the trials with a mean PNR of 27.38 dB ± 3.14 dB and 26.55 dB ± 3.22 dB for the pre- and post BoNT-A trials, respectively. Thus, the findings suggest decomposing hdEMG signals in spastic CP is feasible. Nevertheless, the relatively low number of MUs highlights the need to further improve the decomposition method to extract MUs from hdEMG data with low signal quality.*

Keywords: Cerebral Palsy, spasticity, hdEMG, neuromuscular activation, Botulinum Neurotoxin-A

Introduction

Cerebral Palsy (CP) is a common disorder that develops due to a brain lesion, and affects approximately 3 out of 1000 newborns [1]. While the lesion to the brain is generally non-progressive in CP, muscle pathologies worsen over time and often require costly clinical interventions [2]. For instance, Botulinum Neurotoxin-A (BoNT-A) is a common intervention to treat spasticity [3, 4]. BoNT-A is injected into spastic muscles in order to decrease hypertonia, therefore reducing pain, increasing the potential range of motion of the joint and preventing contractures [2, 5, 6].

High-density electromyography (hdEMG) records muscle activation using multiple electrodes on the skin surface. Through decomposition techniques such as the Convolution Kernel Compensation (CKC), it enables investigating the discharging characteristics of individual motor units (MU) [7]. Due to the high costs of hdEMG systems, the time-consuming measurement procedure and the signals' susceptibility to contamination with noise, the method is mostly limited to scientific research [8, 9, 10]. Nevertheless, continuing efforts in using hdEMG on clinical populations increase the popularity of the method and its transition into clinical practice [11, 12, 13]. To the best of our knowledge decomposition of hdEMG signals has not been applied to children with spastic CP pre and post BoNT-A. Even though BoNT-A is an important clinical intervention for children with CP [3], the effect of BoNT-A on the neural drive of the muscle is unknown. Furthermore, the underlying mechanisms of progressive muscle pathologies are not yet fully understood. Investigating neuromuscular control strategies is therefore important to improve our understanding of CP.

This pilot study aims to investigate the feasibility of decomposing hdEMG signals to identify individual MUs in one child with spastic CP pre and post BoNT-A treatment.

Material and Methods

Participant demographics and clinical assessments: The participant assessed in this case study was a 12 years old male with spastic diplegic CP and a GMFCS level I. His height and weight were 1,63 m and 49,3 kg (BMI: 18,6 kg m^{-2}). His dominant leg was the right side and the non-dominant side was assessed for the study, which was more significantly affected with spasticity according to the Modified Ashworth Scale (MAS). The following clinical assessment scores are provided for the non-dominant limb and pre BoNT-A only: MAS for the gastrocnemius was 2, and the Modified Tardieu Scale (MTS) equalled 3° plantarflexion (R1; i.e. spastic catch angle) and 0° (R2; i.e. passive range of motion). The timed-up and go (TUG) assessment resulted in a time of 8,5 s taken to complete the test. The BoNT-A intervention was part of the patient's standard medical care and was not modified through participation in the study. Written informed assent/consent was provided by the participant and legal guardian following the guidelines outlined by the Southern Health and Disability Ethics Committee, New Zealand (HDEC; Ethics reference: 17/STH/215).

Experimental data: Datasets containing hdEMG and torque data available online with Mendeley data [14] were used for this preliminary study. The participant assessed for this preliminary case study had the identifier 'CP_ankle04' (pre BoNT-A trial) and 'CP_ankle04_post' (post BoNT-A). HdEMG data was recorded using 64 electrodes (16 rows x 4 columns) on the skin surface above the Gastrocnemius medialis. The data were collected during isometric contractions of the plantarflexors one day before and 30 days after BoNT-A treatment. The ankle angle was 90° during the isometric

force ramp contractions. Visual real-time force feedback was provided on a computer screen. A TUG test and two maximum voluntary contractions (MVC) followed by eight isometric force ramp trials with contraction levels ranging between 15-70% MVC were performed: three low force ramps (FRL; 15% MVC), three medium force ramps (FRM; 30% MVC) and two high force ramps (FRH; 70% MVC). Each force ramp consisted of a ramp-up phase (7.5 s), plateau phase (10 s) and a ramp-down phase (7.5 s). Further details about the experimental protocol and data collection can be found elsewhere [15].

Signal analysis: The hdEMG signals were decomposed using the CKC approach [16, 17, 18, 19] to reconstruct individual MU spike trains. Subsequently, identified spike trains were edited manually to disregard erroneous discharges [20]. The accuracy of the decomposition method was assessed for each individual MU by the pulse-to-noise-ratio (PNR) [21, 22]. The number of discharges was evaluated for each MU during the whole force ramp trial, whereas the firing rates were only calculated for the constant contraction phase (i.e. the plateau region) of the force ramps.

Results

The number of identified MUs ranged between 0 and 5 over all force ramps and pre and post BoNT-A treatment (Table 1 and 2). The mean number of discharges pre BoNT-A for the FRLs, FRMs and FRHs were 143 ± 4.24, 131.14 ± 40.52, 159 ± 43.74, respectively. Post BoNT-A the number of discharges were 112 ± 0, 115.64 ± 18.85 and 99.5 ± 33.49 for the FRLs, FRMs and FRHs, respectively. The mean PNR over all force ramps pre BoNT-A was 27.38 dB $\pm$ 3.14 dB. In contrast, the PNR post BoNT-A equalled 26.55 dB $\pm$ 3.22 dB. The mean firing rates of all MUs pre BoNT-A during the plateau phase of the FRLs, FRMs and FRHs equalled 8.05 Hz $\pm$ 0.44 Hz, 7.37 Hz $\pm$ 0.72 Hz and 10.00 Hz $\pm$ 1.92 Hz, respectively. After the BoNT-A treatment, the mean firing rates resulted in 6.89 Hz $\pm$ 0.00 Hz, 8.15 Hz $\pm$ 0.70 Hz and 9.26 Hz $\pm$ 2.45 Hz for the FRLs, FRMs and FRHs, respectively. Fig. 1 demonstrates the decomposed MU firings of one exemplary trial (FRM01, post BoNT-A) and Fig. 2 shows the identified MU action potential shapes of the participant analysed.

Table 1: MU firing characteristics of one participant before the BoNT-A treatment. If multiple MUs were detected, their number of discharges, firing rates and PNR are displayed in separate rows.

Pre BoNT-A	FRL01	FRL02	FRL03	FRM01	FRM02	FRM03	FRH01	FRH02
No. of MUs	0	2	0	3	1	3	2	3
No. of discharges	-	1: 140 2: 146	-	1: 174 2: 179 3: 156	1: 80	1: 110 2: 133 3: 86	1: 156 2: 131	1: 120 2: 156 3: 232
Firing rates [Hz]	-	1: 7.74 2: 8.36	-	1: 8.45 2: 7.78 3: 7.19	1: 7.04	1: 6.50 2: 7.96 3: 6.65	1: 8.78 2: 10.43	1: 7.81 2: 10.14 3: 12.87
PNR [dB]	-	1: 32.5 2: 22.6	-	1: 28.6 2: 28.2 3: 28.0	1: 31.7	1: 29.4 2: 23.0 3: 28.6	1: 30.0 2: 24.3	1: 27.3 2: 25.3 3: 23.8

Table 2: MU firing characteristics of one participant after the BoNT-A treatment.

Post BoNT-A	FRL01	FRL02	FRL03	FRM01	FRM02	FRM03	FRH01	FRH02
No. of MUs	1	0	0	5	3	3	2	4
No. of discharges	1: 112	-	-	1: 148 2: 134 3: 90 4: 137 5: 123	1: 118 2: 115 3: 108	1: 104 2: 106 3: 89	1: 100 2: 74	1: 105 2: 145 3: 122 4: 51
Firing rates [Hz]	1: 6.89	-	-	1: 8.60 2: 9.27 3: 7.12 4: 8.06 5: 7.23	1: 7.38 2: 8.70 3: 8.30	1: 7.87 2: 8.85 3: 8.32	1: 8.24 2: 11.13	1: 7.95 2: 13.37 3: 7.18 4: 7.69
PNR [dB]	1: 33.6	-	-	1: 26.1 2: 22.8 3: 24.3 4: 25.4 5: 31.0	1: 29.1 2: 24.1 3: 21.4	1: 29.6 2: 24.3 3: 24.7	1: 27.6 2: 24.7	1: 29.2 2: 27.5 3: 23.4 4: 29.1
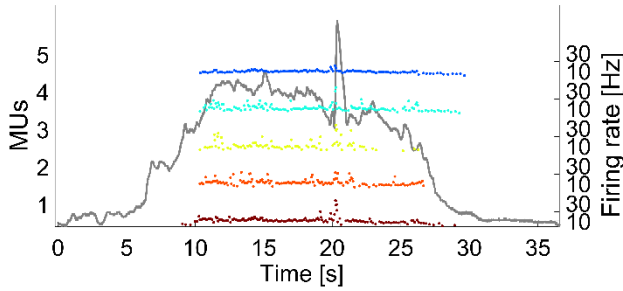
Figure 1: MU firing patterns during the FRM01 trial of the participant after the BoNT-A treatment. Different MUs are illustrated in colour and the force trajectory is grey. The MUs were sorted according to their recruitment order.

Discussion

The main aim of this pilot study was to investigate the feasibility of identifying individual MUs in a child with CP before and after BoNT-A treatment. The ability to evaluate MU firing patterns in this patient group would provide an extremely valuable tool to reveal potential underlying mechanisms leading to differences in muscle physiology compared to typically developed children. For example, it was previously found that MU firing synchronicity was higher in patients with pathological tremor [23] and MU firing modulation was reduced in individuals with diabetes type II [24]. Similar investigations could shed more light on differences in the neural drive in children with CP.

The number of identified MUs in this study was rather low and limited to a maximum of 5 MUs across all trials. In addition, the decomposition method failed to identify MUs in two out of three FRLs in both, the pre- and post BoNT-A conditions. In comparison, other studies found between 0-15 MUs in the Vastus lateralis in patients with diabetes type II [24] and Farina et al. [25] extracted up to 27 MUs with a PNR > 30 dB from patients in targeted reinnervated muscles. In comparison, the PNR of the individual MUs assessed in this case study was often poor. This could be due to environmental noise sources or deep MUs as the muscle volume in children with CP is significantly reduced [5]. Holobar et al. [26] suggested MUs being identified reliably if their PNR is greater than 30 dB and noise is commonly reported to be a problem for hdEMG [10].

It is important to note, that this preliminary study is limited to the decomposition of one child with CP only. Thus, no statistical analysis could be performed to compare MU firing patterns pre and post BoNT-A. Nevertheless, this pilot study reveals the feasibility of the decomposition method in CP before and after BoNT-A treatment. The decomposition of hdEMG remains a promising approach to improve our understanding of CP and the effect of BoNT-A treatment. Future research needs to focus on improving the decomposition method for low-quality signals to obtain a higher number of MUs in children with CP.

Acknowledgement

References

[1]   H. K. Graham, P. Rosenbaum, N. Paneth, B. Dan, and J. Lin, "Cerebral palsy," Nat. Rev., vol. 2, pp. 1–24, 2016.

[2]   H. K. Graham and P. Selber, "Musculoskeletal Aspects of Cerebral Palsy," J. Bone Jt. Surg., vol. 8585, no. 2, pp. 157–66, 2003.

[3]   S. C. Love, I. Novak, M. Kentish, K. Desloovere, F. Heinen, G. Molenaers, S. O'Flaherty, and H. K. Graham, "Botulinum toxin assessment, intervention and

Figure 2: MU action potential shapes for the FRM01 post BoNT-A. Each line represents one channel of the 16x4 EMG grid in bipolar mode. Noisy channels were discarded manually.

after-care for lower limb spasticity in children with cerebral palsy: International consensus statement," Eur. J. Neurol., vol. 17, no. SUPPL. 2, pp. 9–37, 2010.
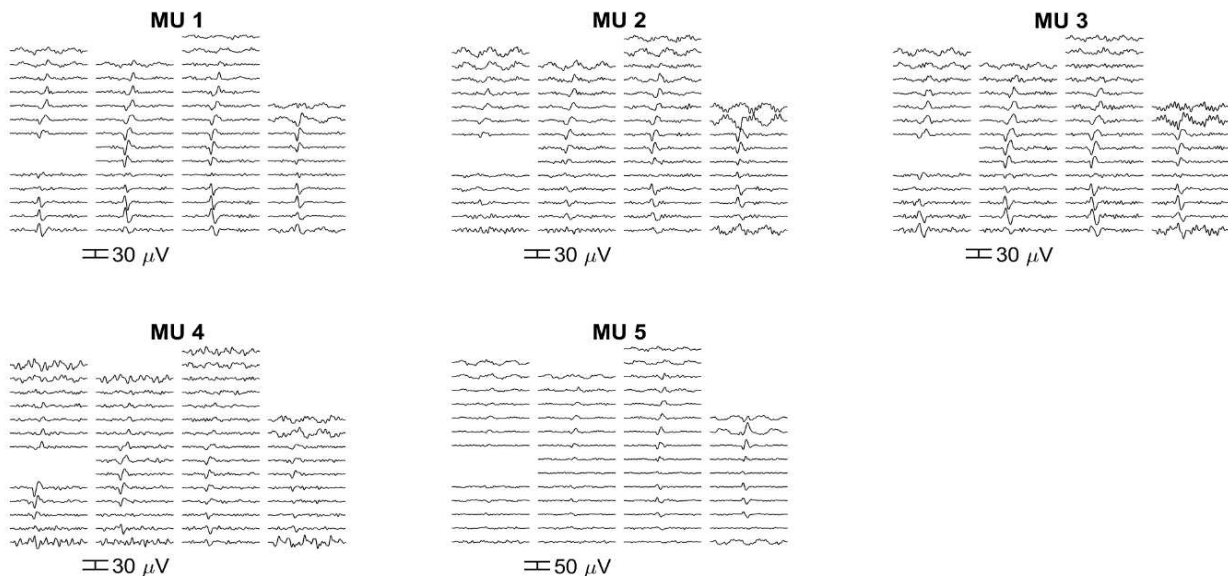
[4]　T. M. O'Shea, "Diagnosis, Treatment, and Prevention of Cerebral Palsy in Near Term/Term Infants," Clin Obs. Gynecol, vol. 51, no. 4, pp. 816–828, 2008.

[5]　S. Dayanidhi and R. L. Lieber, "Skeletal muscle satellite cells: Mediators of muscle growth during development and implications for developmental disorders," Muscle Nerve, vol. 50, no. 5, pp. 723–732, 2014.

[6]　S. K. Chaturvedi, Y. Rai, A. Chourasia, P. Goel, V. K. Paliwal, R. K. Garg, R. K. S. Rathore, C. M. Pandey, and R. K. Gupta, "Comparative assessment of therapeutic response to physiotherapy with or without botulinum toxin injection using diffusion tensor tractography and clinical scores in term diplegic cerebral palsy children," Brain Dev., vol. 35, no. 7, pp. 647–653, 2013.

[7]　A. Holobar and D. Farina, "Blind source identification from the multichannel surface electromyogram.," Physiol. Meas., vol. 35, no. 7, pp. R143-65, Jul. 2014.

[8]　M. A. Mañanas, M. Rojas-Martínez, and J. F. Alonso, "Towards the application of hdEMG decomposition in clinical practice," Clin. Neurophysiol., vol. 127, pp. 2532–2533, 2016.

[9]　S. Dick F., K. Bert U., L. Bernd G., and V. D. Johannes P., "High-density Surface EMG: Techniques and Applications at a Motor Unit Level," Biocybern. Biomed. Eng., vol. 32, no. 3, pp. 3–27, Jan. 2012.

[10]　C. J. De Luca, L. Donald Gilmore, M. Kuznetsov, and S. H. Roy, "Filtering the surface EMG signal: Movement artifact and baseline noise contamination," J. Biomech., vol. 43, no. 8, pp. 1573–1579, 2010.

[11]　M. Jordanic, M. Rojas-Martínez, M. A. Mañanas, and J. F. Alonso, "Spatial distribution of hdEMG improves identification of task and force in patients with incomplete spinal cord injury," J. Neuroeng. Rehabil., vol. 13, no. 1, pp. 1–11, 2016.

[12]　T. Kapelner, N. Jiang, A. Holobar, I. Vujaklija, A. D. Roche, D. Farina, and O. C. Aszmann, "Motor unit characteristics after targeted muscle reinnervation," PLoS One, vol. 11, no. 2, pp. 1–12, 2016.

[13]　X. Li, M. Gazzoni, R. Merletti, and W. Z. Rymer, "Examination of Poststroke Alteration in Motor Unit Firing Behavior Using High-Density Surface EMG Decomposition," vol. 62, no. 5, pp. 1242–1252, 2015.

[14]　L. Wiedemann, S. Ward, E. Lim, N. Wilson, A. Hogan, A. Holobar, and A. McDaid, "Dataset on isometric contractions of the ankle joint in children with spastic Cerebral Palsy: hdEMG and torque." Mendeley Data, 2019.

[15]　L. G. Wiedemann, S. Ward, E. Lim, N. C. Wilson, A. Hogan, A. Holobar, and A. J. McDaid, "High-density electromyographic data during isometric contractions of the ankle joint in children with Cerebral Palsy pre and post BoNT-A treatment," Data in Brief, vol. 24, 2019.

[16]　A. Holobar and D. Zazula, "Multichannel Blind Source Separation Using Convolution Kernel Compensation," IEEE Trans. Signal Process., vol. 55, no. 9, pp. 4487–4496, 2007.

[17]　R. Merletti, A. Holobar, and D. Farina, "Analysis of motor units with high-density surface electromyography.," J. Electromyogr. Kinesiol., vol. 18, no. 6, pp. 879–90, Dec. 2008.

[18]　A. Holobar, D. Farina, M. Gazzoni, R. Merletti, and D. Zazula, "Estimating motor unit discharge patterns from high-density surface electromyogram.," Clin. Neurophysiol., vol. 120, no. 3, pp. 551–62, Mar. 2009.

[19]　D. Farina, A. Holobar, R. Merletti, and R. M. Enoka, "Decoding the neural drive to muscles from the surface electromyogram.," Clin. Neurophysiol., vol. 121, no. 10, pp. 1616–23, Oct. 2010.

[20]　E. Martinez-Valdes, C. M. Laine, D. Falla, F. Mayer, and D. Farina, "High-density surface electromyography provides reliable estimates of motor unit behavior," Clin. Neurophysiol., vol. 127, no. 6, pp. 2534–2541, 2016.

[21]　a Holobar, M. a Minetto, and D. Farina, "Accurate identification of motor unit discharge patterns from high-density surface EMG and validation with a novel signal-based performance metric.," J. Neural Eng., vol. 11, no. 1, p. 016008, 2014.

[22]　H. R. Marateb, K. C. McGill, a Holobar, Z. C. Lateva, M. Mansourian, and R. Merletti, "Accuracy assessment of CKC high-density surface EMG decomposition in biceps femoris muscle," J. Neural Eng., vol. 8, no. 6, p. 066002, 2011.

[23]　a Holobar, V. Glaser, J. a Gallego, J. L. Dideriksen, and D. Farina, "Non-invasive characterization of motor unit behaviour in pathological tremor.," J. Neural Eng., vol. 9, no. 5, p. 056011, Oct. 2012.

[24]　K. Watanabe, M. Gazzoni, A. Holobar, T. Miyamoto, K. Fukuda, R. Merletti, and T. Moritani, "Motor unit firing pattern of vastus lateralis muscle in type 2 diabetes mellitus patients.," Muscle Nerve, vol. 48, no. 5, pp. 806–13, Nov. 2013.

[25]　D. Farina, H. Rehbaum, A. Holobar, I. Vujaklija, N. Jiang, C. Hofer, S. Salminger, H. W. Van Vliet, and O. C. Aszmann, "Noninvasive, accurate assessment of the behavior of representative populations of motor units in targeted reinnervated muscles," IEEE Trans. Neural Syst. Rehabil. Eng., vol. 22, no. 4, pp. 810–819, 2014.

[26]　A. Holobar, M. A. Minetto, and D. Farina, "Accurate identification of motor unit discharge patterns from high-density surface EMG and validation with a novel signal-based performance metric," J. Neural Eng., vol. 11, no. 1, p. 016008, Feb. 2014.

Author's Address

Lukas Gerald Wiedemann
Department of Mechanical Engineering, The University of Auckland, New Zealand
lwie327@aucklanduni.ac.nz
https://www.mdt.auckland.ac.nz/lukas-wiedemann/

Use of High Density EEG to assess schizophrenic patients undergoing TMS treatment: N100-P300 ERP complex

Ovidiu C. Banea [1,2], Sara Marcu [2], Eysteinn Ívarsson [1], Aron D. Jónasson [1], Sigurjón B. Stefansson [1], Eric Wassermann [5], Rún Friðriksdóttir [2] and Paolo Gargiulo [2]

1 National University Hospital of Iceland, Clinical Neurophysiology Unit, Reykjavík, Iceland

2 Reykjavik University and Landspitali/ Institute of Biomedical and Neural Engineering

3 Reykjavik University / School of Business, Department of Psychology, Reykjavik, Iceland

4 Icelandic Psychiatric Hospital Kleppur, National University Hospital of Iceland, Reykjavík, Iceland

5 National Institute of Neurological Disorders and Stroke, National Institutes of Health / Behavioral Neurology Unit, Bethesda, MD, USA

Abstract: The main objectives of this study were to describe P300 cortical topography in patients with schizophrenia and to define a robust methodology of signal quantification using high density EEG 256 channels system. Within a clinical trial in which patients with schizophrenia and auditory verbal hallucinations were submitted to 10 days rTMS treatment, P300 was investigated as possible neurophysiological marker to assess treatment effectiveness together with psychometric scales. This work mainly focuses on the methodological pipeline to extract and process the EEG data and display the results on a patient case, before and after the treatment.

Keywords: Schizophrenia, N100-P300, high-density EEG, TMS

Introduction

Theoretical and research evidence suggests that attention may be important in affect perception which is highly related to schizophrenia patients [1]. Event-related potentials (ERPs) offer a more sophisticated method of extracting specific sensory, cognitive and motor events by using simple averaging techniques. An increase of the N100 or N1 wave amplitude by allocation of attention is often lacking in schizophrenia patients [2] and the decrease of P300 or P3 wave amplitude is well known as a robust neurophysiological marker in schizophrenia [3]. The N1 is a negative deflection peaking between 90 and 200 ms after the onset of an auditory stimulus observed when an unexpected stimulus is presented [3] while the auditory P3 wave is a time-locked ERP component indexing attentional resources allocated to the target stimuli and/or the context updating. The P3 peak is defined as the largest positive deflection in the time range from 270 to 470 ms [4] [5]

We aimed to describe P300 in patients with schizophrenia and auditory verbal hallucinations using 256-channels "high-density" EEG with an auditory oddball paradigm attention task. The research is part of the AVH TMS Icelandic project. The goal of this clinical applied research is to identify the degree of repetitive transcranial magnetic stimulation (rTMS) effectiveness for the treatment of schizophrenic patients with persistent auditory verbal hallucinations (AVH).

In this work, we present data on N100-P300 complex with signal processing in one healthy subject and one patient, before the TMS treatment, after the TMS treatment and three months after the treatment.

Material and Methods

Participants and the Icelandic AVH-TMS study
The patients have been recruited from the psychiatric wards and outpatient clinics through the National Hospital database of diagnosed schizophrenia patients, following the ICD-10 schizophrenia classification (F20). Only those still experiencing persistent auditory verbal hallucinations after finishing at least two 6-8 week drug prescription treatments have been selected. Permission from the Health Research Ethics Committee at the University Hospital of Iceland was obtained (approval no. 21.2018).

Persistent auditory verbal hallucinations have been studied with rTMS, which has been recognized as A level treatment option. The study used a randomized double-blind placebo-control trial design. It included three groups, one group which received active rTMS treatment the second group receiving treatment at a control location and the third healthy control groups without treatment.
A Medtronic MagPro stimulator TMS machine from Denmark was used. In the active treatment the figure of eight coil (MC-B70) was placed on the scalp between T3-P3 as measured with the 10-20 international system, while for control treatment, the coil was placed at the vertex. Stimulation was delivered at 100% of the resting resting motor evoked potential (MEP) threshold (RMT) for the right *abductor pollicis brevis* (APB) muscle, determined before each rTMS. RMT was defined as the minimum intensity needed to evoke five MEPs in 10 consecutive trials. Treatment consisted of ten sessions over the course

of two weeks. Each session lasted 15 minutes and included 900 pulses delivered at 1 Hz.

Task design
In the current study, N100-P300 components were measured with an auditory oddball paradigm attention task. The recordings were carried out between 11AM and 14 PM. The subjects were sitting in a comfortable chair with their eyes closed. The frequent (F) and the rare (R) auditory stimuli were presented binaurally through headphones at an interstimulus interval between tones of constant 1.1 sec. For each subject there was 1 trial of 160 tones which occurred randomly with a probability of 0.2 [6]. Participants were instructed to pay attention to the rare stimuli without counting or moving their fingers.

EEG pre-processing and analysis
Data pre-processing and analysis was performed with Brainstorm [7] and MATLAB 2018b. The data was sampled at 1024Hz and re-referenced to the average of left and right mastoid electrodes (R19R, L19L). A band-pass filter was set between 0.1- 80 Hz. The signals were digitized for each epoch of 1000 ms starting 100 ms prior to the presentation of each auditory stimulus (-100 to +900 ms).

The Regions of Interest (ROI)
The ROI were defined using matlab script (Fig 1), each of them being represented by 15 electrodes (105 electrodes out of 256) as follow: Left Anterior (LA), Left Posterior (LP), Medial Anterior (MA), Medial Central (MC), Medial Posterior (MP), Right Anterior (RA) and Right Posterior (RP).
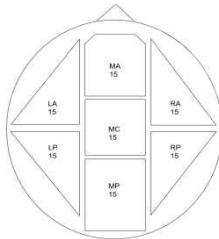
Fig 1. EEG cortical distribution of the seven regions

N100-P300 complex
N100-P300 complex values for each ROI were calculated as the difference between the most positive voltage value and the most negative voltage value within the time range of interest. In this work N1 and P3 wave's signals were represented as the average of the fifteen electrodes of every ROI between 80 and 500 ms.

Results

N100-P300 complex values for each ROI were displayed for one healthy subject (no treatment) and one patient from the T3-P3 scalp location rTMS group before, after and 3 months after the treatment (Fig 2, Table 1)
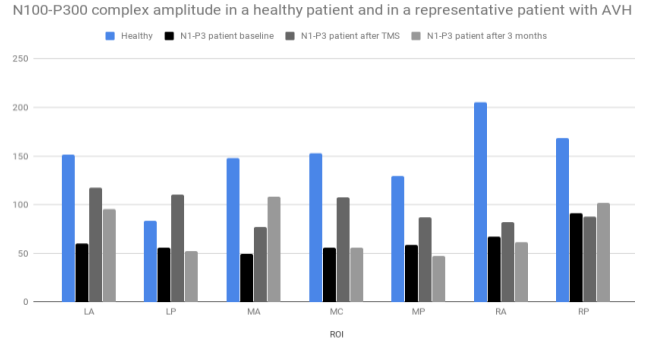
Fig. 2. N100-P300 complex amplitude shown over the seven regions of interest (ROI). The bars represent the N100-P300 complex amplitude difference in one healthy participant (blue), patient baseline (black), patient right after treatment (gray) and patient three months after the treatment (light gray).

Table 1: N100-P300 complex amplitude

ROI	N1-P3 Healthy (mV)	N1-P3 patient baseline (mV)	N1-P3 patient after TMS (mV)	N1-P3 patient after 3 months (mV)
LA	**151,51**	**59,963**	**117,48**	95,644
LP	83,541	**55,645**	110,09	**52,003**
MA	148,2	49,168	76,986	108,05
MC	**152,87**	56,02	**107,91**	55,854
MP	129,62	58,791	**87,062**	47,336
RA	**205,12**	67,046	**82**	61,404
RP	**168,33**	91,044	87,668	101,71

The healthy participant shows maximum deflection of N1-P3 waves on right anterior region of the scalp followed by right posterior, mid central and left anterior regions (Fig. 3).
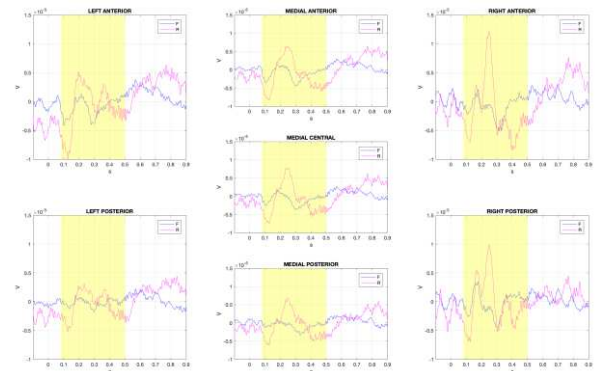
Fig.3. N100-P300 complex shown in a healthy control.

The patient with schizophrenia and auditory verbal hallucinations showed decreased N100-P300 complex values at baseline conditions. After the rTMS treatment the N1-P3 maximum-minimum difference increased mostly over the left hemisphere (LA and LP regions) and central regions (MA, MC, MP) (Fig. 4).
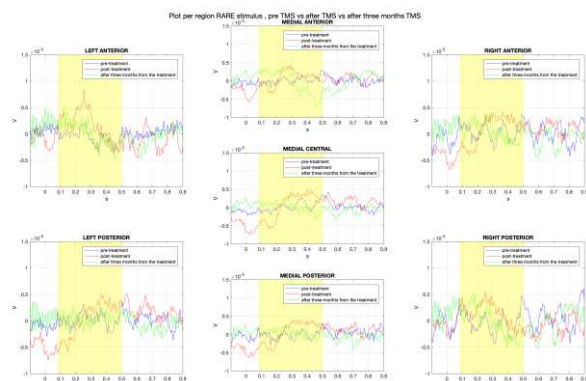
Fig. 4. N100-P300 complex in a patient with auditory verbal hallucinations before (blue traces), after rTMS (red traces) and 3 months after the treatment (green traces).

Conclusions

With this technique of measuring the ERP with high density EEG we were able to observe differences of N100-P300 complex values at the scalp level in the different regions of the interest in a patient with schizophrenia.

The complex values improved after the rTMS treatment but after 3 months the N1-P3 waves signals were as in baseline conditions.

More patients from both T3-P3 scalp location treatment group and vertex control location treatment group will be analysed to better understand these changes and to propose this method as neurophysiological marker to assess rTMS treatment effectiveness in patients with schizophrenia.

References

[1] Combs DR, Gouvier WD. The Role of Attention in Affect Perception: An Examination of Mirsky's Four Factor Model of Attention in Chronic Schizophrenia [Internet]. Schizophrenia Bulletin. 2004. pp. 727–738. doi:10.1093/oxfordjournals.schbul.a007126

[2] Rosburg T, Boutros NN, Ford JM. Reduced auditory evoked potential component N100 in schizophrenia — A critical review [Internet]. Psychiatry Research. 2008. pp. 259–274. doi:10.1016/j.psychres.2008.03.017

[3] Sur S, Sinha VK. Event-related potential: An overview [Internet]. Industrial Psychiatry Journal. 2009. p. 70. doi:10.4103/0972-6748.57865

[4] Strik WK, Dierks T, Franzek E, Stöber G, Maurer K. P300 asymmetries in schizophrenia revisited with reference-independent methods. Psychiatry Res. 1994;55: 153–166.

[5] Toyomaki A, Hashimoto N, Kako Y, Tomimatsu Y, Koyama T, Kusumi I. Different P50 sensory gating measures reflect different cognitive dysfunctions in schizophrenia. Schizophr Res Cogn. 2015;2: 166–169.

[6] Stefánsson SB, Jónsdóttir TJ. Auditory event-related potentials, auditory digit span, and clinical symptoms in chronic schizophrenic men on neuroleptic medication [Internet]. Biological Psychiatry. 1996. pp. 19–27. doi:10.1016/0006-3223(95)00351-7

[7] Tadel F, Baillet S, Mosher JC, Pantazis D, Leahy RM (2011) Brainstorm: A User-Friendly Application for MEG/EEG Analysis Computational Intelligence and Neuroscience, vol. 2011, ID 879716

Author's Address

Name: Ovidiu Constantin Banea
Affiliation: National University Hospital of Iceland
eMail: ovidiuc@landspitali.is
homepage:
https://sites.google.com/view/neurophysiologyplus

SKIN IMPEDANCE IS A RELIABLE PARAMETER FOR AROUSAL MONITORING (STRESS MONITORING)

Bijak M[1], Brettlecker S[1], Cap V[1], Deubner O[1], Lebloch K[2], Schröder S[2]

[1]Department of Medical Physics and Biomedical Engineering, Medical University of Vienna, Austria
[2]Faculty of Computer Science, University of Vienna, Austria

Abstract: *Acute stress is a normal part of daily life and shall help to cope with unusual, challenging situations. When the body is exposed to stress over a longer time period (chronic stress), like in working environments it can cause various serious health problems. The assessment of electrodermal activity (EDA, skin conductance) might be an easy approach to evaluate individual stress conditions over a longer period of time in an objective way. With the help of cvxEDA the monitored skin conductance can be split into the slow skin conductance level (SCL) and the fast skin conductance response (SCR). 20 volunteers were exposed to a relaxing-challenging-relaxing situation to mimic different stress conditions. The SCR rate proofed to be a reliable measure to evaluate sympathetic arousal. During the relaxation phases, the SCR rate was around $6min^{-1}$ and during mathematical challenges it raised to $9min^{-1}$ (p<0.05).*

Keywords: *arousal, stress, EDA, SCL, SCR, cvxEDA*

Introduction

Even if there is not (yet) a comprehensive definition of "stress" nearly everyone knows these days what stress is and has felt how it can influence the behavior, well-being, and health [1].

The literature distinguishes between acute and chronic stress. Acute stress describes the "normal", short-term stress response and is a necessary part of daily life. It is also the one usually observed in a laboratory setting. Contrary, chronic stress is a long-term and strictly pathological stress response. Chronic stress has been linked to many diseases such as depression, cardiovascular diseases, insulin insensitivity and cancer [2]. Chronic stress is often work-related and consequently considered as a serious problem these days [3].

Out of this, it is necessary to find ways to evaluate the stress level of people, preferably as objective as possible. Usual methods are [4]:

Self-assessment: by standardized surveys; useful to evaluate both kinds of stress

Performance measurements: Acute stress can have positive or negative effects on specific tasks like proof-reading. These techniques require a baseline measurement.

Chemical Biomarkers: Cortisol, epinephrine, and catecholamine levels are evaluated. Requires blood samples.

Physiological biomarkers like blood pressure, heart rate, and breathing rate are controlled by the sympathetic nervous system and can be measured non-invasive. Out of the heart rate, the Heart Rate Variability can be calculated and can bring insight into the activity of the parasympathetic nervous system [5].

The listed methods are subjective, time-consuming, invasive, require a baseline and/or are complex in terms of evaluation and setup.

A relatively simple approach, in terms of required equipment and data processing, for stress evaluation is the monitoring of the Electrodermal Activity (EDA). A DC current of a few µAs is sent through the skin and with the measured voltage, the skin conductance [S] is calculated. Common measurement sites are palmar and plantar areas, especially fingers and toes. Areas like shoulders or armpits are also possible but less often used due to generally lower EDA [6].

Skin conductance is made up of two distinct components. A slow, tonic component called skin conductance level (SCL) and a much faster changing, phasic , called skin conductance response (SCR) [7].

We assume that it is possible to evaluate a person's stress level (sympathetic arousal) continuously during a task/work out of the measured skin conductance.

Material and Methods

Measurement protocol:

Students of a seminar were asked to participate in the "stress test" protocol described in the following. 20 persons volunteered, were informed and signed an informed consent. Then they were asked to sit in front of a computer monitor as still as possible and go through the following five phases:

1. Three minutes acclimatization: the participants were asked to relax in total silence – to get insight into the participants' ability to calm down from their previous normal level of arousal.

2. Three minutes anticipation: The participants were asked to relax while watching a relaxation video – to get insight into participants' ability to remain calm while waiting for the first task.

3. Five minutes of easy to moderately difficult mathematical challenges. The participants gave the answers orally. The answers were checked by a voice recognition system and the result (correct/incorrect) was displayed on the monitor. Each challenge had a timeframe with a ticking sound notifying the last few seconds. This phase is the start of the stressor, which simulates work stress.

4. Five minutes moderately to difficult mathematical challenges. Additionally, a supervisor entered the room sat down slightly out of sight participants. The presence of the supervisor put additional social pressure on the person.

5. Three minutes of relaxation. The supervisor left the room and the video from phase 2 was played again – to get insight into the participants' ability to relax after stress.

As EDA measuring device the biofeedback recording system "Neuromaster" from Insight Instruments (Hallein, Austria) was used. The finger sensor was attached to the index finger of the right hand (Fig. 1.)

Fig. 1: Skin conductance measurement with finger sensor (Insight Instruments Hallein, Austria) (left) attached to the index finger of the right hand (right)

Measurement equipment:
The entire procedure was automated with a self-written PC program. The time course was documented automatically. Simultaneously the skin conductance was recorded with 5 samples/second. The time was synchronized between PC and Neuromaster at the beginning of each session.

Data analyses:
All data sets were processed with MatLab (MathWorks Inc.).
For the evaluation of SCRs cvxEDA was used, an algorithm based on convex optimization [8].
Four assumptions are made to isolate single SCRs and evaluate sympathetic arousal out of the recorded skin conductance:

1. SCRs result from sudomotor nerve bursts
2. The number of sweat glands recruited for a burst is linearly proportional to the amplitude of the nerve burst and any SCR is not influenced by previous or following nerve bursts.
3. Sweat diffusion follows a specific Impulse Response Function.
4. Phasic activity is superimposed by slow-moving tonic activity, with a spectrum below 0.05 Hz.

Following assumption 4, cvxEDA separates phasic (SCRs) and tonic (SCL) activity. The tonic activity is estimated via splines. The parameters of these splines are taken from ten seconds long windows and are subtracted from the original data. The isolated SCRs are then used to describe the most likely sympathetic activity based on assumptions 1-3.
To consider the individual differences in the SCR shapes a quadratic optimization algorithm is used to minimize the differences between predicted and recorded data.

As a representation of the momentary arousal level, the SCR frequency was used. CvxEDA creates a vector containing the isolated SCRs and by implementing MatLab's "findpeaks" the local maxima above a certain threshold can be found. Even if SCRs overlap the peaks are still present and can be detected.
According to the literature the SRC rate is typically 1-3min^{-1} during rest, below 10min^{-1} calm, above 10min^{-1} moderate to high sympathetic arousal and over 20 min^{-1} in very high arousal situations [7].

Statistical testing
SCR rates of the different stress test phases were compared using the paired Student's t-test. The level of significance was set to $p < 0.05$.

Results

For all participants, the Electrodermal Activity was recorded throughout the entire session, exemplary represented with the blue line in Fig. 2. From this data, cvxEDA calculates the SCL (magenta line) which is subtracted from the EDA and the SCRs (red line) remain.

Applying the MatLab's "findpeaks" function to the SCRs from above and counting the number of detected peaks for every minute results in, again exemplary Fig. 3.

Stress test results:

Evaluating the SCR activity of all 20 volunteers for each stress test phase showed for the Acclimatization phase 10.7 ± 3.4 min^{-1}, for the Anticipation phase 6.7 ± 3.9 min^{-1}, MAT test 1 9.1 ± 3.4 min^{-1}, MAT Test 2 8.7 ± 3.4 min^{-1} and 5.5 ± 3.6 min^{-1} for the Relaxation phase at the end of the session. All phases showed statistical differences ($p<0.05$) except between the Anticipation and the Relaxation phase and MAT test 1 and MAT test 2.

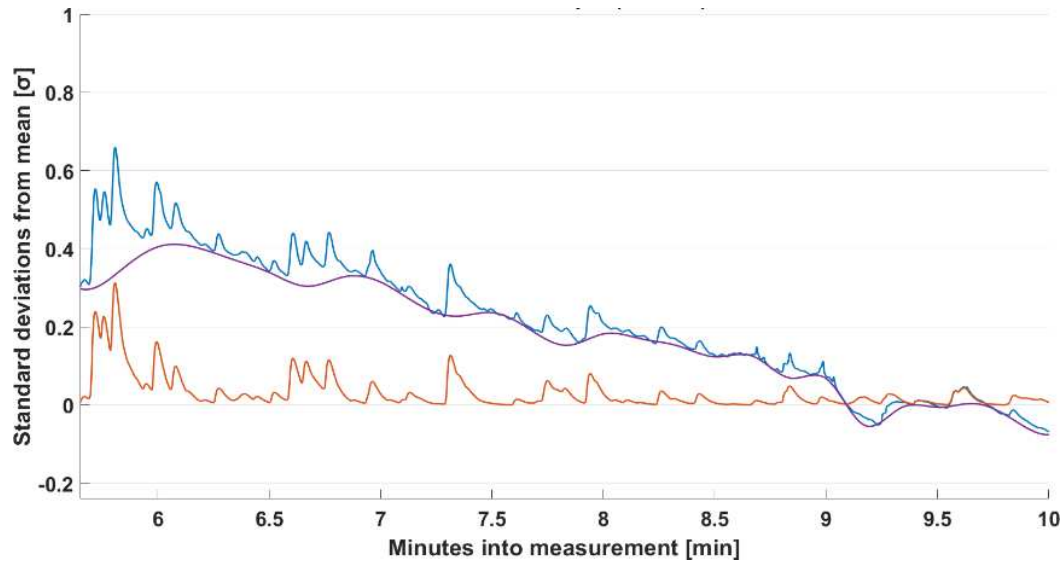*Fig. 2: An example of cvxEDA's functions. EDA / skin conductance (blue); SCL (magenta); SCRs (red). The y-Axis is the data's standard deviation since intra-personal relative values are more meaningful than absolute values.*
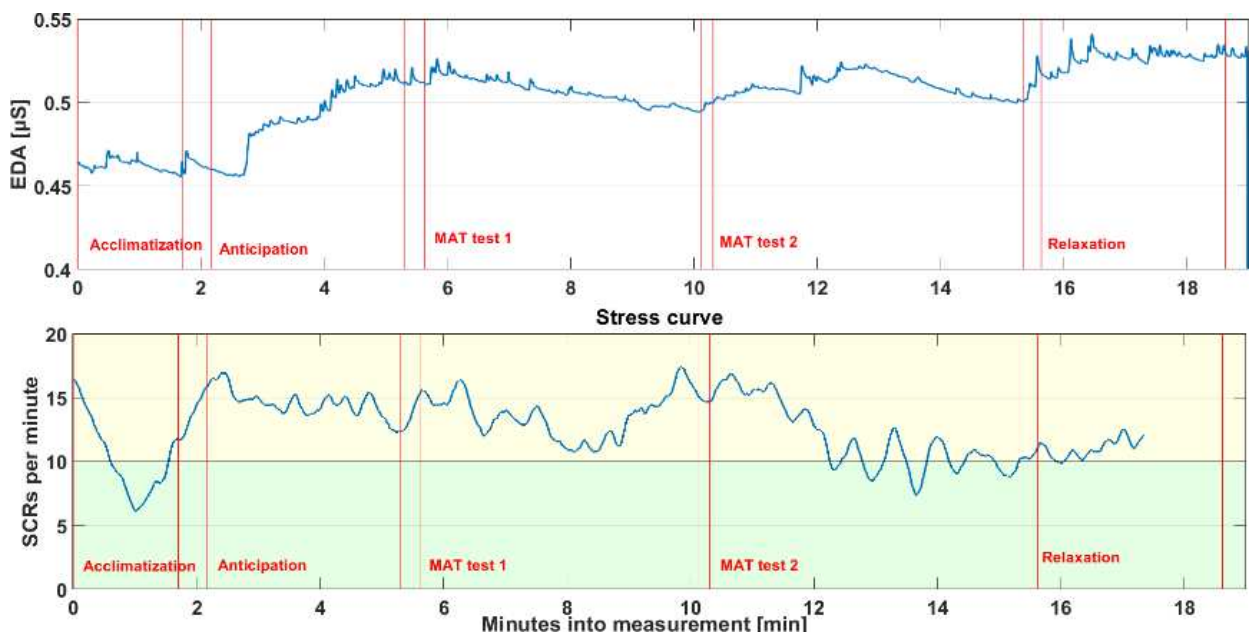

Fig. 3 An example of EDA (skin conductance) (top) and corresponding SCR rate (bottom). The SCR rate curve is evaluated by counting the events in an interval of one minute for every second.

Discussion

Evaluation of the state of arousal ("stress level") becomes more and more important as there is increasing evidence that ongoing work-related stress is a major promotor of various diseases. Since reactions to stress are highly individual the necessity for finding an objective parameter to evaluate the stress level increases.

Electrodermal Activity (EDA, skin conductance) as a combination of the slow, tonic component named skin conductance level (SCL) and a much faster changing, phasic component called skin conductance response (SCR) is investigated.

Especially the usability of the SCR rate, evaluated with cvxEDA was investigated in a setting, that tries to mimic stressful situations by mathematical challenges, preceded and followed by relaxation phases.

20 students volunteered in this study. A significant difference in SCR rates was found between all phases, except, not surprising, between the relaxation phase in the beginning (anticipation) and at the relaxation phase at the end as well as between the 2 Mat tests. Actually, we expected a higher pressure on the volunteers due the presence of the supervisor and the more difficult tasks in MAT test 2. Contrary, even if there was no statistical difference, the mean value of the SCR rate even dropped from 9.1 to 8.7. We assume, that the increased difficulty led to resignation.

The highest individual observed SCR rate was 15 and the lowest around 2, in accordance with the literature [7]. A rate of 20 would indicate a very high arousal state probably only be reached if it comes to life-threatening situations.

In general very different individual responses to the performed stress test could be observed. Some participants showed higher arousal states during Acclimatization, Anticipation and Relaxation as during the MAT test, opposite as expected.

This observation suggests, that a grouping of the participants gives better insight into the particular reactions. In a first approach, a separation into "calm participants", those who show low SCR rates during the Anticipation phase and "anxious" participants looks promising and will be a topic for future research.

Conclusions

SCR rate, evaluated with cvxEDA from the Electrodermal Activity was investigated as an objective measure for the activity of the sympathetic nervous system (arousal level, stress level).

The experiment demonstrated that is possible to distinguish between phases of relaxation and "stressful" periods where mathematical challenges are solved.

References

[1] "The United States of Stress 2019," *EverydayHealth.com*. [Online]. Available: http://www.everydayhealth.com/wellness/united-states-of-stress?nocache=true. [Accessed: 26-Aug-2019]

[2] N. Rohleder, "Stress and inflammation – The need to address the gap in the transition between acute and chronic stress effects," *Psychoneuroendocrinology*, vol. 105, pp. 164–171, Jul. 2019.

[3] "20170222pg-allianz-stressstudiecharts.pdf." [Online]. Available: https://www.allianz.at/v_1487631600000/ueber-allianz/media-newsroom/news/aktuelle-news/pa-download/20170222pg-allianz-stressstudiecharts.pdf. [Accessed: 26-Aug-2019]

[4] A. Baum, N. E. Grunberg, and J. E. Singer, "The use of psychological and neuroendocrinological measurements in the study of stress," *Health Psychol.*, vol. 1, no. 3, pp. 217–236, 1982.

[5] H.-G. Kim, E.-J. Cheon, D.-S. Bai, Y. Hwan Lee, and B. H. Koo, "Stress and Heart Rate Variability: A Meta-Analysis and Review of the Literature," *Psychiatry Investig.*, vol. 15, Feb. 2018.

[6] M. van Dooren, J. J. G. (Gert-J. de Vries, and J. H. Janssen, "Emotional sweating across the body: Comparing 16 different skin conductance measurement locations," *Physiol. Behav.*, vol. 106, no. 2, pp. 298–304, May 2012.

[7] "guide-electrodermal-activity.pdf." [Online]. Available: https://www.birmingham.ac.uk/Documents/college-les/psych/saal/guide-electrodermal-activity.pdf. [Accessed: 26-Aug-2019]

[8] A. Greco, G. Valenza, A. lanatà, E. Scilingo, and L. Citi, "cvxEDA: A Convex Optimization Approach to Electrodermal Activity Processing," *IEEE Trans. Biomed. Eng.*, vol. 2016, pp. 797–804, Apr. 2016.

Author's Address

Manfred Bijak
Center for Medical Physics and Biomedical Engineering,
Medical University of Vienna, Austria
Manfred.bijak@meduniwien.ac.at

Frequency analysis of EMG signals from the triceps surae muscle in Achilles tendon tests by stroke patients in tSCS treatment

Halldór Kárason[1], Vilborg Guðmundsdóttir[2], Gígja Magnúsdóttir[2], Guðbjörg Ludvigsdóttir[2], Belinda Chenery[3],

Þórður Helgason[1,2].

[1]Reykjavik University, Iceland
[2]Landspitali – University Hospital, Reykjavik, Iceland
[3]University of Iceland

Abstract: Effective treatment modalities for alleviating spasticity and pain and enhancing mobility and sleep are limited post-stroke. Some evidence suggests that treatment of transcutaneous spinal cord stimulation (tSCS) may be beneficial. The aim of the current study was to evaluate changes in muscle fibre type composition after daily home-treatment with tSCS by analysing the frequency of EMG (electromyography) signals from the Achilles tendon test. Our results suggest that tSCS treatment has some effects on EMG frequency but to make clear conclusions further investigations have to be made.

Introduction

Spasticity is a common neurological impairment after stroke that correlates with higher levels of disability and pain. It compromises quality of life and movement ability. Anti-spasticity treatments are limited and have adverse side- effects. Transcutaneous spinal cord stimulation (tSCS) has been shown to alleviate spasticity of the lower limbs in people with spinal cord injury (SCI). [1,2] This is believed to be due to inhibitory effects of stimulation of the posterior roots of sensory fibres on motor output. The afferent fibres leads through the neural network of the spine to spinal interneurons and motoneurons that generate the output [3,4]. The question how the tSCS influences the spinal cord circuitry has not been answered. The aim of our research is to evaluate the effect of repetitive tSCS on spasticity, mobility, pain and sleep in community dwelling individuals post-stroke. Here we specifically look at power spectra of electromyography (EMG) signals of the triceps surae muscle obtained during Achilles tendon test by brain insulted people. Frequency of EMG signals during muscle contraction relates to the muscle fibre type composition [5]. Muscles with greater percentage of fast twitch muscle fibres translate into higher frequency EMG signals during muscle contraction.

In this study we want to see if the tSCS treatment causes any change muscle fibre type composition. Shift in frequency could be an indication of muscle fibre type transfer towards faster or slower types.

Material and Methods

This study used a single-case withdrawal research design with four phases (A1, B1, A2, B2) of alternating baseline (A) and intervention (B). The intervention phase included tSCS treatment where electrodes are placed on the skin of the lower back and abdomen to target lumbar segmental neural circuits with electrical stimulation. Four post-stroke individuals were assessed for three weeks in order to establish a baseline (A) followed by another three weeks of home based tSCS (B). In both cases they were assessed once a week. This was repeated twice (phase 1 and phase 2) with an eighteen to twenty four weeks washout period in between.

Electrophysiological and biomechanical assessment methods for spasticity were applied and have been described in our earlier work [2]. Here we look at the frequency of the EMG recorded during an Achilles tendon test. We calculated the power spectrum of the EMG signal from the third week (A1) and the sixth week (B1), after three weeks of treatment, baseline period and intervention period respectively, in phase 1. This 6 weeks procedure was repeated after a washout period of 18 to 24 weeks giving phase 2.

Results

The graphs on figure 1 show the power spectrum, which describes the distribution of power into frequency components of the EMG signal during Achilles tendon test. The results from subject 3 and 6 show a shift of frequency towards lower values, by subject 4 there is no significant change and subject 5 has a slight shift towards higher frequencies. These findings harmonic with findings of other groups [6,7].
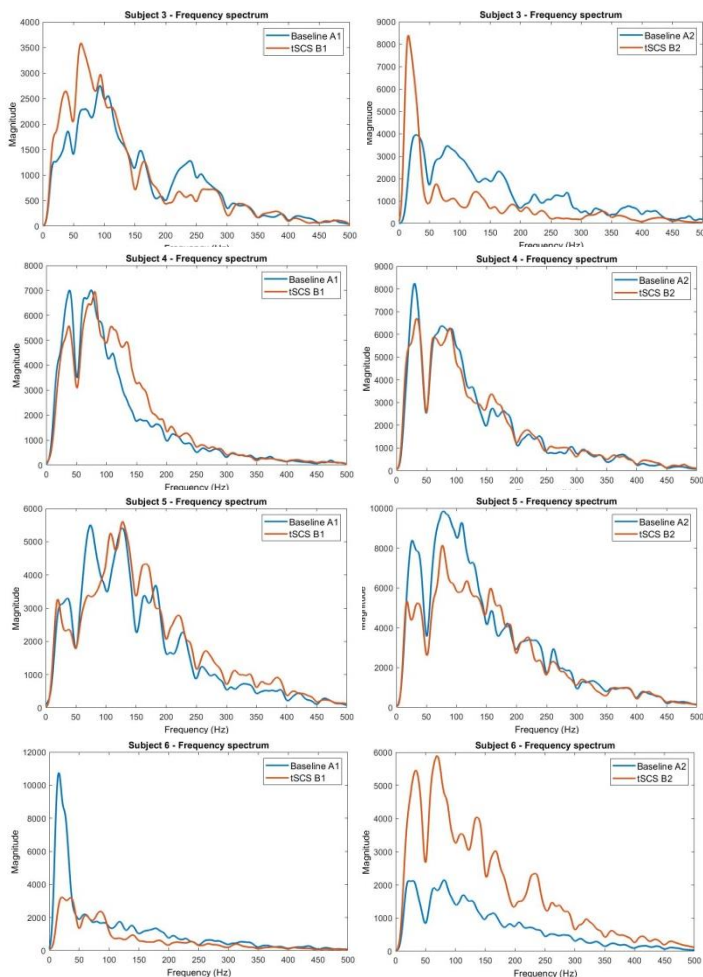
Figure 1: Each graph depicts the power spectrum of EMG of the triceps surae muscle in two Achilles tendon tests of one subject. Each graph shows data from a baseline measurement (blue) and after tSCS assessment (red). The left column is from data gathered in phase 1 and the right column is from data gathered in phase 2. Eighteen to twenty four weeks washout period was between phases.

Discussion

The result of the recordings in Achilles tendon test by stroke patients in tSCS treatment show a shift of the EMG signal from the triceps surae towards lower frequencies in two subjects, no shift in one and towards higher frequencies in one. Whether this is due to transfer of the muscle fibres towards a slower or faster types has to be further investigated. Development in both directions are possible and depend on the lesion of each individual and his spasticity [6,7].

Conclusions

Clear conclusions about changes in muscle structure cannot be made because even after a long search of patients, it was difficult to obtain a sufficiently homogenous group in terms of type and duration of the stroke and the location of the damaged brain tissue. These findings support the possibility that tSCS treatment can affect muscle composition. Four post-stroke individuals participated in this study, to further investigate the effect of tSCS treatment on muscle composition more participants should be investigated. Healthy subjects could also be investigated in the same manner for comparison.

References

[1] Hofstoetter, Ursula S.; McKay, William B.; Tansey, Keith E.; Mayr, Winfried; Kern, Helmut; Minassian, Karen: „Modification of Spasticity by Transcutaneous Spinal Cord Stimulation in Individuals with Incomplete Spinal Cord Injury". In: *The Journal of Spinal Cord Medicine,* 37, M b arz, Nr.2, S. 202-211**,** 2014

[2] Vargas Luna, José L.; Gudfinnsdottir, Halla K.; Magnusdottir, Gigja; Gudmundsdottir, Vilborg; Krenn, Matthias; Mayr, Winfried; Ludvigsdottir, Gudbjorg; Helgason, Thordur: „Effects of Sustained Electrical Stimulation on Spasticity Assessed by the Pendulum Test". In: *Current Directions in Biomedical Engineering* 2, Nr. 1. S. 405-407, 2016

[3] Dimitrijevic, Milan R. (Hrsg.): *Restorative Neurology of Spinal Cord Injury*. New York: Oxford University Press, 2012

[4] Aiva Levins, Chet T. Moritz: Therapeutic Stimulation for Restoration of Function after Spinal Cord Injury. Physiology 32: 391-398, 2017. Doi:10.1152/physiol.00010. 2017

[5] Kupa, E. J., et al. „Effects of Muscle Fiber Type and Size on EMG Median Frequency and Conduction Velocity". *Journal of Applied Physiology*, vol. 79, no. 1, pp. 23–32., doi:10.1152/jappl.1995.79.1.23, 1995

[6] Sudarsan Srivatsan, Xiaogang Hu, Brian Jeon, Aneesha K. Suresch, William Zev Rymer, Nina L. Suresch: „Power Spectral Analysis of Surface EMG in stroke: a preliminary study". *6th Annual International IEEE EMBS Conference on Neural Engineering.* 2013

[7] Silvija Angelova, Simeon Ribagin, Rositsa Raikova, Ivanka Veneva: „Power frequeny spectrum analysis of surface EMG signals of upper limb muscles during elbow flexion – A comparison between healthy subjects and stroke survivors". *Journal of Electromyography and Kinesiology* 38, 7-16, 2018

Author's Address

Halldór Kárason
Reykjavik University, Iceland
halldork15@ru.is

Effects of muscle fatigue on classification accuracy of Pattern recognition in a myoelectrical control system

Baumgartner M[1], Aramphianlert W[2], Mayr W[2]

[1] University of Applied Sciences Technikum Wien, Vienna, Austria

[2] Center of Medical Physics and Biomedical Engineering, Medical University of Vienna, Austria

Abstract: *Upper limb prostheses users state intuitively to use and control reliability as one of their highest priorities. Advances in data processing and classification algorithms have enabled improvement in pattern recognition systems for prosthetics, leading to more accurate control systems. However, muscle fatigue is known to change EMG signals' characteristics, which could affect the classification accuracy of the machine learning-based control systems. To quantify its impact in detail, a machine learning-based myoelectric control system was developed, trained with different data (fatigued, non-fatigued), and tested. For this purpose, EMG data from 10 healthy subjects were collected. A non-linear support vector machine was applied to recognise 7 different arm movements. After an optimisation procedure, the machine classified 99% of movements correctly, however testing the system with fatigued data reduced the classification accuracy by 27% on average (p < 0.001). To compensate for this effect, two strategies which provide improvement of pattern recognition in EMG signals of fatigued muscles were explored and included in this paper.*

Keywords: *Prosthetics, Neuroprosthese, Muscle Fatigue, Myoelectric Control System, Machine Learning*

Introduction

While nowadays prosthetic devices for the upper limb appear promising, a majority of patients rejecting electrically powered prostheses name difficulties in control as a reason of abandonment [1], especially the intuitiveness of use and reliability. The workflow of externally powered prostheses control can be explained as follows: Information is acquired from the amputees' body, the data is processed and interpreted by a control system that maps users' intentions to actuator control signals. Since the electromyography (EMG) signal is mostly used as the input of the control system, the term "myoelectrically controlled prostheses" has become almost synonymous with "externally powered prostheses". For the purpose of daily prosthetic use, EMG data are acquired non-invasively from the muscles via the surface electrode. However, instabilities can occur on the sEMG signal due to several factors, for instance, skin impedance changes, electrode shifting, and muscle fatigue. All these factors have been mentioned to reduce the classification accuracy of the pattern recognition based myoelectric control systems due to the signals' characteristics changes which cause unreliabilities to the system.

Pattern recognition technique has been applied to this application due to it provides more natural movement to the device, thus allows the user to control the device intuitively. However, this approach, in general, is developed and evaluated in controlled environments. Therefore, it is more sensitive to changes in sEMG signals' characteristics. In recent years, advancements in technology have been applied to overcome the factors of the system's unreliability. For example, implantable electrodes have been developed to overcome the challenges of electrode shift and impedance changes. However, there is no solution to counteract muscle fatigue due to it is a common muscle condition which occurs in every person after an interval of muscle contractions.

Although muscle fatigue has been known as a problematic issue, the effects of this phenomenon on the pattern recognition based myoelectric control system have not been clearly and systematically revealed. In this study, a pattern recognition based myoelectric control system was implemented based on the machine learning (ML) technique. The sEMG data were collected from a group of volunteers in two different conditions of non-fatigued and fatigued states. The system was trained, optimized, and tested according to the designed protocol. Hence, the performance of the system whil dealing with fatigued data was evaluated. Additionally, two startegies to compensate for the effects of muscle fatigue have been explored.

Material and Methods

For the purpose of testing the effects of muscle fatigue, a control system was developed based on a machine learning model. This gave the full control over the parameters and therefore allowed for higher transparency of results. The system classified seven movements; hand opening, hand closing, pronation, supination, wrist extension, wrist flexion, and a neutral state.

Developing the control system

As mentioned above, various approaches have proven to achieve satisfying results. For this paper, a Support Vector Machine (SVM) was selected as the myoelectric classifier. The SVM was chosen because of their more transparent approach and the lower need for training data compared to other ML methods, such as Artificial Neural Networks. The SVM was implemented in Python 3.6, using various libraries from Python's Scientific Stack (NumPy, SciPy, pandas, scikit-learn, …).

Participant recruitment

Ten healthy able-bodied participants were recruited to the study. Information and details regarding the study were clearly explained to them prior to the actual data collection procedure and the inform consents were signed. The information of the recruited participants is listed in Table 1.

Table 1: List of participants

| Age [years]	Sex	Height [cm]	Weight [kg]	BMI
23	M	183	70	20.90
59	M	189	77	21.56
22	M	177	78	24.90
23	M	182	73	22.04
59	F	167	58	20.80
32	M	176	80	25.83
29	F	169	65	22.76
30	F	167	60	21.51
20	F	159	59	23.34
25	F	171	60	20.52
avg. 32.2 ±13.88		avg. 174 ±8.60	avg. 67.5 ±8.86	avg. 22.41 ±1.70

Instrumentations

A portable EMG data acquisition device, built at the Medical University of Vienna [2], was used for data acquisition. Eight channels of data were recorded at 2000 Hz sampling rate with 24-bit resolution. The acquired data was transmitted to a personal computer via a universal serial bus (USB). Sixteen self-adhesive AG/AgCl surface electrodes (bipolar configuration, 2 for each of the 8 channels) were placed symmetrically around the proximal third of the forearm with the inter-electrode distance of 20mm. The reference electrode was located on the humerus' medial epicondyle. The first channel was located above the *musculus extensor digitorum*, then the remaining were arranged in equally spaced around the forearm. Figure 1 shows the electrode positioning in one subject.

Figure 1: Electrode placement for data acquisition

Data acquisition process

The data collection procedure was divided into two sections; non-fatigue (I) and fatigued sections (II). Both sections started with a maximum voluntary contraction (MVC) measurement. This is followed by the relevant collection session. Data from this session was later used for the SVM training and evaluation. After the recording session of Section I, a fatiguing exercise was conducted to induce muscle fatigue to acquire fatigued data in later Section II. The diagram of data collection procedure is depicted in Figure 2. the data collection procedure
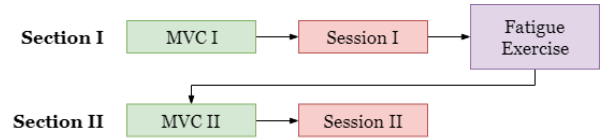
Figure 2: Diagram of data collection protocol

During each MVC measurement, every movement was performed three times with full force. In the recording sessions, each movement was repeated five times. In both the MVC and the session periods, movements were performed in the following way: the subjects were given 5 seconds to prepare, 3 seconds to move into the target position, 5 seconds to hold the position, 3 seconds to move back to the neutral state and 5 seconds to stay relax. The movements were done in a randomised order to avoid potential memory effects. After section I, the participants were requested to repeatedly perform the fatigue exercise until they had felt muscle fatigue and unable to continue the exercise. However, they were allowed to freely stop the exercise when they felt any discomfort or pain. Each iteration of the exercise consisted of 20 repetitions of 1s alternately wrist flexion/extension, and 20s of isometric wrist extension, 20s of isometric wrist flexion with 5s resting in between each movement. Then, the data collection was continued in Section II.

Data processing

To prepare the collected data for the myoelectric classifier implementation, the data was filtered and segmented in contraction-wise. Then, an analysis window (256ms, 64ms sliding step) was applied on the signal segments for myoelectric feature extractions. Eleven myoelectric features [3]; Root Mean Square (RMS), Mean Absolute Value (MAV), Waveform Length (WL), Zero Crossings (ZC), Slope Sign Change (SSC) and 6 autoregressive (AR) coefficients were extracted, hence this resulted as an 88-dimensional (11 features x 8 channels) feature vector for each sliding window in total. Every single feature vector was labelled by its corresponding movement class and collected in the dataset matrix for the myoelectric classifier implementation. Selection of these features is being done in accordance with published literature [4]. The dataset was separated into training and testing data with a ratio of 70:30.

Myoelectric classifier training and optimization

To obtain a high classification accuracy myoelectric classifier, the SVM model was tuned and optimized. Five parameters; kernel type, decision function, and the marginal value C and γ were considered and carefully selected. To find the best parameter combination, an iterative grid search was applied. In the first iteration, kernel type and decision function were selected by a broad grid search. Afterwards, only C and γ values needed to be adjusted in three more iterations, narrowing down the options further until a satisfying result was found. Each combination was tested using 10-fold cross validation. This was done with a stratified sample of 10% of the training data to reduce calculation times.

Fatigued EMG signal analysis

Before testing the model, the data were analysed to determine whether the occurrence of fatigue can be confirmed from the collected data. For this purpose, the contractions of the 20s isometric wrist extension portion from the fatigue exercise were examined. The sEMG data of channel 1 were segmented with a non-overlapping analysis window of 1s, in which four indicators were calculated: median frequency (MDF), mean frequency (MNF), amplitude as Root Mean Square (RMS) and a fatigue index (FI) proposed by Dimitrov et al. in 2006 [5]. The evidence state that during the occurrence of muscle fatigue, the MDF and the MNF shift to the lower frequency, while the RMS and the FI are supposed to increase over time during exercise [6][7]. Therefore, the sEMG dataset which the majority of these four indicators (i.e. at least 3 out of 4) with statistical significance ($p < 0.05$) were accepted as "fatigued" and data was labelled accordingly. The sEMG data of the subjects whose data did not show provable signs of fatigue were excluded in further analysis.

Myoelectric classifier evaluations

The optimized model was tested with rested muscles' signals from Section I. Testing data consisted of 8310 samples were equally divided into 30 subsets, leading to 277 samples per subset. Each subset was tested individually, which resulted in 30 accuracy values. The average accuracy and standard deviation were calculated. Afterwards, data from Section II (fatigued data) was tested in a similar manner to quantify the effects of muscle fatigue.

Results

Myoelectric classifier training and optimization

During the four iterations of grid search procedures, 2311 different models were assessed. The radial basis functions (RBF) gave the best results as the kernel function. The decision function ("one vs. one" or "one vs. rest") showed no effect on the classification accuracy, as they resulted in the same mathematical model each time while the "one vs. rest" method used shorter computational time. In three latter iterations, C and gamma value were selected at C = 10 and gamma = 2.2 with an RBF kernel.

Fatigued EMG signal analysis

In five subjects (No. 1, 2, 4, 6 and 7) three out of four fatigue indicators (MDF, MNF, FI) indicated fatigue during the last isometric contraction in the last isometric contraction with over 95% confidence (2-tailed p-value converted from Pearson correlation coefficient). The other five subjects (No. 3, 5, 8 and 9) were excluded due to the occurrence of muscle fatigue could not be confirmed with the selected indicators.

Myoelectric classifier evaluations

The model was able to classify the data with the averaged classification accuracy of $99.29 \pm 0.47\%$ for the testing on the non-fatigued test samples. The classifier showed the decreasing in classification accury to $72.60 \pm 2.56\%$ when it was tested on the fatigued samples, which is 26% lower than the non-fatigued group. A paired t-test as applied to confirm statistical significance ($p < 0.001$). The most drastic reductions in classification accuracy were seen in less expressive movements such as pronation (-35.74%) and supination (-22.96%). More distinct movements such as wrist flexion (-4.40%) and wrist extension (-3.80%) suffered less reduction.

Compensation strategies

During the myoelectric classifier training, two feasible compensation strategies to mitigate the effects of muscle fatigue data on the classification accuracy were explored, as follow:

(1) Adjusting the dataset: By including fatigued samples to the training dataset, the classification accuracy increased to $99.42 \pm 0.46\%$ while the classification rate when evaluating the classifier with non-fatigued testing data was not affected by this process.

(2) Adjusting the model's parameters: By reducing the values of the C and gamma values, the classification accuracy of the non-fatigue testing data was inevitably decreased. However, while truing to reduce both parameters' values by the step of 10% of the optimized values until they reached 0.1%, the classifier showed increasing in the classification accuracy when dealing with the fatigued testing data as shown in figure 3.
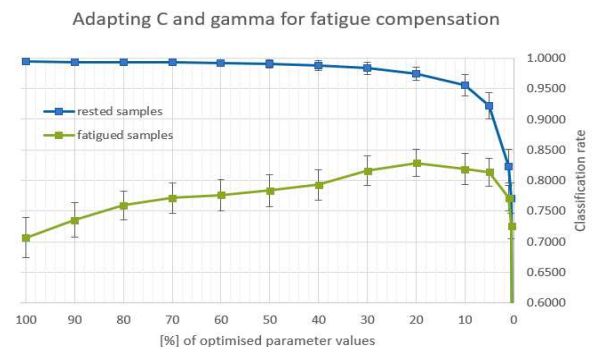
Figure 1: Success rate in reduced parameter strategy

The best trade-off situation was explored at the setting where the values of C and γ were reduced by 20% of their optimized values (C = 8 and γ = 1.76). By using this setting, the classifier was able to classify the non-fatigued data at $97.47 \pm 1.09\%$ accuracy (approximately 3% decreasing) while it was $82.88 \pm 2.21\%$ accuracy when dealing with the fatigued testing data (which is over 10% of increasing).

Discussion

Measurement setup

In this study, the symmetrical electrode placement was chosen over the anatomical selection, since it is easier to be repeated. Since the dataset was exclusively collected from a group of healthy subjects, the accuracy rates were expected to be higher than in amputees who the pathological issues and different muscle conditions could

be found. The electrodes were placed at the most proximal third of the arm to replicate the actual setting of using a myoelectrically controlled arm prosthesis when the hand gets amputated and partial forearm muscles remain. During the data collection, the subjects sat on a chair with their arms were freely hanging down towards the floor. This might affect the quality of the sEMG signals and also the classification rate of the myoelectric control system. However, this sitting position was decided to be used to avoid the situations when the subjects got fatigued from raising their arms. Thus, a clear conclusion could be made.

Data treatment and fatigue analysis

For the grid search optimization, only 10% of data samples were used to find the proper parameter setting over the number of 2300 combinations. This helps to reduce the computational time for the classifier training, as the training time increases exponentially with increased numbers of training samples, especially if the models were under- or overfitting. In order to guarantee that the model was learning with the representative portion of the full data, a stratified sample selection method was used for the data selection.

During the fatigue analysis, only the sEMG data of channel 1 was analyzed due to this was this is the only channel which anatomically attached on a specific muscle, which is the *extensor digitorum*. On the other hand, the other channels were placed with equally spaced around the forearm that might acquire the combined sEMG signal from multiple subjects. This was held to avoid misinterpretation of the fatigue analysis. The result showed that there was no increasing of the sEMG amplitude been observed. This could be explained by the relatively short period of the contractions (20 seconds only). As in the literature, this is the most disputed indicator, suggesting that it should possibly be given less weight in assessing fatigue.

Effects of muscle fatigue and compensation

A decreasing of over 26% is a significant reduction in classification accuracy. Instead of 1 in 100, the prosthesis would fail to execute the correct movement in 3 out of 10 times. This result has proven that the hypothesis that muscle fatigue has no effect can be rejected. The changes in sEMG data during muscle fatigue negatively affects the classification rate of the optimized myoelectric classifier.

In comparison between two proposed compensation strategies, one can easily determine that including a fatiguing exercise and fatiguing data samples in the training protocol is worth the additional effort. The dataset with assorted data was expected to reduce the overall prediction accuracy of both cases (non-fatgiued and fatigued), in fact, this was not observed, as both classification rates were higher than 99%. The latter strategy of adjusting the values of C and γ showed lower performance to maintain the accuracy rate. However, the advantage over another starategy is that there is no need for additional training data. Therefore, by using this strategy, the participants do not have to attent to a long session of data collection, including the fatigue-induced exercise

which would be more practical in clinically and commercially uses of the myoelectrically controlled arm prosthesis. Even though myoelectric control is most known for control of mechanical arm prosthese, it is equally usefull for control of neuroprostheses, namely in the paralyzed upper extremit.

Conclusions

The findings showed that when dealing with the fatigued sEMG data, although the myoelectric classifier is well optimized, the classification accuracy of the system can be decreased drastically. However, with some adjusments, the effects of muscle fatigued sEMG data on the myoelectric control system can be mitigated.

References

[1] E. Biddiss, T. Chau, "Upper-Limb Prosthetics," *American Journal of Physical Medicine & Rehabilitation*, vol. 86, no. 12, pp. 977–987, 2007.

[2] C. Kast, W. Aramphianlert, M. Krenn, C. Hofer, O. C. Aszmann, and W. Mayr, "Development of a closed-loop control system for upper limb prosthesis integrating electromyographic inputs and position feedback," in *"Dreiländertagung" Swiss, Austria, and German Societies for Biomedical Engineering (BMT2016)*, 2016.

[3] M. Hkonen, H. Piitulainen et al., "Current state of digital signal processing in myoelectric interfaces and related applications," *Biomedical Signal Processing and Control*, vol. 18, pp. 334–359, 2015.

[4] T. Lorrain, D. Farina et al., "Surface EMG classification during dynamic contractions for multifunction transradial prostheses," *2010 Annual International Conference of the IEEE Engineering in Medicine and Biology*, 2010.

[5] G. V. Dimitrov, et al. "Muscle Fatigue during Dynamic Contractions Assessed by New Spectral Indices," *Medicine & Science in Sports & Exercise*, vol. 38, no. 11, pp. 1971–1979, 2006.

[6] Marco, G., Alberto, B., & Taian, V. (2017). Surface EMG and muscle fatigue: multi-channel approaches to the study of myoelectric manifestations of muscle fatigue. *Physiological Measurement,* 38(5), R27–R60.

[7] Cifrek, M., Medved, V., Tonković, S., & Ostojić, S. (2009). Surface EMG based muscle fatigue evaluation in biomechanics. *Clinical Biomechanics*, 24(4), 327–340.

Author's Address

Martin Baumgartner, MSc.
Student at UAS Technikum Wien
gr17m008@technikum-wien.at
www.technikum-wien.at

Surface EMG based muscle fatigue level estimation model towards adaptive myoelectric control of mechanical upper-limb prosthesis or neuroprostheses.

Aramphianlert W[1,2], Aszmann O C [2], Mayr W[1,2]

[1]Center of Medical Physics and Biomedical Engineering, Medical University of Vienna, Austria
[2]Christian Doppler Laboratory for Bionic Reconstruction, Medical University of Vienna, Austria

Abstract: *A myoelectric control system is a human-machine interface with its important application for control of electrical powered arm prostheses, or control of neuroprostheses. This system allows the patients with limb loss to intentionally control the bionic arm with the biopotentials generated by the contractions of the residual muscles, so-called surface electromyography (sEMG) signals. Muscle fatigue is an inability to maintain muscle contraction at the desired level. This muscle condition has been mentioned as a factor which causes instability to the sEMG signals, thus results in decreasing the reliability of the myoelectric control system. Therefore, an ability to monitor and apply the proper adaptation to counteract this muscle condition is a further step of the myoelectric controlled prosthesis development. This paper aims to achieve an approach to estimate the level of muscle fatigue based on the sEMG signals. The signals were collected from 8 healthy able-bodied volunteers while attending to a muscle fatigue-inducing exercise. The exercise was designed by replicating the scenario of controlling a myoelectric controlled arm prosthesis. An investigative study was conducted to observe the changes in 4 spectral myoelectric features. Finally, a model for estimating the level of muscle fatigue was created based on the observed pattern of change in myoelectric features.*

Keywords: *Myoelectric control, muscle fatigue, prostheses, neuroprostheses, electromyography, signal processing*

Introduction

Muscle fatigue is defined as an inability to perform and maintain muscle contractions at the desired level. This condition commonly occurs after a period of constantly or repeatedly contracting the muscle. It has been mentioned as a cause of instability of the sEMG signals which affect the efficiency of the myoelectric control system [1]. In general, muscle fatigue can be physically observed via manifestations, e.g., muscle tremor, pain, or reducing in force output. Besides, the muscle fatigue can also be observed via changes in sEMG contents, a so-called *myoelectric manifestation of muscle fatigue* [2] which reveals as a shifting of frequency contents to the lower frequency, an increase in amplitude-related contents, and decreasing in the conductive velocity of muscle fibers [3]. Recently, a number of different sEMG based muscle fatigue detection studies were proposed, for example, investigations on myoelectric variable [4], inventing new muscle fatigue indices [5], or multivariate fatigue detection techniques [6]. However, according to the author's knowledge, there is no standard method which accurately assesses muscle fatigue during the dynamic submaximal contractions so far.

In this paper, an investigative study on myoelectric contents (as also knows as features) was conducted. A muscle fatigue-inducing exercise was designed and aimed to replicate the scenario of using the myoelectric control system. The aim of this study was to achieve a non-invasive approach to monitor the progression of muscle fatigue based on the sEMG signals, hence a proper adaptation could be provided to the myoelectric control system according to the fatigue level. In the following sections, an investigative study on myoelectric features for the progression of muscle fatigue is going to be presented. The outcome of the study resulted in a muscle fatigue level estimation model which was created based on the investigative results.

Material and Methods

Data Collection

The sEMG signals were collected from 2 forearm muscles; *extensor carpi radialis* (ECR) and *flexor carpi ulnaris* (FCU) on the dominant side of 8 able-bodied volunteers; 5 males and 3 females. their age, weight, and height (showing in mean ± S.D.) are 29 ± 3.02 years old, 68.62 ± 13.54 kg, and 175.5 ± 9.4 cm respectively. The volunteers were requested to abstain strenuous exercise to prevent the muscles from tiredness prior to the date of data collection. Information and details of the data collection procedure were clearly explained to the volunteers and the informed consents were signed.

Prior to the data collection procedure, the skins were prepared and cleaned to remove oil, debris, and dead skin cells. The self-adhesive Ag/AgCl surface electrodes were placed over the belly of the two muscles with the inter-electrode distance of 20 mm. The reference electrode was placed over the *medial epicondyle* of the humerus bone.

A custom-made data acquisition device, a so-called 'usbEMG', was used to acquire the sEMG signals [7]. The device was developed based on an analog frontend chip; ADS1299 (Texas Instrument Inc., USA). The chip provides low-noise, 8 channels, 24-bits resolution, up to 16k samples-per-second (SPS), and the gain of each channel can be adjusted individually. The signals were transmitted to the personal computer via the USB 2.0. and stored digitally in HDF5 format. A software application was implemented to work with the device. This software provides the device manipulation and communication, real-time signal visualization, and also data recording. The data collection protocol was designed to replicate the situation of using the myoelectric control system with 2 channels of input. The sampling frequency of the usbEMG device was set to 4k SPS with the gain of 6x. The volunteer sat comfortably on a chair with their recording arm on the

armrest. A monitor was set to display the visual guideline and real-time visualization of the sEMG root-mean-square (RMS) values. The data collection procedure was separated into 2 phases; maximum voluntary contraction (MVC) measurement and muscle fatigue-inducing exercise.

The MVC levels were measured separately on the ECR and FCU muscles. The volunteer was requested to perform 5s wrist extension (WE) and wrist flexion (WF), 3 repetitions for each movement, by following the guidance on the screen. The MVC levels of the ECR (on channel 1) and FCU (on channel 2) muscles were calculated by averaging the maximum root-mean-square (RMS) values across 3 repetitions of WE and WF respectively. Then, the volunteer was allowed to freely observing the sEMG signal visualization and get familiar with the software. A resting interval of 10-15 minutes was given to the volunteer to let the muscles recovered from tiredness and muscle fatigue.

Consequently, the volunteer had to attend to the muscle fatigue-inducing exercise for the sEMG signals recording. The volunteer performed a pattern of WE and WF at 40% of the MVC level. The pattern consisted of 6 repetitions of dynamic contraction (1s transition from resting position, 5s of holding the target movement contraction, and 1s transition back to resting position), and a 10s isometric contraction of the target movement as shown in Figure 1. The visual guidance line and the real-time RMS values of the sEMG signals were displayed on the screen, hence the volunteer had to perform the contraction by following the visual guideline as much as possible. The exercise was iteratively repeated until the volunteer had muscle fatigue and was unable to keep continuing. However, they were able to discontinue the exercise whenever they had pains or discomforts. The recording was performed on the ECR and FCU muscles separately. The procedure started with the ECR muscle followed by 10-15 minutes break for muscle recovery, then the recording was continued on the FCU muscle respectively.
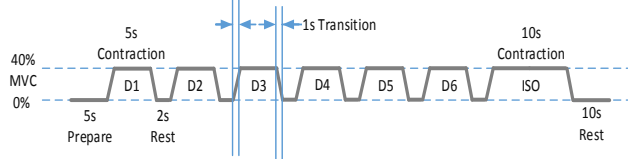
Figure 1: The pattern of muscle fatigue-inducing exercise. *ISO* and *D1-D6* represent the isometric contraction and 6 repetitions of the dynamic contractions respectively.

Data Processing and Analysis
The collected sEMG signals were filtered with the 4th order Butterworth bandpass filter (5-500 Hz) and the 50Hz notch filter to remove the interferences. Then, the signals were segmented into contraction-wise segments. The contractions of the sEMG signals were automatically detected by the instantaneous energy-based segmentation method [8]. The outcomes of this method resulted in a number of files which contained the sEMG signals (2-channels of ECR and FCU muscles) of a single contraction.

The isometric segments were used for fatigue testing in order to confirm the occurrence of muscle fatigue in the collected sEMG signals. The testing was done based on the fatigue test protocol [9]. The isometric segments of the last iteration were used for the assessment, due to they were assumed to be the moment when muscle fatigue had occurred. The slope of the mean frequency (MNF) time plots were analyzed by linear regression analysis (with a significant level of $p < 0.05$). If a significant negative slope was observed, the occurrence of muscle fatigue in the sEMG signal can be confirmed.

The dynamic segments were processed and used for the myoelectric feature investigation. Every dynamic contraction segment was divided into 3 portions; 1s transition (from resting), 5s static contraction, and 1s transition (to resting) as shown in Figure 2.
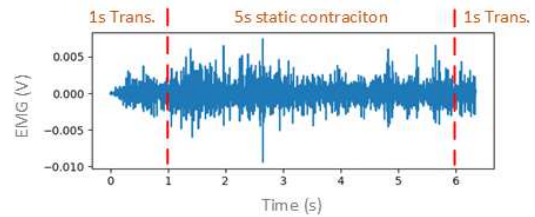
Figure 2: A segment of the sEMG signal from dynamic contraction. The segment consists of 3 portions; 1s transition (from resting), 5s static contraction portion, and 1s transition (to resting).

The transition portions were removed and the static portion was equally segmented into small non-overlapping chunks of 1s interval. In each chunk, the power spectrum of the signal was calculated by applying the short-time Fourier transform (STFT) equation with a *Hanning* window of 256ms and 64ms sliding step. Then, four spectral myoelectric features, i.e., instantaneous root-mean-square voltage (Vrms) [10], instantaneous energy (iE) [8], mean frequency (MNF), and median frequency (MDF) [11] were extracted out of the analysis window. The features were averaged across the other windows within the same corresponding chunk. Therefore, every single chunk was represented by the averaged 4 spectral myoelectric features.

The observation and analysis were done separately on each muscle which corresponded to the movement, for example, only the sEMG signal of the ECR muscle was analyzed during WE and the FCU muscle during the WF. Linear regression analysis (with a significant level of $p<0.05$) was applied to the time series in order to observe significant changes in the myoelectric features.

Results

During the data collection, the volunteers performed a different number of repetitions of wrist movements. There was no report of discontinuing the data collection procedure due to pains or discomfort.

The results of the fatigue test showed that most of the MNF time plot gave the negative slopes. However, only a few of them were statistically significant; ECR of the volunteers 2, 4, 6, 7 and FCU of the volunteers 5, 6, 7. In contrast, insignificant positive slopes could also be

observed in the ECR of the volunteers 1, 3 and in the FCU of the volunteer 4.

The linear regression analysis on the selected 4 spectral myoelectric features, MNF and MDF showed the results in significant negative slope in all cases of the ECR muscle, and in almost all cases of the FCU muscle (insignificant negative slopes were found in volunteers 1, 7 and insignificant positive slope in the volunteer 3). There was no pattern of change to be obviously observed for Vrms and iE.
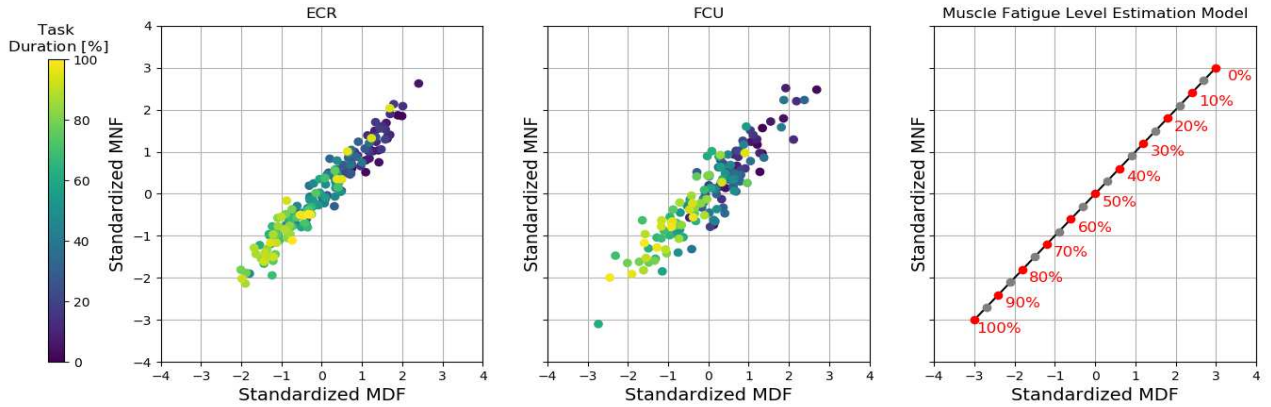
Muscle Fatigue Level Estimation Model

According to the investigative results, the pattern of changes due to the progression of fatigue could be observed by MNF and MDF as significant negative slopes. A new plot of MNF-MDF map was created to visualizes the relationship between the samples of these two features. The MNF and MDF samples were standardized for the purpose of comparing the samples across all volunteers. Figure 3 (left) and (middle) show the standardized MNF-MDF maps of a selected volunteer on the ECR and FCU muscles respectively. The color mapping was added to the MNF-MDF map in order to trace the progression of the feature change along with the task duration.

The progression of muscle fatigue can be observed via the gradually changing of MNF-MDF feature from the top-right to the bottom-left corners of the map. Therefore, the muscle fatigue level estimation model was defined as a diagonal line connecting between two coordinates (3,3) to (-3,-3) as shown in Figure 3 (right). Twenty-one reference points were defined along with the line. To estimate muscle fatigue level, distances from a single feature point to every reference points were calculated by the two-dimensional Euclidean distance equation:

$$Dist(x_i, Ref_k)$$
$$= \sqrt{(MNF_i - MNF_{Ref_k})^2 + (MDF_i - MDF_{Ref_k})^2} \quad (1)$$
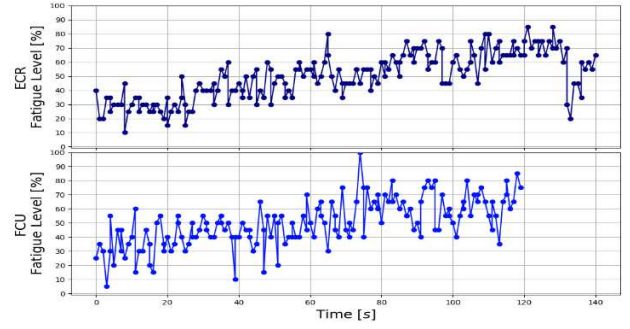
where x_i is the ith feature point, Ref_k is the kth reference point. Then, the reference point with the shortest distance was selected as the corresponding fatigue level of that feature point as in the equation

$$Fatigue\ Level = argmin(Dist(x_i, Ref_k)), \quad k = [1, ..., 21] \quad (2)$$

Figure 4 shows the results of muscle fatigue level estimation calculated by the proposed model.

Figure 4: Fatigue level estimations of the volunteer 5 on (top) ECR muscle and (bottom) FCU muscle.

Discussion

The aim of this study was to achieve an approach to monitor the progression of muscle fatigue based on the sEMG signal. Two superficial forearm muscles; ECR and FCU were selected due to these muscles are frequently used in the myoelectric controlled arm prosthesis. The able-bodied volunteers were recruited to the study instead of the amputated subjects in order to reduce the diversities and pathological conditions of the muscles which might lead to a misinterpretation of the results.

However, in this study, the inconsistent result was found in the fatigue test protocol compared to the original study [9], which the assessment was done on the *biceps* and *triceps brachii* muscles. Those two muscles response to the force exertion and movement of the elbow joint which moves in only 1 degree-of-freedom (DoF) movement of flexion/extension. In comparison to the wrist joint which dominates higher DoF movements, force exertion and movement are responded by multiple muscles around the forearm. Accordingly, the volunteers might perform the WE and WF movements with the superimposed wrist abduction and adduction. Hence, muscle fatigue might occur in the nearby muscles instead of the target muscles. Therefore, the design of the muscle fatigue-inducing exercise needs to be done carefully.

Figure 3: The standardized MNF-MDF maps of the volunteer 5 on (left) ECR and (middle) FCU muscles. (right) The muscle fatigue level estimation model.

So far, there is no direct approach to monitor the progression of muscle fatigue, force exertion level has been frequently used as an indirect approach. Mostly, the participants were requested to keep exerting the force at a specific level until they reach the failure point. In general, a hand dynamometer is an apparatus which can be used to measure the force exerted by forearm muscles. However, in this study, to replicate the scenario of controlling a myoelectric controlled arm prosthesis, it was assumed that the force could not be measured via the hand dynamometer due to the hand got amputated. Therefore, the percentage of MVC was used as an indirect approach to measuring the force level of the muscles.

The result showed that MNF and MDF were the two myoelectric features that revealed the pattern of change in negative slopes as the progression of fatigue, which was consistent with previous studies. The muscle fatigue level estimation model was created based on these two features. The model was designed to estimate the fatigue level in terms of percentage. Therefore, the adaptations which would apply to the myoelectric control system could be varied according to the fatigue level, not only be limited with specific states, e.g., non-fatigue, transition-to-fatigue, or fatigue.

Although the purposed model shows the possibility of muscle fatigue level estimation, there are the limitations and improvements which need to be explored for further studies, for example, i) conducting the investigation on a larger group with higher diversities (including amputated volunteers), ii) there are a number of myoelectric features that are recently proposed which might be more sensitive to muscle fatigue and give better result in estimation, iii) the model needs to be validated under different conditions, e.g., variations of MVC level, duration, and electrical stimulated contractions, iv) implementing the real-time fatigue level estimation for instantly monitoring the progression of fatigue during the fatigue-inducing exercise.

Conclusion

The myoelectric feature investigations showed that the negative slopes were revealed by the MNF and MDF while Vrms and iE showed no pattern. The muscle fatigue level estimation model was created based on the MNF-MDF map to estimate fatigue level in terms of percentage. This model showed the feasibility of monitoring the progression of muscle fatigue which could be applied to many related studies.

References

[1] A. G. Barszap, I.-M. M. Skavhaug, and S. S. Joshi, "Effects of muscle fatigue on the usability of a myoelectric human-computer interface," *Hum. Mov. Sci.*, vol. 49, pp. 225–238, Oct. 2016.

[2] R. Merletti, "Muscle Fatigue and Time-Dependent Parameters of the Surface EMG Signal," in *Muscles Alive, Their Functions Revealed By Electromyography*, J. V. Basmajian, Ed. Williams & Wilkins, 1985, pp. 201–222.

[3] D. Farina, M. Pozzo, E. Merlo, A. Bottin, and R. Merletti, "Assessment of average muscle fiber conduction velocity from surface EMG signals during fatiguing dynamic contractions," *IEEE Trans. Biomed. Eng.*, vol. 51, no. 8, pp. 1383–1393, 2004.

[4] S. Thongpanja, A. Phinyomark, P. Phukpattaranont, and C. Limsakul, "A feasibility study of fatigue and muscle contraction indices based on EMG time-dependent spectral analysis," *Procedia Eng.*, vol. 32, pp. 239–245, 2012.

[5] G. V. Dimitrov, T. I. Arabadzhiev, K. N. Mileva, J. L. Bowtell, N. Crichton, and N. A. Dimitrova, "Muscle fatigue during dynamic contractions assessed by new spectral indices," *Med. Sci. Sports Exerc.*, vol. 38, no. 11, pp. 1971–1979, 2006.

[6] D. T. MacIsaac, P. A. Parker, K. B. Englehart, and D. R. Rogers, "Fatigue estimation with a multivariable myoelectric mapping function," *IEEE Trans. Biomed. Eng.*, vol. 53, no. 4, pp. 694–700, 2006.

[7] C. Kast, W. Aramphianlert, M. Krenn, C. Hofer, O. C. Aszmann, and W. Mayr, "Development of a closed-loop control system for upper limb prosthesis integrating electromyographic inputs and position feedback," in *"Dreiländertagung" Swiss, Austria, and German Societies for Biomedical Engineering (BMT2016)*, 2016.

[8] E. F. Shair, A. R. Abdullah, T. N. S. Tengku Zawawi, S. A. Ahmad, and S. Mohamad Saleh, "Auto-segmentation analysis of EMG signal for lifting muscle contraction activities," *J. Telecommun. Electron. Comput. Eng.*, vol. 8, no. 7, 2016.

[9] D. R. Rogers and D. T. MacIsaac, "EMG-based muscle fatigue assessment during dynamic contractions using principal component analysis," *J. Electromyogr. Kinesiol.*, vol. 21, no. 5, pp. 811–818, 2011.

[10] T. N. S. T. Zawawi, A. R. Abdullah, E. F. Shair, I. Halim, and S. M. Saleh, "EMG Signal Analysis of Fatigue Muscle Activity in Manual Lifting," *J. Electr. Syst.*, vol. 11, no. 3, pp. 319–325, 2015.

[11] S. Thongpanja, A. Phinyomark, P. Phukpattaranont, and C. Limsakul, "Mean and median frequency of EMG signal to determine muscle force based on time dependent power spectrum," *Elektron. ir Elektrotechnika*, vol. 19, no. 3, pp. 51–56, 2013.

Author's Address

Weerayot Aramphianlert, M. Eng.
Center for Medical Physics and Biomedical Engineering,
Medical University of Vienna, Austria
n1442050@students.meduniwien.ac.at
weerayot.a@gmail.com

Session 5:
Early Career Panel Discussion

Session 6:
Parameters and Technology

A percutaneous electrode for dorsal genital nerve stimulation; Comparison with a surface electrode

Rijkhoff NJM[1], Hennings K[1], Hellevik J[1], Knudsen DM[2]

[1] Department of Health Science and Technology, Aalborg University, Denmark
[2]InnoCon Medical, Aalborg, Denmark

Abstract: Several clinically available devices use electrical stimulation to treat urinary bladder dysfunction. For treatment of overactive bladder they either employ sacral root stimulation or tibial nerve stimulation. Clinical experiments have shown that dorsal genital nerve (DGN) stimulation can also be used to treat overactive bladder. Especially on-demand DGN stimulation has the potential to have a significant better clinical outcome than stimulation of the sacral roots or tibial nerve. However, there is currently no electrode available that can meet the requirements for clinical practice. In this study we tested the feasibility of a new electrode for DGN stimulation: a percutaneous electrode. We compared a percutaneous electrode with a standard surface electrode by measuring electrical impedance and stimulation thresholds in healthy volunteers. The results show that the differences in impedance and stimulation thresholds for percutaneous electrode and surface electrode are not very large. It can therefore be concluded that, from an electrical point, a percutaneous electrode would be as good as a surface electrode for DGN stimulation.

Keywords: Bladder, incontinence, percutaneous electrode, genital nerve stimulation

Introduction

Electrical stimulation has been used to treat symptoms of overactive bladder, e.g. incontinence, for many years. Clinically available neuromodulation therapies either use the sacral nerve roots or the posterial tibial nerve as target for stimulation [1]. But, although these therapies reduce symptoms, only a small fraction of the patients become symptom free.

Another stimulation target is the dorsal genital nerve (DGN). Studies have shown that DGN stimulation can suppress detrusor contraction [2] and could thus be used to prevent incontinence when stimulation is started soon after the onset of a detrusor contraction (on demand stimulation). This on demand stimulation has the potential to drastically increase the fraction of patients that become symptom free.

The main problem in the development of a clinically available DGN stimulation system is the electrode-nerve interface. Most attractive would be an implanted electrode. However, an implanted electrode is invasive and without good options for fixation the electrode will most likely migrate. The alternative is using surface electrodes. They are cheap, non-invasive and easy to place. For that reason have they been used extensively in research settings.

But long-term use of surface electrodes is challenging, at least in women, although they could be used in males. In male patients, at least one electrode is placed on the dorsal side of the penis. This may be suitable in a long term application providing that the patient is no longer incontinent. In female patients, one electrode is placed on the clitoris. Long-term adherence at this location is nearly impossible due to the moist environment. So, at least for females, another type of stimulation electrode is necessary.

Because the DGN lies just below the skin, a percutaneous electrode may solve this problem. The idea is to use an electrode that is anchored to the skin using a fistula like a piercing. Such an electrode would have a number of advantages as compared to a surface electrode. As the electrode is attached to the skin it will not migrate or become detached. In addition, it can stay there as a permanent electrode that doesn't require any attention or maintenance.

This study was conducted to investigate whether using a percutaneous electrode is feasible. Such an electrode is not available yet so a simple metal rod was used to test the idea.

In this study, we compared a percutaneous electrode and a standard surface electrode. We investigated the electrical impedance and thresholds to stimulation (perception threshold and maximum tolerance amplitude).

Material and Methods

For this study we used healthy volunteers with a nipple piercing, belly button piercing and/or genital piercing. The study was approved by the local ethical committee in North Jutland (approval N-20180002). Experiments were conducted while the subject was lying on his/her back on a bed. The existing piercing was removed and a surface electrode (3.2 cm diameter, round, Pals, Axelgaard, Denmark) was placed over the area where the piercing had been. A return electrode (5x5 cm, square, Pals, Axelgaard, Denmark) was placed about 5 cm away. Both electrodes were connected to stimulator 1 (DS5, Digitimer, UK) for impedance measurement or to stimulator 2 (DS7A, Digitimer, UK) to measure perception threshold and maximum tolerable stimulation amplitude.

Impedance was measured using a sinewave current of 1

Table 1: Mean impedance data. All impedances are given in kΩ. N = number of subjects

Stimulation site	Surface electrode			Percutaneous electrode		
	0.1 kHz	1 kHz	10 kHz	0.1 kHz	1 kHz	10 kHz
Genital (N=3)	7.06	2.68	1.10	7.25	5.44	1.63
Nipple (N=3)	21.11	4.67	1.13	6.24	1.45	0.79
Belly (N=4)	27.68	6.37	1.66	14.99	10.31	2.50

mA at 3 different frequencies (0.1 kHz, 1 kHz and 10 kHz). At each frequency the corresponding voltage was measured using an oscilloscope and the impedance was calculated by dividing the peak voltage by 1 mA.

To determine sensation threshold, 200 μs monophasic square current pulses at a frequency of 20 Hz were used. The return electrode was anode while the other was cathode. The amplitude was slowly increased until the subject reported sensation. This was taken as perception threshold. The amplitude was further increased until the subject asked to stop stimulation. This amplitude was taken as maximum tolerance amplitude.

After the measurements for the surface electrode were finished, the surface electrode over the piercing area was removed and a custom made stainless steel rod was inserted into the fistula. Care was taken that the ends of the rod were not in contact with skin. Both metal rod and return electrode were again connected to the stimulator and the measurements for impedance, perception threshold and maximum tolerance level were conducted in the same way as for the surface electrode.

Results

A total of 10 healthy subjects with relevant piercings were included. There were 3 subjects with a genital piercing, 3 with a nipple piercing and 4 with a belly piercing. All experiments were conducted without any complications. The impedances are shown in Table 1. It shows that for the nipple, surface electrodes had a higher impedance than the percutaneous electrodes. For the other 2 locations, the impedance of surface electrode was somewhat lower than the impedance of the percutaneous electrode.

Perception and max tolerance thresholds (Table 2) show that, compared with the surface electrodes, the percutaneous electrodes has the lowest threshold for perception.

Table 2: Mean perception and tolerance thresholds. Data is presented as mean (range) in mA. N=10

Surface electrode		Percutaneous electrode	
Perception	Max tol.	Perception	Max tol.
5.0 (1.8-11.7)	17.9 (8.8-30.0)	3.3 (1.3-6.3)	12.0 (6.8-27.5)

Discussion

It was expected that the impedance of the surface electrode would be much lower than the impedance of the percutaneous electrode. This because (1) the contact area between tissue and electrode is much larger for the surface electrode and (2) the surface electrode contains gel to reduce impedance. It turned out that the difference in impedance between percutaneous and surface electrode is not very large. The surface electrode impedance at both nipple and belly was higher compared with genital. The reason may be that the surface at both nipple and belly button is not flat. It is therefore likely that not the whole area of the surface electrode was in contact with the skin, which may have increased the impedance.

The thresholds for perception and tolerance were lowest for the percutaneous electrode while still sufficiently high to allow DGN stimulation if the electrode is at the right location.

Conclusions

It is known that DGN stimulation using surface electrodes can be used to treat incontinence caused by detrusor overactivity. However, using surface electrode 24/7 on the genitals is very problematic [3]. Percutaneous electrodes may solve this problem. Placing them is a simple procedure, just as removing them if the clinical benefits are unsatisfactory. They are anchored to the skin so they could provide a stable stimulation interface. This study shows that the electrical impedance is similar to that of a surface electrode and that the perception and max tolerance level are only a little lower compared to a surface electrode. This suggests that a percutaneous electrode could be used for stimulation of the DGN when located near the clitoris in females or near the dorsal penile nerve in males. In fact some volunteers with a genital piercing reported sensation in the DGN upon stimulation. Further work is needed to show that bladder contraction can be suppressed by DGN stimulation using a percutaneous electrode.

References

[1] M. Tutole, E. Ammirati, F. Van der Aa: What is new in neuromodulation for overactive bladder?, *Eur. Urol. Focus.*, vol. 4, pp. 49-53, 2018.

[2] J. Hansen, S. Media, M. Nøhr, F. Biering-Sørensen, T. Sinkjær, N.J.M. Rijkhoff: Treatment of neurogenic detrusor overactivity in spinal cord injured patients by

conditional electrical stimulation, *J. Urol.,* vol. 173, pp. 2035-2039, June 2005.

[3] F.M.J. Martens, J.P.F.A. Heesakkers, N.J.M. Rijkhoff: Conditional genital nerve stimulation to suppress detrusor overactivity using a needle electrode, *Spinal Cord,* vol. 49, pp. 566-572, 2011.

Author's Address

Nico J.M. Rijkhoff
Center for Sensory-Motor Interaction (SMI)
Department of Health Science and Technology
Fredrik Bajers Vej 7, 9210 Aalborg
Aalborg University, Denmark
nr@hst.aau.dk

Multi-channel transcutaneous auricular nerve stimulation

Rozman J[1,2], Pečlin P[3], Ribarič S[2]

[1]Center for Implantable Technology and Sensors, ITIS d. o. o. Ljubljana, Lepi pot 11, 1000 Ljubljana, [2]Institute of Pathophysiology, Faculty of Medicine, University of Ljubljana, Zaloška 4, 1000 Ljubljana, [3]Division of Gynaecology and Obstetrics, Šlajmerjeva 3 and Zaloška 7, 1000 Ljubljana, Republic of Slovenia

Abstract: The purpose of this study was to design and test a four-channel system for the selective transcutaneous stimulation (tVNS) of an auricular branch of the vagus nerve at the cymba conchae (CC) region to assess clinical benefits and limitations of tVNS when used for modulation of a heart function, modulation of respiratory rhythm or induction of hormone secretion.

The tANS was accomplished in a 62-year-old individual with angina pectoris, coronary artery disease, and moderate insomnia. Four sites identified at the CC were selectively stimulated using a silicone plug containing four globule-like platinum cathodes. A common anode, crafted from ribbon made of water absorptive sponge, was attached to the neck. For the tANS, current regulated stimulating pulses with an intensity of i_c=20 mA, a pulse width of 200 µs, and a frequency of f=25 were used. The performance of the system was investigated via an equivalent circuit model (ECM) of the interface at the cathode and the anode.

The results of tANS show that the melatonin level was significantly lower in all tANS sites before daylight selective tANS than after daylight selective tANS. ECM elements were independent on changes in pressure on the anode and highly dependent on the pressure on the cathode. The negative chronotropic effect was suppressed, presumably due to the prescribed beta blockers. The eventual effect on heart function could be confirmed once HRV is assessed. Results of tANS show that the cathodic charge density for optimum tANS was 2.4 µC/mm², while anodic charge one was of orders lower. To minimize variations of ECM elements and thus to optimize the tANS, the plug should be pushed into an external ear using a low steady force.

Keywords: Transcutaneous vagus nerve stimulation, cymba conchae, auricular nerve, melatonin, HRV, platinum electrodes, Equivalent Circuit Model.

Introduction

Neuromodulation is among the fastest growing areas of medicine. Over the last several decades, vagus nerve stimulation (VNS) has been established on a long history of investigating the relationship of autonomic signals to internal organs and glands with cortical function [1–5].

Transcutaneous vagus nerve stimulation (tVNS), however, is a diagnostic and therapeutic approach used to attempt to normalize the body's dysfunction through the stimulation of particular areas of the external ear [6–9]. These areas exhibit high availability and density of receptors, such as nociceptor Golgi-tendon receptors, Meissner corpuscles, Krause's end-bulbs, and glomus-bodies that respond to stimuli by sending signals via slowly conducting afferent Aδ and C fibres to the spinal cord and the brain [10–12]. Mechanisms of the tVNS have been described by Frangos et al. [13], who demonstrated that in humans, the auricular branch of the vagus nerve, via the CC, projects to the nucleus of the solitary tract. Thereafter, it was proposed that transcutaneous stimulation of afferent nerve fibres within the auricular branch (tANS) of the vagus nerve can potentially produce an effect similar to that of invasive VNS. Specifically, the external ear is the only place on the surface of the human body where there is a high density of afferent vagus nerve fibres [14].

All applications of tANS, however, require electrodes with high spatial selectivity, low impedance, and safe reversible charge delivery to specific populations of receptors through the electrode-tissue interface [15, 16]. For tANS, pure platinum can be used as a stimulating electrode material because it can effectively supply high-density electrical charge to excitable tissue by capacitive and faradaic mechanisms [17, 18]. To determine the efficiency and selectivity of the tANS, characterizing the electrical impedance of the electrode-tissue interface is crucial in all applications. This work is focused on modelling selective tANS of fibres supplying the CC, developing a multi-electrode plug for insertion into the external ear, and describing the stimulating cathode-skin interface at the CC [14].

The present study was also aimed at demonstrating that selective tANS can be potentially used as a method for the external modulation of heart function, respiratory function, and the induction of melatonin hormone secretion [19]. Melatonin, a naturally occurring hormone produced mainly by the pineal gland, regulates the sleep-wake cycle. Its peak secretion and level in the blood occurs in the middle of the night and gradually fall until morning [20]. If this sleep-wake cycle is disturbed, insomnia that presents a subjective perception of dissatisfaction with the amount and/or quality of the sleep can occur [21].

Material and Methods

The protocols of the measurements were approved by the National Medical Ethics Committee, Ministry of Health, Republic of Slovenia (Unique Identifier No. 0120-297/2018/6). The tANS trials were conducted in a 60-year-old individual treated with various drugs, such as beta-blockers which may be responsible for mild insomnia [22].

At the CC in which innervation corresponds to the auricular branch of the vagus nerve, four sites are identified for selective tANS (see Fig.1).
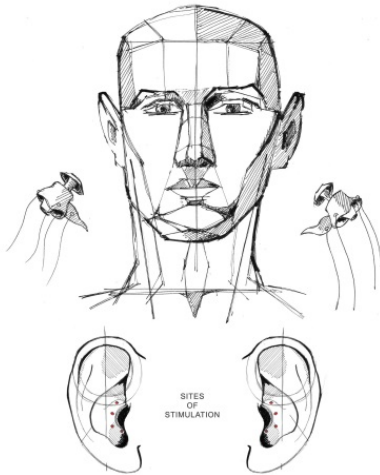

Fig. 1. Four sites at the CC identified for selective tANS.

The silicone plug to be inserted into the external ear contains four globule-like cathodes of about 1.2 mm in diameter. They were then welded to the lead wires and attached to specified sites of the silicone plugs. The anode is crafted using a 300-mm-long and 25-mm-wide ribbon made of sponge situated below the stainless-steel mesh. During the tANS, the anode was placed at the neck.

The elements C, R, $|Z|$ and θ of an ECM of the cathodic and anodic interfaces were measured at 1 and 2.5 kHz using the LCR meter (AT2816A Precision Digital LCR Meter, Changzhou Applent Instruments, Ltd., Jiangsu, China) [23]. The voltage response at a particular cathode with respect to the anode and i_c was measured using a real-time digital oscilloscope (Hantek DSO5102B, 2-Channel Digital Oscilloscope, High-tech Zone, Qingdao, Shandong, China).

During tANS, the plug is pushed into an external ear using a force of approximately 2.5 N produced by the vice within the dummy headphones. Thus, the globule is pressed into the skin, so that the skin is bent into a basin encircling about half of the globule.

The stimulus used was a current, biphasic pulse with a rectangular cathodic component and an exponentially decaying anodic component with the following parameters: a 1-second pulse train at f=25 Hz; intensity i_c=20 mA and a width τ=200 µs. The tANS can be triggered manually or synchronized by a piezo diaphragm sensor or by heart rate using a pulse oximeter. The stimulus pulse train, once triggered, began at 25 µs pulse width and linearly increased to 200 µs during the stimulation duration. This mode of stimulation intensity enabled the gradual onset of tANS and acceptable discomfort of the subjects. Stimulation intensity i_c was set at the level for which a low level of discomfort at the deployed cathode is produced.

For ECG measurements, a customized HKD-10A single lead ECG acquisition module with analogue signal output is used. For the assessment of respiration rhythm, a custom-designed piezo diaphragm sensor is used. For assessment of oxygen saturation, a customized low-cost acquisition fingertip pulse oximeter module is used. tANS trials were performed in a sitting position of the individual being exposed to a defined level of daylight illumination. Afterwards, saliva samples were collected just before and just after a 30 min tANS and analyzed using ELISA (Non-Extraction), enzyme immunoassay.

Results

Table 1 shows the level of melatonin before and after daylight selective tANS of the left and right CC in samples for which the maximum and minimum differences in melatonin secretion were obtained.

tVNS SITE	DIFFERENCE OF MELATONIN LEVEL WITH AND WITHOUT tVNS [pg/ml]	
UPPER LEFT CC	MAX	26,6
	MIN	1
LOWER LEFT CC	MAX	42,3
	MIN	5,2
UPPER RIGHT CC	MAX	72
	MIN	4,8
LOWER RIGHT CC	MAX	12,6
	MIN	2,4

Table 1. Level of melatonin before and after daylight selective tANS.

It is shown in Table 1 that the melatonin levels were significantly lower in the upper and lower CC of both ears before daylight selective tANS than after daylight selective tANS.

The results also show that all the averaged ECM elements have larger values when measured at 1 kHz than when measured at 2.5 kHz. In particular, the absolute impedance magnitude $|Z|$ is reduced from approximately 50 kΩ at 1 kHz to approximately 48 kΩ at 2.5 kHz. The contribution of the anode to ECM elements was independent on changes in pressure while the contribution of the cathode was highly dependent on changes in pressure.

Even though a negative chronotropic effect could be expected, this was not the case, presumably due to the

beta blockers prescribed to the individual to treat hypertension and angina pectoris. This could be the reason that the heart rate was not lowered as expected. More significant effect on heart function could be expected once HRV is assessed. It can be seen in Fig. 2 that the most significant effect of tANS was observed the in respiration rhythm: during tANS and shortly afterwards, the respiration rhythm was significantly reduced.
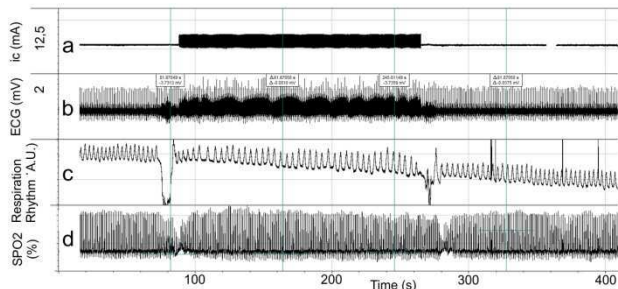

Fig. 2. tANS of the left CC: (a) i_c before tANS, with tANS and after tANS; (b) ECG before tANS, with tANS and after tANS; (c) respiration rhythm before tANS, with tANS and after tANS; (d) SPO2 before tANS, with tANS and after tANS.

Discussion

In the developed system, selective tANS drives current from the cathode in the direction that is perpendicular according to the globule so a limited population of nerve fibres can be stimulated. It was presumed that i_c, which spreads radially from half of the globular cathode, is more effective in the tANS of nerve fibres than when spreading in a single direction. Regardless, the activation function for a particular group of nerve fibres must be positive; otherwise, only specific receptors can be activated. The greatest concern in shaping and dimensioning the cathodes was to provide effective activation of particular nerve fibres at the targeted locations of the CC so that no pain and no high i_c density peaks could cause skin burns and irritation. One weakness of the system is a dependence of the ECM elements on the force applied onto the plug during the tANS. To optimize the tANS, the plugs should be pushed into the external ear using steady force.

To help judge the autonomic nervous system functions elicited by tANS, however, software that analyses the beat-to-beat time intervals of the heart rate and displays Heart Rate Variability (HRV), should be used.

Conclusions

Melatonin levels were significantly lower in all tANS sites of both ears before daylight selective tANS than after daylight selective tANS. ECM elements were independent of changes in pressure on the anode and highly dependent on the pressure on the cathode. A negative chronotropic effect was not obtained, presumably due to the medicine Concor prescribed to the individual. A specific effect on heart function could be confirmed once HRV is assessed. Finally, the goal of developing, designing, and testing a four-channel system for the selective tANS at the CC was achieved.

References

[1] A. M. Bilgutay, I. M. Bilgutay, F. K. Merkel, C. W. Lillehei, Vagal tuning. A new concept in the treatment of supraventricular arrhythmias, angina pectoris, and heart failure, J. Thorac. Cardiovasc. Surg., 56 (1968) 71–82

[2] J. P. Beekwilder, T. Beems, Overview of the clinical applications of vagus nerve stimulation, J. Clin. Neurophysiol., 27 (2010) 130–8, doi: 10.1097/WNP.0b013e3181d64d8a

[3] A. P. Amar, M. L. Levy, C. Y. Liu, M. L .J. Apuzzo, Vagus nerve stimulation, in: E. Krames, P. Peckham, A. Rezai, editors, Neuromodulation, Academic Press, London 2009, p. 625–37

[4] R. H. Howland, Vagus Nerve Stimulation, Curr. Behav. Neurosci. Rep.,1 (2014) 64–73, doi: https://doi.org/10.1007/s40473-014-0010-5

[5] G. M. de Ferrari, P. J. Schwartz, Vagus nerve stimulation: from pre-clinical to clinical application: challenges and future directions, Heart Fail Rev., 16(2) (2010) 195–203, doi: 10.1007/s10741-010-9216-0

[6] S. Dietrich, J. Smith, C. Scherzinger , K. Hofmann-Preiß, T. Freitag, A. Eisenkolb, R. Ringler, A novel transcutaneous vagus nerve stimulation leads to brainstem and cerebral activations measured by functional MRI, Biomed. Tech. Biomed. Eng., 53(3) (2008) 104–11, doi: 10.1515/BMT.2008.022

[7] L. Gori, F. Firenzuoli, Ear acupuncture in European traditional medicine, Evid Based Complement. Altern. Med., 4(Suppl 1) (2007) 13–6, doi: 10.1093/ecam/nem106

[8] P. M. Nogier, External ear: Zones and reflex points [in French], Bull. Soc. d'Acupunct., 20 (1956) 51–7.

[9] P. M. Nogier, From auriculotherapy to auriculomedicine, Moulins-les-Metz, Maisonneuve 1983, 231

[10] X. Y. Gao, Y. H. Li, K. Liu, P. J. Rong, H. Ben, L. Li, B. Zhu, S- P. Zhang, Acupuncture-like stimulation at auricular point Heart evokes cardiovascular inhibition via activating the cardiac-related neurons in the nucleus tractus solitarius, Brain Res., 1397 (2011) 19–27, doi: 10.1016/j.brainres.2011.04.034

[11] M. T. Cabioglu, A Glance at the Acupuncture Point from the Perspective of Current Technology, Open Access Library Journal, 3 (2016) 1–5, doi: 10.4236/oalib.1102237

[12] H. G. Kho, E. Robertson, The mechanisms of acupuncture analgesia: review and update Am. J. Acupunct., 25 (1997) 261–81

[13] E. Frangos, J. Ellrich, B. R. Komisaruk, Non-invasive access to the vagus nerve central projections via electrical stimulation of the external ear: fMRI evidence in humans, Brain Stimul., 8(3) (2015) 624–36, doi: 10.1016/j.brs.2014.11.018

[14] E. T. Peuker, T. J. Filler, The nerve supply of the human auricle, Clin. Anat., 15(1) (2002) 35–7, doi: 10.1002/ca.1089

[15] L. S. Robblee, T. L. Rose, Electrochemical guidelines for selection of protocols and electrode materials for neural stimulation, in W. F. Agnew, D. B. McCreery, editors, Neural Prostheses: Fundamental Studies, Prentice-Hall, Englewood Cliffs 1990, p. 25–66

[16] E. Gileadi, E. Kirowa-Eisner, J. Penciner, Interfacial electrochemistry: an experimental approach, Reading, Massachusetts: Addison-Wesley Pub. Co., Advanced Book Program, 1975

[17] L. A. Geddes, R. Roeder, Criteria for the Selection of Materials for Implanted Electrodes, Ann. Biomed. Eng., 31(7) (2003) 879–90. doi: 10.1114/1.1581292

[18] S. B. Brummer, M. J. Turner, Electrochemical Considerations for Safe Electrical Stimulation of the Nervous System with Platinum Electrodes, IEEE Trans. Biomed. Eng., BME-24(1) (1977) 59–63. doi: 10.1109/TBME.1977.326218

[19] S. Wang, X. Zhai, S. Li, M. F. McCabe, X. Wang, P. Rong, Transcutaneous Vagus Nerve Stimulation Induces Tidal Melatonin Secretion and Has an Antidiabetic Effect in Zucker Fatty Rats, PloS ONE 10(4): e0124195. doi:10.1371/journal.pone.0124195

[20] B. Claustrat, J. Brun, G. Chazot, The basic physiology and pathophysiology of melatonin, Sleep Med. Rev., 9(1) (2005) 11-24

[21] V. Rajput, S. M. Bromley, Chronic insomnia: A practical review Am. Fam. Physician, 60 (1999) 1431–8. discussion 1441-2

[22] S. Saddichha, Diagnosis and treatment of chronic insomnia, Ann. Indian Acad. Neurol., 13(2) (2010) 94–102. doi: 10.4103/0972-2327.64628

[23] J. E. B. Randles, Kinetics of rapid electrode reactions, Discuss Faraday Soc., 1 (1947) 11-19. doi: http://dx.doi.org/10.1039/DF9470100011

Author's Address

Janez Rozman, Center for Implantable Technology and Sensors, ITIS d. o. o. Ljubljana, Lepi pot 11, 1000 Ljubljana, Republic of Slovenia,
janez.rozman@guest.arnes.si

Polona Pečlin, Division of Gynaecology and Obstetrics, Šlajmerjeva 3 and Zaloška 7, 1000 Ljubljana, Republic of Slovenia, polonapeclin@gmail.com, https://www.kclj.si/index.php?dir=/divisions__departments/division_of_gynaecology_and_obstetrics

Samo Ribarič, Institute of Pathophysiology, Faculty of Medicine, University of Ljubljana, Zaloška 4, 1000 Ljubljana, samo.ribaric@mf.uni-lj.si, https://www.mf.uni-lj.si/pafi/predstavitev

Influence of electrode configuration on the effect of subthreshold pre-pulses: An explanation for two decades of conflicting data

Eickhoff S[1], Jarvis JC[1]

[1]School of Sport and Exercise Science, Liverpool John Moores University, United Kingdom

Abstract: The scientific literature of over two decades on sub-threshold conditioning pre-pulses is confused and lacks clear explanations for the conflicting data. We investigated the effect of depolarizing (DPPs) and hyperpolarizing (HPPs) sub-threshold pre-pulses on neural excitability in an animal model. The common peroneal nerves in anaesthetized Wistar rats were stimulated with biphasic stimuli with and without ramp and square DPPs and HPPs of 1, 5 and 10ms duration and 10% - 20% intensity of the following pulse. Monopolar and bipolar electrode configurations were compared. With monopolar electrodes DPPs increased the amplitude required to activate 50% of the motoneuron pool (11.3 ± 2.4% increase with 5ms Square DPP) and HPPs decreased the threshold (7.3 ± 3.1% decrease with 10ms Square HPP). With bipolar electrodes both pre-pulse types consistently had the opposite effect: DPPs decreased thresholds (6.7 ± 0.2% decrease with 1ms Square DPP) while HPPs led to threshold increases (6.1 ± 2.9% increase with 10ms Ramp HPP). Electroneurogram recordings of the stimulated nerve revealed that these differences in the effects of pre-pulses for monopolar versus bipolar electrodes originate in different mechanisms of action potential generation. In bipolar biphasic stimulation, the nerve was excited at the anode as a response to the second (anodic) phase. These findings explain the contradictions in published data on sub-threshold conditioning pre-pulses and highlight the fundamental influence of electrode configuration on the effect of pulse shaping.

Introduction

Electrical stimulation (ES) is a neuromodulation technique that applies artificial electrical stimuli to alter the activity of a target nervous structure. The stimuli are delivered via an active electrode, the cathode, near the target nerve. The anode, i.e. the passive return electrode, can either be situated in similar proximity to the target structure, this configuration is called *bipolar*, or can be placed further away, in which case the configuration is *monopolar*. For some applications of ES either electrode setup might be used, but for others specific requirements predetermine the electrode configuration. For example, in the emerging field of miniaturized neuromodulation implants, so called "electroceuticals" [1], in which electrodes are envisaged as integral with the stimulator, the small device size does not allow substantial electrode separation so the configuration is inevitably bipolar.

The pursuit of stimulation selectivity, that is the activation of a specific neuronal population without coactivation of other fibres, led to numerous investigations of ES with waveforms varying from the standard biphasic rectangular pulse. One such modification is the addition of a sub-threshold conditioning pre-pulse immediately prior to the stimulating pulse. Sub-threshold means that the pre-pulse itself does not elicit action potentials. A pre-pulse in the cathodic phase is called a depolarizing pre-pulse (DPP), whereas a hyperpolarizing pre-pulse (HPP) is an anodic pre-pulse. Literature on the effect of these sub-threshold pre-pulses in computer simulations and various experimental settings is contradictory [2]. Mortimer and Grill, the pioneers in the field of pre-pulses to selectively alter excitability of certain fibre populations, described a threshold decreasing effect of HPPs [3] and an increase of threshold with DPPs [3]–[5]. Over the decades following, several studies agreed with these original findings [6]–[8], while other research groups reported opposing results, describing decrease of stimulation threshold with DPPs [2], [9]–[11].

The aim of this study was to investigate comprehensively the effect of DPPs and HPPs on motor nerve recruitment. The pre-pulses were studied under conditions relevant to neuromodulating implants: The stimulation pulses preceded by DPPs and HPPs were biphasic and of a phase duration near the chronaxie, that is, near the energy-optimal stimulus duration. Both principal electrode configurations, bipolar and monopolar, were tested and for the first time, detailed comparisons of the electroneurogram (ENG) of the stimulated nerve were analysed.

Material and Methods

Surgical Procedure: All experiments were carried out under strict adherence to the Animals (Scientific Procedures) Act of 1986. The procedures were approved by the Home Office (PPL 40/3743) and were conducted in three terminal experiments in adult Wistar rats.

Anaesthesia was induced using 3% isoflurane in oxygen. To maintain stable, deep anaesthesia, respiration rate was monitored and the isoflurane concentration adjusted between 1% and 2%. 0.05 mg kg^{-1} of Buprenorphine (Temgesic, Indivior, Slough, UK) was administered intra muscularly for analgesia. The body temperature was kept between 37-38°C with an adjustable heatpad (E-Z Systems Corporation, Palmer, Pennsylvania, USA).

Stimulation and ENG recording electrodes were made from PVC insulated stainless steel wire (Electrode wire AS634, Cooner Sales Company, Chatsworth, California,

U.S.A.). Loops of 1mm diameter were formed from the uninsulated wire ends and placed under the common peroneal nerve (CPN). Two stimulation electrodes were placed 2mm apart, approximately 5mm distal to the CPN branch from the sciatic nerve. The more distal electrode was the cathode and the proximal electrode the anode for bipolar stimulation. For monopolar stimulation the nerve anode was not connected and a hypodermic needle (21G x 1-1/2") under the dorsal skin of the animal was used as a remote return electrode (anode). A second electrode pair, also 2mm apart, was placed approximately 10mm distal to the stimulation electrodes and used for ENG recording, with the more distal electrode as reference.

After freeing the extensor digitorum longus (EDL) muscle by dissecting the distal tendon of the overlying tibialis anterior, the proximal EDL tendon was clamped at the knee joint with a artery forceps which was firmly mounted to a steel table. The distal EDL tendon was dissected, fixed to a miniature titanium alloy hook, and connected to a force transducer (Gould Inc, Statham Instrument Division, Oxnard, California, U.S.A.). This procedure allowed us to mechanically isolate the EDL muscle and record isometric contractions, while blood supply and innervation were preserved. The proportion of isometric force generated was taken as indicative of the proportion of neural acivation among the population of motorneurones within the common peroneal nerve.

Stimulation: Stimulation pulses were generated at a 1MS/sec sampling rate with LabVIEW™ 2016 (National Instruments Corporation, Austin, Texas, U.S.A.) and sent over the analogue output of a NI PCIe 6351 Data Acquisition Card (National Instruments Corporation, Austin, Texas, U.S.A.) to a galvanically isolated voltage-to-current converter. The current-controlled stimulation pulses were delivered to the cathode at the nerve. A relay unit was used to select between the nerve anode and the remote anode. Combinations of stimulation parameters (amplitude, pre-pulse type, intensity, duration and anode position) were applied in randomized order. Every 20 stimulations a standard control pulse, set to ensure full nerve activation, and therefore to elicit maximal isometric twitch force, was delivered to the electrodes. All force responses were measured relative to the nearest control response. This means that final recruitment curves were built from test pulses that were placed randomly from start to finish of the recording period, and therefore are not affected by variations of temperature, level of anaesthesia or fatigue.

Full recruitment curves were recorded in 2 animals in 50μA increments for square and ramp DPPs and HPPs with 1, 5 and 10ms duration at 10% and 20% of the amplitude of the subsequent stimulation pulse in both electrode configurations (n=3 animals for 10% DPPs, 5 and 10ms). The stimulation pulses were biphasic with phase widths (PhWs) of 40μs, cathodic phase first.

Additionally, in n=2 animals ten repetitions of PhW 100 and 200μs standard biphasic stimulations (without pre-pulses) with amplitudes that ensured full neural activation were recorded with bipolar and monopolar anode position.

Recording: Isometric twitch force and ENG were recorded at 100kS/sec with a PowerLab 16/35 (ADInstruments Pty Ltd, Bella Vista, New South Wales, Australia) and stored, pre-processed and exported using ADInstruments LabChart 7 Pro (ADInstruments Pty Ltd, Bella Vista, New South Wales, Australia).

Data analysis and statistics: The 50% activation thresholds were determined for every recruitment curve by linear interpolation of experimental data points (Fig. 1). The normalized data followed the same patterns in each of the 2 or 3 experiments performed. Rather than formal statistical tests we have shown the consistency of the data by plotting individual data points with the means (Fig. 2).
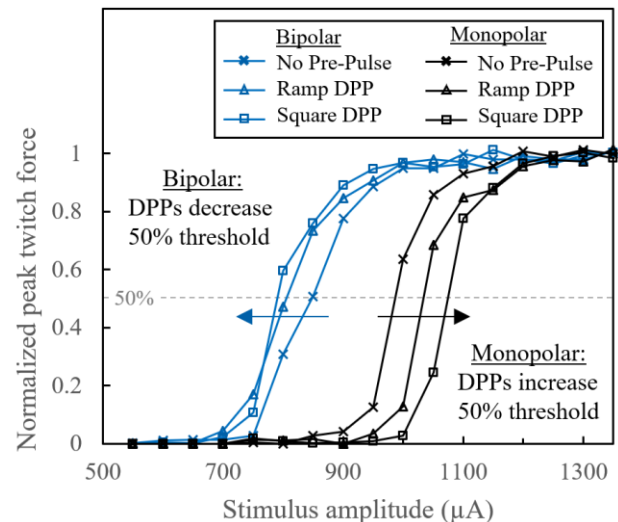

Figure 1: Recruitment curves for 40μs biphasic stimulation with and without 5ms DPPs of 20% stimulus intensity in monopolar (black) and bipolar (blue) setup.

Results

Depolarizing Pre-pulses: All tested DPPs increased the 50% activation thresholds in the monopolar electrode configuration and decreased stimulation thresholds in the bipolar configuration (Fig. 2.a-b). DPPs with 10% of the stimulation pulse amplitude increased thresholds in the monopolar configuration up to 7.5% (10ms Square DPP, ±0.6% SEM) and decreased thresholds up to 3.5% (5ms Square DPP, ±0.2% SEM) in the bipolar configuration. Larger threshold changes of up to 11.3% increase (5ms Square DPP, ±2.4% SEM) in monopolar and 6.7% decrease (1ms Square DPP, ±0.2% SEM) in bipolar configurations were observed when the DPP amplitude was set to 20% of the stimulus amplitude.

Hyperpolarizing Pre-pulses: HPPs decreased stimulation thresholds in monopolar and increased thresholds in bipolar configurations (Fig. 2.c-d). The threshold decreases with 10% HPPs ranged up to 4.9% (10ms Square HPP, ±1.3% SEM) for monopolar stimulation. The same pre-pulses increased thresholds by up to 6.1% (10ms Ramp HPP, ±2.9% SEM) in the bipolar case. Thresholds were decreased up to 7.3% (10ms Square HPP, ±3.1% SEM) in monopolar and increased by up to 3.5% (1ms Square HPP, ±2.2% SEM) in bipolar setup, when HPPs of 20% stimulus amplitude were used.
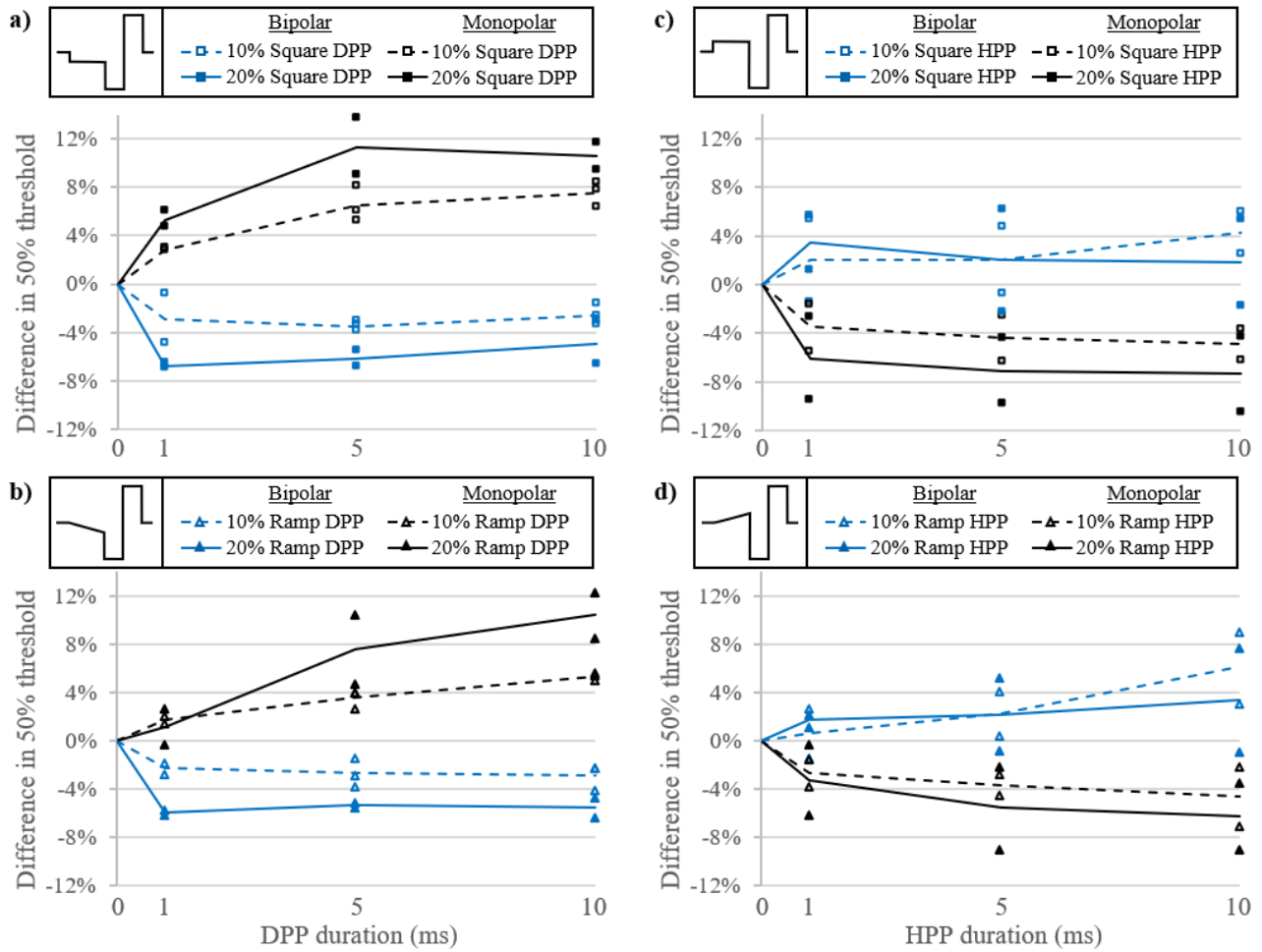
Figure 2: Changes in 50% activation threshold with 10% (dashed lines and empty markers) and 20% (solid lines and full markers) **a)** square DPPs, **b)** ramp DPPs, **c)** square HPPs and **d)** ramp HPPs. Pre-pulses have opposite effects on 50% activation threshold with monopolar (black) and bipolar (blue) electrode configuration. Negative values of '*Difference in 50% threshold*' indicate that the activation threshold with biphasic stimulation PhW=40µs decreased with the tested pre-pulse compared to standard stimulation without pre-pulse. Lines represent mean n=2 animals (except for 5 and 10ms 10% DPPs with n=3).

Electroneurogram recordings: ENG recordings of compound action potentials (CAPs) evoked by 100µs biphasic stimulation had an average delay of 1.67ms of the prominent first downward signal deflection to the stimulus artefact with monopolar, and an approximately one PhW greater delay of 1.79ms with bipolar electrodes (Fig. 3.a). Biphasic stimulation with 200µs PhW led to a delay of 1.72ms in the monopolar and 1.91ms, one PhW greater, in the bipolar setup (Fig. 3.b).

Discussion

The observed effects of DPPs and HPPs on the excitability of the nerve with a succeeding stimulus in monopolar electrode configuration are in good agreement with the original research by Mortimer and Grill. In their first publication on subthreshold pre-pulses, the authors used a cable model of a mammalian myelinated axon with 500µs monophasic stimuli applied via a monopolar point source and reported increased thresholds when the stimulation pulse was preceded by 500µs DPPs of 95% threshold amplitude [4]. Further computer simulations employed a single space-clamped node of Ranvier as well as a

compartment cable model of a mammalian nerve fibre, both modelled exclusively as monopolar electrode configurations, and described threshold increases with 500µs DPPs of 90% threshold amplitude and threshold decreases with similarly parametrized HPPs [3]. In later in-vivo experiments on cat sciatic nerve stimulation, Mortimer and Grill demonstrated that 500µs DPPs of 90% threshold amplitude applied via a monopolar electrode contact selectively increased stimulation thresholds of nerve fibres that otherwise showed the lowest threshold for recruitment [5].

Using the bipolar electrode configuration we observed opposite effects of pre-pulses on stimulation threshold that are also in line with published literature that opposes the pioneer work by Grill and Mortimer [2], [9]–[11]. Most of these studies were carried out with human transcutaneous stimulation, either in a clearly bipolar configuration [9], [10] or in a monopolar setting in which the reference anode was still relatively close to the stimulated nervous structure [2]. The consistent differences of pre-pulse effects in monopolar and bipolar electrode setup in both the data described in the present study and in previously published
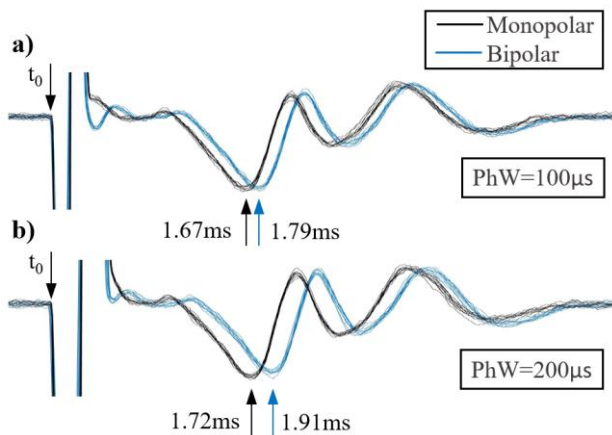
Figure 3: ENG recordings of the CPN during biphasic stimulation of **a)** PhW=100μs and **b)** PhW=200μs with monopolar (black) and bipolar (blue) electrode configuration (10 superimposed recordings each). Arrows indicate mean delays of first signal downward deflection with respect to the stimulation artefact t_0.

literature, led us to hypothesize that excitation might occur at the anode in bipolar stimulation setups at near threshold conditions. This hypothesis of excitation at the anode provides a satisfying explanation for the opposite effects of pre-pulses in bipolar versus monopolar stimulation described in this study. Like the stimulation phases themselves, the pre-pulses are inverted at the anode: DPPs have a hyperpolarizing effect and thus decrease thresholds at the anode, whereas HPPs have depolarizing effects that render the membrane less excitable at this location. The ENG recordings verify the hypothesis by showing a shift correlating to the duration of one PhW between responses elicited by monopolar and bipolar stimulation setups (Fig. 3). Our interpretation is that while in monopolar stimulation excitation occurred as a response to the cathodic (first) phase, the effective part of the pulse for the bipolar setup was the anodic (second) phase. This provides a potent explanation for the differences in pre-pulse effects that were observed between monopolar and bipolar configurations in this study. Furthermore, the possibility of excitation at the anode explains apparently contradictory findings in published literature with bipolar electrodes [9], [10].

The present study is the first to investigate comprehensively the effect of DPPs and HPPs on biphasic stimulation thresholds under conditions of direct relevance to contemporary miniature implantable neuromodulation devices. The consistent finding of reversed pre-pulse effects in bipolar setup due to excitation at the anode clearly stresses the strong influence the electrode configuration has on the effect of variations in pulse shape. A better understanding of the differences between monopolar and bipolar stimulation is of particular relevance to the emerging field of miniaturized neuromodulators, so called *electroceuticals*, where the small implant size does not allow for substantial separation of the electrodes. The majority of published literature on well-established pulse shape variations such as inter phase gaps (IPGs) [12] is, like the literature on subthreshold pre-pulses, primarily based on monopolar findings and is not applicable to these bipolar scenarios.

References

[1]   C. C. Horn, J. L. Ardell, and L. E. Fisher, "Electroceutical Targeting of the Autonomic Nervous System," *Physiology*, vol. 34, no. 2, pp. 150–162, 2019.

[2]   J. L. Vargas Luna, W. Mayr, and J. A. Cortés-Ramirez, "Sub-threshold depolarizing pre-pulses can enhance the efficiency of biphasic stimuli in transcutaneous neuromuscular electrical stimulation," *Med. Biol. Eng. Comput.*, 2018.

[3]   W. M. Grill and J. T. Mortimer, "Stimulus Waveforms for Selective Neural Stimulation," *IEEE Eng. Med. Biol. Mag.*, 1995.

[4]   W. M. Grill and J. T. Mortimer, "Selective activation of distant nerve fibers," in *Proc. 15th Annu. Int. Conf. IEEE Eng. Med. Biol. Soc. IEEE*, 1993, pp. 1249–1250.

[5]   W. M. Grill and J. T. Mortimer, "Inversion of the current-distance relationship by transient depolarization," *IEEE Trans. Biomed. Eng.*, 1997.

[6]   C. J. Poletto and C. L. Van Doren, "Elevating pain thresholds in humans using depolarizing prepulses," *IEEE Trans. Biomed. Eng.*, 2002.

[7]   T. D. Blumenthal, T. T. Burnett, and C. D. Swerdlow, "Prepulses reduce the pain of cutaneous electrical shocks," *Psychosom. Med.*, 2001.

[8]   K. E. I. Deurloo, J. Holsheimer, and P. Bergveld, "The effect of subthreshold prepulses on the recruitment order in a nerve trunk analyzed in a simple and a realistic volume conductor model," *Biol. Cybern.*, 2001.

[9]   M. P. Willand and H. de Bruin, "Design and testing of an instrumentation system to reduce stimulus pulse amplitude requirements during FES.," *Conf. Proc. IEEE Eng. Med. Biol. Soc.*, 2008.

[10]   K. Hennings, L. Arendt-Nielsen, and O. K. Andersen, "Orderly activation of human motor neurons using electrical ramp prepulses," *Clin. Neurophysiol.*, 2005.

[11]   N. Vastani, B. Seifert, D. R. Spahn, and K. Maurer, "Preconditioning depolarizing ramp currents enhance the effect of sodium channel blockers in primary sensory afferents," *Neuromodulation*, 2013.

[12]   C. van den Honert and J. T. Mortimer, "The response of the myelinated nerve fiber to short duration biphasic stimulating currents," *Ann. Biomed. Eng.*, 1979.

Author's Address

Steffen Eickhoff
Liverpool John Moores University
Tom Reilly Building, Byrom Street,
Liverpool L3 3AF, United Kingdom
S.Eickhoff@2017.ljmu.ac.uk

A Computational Model for Neuromuscular Electrical Stimulation - Featuring Excitation Contraction Dynamics

Narrendar RaviChandran[1], Kean Aw[2,] and Andrew McDaid[1]

[1] Medical Devices and Technologies group, The University of Auckland, 20 Symonds Street, Auckland, New Zealand.

[2] Smart Materials and Microtechnologies group, The University of Auckland, 20 Symonds Street, Auckland, New Zealand.

Abstract: Computational models have brought a significant advancement to the field of electrical stimulation. Still, it is quite challenging to develop a representative model for neuromuscular stimulation, given its intricate physiology. This study aims to extend the capability of a finite element (FE)-based nerve excitation model to accommodate subsequent muscle contraction that embodies neuromuscular stimulation by coupling an active nerve fiber with a constitutive muscle fiber model. Both the nerve and the muscle elements were embedded in a volume conductor of the tissue layers. The model was solved under transient conditions, wherein an external stimulus created a distributed electric field to excite the nerve fibers that subsequently initiated muscle contraction. The validity of the model was further verified against experimental data on nerve excitability. The model was able to predict the stress developed during muscle contraction, which contributed to the total force exertion. The proposed model is a novel attempt towards a continuum description for neuromuscular stimulation, that can be deployed to test various stimulation protocols and assessing their physiological outcome.

Keywords: Strength duration curve, FH nerve, Hill-type muscle, Twitch contraction, Finite element approach

Introduction

Transcutaneous neuromuscular electrical stimulation (tNMES) represents a non-invasive and a convenient way to elicit dormant motor function. Axons branching from a peripheral nerve arborize into individual muscle fibers to form motor units [1]. With tNMES, such axons are targeted to activate several motor units, which causes muscle contraction. Hence, the number of axons being excited directly impacts the recruitment of muscle fibers [1], [2]. Furthermore, a sustained muscle contraction is achieved by inducing a continuous excitatory response of motor axons using a pulsated stimulation [1], [3].

Driven by electrophysiological indices, computational models could replicate neuromuscular function at the subject-specific level. In this way, such tools can aid to understand the physiological recruitment and the neuromuscular response to various stimulation protocols [2], [4], [5]. This could potentially reduce evaluation times on patients and can serve as a test-bench to validate motor control strategies. However, a complete biophysical representation of neuromuscular stimulation is very challenging. Such modeling needs to embody (i) the spatial distribution of electric field inside tissue layers [2], (ii) excitation of nerve fibers based on the spatially distributed electric field [6], (iii) the excitation-contraction coupling to transduce nerve activation into corresponding muscle fiber recruitment [7] and (iv) the contraction dynamics to dictate the whole muscle response [7]–[9]. Separate studies have modeled these representations. So far, an integral approach has not been attempted for tNMES.

Two-step models are used to predict the nerve response to external excitation [2]. Herewith, the spatial distribution of the electric field within tissues are solved as volume conductors, and the excitatory field is later applied to analytical nerve models. However, these models have limited applicability as the calculation of field distribution, and the resulting excitatory response secedes. The constitutive representation is widely adopted in biomechanics towards full-scale muscle modeling. Active stress development that initiates muscle contraction is modeled based on macroscopic, phenomenological models like the Hill-type [3] or microscopic models based on cross-bridge sliding, like the Huxley-type models [5], [9]. The choice of the two methods varies based on their applicability and computational limitations [10]. To couple the previously mentioned nerve activation with the muscle models, depolarization of a muscle fiber is modeled based on the alterations in its calcium ion concentration with respect to the transient excitatory nerve response [5], [7], [9]. Coupling the physiological process of nerve recruitment into these models is actively researched [9].

Three-dimensional modeling represents a compelling approach to include the geometrical and biophysical features of the neuromuscular system for deriving personalized models. Furthermore, the above-mentioned physiological mechanisms and their transient behavior are represented by differential equations, hence, to accommodate such a modeling feat with reduced computational complexity, the finite element (FE) approach is favored [2], [5], [9], [10]. Accordingly, this study aims to develop a model that can predict muscle forces for a transient external stimulation using the FE approach.

Material and Methods

This paper presents a methodological approach in deriving a neuromuscular multi-scale model using the FE approach. To couple individual elements that represent tNMES, the excitation of an active myelinated nerve fiber in a volume conductor of tissues was coupled with a constitutive muscle model with its active stress generation characterized by the Hill-type formulations. The entire computational model was implemented using *COMSOL Multiphysics®, Version 5.4 (COMSOL, Inc., MA, USA)*. The model represented the transcutaneous stimulation of the median nerve for its consequent contraction of the Brachioradialis (BRD) muscle upon excitation. The forearm tissues and the BRD muscle were modeled as 3D geometry [2],[8] (Fig. 1a). Additionally, the median nerve with its axons was modeled as 1D elements to reduce the computational complexity.
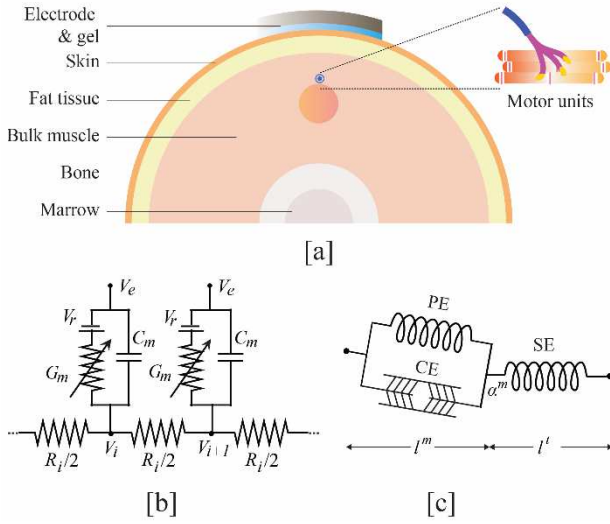

Figure 1: [a] A stylized representation of the neuromuscular model. [b] Electrical equivalent of the compartmentalized myelinated nerve model. [c] Biomechanical equivalent of a muscle with active and passive elastic components.

Firstly, the tissue layers were idealized as volume conductors with respective conductivity (σ), permittivity (ε_0). Using Poisson's equation for electrical conduction (1), the spatial distribution of the electric field as a potential gradient (∇V_e) was calculated for the externally induced stimulation (J).

$$-\nabla \cdot \left(\sigma \nabla V_e - \varepsilon_o \nabla \frac{\delta V_e}{\delta t} \right) = J \qquad (1)$$

The axons of the nerve fiber were modeled based on an established myelinate nerve [6]. Each nerve axon was compartmentalized with 21 interconnected nodal and internodal segments. The nerve fiber was at a depth of $12mm$ from the skin surface with 25 of such $10\mu m$ compartmentalized nerve axons distributed within $20mm^2$ [2]. The current density across each compartment of the nerve segment was computed as (2), based on the membrane capacitance (C_m), conductance (G_m) and the

resistivity of the intracellular fluid (R_i) (Fig. 1b). The potential gradient, ∇V_e from the volume conductor is directly coupled into (2), thus perturbations to the intracellular potential (V_i) can depolarize the nerve causing an action potential.

$$c_m \left(\frac{\partial V_i}{\partial t} - \frac{\partial V_e}{\partial t} \right) = \frac{d_a}{4\rho_i} \left(\frac{\partial^2 V_i}{\Delta x^2} \right) - g_a (V_i - V_e - V_{rest}) \qquad (2)$$

This action potential can further depolarize the motor-end plates of several muscle fibers within a motor unit (Fig. 1a). Activation of motor units depends on its type [3], stimulation amplitude (recruitment) [2] and frequency (tetanus) [1]. In this study, only the recruitment-based activation was considered. Hence, a scale factor (S_f) was introduced in (5). Based on the innervation ratio and the number of constituent muscle fibres within BRD [1], the total muscle contraction was graded based on the number of excited nerve axons. Based on the transmembrane potential (V_a), the motor unit activation was considered (3). Also, the dynamics between nerve activation and the resulting depolarization for subsequent muscle activation was included (4) [11].

$$u(t) = \begin{cases} 0, if\ V_a\ < 20\ mV \\ 1, if\ V_a\ \geq\ 20\ mV \end{cases} \qquad (3)$$

$$\dot{a}(t) = \frac{u-a}{\tau_a(a,u)} \qquad (4)$$

A muscle-tendon complex (MTC) has the muscle fiber arranged in series with the tendon. The Hill-type model was used to represent the MTC, Fig. 1c. The muscle component included the active contractile element (CE) and the passive connective tissue element (PE). The force generated by the muscle (F^m) depended on the (i) respective passive force-length relationships of CE [12] and PE [7] elements $f_{fl}^{CE}(\tilde{l}^m)$ and $f_{fl}^{PE}(\tilde{l}^m)$, Fig. 2a. (ii) dynamic force-length relationship of the CE [12], $f_{fv}^{CE}(\tilde{v}^m)$, Fig. 2b and (iii) muscle activation $a(t)$. Thus F^m was the sum of active and passive forces (5). As the hill-type parameters are scalable to model different muscle types, we characterized it for BRD. Accordingly, the optimal muscle length ($\tilde{l}^m$), tendon stack length (l_s^t) and pennation angle (α^m) were determined [7], [8]. The maximum muscle force (F_o^m) was estimated from the muscle's cross-sectional area and its specific tension [8].

$$F^m = F_o^m S_f \left[\left(f_{fl}^{CE}(\tilde{l}^m) f_{fv}^{CE}(\tilde{v}^m) \dot{a}(t) \right) + f_{fl}^{PE}(\tilde{l}^m) \right] \qquad (5)$$

$$f_{fl}^{CE}(\tilde{l}^m) = \begin{cases} -4(\tilde{l}^m - 1)^2 + 1, & 0.5 \leq \tilde{l}^m \leq 1.5 \\ 0, & otherwise \end{cases} \qquad (6)$$

$$f_{fv}^{CE}(\tilde{v}^m) = \begin{cases} 0 & , \tilde{v}^m < -10s^{-1} \\ -\frac{\arctan(\tilde{v}^m - 0.5)}{\arctan(5)} + 1, & -10s^{-1} \leq \tilde{v}^m \leq 2s^{-1} \\ \frac{\pi}{4\arctan(5)} + 1, & \tilde{v}^m > 2s^{-1} \end{cases} \qquad (7)$$

$$f_{fl}^{PE}(\tilde{l}^m) = \frac{e^{10(\tilde{l}^m - 1)}}{e^5}, 1 \leq \tilde{l}^m \leq 1.5 \qquad (8)$$
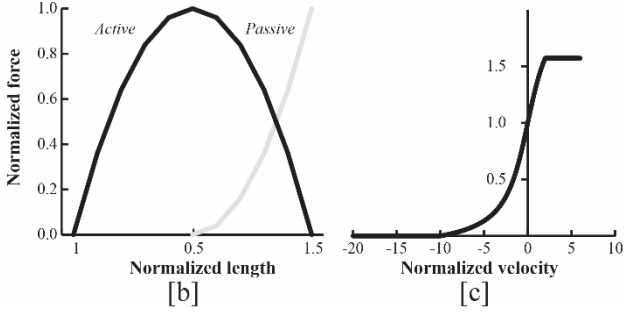
Figure 2. [a] Normalized force-length relationship for active and passive muscle elements. [b] Normalized force-velocity relationship for the active muscle element.

The 3D MTC was modeled as cylindrical geometry with the muscle connected to a tendon. The material properties [13] of MTC is given in Table 1. The mechanical behavior of the muscle upon its activation $\dot{a}(t)$ from the previous sections was assigned to the MTC. Further to this, the model was solved for its displacement, and the von Mises stress was obtained. External stimulation was implicated into the model using the Neuman boundary condition applied at the active electrode, the reference electrode was held as ground using the Dirichlet boundary condition, and the lateral edges were insulated.

Table 1: Material properties of the muscle-tendon complex

	Young's modulus MPa	Poisson's ratio $-$	Density kgm^{-3}
Muscle	1.162	0.4	1056
Tendon	1.6	0.49	1670

The model was validated based on experimental data from two subjects. Through motor point-based stimulation [14], the BRD muscle was evoked for wrist flexion. A monophasic stimulation with amplitude varied from 1-30 mA, and the pulse-width between 100-500 µs was delivered via surface electrodes. The stimulation was delivered via a current controlled stimulator, RehaStim™ 2 (Hasomed GmBH, Magdeburg, Germany). The strength-duration curve was measured to quantify nerve excitation to transcutaneous stimulation and, the twitch response was also recorded using a dynamometer [2]. The twitch response was normalized based on the maximum voluntary isometric contraction (MVIC).

Results

The activation of nerve fibers and the resulting muscle contraction were represented by a collection of coupled differential equations. The computational domain was discretized into finite elements using tetrahedral and edge mesh elements. A mesh convergence study resulted in 300000 mesh elements that were solved using a fully coupled, direct solver as a time-dependent study. The model was studied by simulating the experimental protocol.

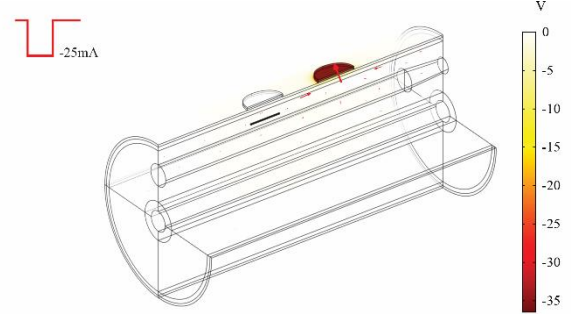The permeation of the externally induced electric field, Fig. 3. Based on the spatial distribution of electric field, the number of nerve axons being excited varied. Fig.4 shows the comparison of model predicted excitability against experimental data. Although the time constants for model predictions fall within the acceptable range [2], the discrepancy was due to the choice of nerve model [2], [6]. Wherein, the rheobase for the model [6] was four times of experimental data.

Fig 3. Potential distribution along the forearm model for a transient-external stimulus.
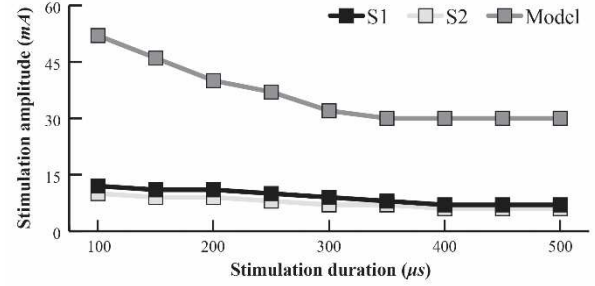

Fig 4. Comparison of model-predicted and experimentally obtained strength-duration curve.

The experimentally obtained twitch responses were <10% of MVIC. The transient-external stimulus applied to the model recruited several nerve axons that initiated muscle contraction. After solving the active stress development with the hill-type formulations for various recruitment levels, the resulting muscle contraction was evaluated for its deformation. A visual representation of muscle displacement is shown in Fig. 5. Stresses were induced due to the stretching of muscles. Moreover, the maximum stress of 17 MPa was developed when F_o^m was at its maximum.
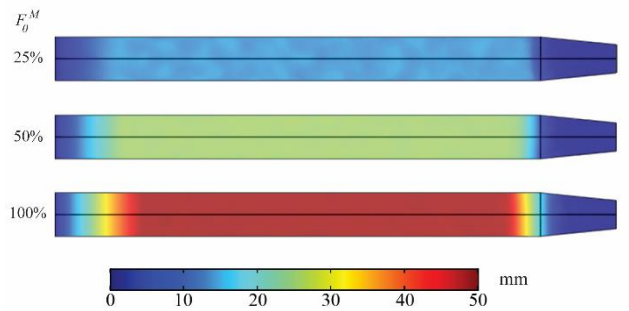

Fig 5. Deformation of the muscle with increasing levels of active stress development (25%, 50%, 100% of F_o^m).

Discussion

The proposed multi-scale model reproduces the critical characteristics of tNMES. The interactions between a spatially distributed electric field, nerve activation, and the resulting muscle contraction were modeled as a fully coupled system of differential equations. Embracing the advantages of FE-based discretization, the modeling approach is a novel contribution to the field, that provides an alternative solution approach to capture time-dependent and spatial effects. The standard volume conductor-based implementation was able to replicate the permeation of electric field across forearm tissues [2]. Furthermore, the model also included an established myelinated nerve that was compartmentalized. Although its excitability was times higher than the experimental data, the model can accommodate physiologically realistic nerve representations to improve its excitability response. Compared to the Huxley-type models, the constitutive 3D muscle utilizing the Hill-type model demonstrated to be computationally effective. In this way, the critical characteristics of a parameterized muscle model were able to oblige the macroscopic-whole muscle level responses: the force-length and the force-velocity relation. [10]. Finally, the active stress developed in the muscle was coupled with the deformation response of the muscle.

As future work, we aim to expand the model's capability to predict muscle response to frequency-induced stimulation effects based on the calcium accumulation dynamics at the muscle fiber level. In this way, the model can predict muscle response to different stimulation protocols. Also, higher stimulation frequencies will dramatically increase the muscle output to its maximum, causing fatigue. Inclusion of frequency-dependent muscle activation and the effects of fatigue can aid with the identification of suitable stimulation parameters needed to achieve desired force output.

Conclusion

In this study, the physiological processes representing tNMES were modeled using the finite element approach. The model can predict muscle forces for an externally induced transient stimulation. The activation of a myelinated nerve with a volume conductor was coupled to a parameterized Hill-type muscle model. The active stress developed during muscle contraction was later integrated into constitutive muscle models. The model represents a continuum for neuromuscular stimulation, which encourages its use as a testbed for evaluating various tNMES-based protocols.

References

[1]   M. K. Floeter, "Structure and function of muscle fibers and motor units," in *Disorders of Voluntary Muscle*, vol. 76, no. 12, G. Karpati, D. Hilton-Jones, K. Bushby, and R. C. Griggs, Eds. Cambridge: Cambridge University Press, 2011, pp. 1–19.

[2]   A. Kuhn, T. Keller, M. Lawrence, and M. Morari, "A model for transcutaneous current stimulation: Simulations and experiments," *Med. Biol. Eng. Comput.*, vol. 47, no. 3, pp. 279–289, 2009.

[3]   M. Böl and S. Reese, "Micromechanical modelling of skeletal muscles based on the finite element method," *Comput. Methods Biomech. Biomed. Engin.*, vol. 11, no. 5, pp. 489–504, 2008.

[4]   J. Martinek, Y. Stickler, M. Reichel, W. Mayr, and F. Rattay, "A novel approach to simulate Hodgkin-Huxley-like excitation with COMSOL Multiphysics," *Artificial Organs*, vol. 32, no. 8, pp. 614–619, 2008.

[5]   T. Heidlauf and O. Röhrle, "Modeling the Chemoelectromechanical Behavior of Skeletal Muscle Using the Parallel Open-Source Software Library OpenCMISS," *Comput. Math. Methods Med.*, vol. 2013, pp. 1–14, 2013.

[6]   D. R. McNeal, "Analysis of a Model for Excitation of Myelinated Nerve," *IEEE Trans. Biomed. Eng.*, vol. BME-23, no. 4, pp. 329–337, Jul. 1976.

[7]   T. S. Buchanan, D. G. Lloyd, K. Manal, and T. F. Besier, "Neuromusculoskeletal modeling: estimation of muscle forces and joint moments and movements from measurements of neural command.," *J. Appl. Biomech.*, vol. 20, no. 4, pp. 367–95, Nov. 2004.

[8]   K. R. S. Holzbaur, W. M. Murray, and S. L. Delp, "A model of the upper extremity for simulating musculoskeletal surgery and analyzing neuromuscular control," *Ann. Biomed. Eng.*, vol. 33, no. 6, pp. 829–840, 2005.

[9]   C. W. J. Oomens, M. Maenhout, C. H. Van Oijen, M. R. Drost, and F. P. Baaijens, "Finite element modelling of contracting skeletal muscle," *Philos. Trans. R. Soc. B Biol. Sci.*, vol. 358, no. 1437, pp. 1453–1460, 2003.

[10]   L. Marcucci, C. Reggiani, A. N. Natali, and P. G. Pavan, "From single muscle fiber to whole muscle mechanics: a finite element model of a muscle bundle with fast and slow fibers," *Biomech. Model. Mechanobiol.*, vol. 16, no. 6, pp. 1833–1843, 2017.

[11]   D. G. Thelen, "Adjustment of Muscle Mechanics Model Parameters to Simulate Dynamic Contractions in Older Adults," *J. Biomech. Eng.*, vol. 125, no. 1, p. 70, 2003.

[12]   J. A. C. Martins, M. P. M. Pato, and E. B. Pires, "A finite element model of skeletal muscles," *Virtual Phys. Prototyp.*, vol. 1, no. 3, pp. 159–170, 2006.

[13]   J. M. Ford, "Skeletal Muscle Contraction Simulation: A Comparison in Modeling," no. November, pp. 1–104, 2013.

[14]   N. RaviChandran, K. Aw, and A. McDaid, "Characterizing the Motor points of Forearm Muscles for Dexterous Neuroprostheses," *IEEE Trans. Biomed. Eng.*, pp. 1–1, 2019.

FES Testbed for Multi-Channel Transcutaneous Stimulation Systems

Valtin M.[1], Schauer T.[1]

[1]Control Systems Group, Technische Universität Berlin, Germany

Abstract: *Troubleshooting advanced FES applications or stimulation devices by measuring the stimulation current and voltage over several minutes is often not possible because of the limited memory available in standard oscilloscopes. The developed FES Testbed, a specialised data acquisition system for transcutaneous electrical stimulation, enables such measurements. The galvanic isolated measurement system transfers the high-resolution data of every detected stimulation pulse via USB to a PC or Laptop. The stimulation pulse can use one of the 3 included skin replacement models or can be forwarded to standard electrodes, allowing to record a normal FES application. Modular postprocessing MATLAB functions round up the FES Testbed. These functions handle the data conversion, pulse detection, gathering of statistics, data management and data visualisation. A MATLAB GUI for efficient pulse examination completes the FES Testbed.*

Keywords: *Stimulation Device, FES, Current Measurement, Data Acquisition, Skin Model*

Introduction

Research involving functional transcutaneous electrical stimulation often includes some kind of control over the electrical stimulation. This may include the timing of the stimulation and/or the stimulation intensity, often based on sensor data [1]. Prominent examples of this structure are the FES based drop-foot correction [2] and the rehabilitation of the upper extremities, e.g. the hand [3]. In both cases, complex stimulation patterns are generated based on real-time sensor data. Monitoring and validating these stimulation patterns is often not easily possible, because the necessary measurement equipment is to large, to expensive, or to difficult to operate outside a lab environment.

Traditionally, the generated stimulation pulses are measured with an oscilloscope or with a data acquisition card for the PC. With a little bit of additional hardware, the stimulation voltage, as well as the stimulation current can be measured with these systems. Both methods usually use grid powered devices with no galvanic isolation, so the electrical safety of the whole setup must be kept in mind to protect the devices or the subject.

While oscilloscope measurements are great for real-time feedback, they cannot be used for long term evaluation (e.g. several minutes) or tracking of randomly occurring stimulation errors, because of the limited amount of memory available.

PC based data acquisition systems do not have this limitation, however, these, often stationary systems, are generally less practical because of the costs, system size and complexity. Data acquisition systems also require elaborate postprocessing to go through the millions of samples to extract the short stimulation pulses and convert the integer raw-data samples into ampere/volt.

The presented *FES Testbed* is a specialised data acquisition system for transcutaneous electric stimulation,

enabling researchers to check and validate the safety and functionality of their advanced FES applications.

The second application of the *FES Testbed* is the validation and comparison of different stimulators and support of the development of new stimulation devices.
Since the various stimulators used in FES research all generate an electrical pulse, suitable to trigger a muscle contraction, the subtle and not so subtle differences, like symmetric and asymmetric biphasic pulses, are often neglected, conveying the idea that every stimulation pulse form is equally effective and can be easily exchanged.
With the *FES Testbed*, the high-resolution voltage and current wave forms of multiple stimulation pulses can be recorded and compared. Additionally, multiple realistic loads included in the *FES Testbed* simulate the electrode-skin interface and allow comparing different stimulators under the exact same load conditions.

Material and Methods

The *FES Testbed* consists of three individual parts:
- a small data acquisition system, specialised for FES,
- a PC based data recorder program,
- and MATLAB (MathWorks Inc., USA) post-processing scripts for efficient evaluation of the recorded stimulation pulses.

The FES data acquisition system is controlled by the PC data recorder, which saves the raw data for post-processing by the MATLAB scripts.

FES Data Acquisition System

Figure 1 depicts the basic structure of the whole system, with the PC or Laptop controlling the FES data acquisition system and the stimulation device. An optional demultiplexer, as well as the modules for additional input channels, are shown in grey.

Figure 1: Overview of the FES Testbed, including the structure of the data acquisition system.

All devices are connected via USB to the PC, which also supplies the power for the data acquisition system. The power supply, as well as the USB communication channel, are galvanically isolated from the PC, to protect the PC from the high stimulation voltage and to protect against any ground loops, in case the FES Testbed is connected to a person. The power supply uses isolated DC/DC modules with at least 5.2kV isolation voltage (MEJ2 series, Murata, Japan). For the communication channel, the USB isolation IC ADUM4160BRWZ (Analog Devices Inc., USA) is used.

The *FES Testbed* supports 4 stimulation channels directly and up to 96 additional channels with optional extension modules, e.g. if a demultiplexer for electrode arrays needs to be tested. However, only one of these input channels can be active at a time. So, the stimulator must have a multiplexed current source, if this feature is used. The input stage is identical for every input channel and consists of a 'stimulation active' detection, which determines which stimulation channel is used. This is realised with an opto-coupler, which is driven directly by the stimulation current. An opto-coupler is used, because the stimulation current is not altered and because the resulting digital signal voltage is isolated from the stimulation voltage. Each input stage also has visual feedback of the stimulation pulse using LEDs.

After the input stage, all channels are connected to one single stimulation channel, which is routed to the current measurement resistor R_{mess} and the selected load.

Four via jumper selectable loads are included:
- a 1kΩ load for simple tests and comparison with oscilloscope measurements (1kΩ),
- a simplified linear skin model [4] (SkinModel),
- a model of the electrode interface according to test specification 09-01 03/2007 MDS-Hi (AuditModel),
- and a connector for standard stimulation cables (Skin).

The voltage drop over the measurement resistor R_{mess} and the voltage over the load are measured with a two channel, 16-bit analogue to digital converter (ADC) MAX11198 (Maxim Integrated Inc., USA). The ADC's sampling rate can go up to 2 MSample/s and is controlled via an external clock signal. The ADC features a dual serial peripheral interface (SPI), with one SPI output channel for each ADC channel and a maximum SPI clock frequency of 50MHz. However, it is not possible, to use two traditional SPIs, since only one SPI clock input is available. Therefore, one SPI interface was used in the master configuration to drive the SPI clock, accompanied by a second SPI interface in slave configuration, using the SPI clock generated by the SPI master. This allows the microcontroller (MCU) to utilise the direct memory access (DMA) unit for the data transfer, significantly reducing the MCU workload. The data transfer is triggered by the same MCU timer, which generates the ADC's clock, guaranteeing a valid data transfer after the ADC's data registers were updated.

The ADCs sampling rate was chosen to 1 MSample/s. This is because the stimulation pulse has a time resolution

of 1µs or greater. Passive first order anti-aliasing filters with ~500 kHz cut-off frequency are included in the signal preconditioning circuitry, before the ADC.

An ARM© based microcontroller (STM32L433, STMicroelectronics, Netherlands) was used to receive the SPI data, as well as the USB data. Because of the embedded USB 2.0 module, supporting 12 MBit/s, no USB to serial converter is needed. Since the highest data rate supported by the USB isolator IC is USB 2.0 'Full Speed' with 12 MBit/s, no faster external USB solutions are viable. Because the data rate is limited, the MCU needs to pre-process the continuous ADC data stream to identify the stimulation pulses, so that only the parts containing stimulation pulses are sent to the PC. This is done via configurable thresholds for the measured stimulation current and voltage. The data is buffered using the MCU's RAM and send out in packages of two times 1000 samples. A 32-bit sample counter is sent with every package to enable the PC program to reconstruct the correct time vector of the stimulation pulses.

Data Recorder Program

The FES data acquisition system is controlled from a Linux PC via the Data Recorder program. This program initiates the measurement, receives, and saves the data excerpt. The following parameters are set during initialisation of the FES data acquisition system: data type to send (only the stimulation pulses or a continuous down-sampled data stream), sample rate divider, search width (number of samples to skip if detecting a stimulation pulse), detection thresholds, and if a demultiplexer is used. This initial setup is also stored in the custom binary format, used to store the measurement data. This allows the postprocessing script the correct conversion of the raw data stored. The data format is optimised for read-in speed and size, so only the time as a float value, and the raw 16-bit integer values for current and voltage are stored as vectors for one pulse. Therefore, before each pulse section, a small header is added with the meta information about the pulse, like the number of samples, the active stimulation channel(s), and so on. Figure 2 depicts the general structure of the resulting data file.
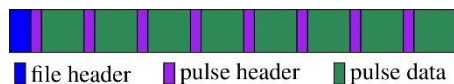
Figure 2: File structure of the custom binary data file.

The data about each stimulation pulse is also available via TCP/IP connection, to allow real-time visualisation and monitoring by other programs or scripts.

MATLAB based Postprocessing

Since the PC program only saves the raw data, the bulk of the conversion and postprocessing is done by modular MATLAB functions. A first function reads the binary file and converts the 16-bit raw data into volt and milliampere. The function also creates a MATLAB structure (struct) for the data, with an array of structs containing the stimulation pulse data. The meta data for

each pulse is also taken over from the raw data and re-formatted for easy access in MATLAB. A second function is used to search for the expected pulse form, e.g. symmetric bi-phasic, and aligns the found pulse data, so that the pulses can be automatically compared and analysed. This function also collects various stats like the current or pulse width for later use. This step also saves all pulses which do not follow the expected form, so that they can be inspected manually later. Custom functions which, e.g., identify skin-model parameters can now be used on these normalised datasets.

Plotting these datasets is also very easy. A custom MATLAB GUI was developed to efficiently view the results and compare various stimulation pulses. This GUI has an overview function, where the complete, down-sampled vector of the stimulation current is plotted over time in subplot 1. One stimulation pulse, highlighted in the overview plot, can be selected via slider and shown in subplot 2. If the overview is disabled, subplot 1 is going to display the stimulation current of N pulses, while subplot 2 is going to display the stimulation voltage for these N pulses. N, the number of pulses to display, is configurable in the GUI and includes the selected pulse as well as the previous N-1 pulses.

The MATLAB data structure containing all this information can be saved directly from the GUI with varying degree of raw data included, significantly reducing the needed file size.

Results

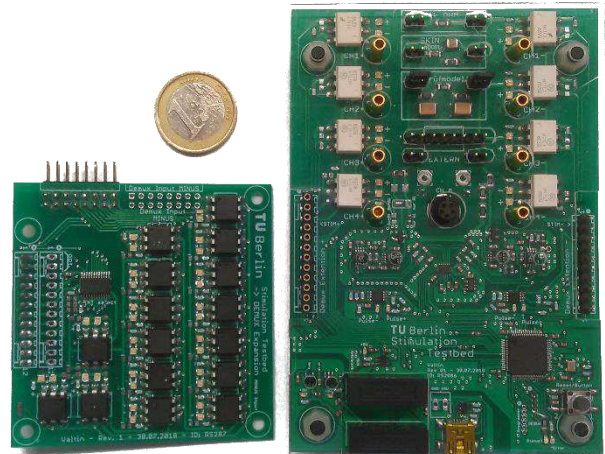The FES data acquisition device with an extension module for additional 16 input channels is depicted in Figure 3.

Figure 3: FES Testbed (right) and one 16 channel extension module (left).

The small size (115 mm × 80 mm × 20 mm) and the single USB connection makes the device very portable and easy to operate.

The quality of the measured data is also very good for such a simple system. The time resolution of 1 µs is sufficient to capture even very short spikes and sharp transients. The 16-bit ADC resolution provides a theoretical resolution for the stimulation current of ~5 µA

and enables low noise measurements from 0 mA up to ±150 mA without the need to adjust the measurement range. Figure 4 shows the stimulation voltage of a stimulator with adaptive high voltage generation [5] over the AuditModel, measured with the FES Testbed and with a 10-bit oscilloscope (Rode&Schwarz, RTM3004).
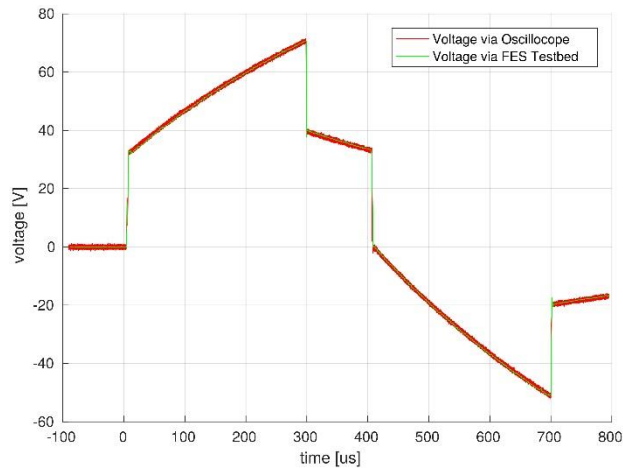

Figure 4: Stimulation voltage over the electrode interface model, measured with the FES Testbed (green) and an oscilloscope (red) (cur=25 mA; pw=300 µs).

Figure 5 shows the MATLAB GUI for a data set of 60 seconds or 1200 pulses (cur=25 mA; pw=300 µs) with 50 ms between each pulse. In the lower part of the GUI, stimulation current (blue) and voltage (orange) is displayed as well as the automatically detected boundaries of the different parts of the pulse (red). The file size of this one-minute long data set is about 34.9 MB. The postprocessing is also very fast, taking less than one second for the 1-minute data set, which would make the postprocessing real-time capable.
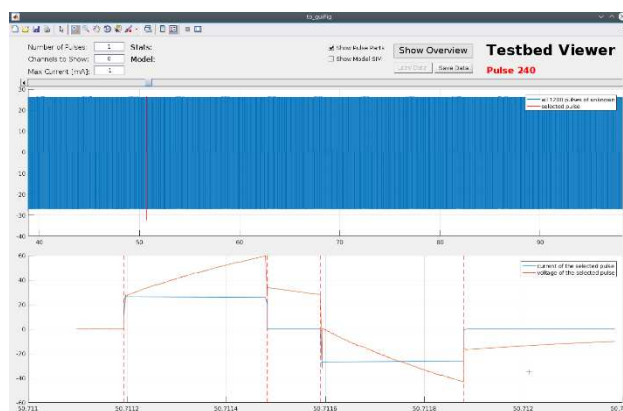
Figure 5: FES Testbed GUI showing the overview with 1200 pulses and the details for pulse 240.

The only limitation of the FES data acquisition system is its inability to continuously stream the data with 1 MSample/s. However, the need for galvanic isolation requires this compromise. On the other hand, most of this data would be discarded anyway, since the relevant stimulation pulse is very short, compared to the stimulation period. The MCUs buffer capability of 2 ms (sampling rate 1 MSample/s) should be sufficient for most applications, even where multiple pulses are used. In all other cases, reducing the sample rate will increase the pulse length the buffer can hold accordingly.

Conclusions

We developed a testbed aimed at supporting developers of intelligent stimulators, researcher who study electrical stimulation and its effects on the body, and clinicians who want to check and monitor the stimulation pulses generated by their FES application, over the entire treatment session.

The FES Testbed gives new insight into the physical effects of electrical stimulation and may aid in the development of smarter stimulators, which e.g., warn the health care professional if the stimulation voltage saturates because of poor electrode-skin contact. The FES Testbed could also prove invaluable for the validation and accreditation of complex stimulation systems.

Future work will focus on the automatic parameter identification for various skin models [6] [7] and the change of these parameters over stimulation intensity and time.

References

[1] T. Schauer: Sensing motion and muscle activity for feedback control of functional electrical stimulation: Ten years of experience in Berlin, *Annual Reviews in Control,* vol. 44, pp. 355-374, 2017

[2] T. Seel, C. Werner, T. Schauer: The Adaptive Drop Foot Stimulator – Multivariable Learning Control of Foot Pitch and Roll Motion in Paretic Gait, *Medical Engineering Physics,* vol. 38, pp. 1205-1213, 2016

[3] C. Salchow-Hömmen, T. Thomas et. al.: Automatic control of grasping strength for functional electrical stimulation in forearm movements via electrode arrays, *at-Autom,* vol. 66, pp. 1027-1036, 2018

[4] A. Boxtel: Skin resistance during square-wave electrical pulses of 1 to 10 mA, *Medical & biological engineering & computing,* vol. 15, pp. 679-687, 1977

[5] C. Wiesener: Current-Controlled Stimulator with Variable High Voltage Generation, *Submitted to Proc. of the 13th Vienna International Workshop on Functional Electrical Stimulation,* 2019

[6] J. L. Vargas Luna et. al.: Dynamic impedance model of the skin-electrode interface for transcutaneous electrical stimulation, *PloS one*, 2015 10(5), e0125609

[7] S. Dorgan, R. Reilly: Model for human skin impedance during surface functional neuromuscular stimulation, *IEEE transactions on rehabilitation engineering,* vol. 7, pp. 341-348, 1999

Author's Address

Markus Valtin
Technische Universität Berlin
Sekretariat EN 11
Einsteinufer 17
D-10587 Berlin, Germany
markus.valtin@campus.tu-berlin.de
http://www.control.tu-berlin.de

Current-Controlled Stimulator with Variable High Voltage Generation

Wiesener C.[1], Valtin M.[1], Schauer T.[1]

[1]Control Systems Group, Technical University Berlin, Germany

Abstract: *The currently available and certified FES cycling systems are tabletop units which are not certified for portable use or to be worn at the body and cannot be configured via a smart device. Therefore, a new stimulation module was developed which can be triggered via integrated or external wireless IMU sensors. The module can be controlled via a smart device. It offers a variable high voltage generation which can be adjusted in real-time. The use of a demultiplexer makes the design very compact and versatile. Due to its small size, it can be directly integrated into a sleeve.*

Keywords: Neuromuscular Stimulator, Variable Stimulation Voltage

Introduction

There are many stimulation systems available for paraplegic rehabilitation. One of the most frequently used systems in FES cycling is the RehaStim1 by Hasomed GmbH which offers the so-called Sciencemode library[1] for stimulation configuration if used together with an ergometer or tricycle. It consists of two separate stimulation modules each with four channels where each module includes a DC/DC converter cascade to produce the galvanically isolated high voltage. The stimulation pulses are then generated via discrete H-bridges. A comparable architecture can be observed for the clinical research system Rehamove Science [1] or in scientific approaches like [2], [3]. The advantage of this architecture is that only one high voltage source is needed and depending on the amount of H-bridges several channels can be stimulated. The main drawback is the high volume, cost, and weight of the DC/DC converters and the high amount of discrete power switches for the H-bridge realization.

A different approach was presented in [4] and [5] where a flyback transformer is used for each stimulation channel which charges a capacitor. This capacitor is then directly switched to the electrodes via a current controller. Using this architecture each channel can act separately with a very low rise time of the current and with voltages for up to 300 V. The drawback is the high volume, weight and cost of the flyback transformer for each channel which limits the number of available channels.

In [6] an optimization of the first architecture is presented which uses only one DC/DC converter for high voltage generation and an integrated high voltage demultiplexer for H-bridge switching.

Requirements Analysis and Design

Since a neuromuscular stimulator is a class II medical device, there are several guidelines for the development, production process as well as standards to asure safety for the user. According to ISO 13485, a controlled development process is mandatory, therefore essential requirements are derived. In summary, to enable mobile applications, the entire circuit should be compact, portable and battery powered only.

Therefore, a common connector is used for either charging or stimulating which makes it possible to omit galvanic isolation of the high voltage generation to the battery power. To stimulate a large number of muscle groups up to 8 channels shall be offered.

The current source of the stimulator shall be able to drive 100 mA for resistive loads for up to 2 ms. As a conseqeuence, internally, a voltage source of up to 115 V is needed to drive the requested currents even for high contact resistances. Furthermore, the design of the DC-DC converter has to be optimized to avoid power loss during stimulation. Finally, the stimulator shall be configured and controlled via a smart device using a wireless protocol. The overall hardware architecture is summarized in Figure 1 which will be referenced and explained in the following sections.
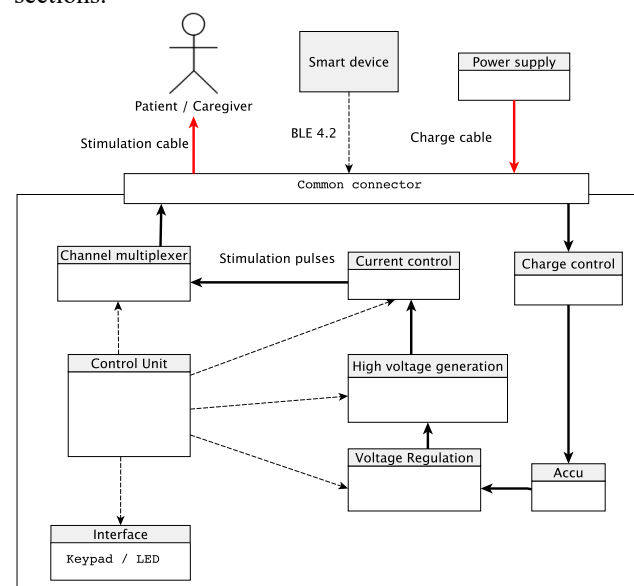

Figure 1: Architecture overview of the neurostimulator. Dashed lines indicate low power control signals (e.g. SPI, I2C, GPIO), solid lines indicate power signals, e.g., stimulation current or charging current.

---

[1] http://sciencestim.sourceforge.net

Variable High-Voltage Generation

The high-voltage source is needed to drive the current through the load attached to the electrodes. According to the requirements, a stimulation voltage of up to 115 V is needed. As stated in the introduction, the use of a common connector for either charging or stimulation makes it possible to omit the need for galvanic isolation for the high voltage source. Therefore, a standard switching converter can be used. The aim of the design is to minimize the size of the switching converter and at the same time to keep the efficiency as high as possible. The higher the frequency of the switching converter, the smaller the inductance can be selected. However, the duty cycle has to be kept small for high efficiency. To keep the duty cycle below 95% a coupled inductor for a cascaded switching converter can be used which is called SEPIC (Single-ended primary inductance converter). The resulting schematic is shown in Figure 2.
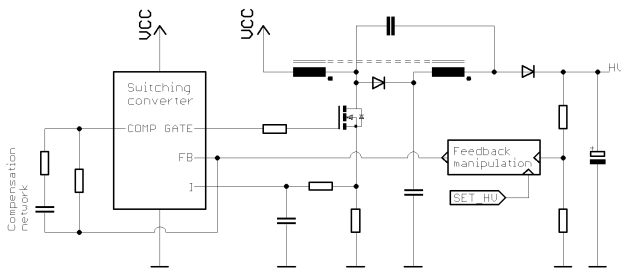
Figure 2: High-voltage generation consisting of a SEPIC converter with feedback manipulation.

The compensation network is used to guarantee an adequate phase margin of the switching converter's current mode control. The voltage VCC represents the battery voltage. The optimized circuit only uses 7.2 cm^2 of PCB space and still guarantees high efficiency.

With the standard SEPIC circuit, only a fixed high voltage can be generated. If the electrode impedance is high the maximum voltage level is needed to drive the requested current. If the impedance is low the unused voltage level drops over the low side current control MOSFET which results in low efficiency due to power dissipation. Hence, an adequate voltage level for the actual electrode impedance is needed. Therefore, the feedback manipulation can be used to adjust the feedback voltage which is the control input of the switching converter. The feedback manipulation can be seen as an applied bias of the feedback line. Furthermore, for applications with low current requirements (e.g. facial stimulation or transcranial stimulation) the stimulation voltage can be adjusted to a minimum level of 30 V.

Multiplexer

To distribute the current pulses to the different channels, a multiplexer is used. In order to be able to generate bipolar current pulses, a full bridge is necessary for each of the 8 channels resulting in a total of 32 high voltage power transistors. Standard bipolar transistors cannot be used to avoid corruption of the controlled stimulation current by the basis current of the transistor which would change the current over the measurement shunt. Furthermore, a discrete

assembly using SMD parts would occupy a large area on the PCB and a high number of soldering contacts. Therefore, an integrated circuit is used, which is controlled via SPI. There are several different multiplexers available with a different number of channels and voltage levels. The HV2801 (Microchip, USA) consists of 32 high voltage MOSFETs in half bridges which can be connected to form 8 full bridges for a maximum stimulation voltage range of [-200V, 200V]. In case of an event, the output voltage can be switched off in a few nanoseconds via one digital line. The overall quiescent current for a switching rate of approx. 100 Hz is rated in the datasheet with approx. 78 μA.

Current controller and Control Unit

To drive a current through the skin via transcutaneous electrodes means controlling the current through a floating impedance consisting of a resistive and capacitive load as shown in Figure 3.
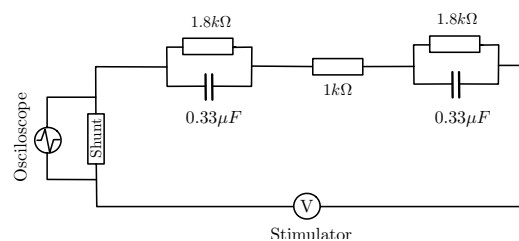

Figure 3: Skin model is taken from medical device verification according to 09-01 03/2007 MDS-Hi.

This means that either low- or high-side current control can be applied. Since the control circuitry is sitting on the low side of the power (3.3V), driving low side switches is usually easier than driving high side switches. Therefore, with a floating load that does not care whether it is switched at the low or high side, low side control is preferred. Furthermore, low-side control means that the lowest level of stimulation voltage which will be switched by the demultiplexer will be always > 0V due to the voltage drop over the low-side switch and shunt resistor.

For this task, it is conceivable to use a n-channel MOSFET as the control switch. If the MOSFET is directly driven by an analog output of the micro controller a certain drain current can be realized. The characteristic drain current to drain-source relation is a nonlinear and temperature dependent function which cannot be pre-determined. At the low-side MOSFET, a certain power loss can be expected which results in a temperature variation of up to 30°C.

According to standard characteristic temperature curves for n-channel MOSFETs, a variation of up to 5 % for the gate-source threshold voltage is expected. Therefore, an analog PI controller is designed that controls the MOSFET in the linear mode, above the gate-source threshold voltage. The value for the setpoint current is provided via DAC from the stimulation control unit. The actual value of the current is measured via a shunt resistor between the source of the MOSFET and ground. This additionally realizes negative current feedback, which ensures higher temperature stability of the current controller. To assure a fast control behavior the analog controller is

designed with a single operational amplifier as shown in Figure 4.
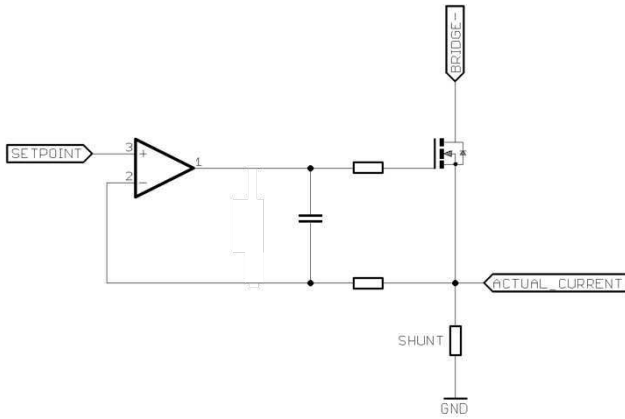

Figure 4: Designed current PI-controller for low-side current control.

The potential at the shunt is only marginally affected by the operational amplifier. Therefore, no additional impedance converter is needed. Furthermore, dependencies on the drain voltage and temperature are adequately adjusted by this topology.

To handle applications like FES cycling and to provide a user interface the stimulator's control unit consists of a stimulation and an application micro controller. The latter incorporates a standard Arm Cortex M4F processor and a Bluetooth low energy radio module. Additionally, an inertial measurement unit is added to control FES cycling when integrated into an electrode sleeve or attached to the patient's segments.

The stimulation controller handles current control, high voltage control, pulse generation, and electrode error detection. For communication with peripheral parts and the application controller different digital interfaces such as SPI and UART are used. The stimulation controller uses a 32-Bit timer to guarantee a high timing resolution of the pulse generation. Furthermore, the stimulation current and voltage are monitored via ADCs. The target values for current and high voltage control are applied via integrated DACs.

Results

First, the generated high voltage was tested for different input and output voltages. For this test, two resistive impedances were used for two different high voltage settings (V_{Out} = 77 V and 49 V) to guarantee the same stimulation current (I_{Out} = 73 mA), as shown in Figure 5.
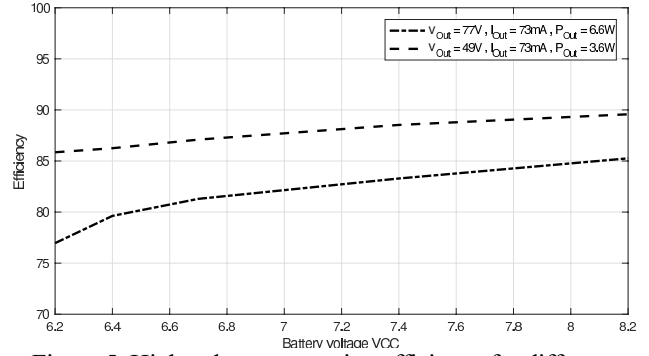
Figure 5: High voltage generation efficiency for different battery voltage levels and different output voltages. The resistive load was adjusted to yield the same current amplitude.

The resulting efficiency varies between 77-85 % for low and between 86-90 % for high electrode impedance depending on the battery voltage level.

To test the stimulation device under real conditions a so-called skin model is used which mimics the worst case impedance of both electrodes and the tissue (see Figure 3). For high stimulation currents at high pulse width and high frequency, the SEPIC is not able to transfer enough charge into the buffer capacitor during the stimulation pulse. Hence, the high voltage starts to drop during stimulation and rises during stimulation pause as shown in Figure 6. This results in a voltage ripple of 1.5 V peak-to-peak, which is compensated by the current controller.
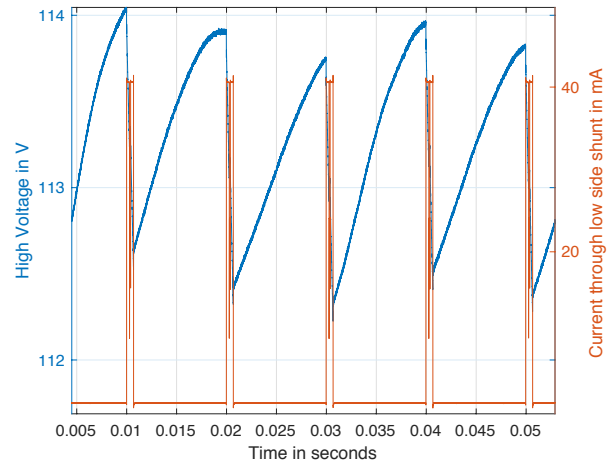
Figure 6: Voltage ripple during biphasic stimulation (40 mA,100 Hz, 300 μs) over a skin model. The blue line shows the high voltage which was set to 115 V.

Despite the voltage ripple, the current controller fulfills the required performance parameters in all aspects. Figure 7 shows as an example of the stimulation voltage and the resulting stimulation current at the skin model for a biphasic stimulation pulse with 40 mA and a pulse width of 300 μs.
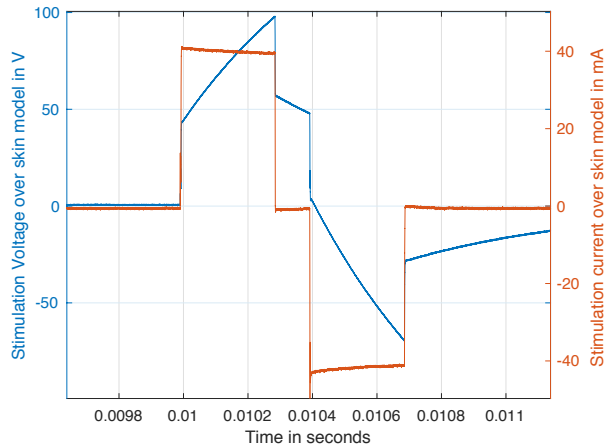
Figure 7: Stimulation voltage and current of biphasic stimulation pulse (40 mA, 300 µs) over worst case skin model.
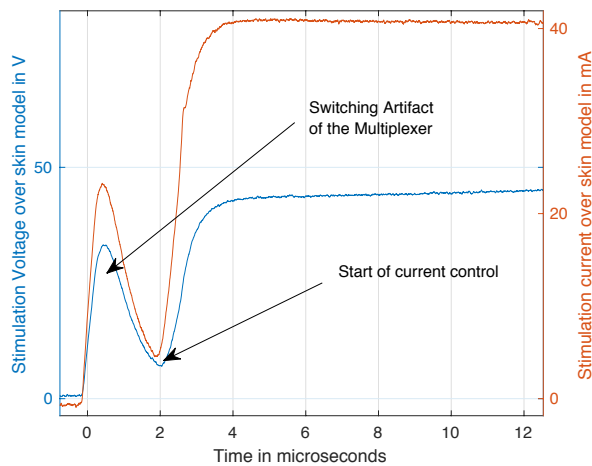

Figure 8: Onset of the same stimulation pulse

The ascending slope of the voltage during the stimulation is normal for a capacitive load as well as the remaining charge during the interpulse phase which results in a nonzero voltage level at the beginning of the negative stimulation pulse. This leads to a small overshoot of the stimulation current at the beginning of the negative pulse. In Figure 8, the pulse is shown in more detail. The current control needs approximately less than 2 µs to reach the target current. But the slope starts with a small switching artifact of the multiplexer. These effects cannot be avoided by the current controller since the current does not go through the low-side shunt and the current control is enabled afterwards.

Discussion and Conclusions

The presented current controlled stimulator fulfills all requested requirements while being ultra-compact with low manufacturing costs. Up to 8 stimulation channels can be independently controlled and configured via a standard smart device. The variable high voltage generation can be used to adjust the stimulation voltage in the case of electrode impedance changes. For the final release of the device, this adaptation can be used for energy harvesting or applications where only a low stimulation voltage is needed. Finally, if the demultiplexer is configured with a constant switching matrix, low DC currents can be generated with up to 30 mA for iontophoresis applications.

References

[1]   M. Valtin, K. Kociemba, C. Behling, B. Kuberski, S. Becker, and T. Schauer, "RehaMovePro: A versatile mobile stimulation system for transcutaneous FES applications," *Eur J Transl Myol*, vol. 26, no. 263, pp. 203–208, 2016.

[2]   H. P. Wang, Z. G. Wang, X. Y. Lu, Z. H. Huang, and Y. X. Zhou, "Design of a pulse-triggered four-channel functional electrical stimulator using complementary current source and time division multiplexing output method," in *Proceedings of the Annual International Conference of the IEEE Engineering in Medicine and Biology Society, EMBS*, 2015, vol. 2015-Novem, pp. 1671–1674.

[3]   A. Tamtrakarn, "A 115V bi-phasic pulse electrical muscle stimulator by using inductor-sharing dual-output boost converter with supply-stepping switch driver," in *2017 24th IEEE International Conference on Electronics, Circuits, and Systems (ICECS)*, 2017, pp. 410–413.

[4]   R. Thorsen and M. Ferrarin, "Battery powered neuromuscular stimulator circuit for use during simultaneous recording of myoelectric signals," *Med. Eng. Phys.*, vol. 31, no. 8, pp. 1032–1037, Oct. 2009.

[5]   S. C. Huerta, M. Tarulli, A. Prodic, M. R. Popovic, and P. W. Lehn, "A universal functional electrical stimulator based on merged flyback-SC circuit," in *15th International Power Electronics and Motion Control Conference and Exposition, EPE-PEMC 2012 ECCE Europe*, 2012, p. LS5a.3-1-LS5a.3-5.

[6]   S. Simcox *et al.*, "A portable, 8-channel transcutaneous stimulator for paraplegic muscle training and mobility-A technical note," *J. Rehabil. Res. Dev.*, vol. 41, no. 1, p. 41, 2004.

Author's Address

Constantin Wiesener
Technische Universität Berlin
Sekretariat EN 11
Einsteinufer 17
D-10587 Berlin
Germany
wiesener@control.tu-berlin.de
www.control.tu-berlin.de

High-frequency transcutaneous cervical electrical stimulation: A pilot study

Villar Ortega E.[1], Ansó J.[2], Buetler K. A.[1], Marchal-Crespo L.[1,3]

[1]Motor Learning and Neurorehabilitation Laboratory, ARTORG Center for Biomedical Engineering Research, University of Bern, Bern, Switzerland
[2]Image Guided Therapy, ARTORG Center for Biomedical Engineering Research, University of Bern, Bern, Switzerland
[3]Sensory-Motor Systems (SMS) Lab, Institute of Robotics and Intelligent Systems (IRIS), Department of Health Sciences and Technology (D-HEST), ETH Zurich, Switzerland

Abstract: Early results suggest that transcutaneous stimulation of cervical regions may have a positive effect on recovery of upper limb motor function after neurological injuries. However, in clinical applications, patients find transcutaneous low-frequency spinal cord stimulation (LF-tSCS) unpleasant. Transcutaneous high-frequency spinal cord stimulation (HF-tSCS) has been presented as an option to reduce pain and discomfort produced by LF-tSCS. We performed a pilot study with 3 participants to compare the effects of HF-tSCS and LF-tSCS on upper limb reflex responses and reported pain level and discomfort. In the first part of the experiment, high- (i.e., monophasic and biphasic burst) vs low-frequency (i.e., monophasic pulse) single waveform cervical tSCS was applied and motor response threshold identified via electromyography (EMG). In the second part of the experiment, the three waveforms were administered as train pulses and the stimulation intensity was increased in four steps from 20% to 80% of the individual motor response threshold. Participants indicated the pain level for each stimulation intensity increment and waveform. We find that participants reported stronger discomfort in HF-tSCS than LF-tSCS stimulation at motor threshold level. Further, stimulation at subthreshold level was associated with strong discomfort in HF- and LF-tSCS train pulses, especially in participants with relatively high motor response threshold. We conclude that cervical HF-tSCS may not (yet) be an option for clinical application, even though acceptability may depend on the individual motor response threshold of the patient.

Introduction

In the last few decades, experts in the field of neurorehabilitation have employed electrical stimulation to treat neurological injuries, namely epidural electrical stimulation to support gait recovery in patients with spinal cord injury [1]. In contrast, only few studies elaborated on the use of electrical stimulation for stroke recovery. Epidural spinal cord electrical stimulation has shown promising results in improving cerebral and cerebellar blood flow in stroke patients [2]. However, epidural electrical stimulation employs invasive implantable electrodes located over the spinal cord (e.g., at the lumbar and/or upper sacral area), limiting its application in stroke patients. An alternative may be the use of noninvasive stimulation techniques such as transcutaneous spinal cord stimulation (tSCS). The use of tSCS, in combination with active training, has shown promising results in improving locomotion function in spinal injured patients [3], [4].

Most of the research effort has concentrated on stimulating the lower lumbosacral vertebrae to enhance locomotor recovery, while transcutaneous stimulation of cervical region for improving hand and arm function is still in nascent stage [3]. The basic mechanisms underlying the effects of cervical tSCS likely also rely on activation of the sensory afferent system [5]. It has been recently shown that cervical tSCS activate posterior roots that transsynaptically modulate motor pools projecting to upper limb muscles (i.e., posterior root-muscle reflexes) [6]. Continuous stimulation at subthreshold intensity levels of motor reflex response (e.g. <80% of motor threshold) modulate the level of sustainable spinal cord excitability [4].

Early results suggest that transcutaneous stimulation of cervical regions may confer similar benefits to those of epidural stimulation [7]. Cervical tSCS seems to facilitate recovery of upper limb motor function after paralysis. In a recent study, non-invasive electrical stimulation resulted in improved voluntary control of hand function in tetraplegic subjects [8]. These promising results make cervical tSCS an appealing therapeutic approach for recovery of arm function after brain injuries. However, before trying this technology in stroke patients, it is important to first gain a better understanding of the feasibility and acceptance of the technology in healthy participants.

Benefits and acceptance of electrical stimulation are limited by stimulation parameters such as intensity, frequency, pulse duration, stimulus pattern, stimulation time and location of electrodes. Conventional noninvasive electrical stimulation setups that stimulate at low frequencies have been associated with tingling sensation, pain and discomfort [9]. High-frequency tSCS (HF-tSCS) (up to 10 kHz) is considered to be less painful and free-paraesthesia stimulation compared to conventional electrostimulation [9]. It has been suggested that HF stimulation modulates Aα and Aβ fiber activity more effectively than traditional SCS [10]. However, it is unclear whether high-frequency tSCS can evoke cervical posterior root reflexes using similar levels of intensity than low-frequency tSCS (LF-tSCS).
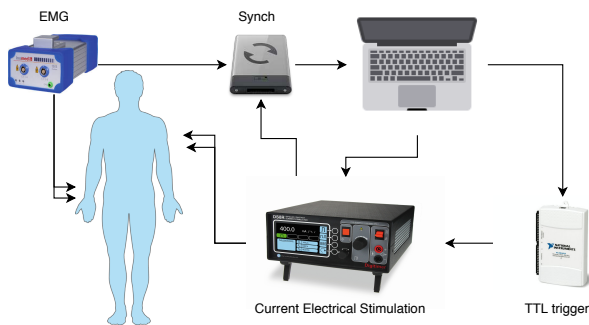
Figure 1: Experimental set-up.

The motivation of this pilot study was to test the feasibility and acceptance of different non-invasive spinal cord stimulation protocols for potential application in stroke patients. We performed a pilot study with 3 participants to compare the effects of HF-tSCS and LF-tSCS on upper limb muscle reflexes and assess the participants' acceptability using a subjective pain rating scale. We hypothesized that high-frequency spinal cord stimulation would be associated with reduced pain and discomfort compared to low-frequency stimulation, but might require higher intensity levels to evoke motor responses.

Material and Methods

Participants

Three authors of this study participated in the experiment. Participant 1 (age 38, male), participant 2 (age 29, male) and participant 3 (age 34, female). The intervention was supervised by a neurophysiologist who monitored the setup and electrode placement.

Experimental Setup

Participants were sitting in a low backrest chair with their arms comfortably placed on the side rests. The experimental setup is shown in figure 1. Transcutaneous cervical electrical stimulation was delivered via adhesive round electrodes (Axelgaard, USA, 2.5 cm diameter) placed over the C6 and T1 vertebrae (figure 2a) [11]. A bipolar arrangement was selected for precaution, in order to prevent any electrical current passing through the back, heart, chest, anterior neck and/or the carotid sinus [12]. Electrical stimulation was applied via a modified version of a constant current stimulator device (DS8R, Digitimer, UK). A special firmware is provided by the manufacturer to reach stimulation frequencies up to 10kHz.

Upper limbs reflex responses were recorded via electromyography (EMG) (ISIS Headbox, inomed, Germany). Adhesive surface recording electrodes (inomed, Germany, 23x23 mm) were positioned over the flexor carpi radialis (FCR) as shown in figure 2b. EMG and tSCS were synchronized via a triggering system provided by the manufacturer (ISIS trigger-box, inomed, Germany). A graphic user interface was developed in MATLAB (MathWorks, USA) to control and trigger the DS8R using a TTL analog output signal from a host computer through a NI-USB 6215 I/O device (National Instrument, USA).
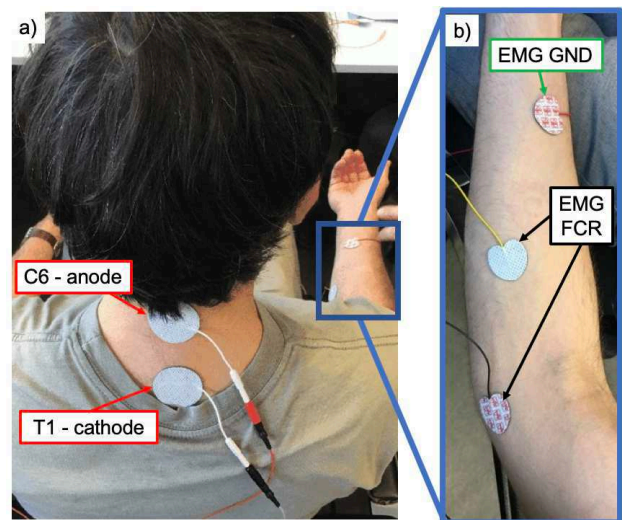
Figure 2: Electrode set-up. a) tSCS electrodes over C6 (stimulation anode) and T1 vertebrae (stimulation cathode). b) EMG electrodes over flexor carpi radialis (FCR) with the EMG ground electrode (EMG GND) located between FCR and wrist.

Stimulation Parameters and Protocol

Single stimulation

Within the first part of the experiment, upper limb reflex responses to a single stimulation event were evaluated. Motor evoked potential response to a single stimulation event was recorded for three different waveform types: i) monophasic pulse (MP), ii) monophasic burst (MB), and iii) biphasic burst (BB). Pulse duration was set to 1 millisecond and burst carrier frequency was 10 kHz. Stimulation intensity was increased by +5 mA until an EMG response was detected in the flexor carpi radialis per each participant and waveform. Threshold response was defined as the lowest stimulation intensity at which upper limb reflexes were consistently elicited. Participants indicated pain level after each stimulation increment (+5 mA) on a scale ranging from 1 (no pain) to 6 (worst pain possible). Intervention per each waveform was interrupted if participants indicated the worst pain possible, even if a reflex response was not yet induced.

Stimulation train

In the second part of the experiment, we administered single monophasic pulses (i.e., LF-tSCS) and monophasic and biphasic bursts (i.e., HF-tSCS) as train of pulses at 10 Hz during 4 s (i.e., three different train pulses). Although we originally aimed to compare train of pulses at different frequencies (i.e., 10, 20, 30 and 40 Hz), we decided to stop once the test with 10 Hz was finished, due to the participants' reported levels of discomfort. We employed four levels of stimulation intensities (20%, 40%, 60%, 80%) relative to the individual motor response threshold extracted from the first part of the experiment. Participants indicated the pain level after each stimulation. The test (per each waveform) was interrupted if participants indicated the worst pain possible. Tests were not blinded to the participants.
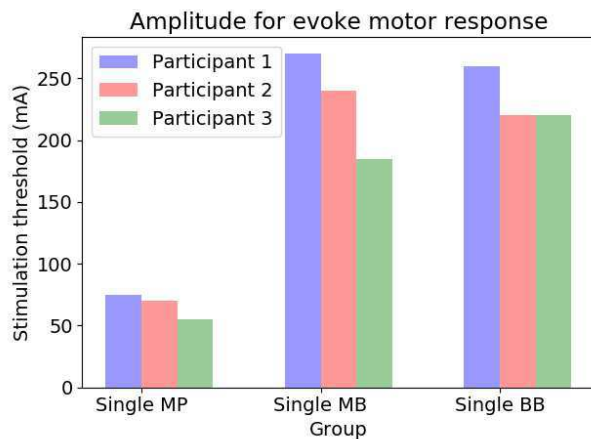
Figure 3: Stimulation thresholds MP: Monophasic pulse, MB: monophasic burst, and BB: biphasic burst.

Results

Motor Response to single stimulation

Participant 1 and 2 exhibited similar motor response thresholds in response to cervical tSCS with the single monophasic pulse (MP) (75 mA and 70 mA, respectively), while the motor threshold in participant 3 was slightly lower (55 mA) (figure 3). For the single burst monophasic (MB) and biphasic (BB), the stimulation intensity required to evoke a motor response was at least 3 times higher than the single monophasic pulse. For example, in the single burst monophasic, participant 1 had a motor response threshold at 260 mA. The motor response threshold for single burst biphasic was only slightly lower than single burst monophasic (240 mA). Participant 2 had similar results as participant 1. Congruent with the single monophasic trial, during the single monophasic burst trial, participant 3 had a motor response threshold lower (185 mA) than participant 1 and 2. Interestingly, participant 3 required higher stimulation thresholds for biphasic than for monophasic bursts, opposite than in participants 1 and 2.

Pain level related to single stimulation

The three participants reported higher pain levels at the motor response threshold during bursts compared to the single pulse waveform (figure 4). However, the three participants reported lower pain with burst than with pulse stimulation for the same intensity of stimulation. For example, participant 1 reported no pain when we delivered a single burst of 75 mA (i.e., at motor response threshold to single pulse), but when we applied 260 mA (i.e., at motor response threshold to the single burst) he reported severe pain.

For each of the three waveforms, participants 1 and 2 reported similar pain levels at the motor threshold intensity (figure 4). Participant 3 reported lower levels of pain compared to participants 1 and 2 through the experiment. Participants 1 and 2 rated the interventions as mild (MP) and moderate pain (MB & BB), while participant 3 rated no pain (MP) and mild (MB & BB).

Pain level related to stimulation train

To analyze the pain related to the train of pulses at 10 Hz, we calculated the sum of the pain score across the 4 stimulation intensities (20%, 40%, 60% and 80% of the motor response threshold). Participants reported lower pain levels for the constant bursts monophasic (MB) and biphasic (BB) than constant pulse monophasic (MP) at 20% and 40% of muscle threshold amplitude level (figure 5). Participant 1 and 2 reported less pain in the train of constant bursts biphasic (i.e., no pain and mild pain) than monophasic (i.e., no pain and moderate) at 20% and 40% of motor threshold stimulation intensity, while participant 3 reported less pain for the constant bursts monophasic than biphasic (i.e., no pain).
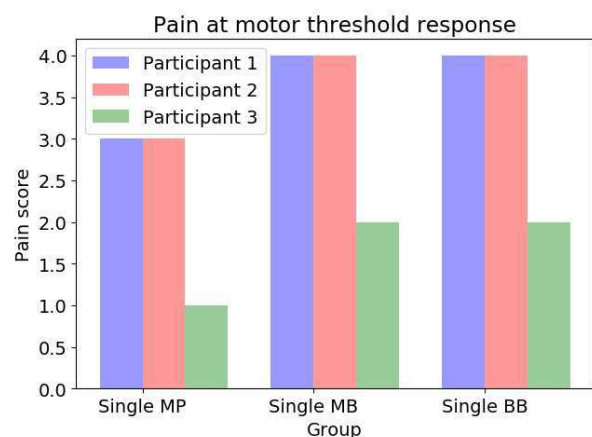

Figure 4: Pain score at muscle threshold response. MP: Monophasic pulse, MB: monophasic burst, BB: biphasic burst.
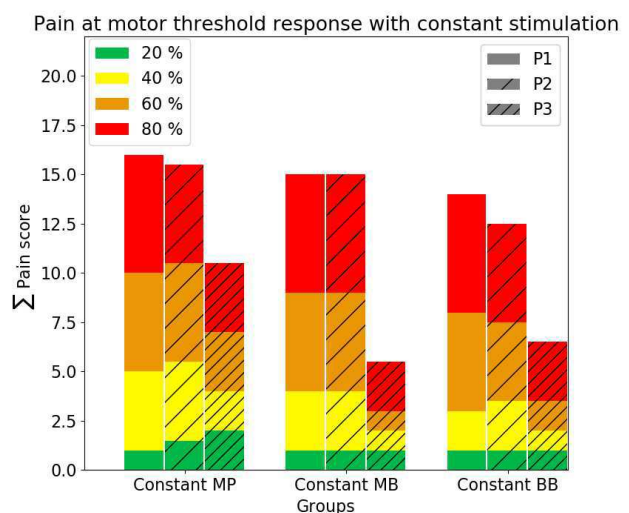

Figure 5: Sum of pain score during stimulation train. The y-axis represents the sum of pain score across stimulation intensities (20%, 40%, 60% and 80% of the motor response threshold) and x-axis the waveforms: pulses monophasic [MP], bursts monophasic [MB] and burst biphasic [BB]).

When applying the train pulses at 60% and 80% of the motor response threshold, the constant bursts monophasic (MB) and biphasic (BB) were not associated with lower pain levels than the constant pulse monophasic (MP). Participant 1 and participant 2 rated the relative stimulation

thresholds of 60% and 80% as very severe and worst pain possible across the three waveforms. Participant 3 reported stimulation intensity at 60% of the muscle response threshold as no pain (constant MB and BB) and moderate pain (constant MP) and 80% of the muscle response threshold as mild (constant BB) and moderate pain (constant MB and MP).

Discussion

Single waveform high-frequency spinal cord stimulation (HF-tSCS) reduced pain and discomfort compared with low-frequency stimulation (LF-tSCS) when applied with the same stimulation intensity. However, while HF-tSCS reduced the pain at LF-tSCS threshold intensity, it did not evoke any motor response. In fact, the current required to evoke a motor response was three times higher for HF-tSCS than LF-tSCS. This resulted in participants reporting more severe pain in high frequency than in low frequency stimulation when stimulating at motor threshold intensity.

Our results suggest that the acceptability of cervical tSCS may vary between participants depending on the patient's individual stimulation intensity required to evoke the posterior root reflex. Motor reflex excitability is known to be influenced by various parameters such as age, body mass and gender [11]. Participants 1 and 2 indicated higher pain levels than participant 3 throughout the intervention. The lower pain level reported by participant 3 (female) could be due to the lower absolute muscle response threshold compared with the other two participants (male).

In conclusion, our results suggest that cervical high frequency stimulation may not (yet) be an option for clinical application, even though acceptability may depend on the patient's individual posterior root reflex excitability. Further investigations on the stimulation parameters (e.g., using biphasic pulse wave-form, different frequencies -i.e., 20, 30, 50 Hz, longer bursts durations -e.g., 3~4 ms, and electrode locations) should be performed. Finally, stimulation while subjects are lying supine might reduce the motor response threshold, resulting in a less painful intervention [6].

Acknowledgments

References

[1] E. Formento *et al.*, "Electrical spinal cord stimulation must preserve proprioception to enable locomotion in humans with spinal cord injury," *Nat. Neurosci.*, vol. 21, no. 12, pp. 1728–1741, 2018.

[2] M. Visocchi, A. Giordano, M. Calcagni, B. Cioni, F. Di Rocco, and M. Meglio, "Spinal Cord Stimulation and Cerebral Blood Flow in Stroke: Personal Experience," *Stereotact. Funct. Neurosurg.*, vol. 76, no. 3–4, pp. 262–268, 2001.

[3] Y. Gerasimenko, R. Gorodnichev, T. Moshonkina, D. Sayenko, P. Gad, and V. Reggie Edgerton, "Transcutaneous electrical spinal-cord stimulation in humans," *Ann. Phys. Rehabil. Med.*, vol. 58, no. 4, pp. 225–231, Sep. 2015.

[4] U. S. Hofstoetter *et al.*, "Augmentation of Voluntary Locomotor Activity by Transcutaneous Spinal Cord Stimulation in Motor-Incomplete Spinal Cord-Injured Individuals," *Artif. Organs*, vol. 39, no. 10, pp. E176–E186, 2015.

[5] M. Alam *et al.*, "Electrical neuromodulation of the cervical spinal cord facilitates forelimb skilled function recovery in spinal cord injured rats," *Exp. Neurol.*, vol. 291, pp. 141–150, 2017.

[6] M. Milosevic, Y. Masugi, A. Sasaki, D. G. Sayenko, and K. Nakazawa, "On the reflex mechanisms of cervical transcutaneous spinal cord stimulation in human subjects," *J. Neurophysiol.*, vol. 121, no. 5, pp. 1672–1679, May 2019.

[7] A. Ievins and C. T. Moritz, "Therapeutic Stimulation for Restoration of Function After Spinal Cord Injury," *Physiol. Bethesda Md*, vol. 32, no. 5, pp. 391–398, Sep. 2017.

[8] P. Gad *et al.*, "Non-Invasive Activation of Cervical Spinal Networks after Severe Paralysis," *J. Neurotrauma*, vol. 35, no. 18, pp. 2145–2158, Sep. 2018.

[9] K. Leonardo and A.-K. Adnan, "Chapter 54 - Ten Kilohertz (10kHz) High-Frequency Spinal Cord Stimulation," in *Neuromodulation (Second Edition)*, E. S. Krames, P. H. Peckham, and A. R. Rezai, Eds. Academic Press, 2018, pp. 693–699.

[10] R. Shechter *et al.*, "Conventional and Kilohertz-frequency Spinal Cord Stimulation Produces Intensity- and Frequency-dependent Inhibition of Mechanical Hypersensitivity in a Rat Model of Neuropathic Pain," *Anesthesiol. J. Am. Soc. Anesthesiol.*, vol. 119, no. 2, pp. 422–432, Aug. 2013.

[11] S. Massey SJE, Y. Al'Joboori, A. Vanhoestenberghe, and L. Duffell, "The Effects of Neuromodulation on Central Excitability of the Upper Limb in Healthy, Able-bodied Adults," presented at the International Functional Electrical Stimulation Society Conference 2018, Nottwil, Switzerland, 2018.

[12] S. Rennie, "ELECTROPHYSICAL AGENTS - Contraindications And Precautions: An Evidence-Based Approach To Clinical Decision Making In Physical Therapy," *Physiother. Can. Physiother. Can.*, vol. 62, no. 5, pp. 1–80, 2010.

[13] N. A. Maffiuletti *et al.*, "Effect of gender and obesity on electrical current thresholds," *Muscle Nerve*, vol. 44, no. 2, pp. 202–207, Aug. 2011.

Author's Address

Eduardo Villar Ortega
Motor Learning and Neurorehabilitation Laboratory, ARTORG Center for Biomedical Engineering Research, University of Bern, Bern, Switzerland
eduardo.villarortega@artorg.unibe.ch
http://www.artorg.unibe.ch/research/mln/index_eng.html

Short Impulse Stimulation for predominant Activation of proprioceptive Afferents

Kast C[1,2], Vargas Luna J[1], Hofer C[2,3], Aszmann OC[2], Mayr W[1,2]

[1] Center for Medical Physics and Biomedical Engineering, Medical University of Vienna, Austria
[2] Clinical Laboratory for Bionic Limb Reconstruction, Medical University of Vienna, Austria
[3] Otto Bock Healthcare Products GmbH, Vienna, Austria

Abstract: *Complementary to visual feedback, proprioception is essential for awareness of the body image and particular the actual arm and hand position. Information on the object's surface, grip force, or proprioception is possible even without visual feedback in the physiologically intact upper extremity. Within a broader project on upper extremity reconstruction after amputation, we work on inducing near-natural impressions artificially to persons with amputation, helping to integrate mechanical prosthesis into the body schema and facilitating acceptance and handling of artificial limbs. Using a specific stimulation protocol, with very short stimulation pulses (10 µs), and high amplitudes it is possible to elicit proprioceptive feedback with surface electrodes in persons with upper limb loss while avoiding unpleasant skin sensation in the application area of the stimulation electrode. Single-pulse stimulation (1 Hz) with very short stimuli were able to induce stimulus threshold perception first as proximal sensation (distal proprioception threshold), with increased stimulus intensity as local skin sensation in the contact area of the active electrode (local sensory threshold) and finally as distal movement (motor threshold).*

Keywords: *proprioception, afferent nerve stimulation, amputation, phantom limb, neuroprosthesis*

Introduction

In a physiologically intact upper extremity, sensory perception provides haptic information, like on an object surface and grip force, and proprioception gives permanent information on the position of all arm- and hand segments in space, even without support by visual feedback. Within a wider project on upper extremity reconstruction after amputation, we work on inducing similar impressions artificially to persons with amputation, helping to integrate mechanical prostheses into the body schema and facilitating acceptance and handling of artificial limbs.

The knowledge on the position of the arm without the need for support by visual perception is a feature of the natural limb that is very difficult to copy. So far, several studies are trying to create some kind of artificial sensing to the arm prosthesis by using haptic feedback modalities (e.g., vibration, electrical stimulation, etc.) [1]–[7]. Several studies stated that sensory feedback not only helps to improve dexterity but also the reliability of myoelectric control in grasping tasks [1], [8], [9].

It has also been shown, that electrical stimulation can not only reduce phantom pain in a stump after amputation but can be applied for evoking sensory feedback like touch, joint movement, and limb position in individuals with amputations [10]–[13]. Using specific stimulation patterns, it has even been demonstrated to convey varying sensory feelings [9] or even correctly identify objects [1].

The drawback in these studies is the necessity of patients having an identifiable projected finger map or using implanted electrodes that are accompanied by high costs and surgical risks. Current solutions with surface electrodes are not entirely satisfactory for sensory feedback with practical value yet, in particular in commercial products.

Afferent nerve fibers can be activated by electrical stimulation at peripheral sites where multiple types of neurons, including Ia, Ib, and cutaneous afferents (type II) would be recruited. Stimulation of these afferent fibers at a sufficiently high frequency (100 Hz) evokes temporal summation of excitatory postsynaptic potentials in motorneurons, indicating the potential for activity patterns more similar to physiological activation. [14], [15]

First experiments with very short impulses were performed by Macdonald et al. in 1995, where they placed surface electrodes on the mid-line of the back for electrotherapy which they called transcutaneous spinal electroanalgesia (TSE) [16]. The authors decided to use very short pulses (typically 4 µs) with sufficient voltage (above 100 V) to reach the nerve. TSE was applied to the skin overlying the vertebral spine and the stimulation frequencies were far higher (2500+ Hz) than those for transcutaneous electrical nerve stimulation (TENS) (circa 1 - 150 Hz). The pulse widths used are also substantially different: 4 - 10 µs for TSE compared with 50 - 200 µs for TENS [16], [17].

Here, we present observations on eliciting basic anatomical perception in phantom limbs by means of combining TENS and TSE. The parameters chosen, have the advantage of reducing the uncomfortable skin sensation known by conventional TENS while predominantly activating afferent nerve fibers.

Material and Methods

Subjects
Experiments were performed on eight volunteers (seven men and one woman; mean age ± SD = 40 ± 17). Three

abled-bodied persons and five with an upper limb amputation (three transradial, two transhumeral). The inclusion criterion was a unilateral upper limb amputation with intact plexus and a generally healthy condition.

All experiments were conducted in accordance with the Declaration of Helsinki and approved by the Ethics Committee of the Medical University of Vienna. All participants were informed about all experimental procedures and signed the informed consent.

Table 1: General information on subjects with upper limb amputation.

Subject (Gender, age)	Amputation side, cause and years since the incident
1 (M, 53)	Left, trauma, 2
2 (M, 54)	Right, trauma, 2
3 (F, 34)	Left, trauma, 33
4 (M,35)	Right, trauma, 20
5 (M, 51)	Left, trauma, 4

Experimental setup
The subject had his arm (stump) positioned on a cushioned pedestal, lifted to 90° in relation to the vertical body axis. This position was comfortable for the subject and allowed access to the armpit to place the stimulation electrode. A self-adhesive reference electrode (75 x 140 mm, Dr. Schuhfried Medizintechnik GmbH) was applied on top of the shoulder of the (amputated) arm. The active counter electrode was a ball-shaped stainless steel (316L) electrode that was placed in the armpit right under the ulnar nerve / median nerve / radial nerve and fixed with a strap that allowed applying contact pressure on the active electrode. To enhance the electrical conductivity, electrode gel was applied.

Stimulation protocol
Voltage-controlled bipolar rectangular pulses with a phase width of 10 µs to 100 µs were applied in a continuous train of 1 Hz or 80/100 Hz. It has been shown that using vibratory stimulation with a frequency range of around 70 Hz was described as kind of movement illusions [18]. In our initial preliminary experiments, the subject's reported similar impressions to electrical stimulation with a frequency above 70 Hz. The experiments have shown that there is no difference in perception if the stimulation frequency is 80 Hz or 100 Hz.
The stimulation output was controlled with a LabVIEW 2017 program (National Instruments Corporation) that transferred the digital output to NI USB-6216 (National Instruments Corporation), an isolated USB-multifunction I/O device. That output was finally conveyed to the input of the stimulator (STMISOLA, Biopac Systems Inc.) to deliver the stimulus.

Since the aim of this study was to induce near-natural sensations without feeling the undesirable electrical tingling at the contact area of the active electrode, the appropriate stimulation intensity needed to be identified. To find the thresholds for distal perception and skin sensation at the electrode site, a modified version of the staircase method, as described in [19], a variation of the method of limits was applied. During stimulation with a continuous train of pulses which progressively increased in amplitude, the subject was asked to say yes if there was a sensation felt at the stimulation electrode. Then the descending sequence started which was terminated when there was no sensation present, at that point the sequence was reversed again. The threshold was calculated as the average of the transition points.

Experiment 1: Evaluation of perceptual attributes
The experimenter was moving the stimulation electrode near the Musculus coracobrachialis, right above the radial, median, and ulnar nerve. The subjects were asked to inform the experimenter if they feel anything unusual. In that case, the experimenter asked where precisely this feeling was occurring and how they would describe what they feel. The phase duration was set to 10 µs while the stimulation amplitude was increased in steps of 1 V if the subject could not sense any excitation.

Experiment 2: Evaluation of sensory thresholds
At the position where the subject reported distal perception, experiment 2 began. The phase duration was set to 10 µs and increased in steps of 10 µs up to maximal 80 µs, while the frequency was fixed to 80 Hz and the initial stimulation amplitude set to 1 V. Before increasing the phase duration, the subject was asked if there is distal excitation or a sensation at the electrode position. If any muscle activation occurred, the experimenter noted the motor threshold. When the subject reported beginning discomfort or a motor threshold was reached, the trial ended. The amplitude was increased by 1 V, and the procedure was repeated.
In abled-bodied subjects, the same experiment was performed with the frequency set to 1 Hz.

Data analysis
All data analyses were conducted using MATLAB R2015b (MathWorks, Natick, Massachusetts).

Results

Experiment 1: Evaluation of perceptual attributes
All subjects were comfortable with the stimulation. Due to the stimulation below the threshold of tingling at the stimulation electrode, no pain was caused, and no local stimulation could be detected at the site of stimulation. At specific electrode locations and 80 Hz stimulation, the patients reported a feeling of a "pressure sensation" in specific areas of the missing limb, or a feeling similar to having the arm "outstretched" in the 3-dimensional space, or even selective perception of single phantom fingers. Stimulation above the accepted maximum level usually caused local discomfort, but no uncomfortable distal sensation. These findings correlate with [13], where the authors had comparable results but used an invasive approach.

The proprioceptive feeling was localized in the distal branches of the nerves, like the lower arm, the hand or the fingers.

Table 2: Proprioceptive feelings

Location	Sensation elicited
Thumb	Bent, Pressure
Pointer	Pulsation, Tingling, Outstretched
Middle finger	Rubbing
Ring finger	Rubbing
Little finger	Outstretched
Lower arm	Bent, Pressure

The sensations described by the subjects ranged from tingling in individual fingers to the feeling of an arm being bent (Tab. 2). A pinprick sensation could be elicited in every subject.

Experiment 2: Evaluation of sensory thresholds
Single-pulse stimulation (1 Hz) with very short stimuli were able to induce stimulus threshold perception first as proximal sensation (distal proprioception threshold - paresthesia), and then with increased stimulus intensity as local skin sensation in the contact area of the active electrode (local sensory threshold) and finally as distal movement (motor threshold). E.g., one able-bodied subject could feel his little finger at 20 V and 10 μs whereas first muscular responses could be seen starting with 28 V.
Using 80 Hz stimuli the thresholds to elicit distal proprioceptive sensations before reaching the motor threshold were even more clearly separated. In subjects having an upper limb loss, it was not possible to elicit visible local motor responses with 10 μs pulses, before reaching uncomfortable stimulation amplitudes.
The measured values (Fig. 1) nicely fit Lapicque's strength-duration curve, including all influences on the separation of sensory and motor thresholds like electrode placement and the pressure applied.
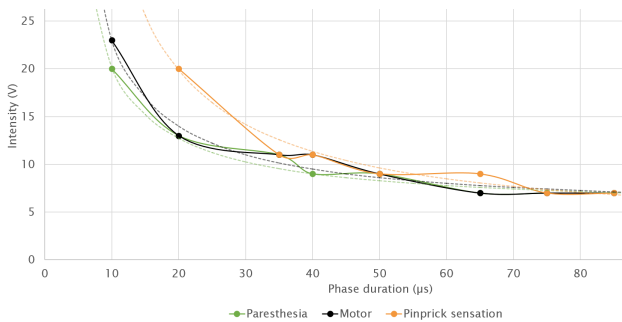
Figure 1: Measured paresthesia, motor and pinprick sensation thresholds (1 Hz); dashed curves show the corresponding Lapicque's equation

Discussion

To enhance the functionality of prosthesis control, sensory feedback is crucial to provide the user status information of the device in real-time. Especially feedback by means of natural sensory pathways is missing in clinical prosthetic systems [8]. Although there are several approaches for sensory feedback with intraneural stimulation, it has always been a challenge to selectively evoke near-natural proprioceptive feedback.

This work shows that it is possible to elicit proprioceptive feedback with surface electrodes using very short stimulation impulses with high amplitudes in subjects with upper limb loss without feeling the undesirable electrical tingling at the contact area of the active electrode. It is even possible to selectively discriminate individual fingers.

The threshold data presented in Fig. 1 were recorded on an able-bodied person. Nevertheless, it is consistent with the data from subjects with upper limb loss. The trend in the data shows that first, the distal proprioceptive threshold is reached, followed by local sensory and motor threshold. The pressure dependence observed in the experiments will be faced in future studies by integrating a pressure sensor in the stimulation electrode.

The test for the evaluation of sensory thresholds in intact individuals turned out to be difficult, as the motor threshold for muscle twitch reactions in the distal arm got quite strong before the local cutaneous threshold was reached. With longer pulses, e.g., 100 μs, the threshold amplitudes for distal proprioception and local sensory perception got more similar, and selective stimulation for distal perception got difficult.

Conclusions

There is strong evidence that it is possible to provide some kind of proprioceptive feedback from a phantom limb of amputated subjects while avoiding uncomfortable skin sensation at the surface electrodes site. This could only be observed with very short stimulation pulses (around 10 μs) and disappeared with increasing pulse duration. Further work will focus on the applicability of these findings in prosthesis control and to what extent inconvenience in other applications of electrical stimulation can be reduced. Due to the non-invasive approach, this could be a practical way to restore near-natural proprioceptive feedback to some extent or reduce sensible discomfort in FES applications. By applying proprioceptive feedback, the control-loop in prosthesis control techniques could be closed, and dexterity and reliability of myoelectric control in daily tasks could be improved.

Acknowledgment

References

[1]   K. Horch, S. Meek, T. G. Taylor, and D. T. Hutchinson, "Object discrimination with an artificial hand using electrical stimulation of peripheral tactile and proprioceptive pathways with intrafascicular electrodes," *IEEE Trans. Neural Syst. Rehabil. Eng.*, vol. 19, no. 5, pp. 483–489, 2011.

[2]   X. X. Liu, G. H. Chai, H. E. Qu, and N. Lan, "A sensory feedback system for prosthetic hand based on evoked tactile sensation," *Proc. Annu. Int. Conf.*

IEEE Eng. Med. Biol. Soc. EMBS, vol. 2015-Novem, pp. 2493–2496, 2015.

[3]   M. Štrbac *et al.*, "Integrated and flexible multichannel interface for electrotactile stimulation," *J. Neural Eng.*, vol. 13, no. 4, p. 046014, 2016.

[4]   E. Rombokas, C. E. Stepp, C. Chang, M. Malhotra, and Y. Matsuoka, "Vibrotactile sensory substitution for electromyographic control of object manipulation," *IEEE Trans. Biomed. Eng.*, vol. 60, no. 8, pp. 2226–2232, 2013.

[5]   C. E. Stepp and Y. Matsuoka, "Object manipulation improvements due to single session training outweigh the differences among stimulation sites during vibrotactile feedback," *IEEE Trans. Neural Syst. Rehabil. Eng.*, vol. 19, no. 6, pp. 677–685, 2011.

[6]   B.- Sheridan and S. St, "Apparatus For Providing Vibrotactile Sensory Substitution Of Force Feedback," 1997.

[7]   C. E. Stepp and Y. Matsuoka, "Relative to direct haptic feedback, remote vibrotactile feedback improves but slows object manipulation," *2010 Annu. Int. Conf. IEEE Eng. Med. Biol. Soc. EMBC'10*, pp. 2089–2092, 2010.

[8]   D. Farina and O. Aszmann, "Bionic Limbs: Clinical Reality and Academic Promises," *Sci. Transl. Med.*, vol. 6, no. 257, pp. 257ps12-257ps12, Oct. 2014.

[9]   G. Chai, X. Sui, S. Li, L. He, and N. Lan, "Characterization of evoked tactile sensation in forearm amputees with transcutaneous electrical nerve stimulation," *J. Neural Eng.*, vol. 12, no. 6, p. 066002, 2015.

[10]   M. R. Mulvey, H. J. Fawkner, H. Radford, and M. I. Johnson, "The use of transcutaneous electrical nerve stimulation (TENS) to aid perceptual embodiment of prosthetic limbs," *Med. Hypotheses*, vol. 72, no. 2, pp. 140–142, 2009.

[11]   R. R. Riso, "Strategies for providing upper extremity amputees with tactile and hand position feedback--moving closer to the bionic arm.," *Technol. Health Care*, vol. 7, no. 6, pp. 401–409, 1999.

[12]   M. R. Mulvey, H. J. Fawkner, H. E. Radford, and M. I. Johnson, "Perceptual embodiment of prosthetic limbs by transcutaneous electrical nerve stimulation," *Neuromodulation*, vol. 15, no. 1, pp. 42–47, 2012.

[13]   A. B. Anani, K. Ikeda, and L. M. Körner, "Human ability to discriminate various parameters in afferent electrical nerve stimulation with particular reference to prostheses sensory feedback," *Med. Biol. Eng. Comput.*, vol. 15, no. 4, pp. 363–373, 1977.

[14]   J. L. Dideriksen, S. Muceli, S. Dosen, C. M. Laine, and D. Farina, "Physiological recruitment of motor units by high-frequency electrical stimulation of afferent pathways.," *J. Appl. Physiol.*, vol. 118, no. 3, pp. 365–76, 2015.

[15]   U. Proske and S. C. Gandevia, "The Proprioceptive Senses: Their Roles in Signaling Body Shape, Body Position and Movement, and Muscle Force," *Physiol. Rev.*, vol. 92, no. 4, pp. 1651–1697, 2012.

[16]   A. J. Macdonald and T. W. Coates, "The Discovery of Transcutaneous Spinal Electroanalgesia and Its Relief of Chronic Pain," *Physiotherapy*, vol. 81, no. 11, pp. 653–661, 1995.

[17]   J. W. Thompson, S. Bower, and S. P. Tyrer, "A double blind randomised controlled clinical trial on the effect of transcutaneous spinal electroanalgesia (TSE) on low back pain," *Eur. J. Pain*, vol. 12, no. 3, pp. 371–377, 2008.

[18]   T. Kito, "Does vibration-induced kinesthetic illusion accompany motor responses in agonistic and antagonistic muscles?," *J. Phys. Fit. Sport. Med.*, vol. 5, no. 1, pp. 73–76, 2016.

[19]   T. N. Cornsweet, "The staircrase-method in psychophysics.," *Am. J. Psychol.*, vol. 75, pp. 485–491, 1962.

Author's Address

Christoph Kast
Center for Medical Physics and Biomedical Engineering, Medical University of Vienna, Vienna, Austria
christoph.kast@meduniwien.ac.at

Session 7:
Hybrid systems for exercising cyclic functional movements

The Role of Functional Electrical Stimulation in Hybrid Systems for Rehabilitation

Popović, D.B.

Serbian Academy of Sciences and Arts, Belgrade, Serbia and Aalborg University, Aalborg, Denmark

Abstract: *The current approach in the rehabilitation favours maximum intensity training of functional movements. The evidence from clinical studies where constraint-induced movement therapy, robot-assisted therapy, and functional electrical stimulation (FES) have been compared with conventional treatments suggested a significant increment in the speed and level of recovery of compromised functions. In parallel, clinical studies where two therapies have been compared with only one indicate that the more action is induced, especially during the early period after the onset of impairment, the carry-over effects are pronounced. The development of exercise machines like training bicycles, tricycles, body suspension systems, and robot mechanisms which drive the leg combined with the FES and integrated into the training protocol where the person with impairment must work hard seems to be the solution which deserves much attention. The biggest problem is the integration where the external support will be minimized, while the remaining motor abilities will be used as much as possible. Ultimately, the biological control should be mimicked and necessary compensatory motor control strategy developed by the user after the onset of the impairment allowed. Forcing the recovery of normal function is not necessarily an optimal solution since the motor capacity after the lesion of the central nervous system is not normal. The user of the system must feel that he is in control of a motor function. The FES provides conditions for the intensive parallel exercise of "healthy" and "impaired" motor systems. The likely significant effect of the stimulation is the activation of sensory systems that directly contribute to the modified excitability of the brain systems. The altered excitability leads to "plastic" changes (reorganization of the motor schema), but also to the generation of motor signals that assist in the normalization of spinal networks operation. The FES facilitated exercise contributes to the prevention of muscle loss and the range of movement and provides a condition for better functioning of the cardiovascular and pulmonary systems. The FES is an ideal add-on to exoskeletons and increases the efficacy of the rehabilitation. The features of the FES systems which will make the difference are the simple interface allowing the implementation by clinicians and individual home users and physiological like synergistic activation of the sensory-motor systems.*

Keywords: *The hybrid system, FES, exoskeleton, intensive exercise, restoration of function*

Author's Address

Name: Dejan B. Popović

Affiliation: Serbian Academy of Sciences and Arts, Belgrade, Serbia, and Aalborg University, Denmark

Knez Mihailova 35, 11000 Belgrade, Serbia

e-mail: dbp@etf.bg.ac.rs

homepage: https://vbn.aau.dk/en/persons/100233

STIMULATION PARAMETERS FOR CYCLING IN PERSONS WITH DENERVATED AND ATROPHIED MUSCLES DUE TO INJURY OF THE CENTRAL NERVOUS SYSTEM

Mayr W

Department of Medical Physics and Biomedical Engineering, Medical University of Vienna, Austria

Abstract: Functional Electrical Stimulation (FES) of denervated muscles has long been regarded as generally insufficient, only some limited capability of slowing down degenerative processes in muscle tissue with lost nerve supply has been attributed to application of sequences of long-duration triangular stimuli ("Exponential Current") via skin attached electrodes. After growing evidences that more effective direct muscle stimulation is possible with appropriate stimulation patterns, this question was addressed on a broader basis in the European Research and Development Project "RISE", that was focused to individuals with flaccid paraplegia with clinically complete denervation of both lower extremities. Deliverables of RISE were validated clinical guidelines for maintaining intact or retraining degenerated denervated muscles and equipment for stimulation and assessment of muscle status for intervention planning and monitoring. The method provides effective prophylaxis against pressure sores and osteoporosis, and opens new exercising means for cardiovascular fitness for persons with flaccid paraplegia. Within RISE this was accomplished by stand-up and stepping exercises, now, as an additional modality, cycling was tested. In comparison to established FES-cycling, in case of lower motor neuron lesion specific strategies are needed to achieve fused muscle contractions for propelling, as effective stimuli have a minimum length of 30ms. Preparatory conditioning of muscle excitability is necessary before appropriate patterns are applicable. An alternative cycle design applies rowing-like leg movements instead of classical pedalling for more efficient propulsion and simpler control, just involving Mm. quadriceps contractions.

Keywords: denervated muscles, lower motor neuron lesion, direct muscle stimulation, FES-cycling

Author's Address

Winfried Mayr
Center for Medical Physics and Biomedical Engineering,
Medical University of Vienna, Austria
Winfried.mayr@meduniwien.ac.at

THE IMPORTANCE OF MODELING FOR CONTROL OF ELECTRICAL STIMULATION FOR CYCLING

Laczko J

Wigner Research Centre for Physics, University of Pecs, Hungary

Abstract: *The proper execution of limb movements requires well-coordinated interaction between neural, muscular and skeletal structures. The multilevel control of limb movements and locomotion is known and has already been modeled for various types of motor tasks. Models are applied to study healthy human limb movements as well as provide research tools that can be used in rehabilitation of spinal cord injured (SCI) persons. This strongly relates to control of devices and approaches that help to substitute lost motor functions. One particular application is functional electrical stimulation (FES). Modeling is very important to define stimulation patterns for FES cycling on a stationary cycle-ergometer or mobile tricycle. There are several commercially available FES cycling systems which can be used in passive and active mode. In active mode not only the amplitude, pulse with, wave forms and stimulation frequency influence the performance of the cyclist participant. Besides these factors, the timing of muscle activities also influences the power and energy output of the participant. In FES cycling, stimulation intervals of muscles are usually given as a function of the crank angle and that function is mapped to the time domain. Recorded muscle activity patterns (time series of EMG signals) may be averaged across healthy subjects and the averaged patterns are used to define stimulation patterns for cycling movements of SCI individuals. However, individual differences are significant, and the muscle properties of SCI individuals differ from that of able-bodied persons. Intrinsic, biomechanical and geometric properties of the particular musculo-skeletal system and external conditions as gravity, or crank resistance affects the cycling performance and success of FES cycling trainings. Changing pedaling cadence or changing crank resistance is associated with altered timing of muscle activities and altered muscle synergies. For instance, cycling against higher crank resistance or cycling with higher cadence may be achieved by increasing stimulation current amplitude or altering the length of co-activation time-intervals of several muscles. Modeling can help to discern relation between extrinsic variables and muscle stimulation patterns. Recently dimension reduction methods as non-negative matrix factorization is applied to model synergistic control of sets of muscles. All of these modeling techniques may help to design efficient FES cycling trainings for spinal cord injured persons.*

Keywords: *denervated muscles, lower motor neuron lesion, direct muscle stimulation, FES-cycling*

Author's Address

Jozsef Laczko
Wigner Research Centre for Physics,
University of Pecs
jozseflaczko1@gmail.com

FES Cycling in Persons with Paralyzed Legs: Force Feedback for Setup and Control

Popović Maneski Lana[1], Amine Metani[2]

[1]Institute of Technical Sciences of the Serbian Academy of Sciences and Arts (ITS-SASA), Belgrade, Serbia
[2]Univ Lyon, ENS de Lyon, Univ Claude Bernard, CNRS, Laboratoire de Physique, F-69342 Lyon, France

Abstract*:*

Cycling assisted by functional electrical stimulation (FES cycling) has many positive effects on the overall health in persons with paralyzed legs due to the injury of the central nervous system (i.e., increases bulk of stimulated muscles, preserved range of movements in the joints, preserved cross-section geometry of long bones that are axially loaded, reduced body fat content, preserved functioning of the cardiovascular and pulmonary systems, reduced frequency of urinary infections, reduced spasticity in stimulated muscles). If the FES cycling exercise starts shortly after the central nervous system lesion, then the muscles will not be atrophied. The FES needs to provide sufficient muscle power to turn the pedals of the bicycle. If the pedals don't rotate, then the exercise would be discouraging for the patient and many among them would give up on this type of training. The FES assistance must provide strong enough stimulation that is tolerable by the user, and the correct timing of stimulation bursts to push and pull when needed. If the stimulation power is not sufficient, then the external power coming from the motor built into the exercise bike is required. The temporal pattern (on-off) need to match the pushing and pulling on the pedals at the appropriate positions to generate the driving momentum; hence, it is linked to the angle of the pedals (from 0° to 360°). The optimal setup of the temporal pattern benefits from the assessment of the interface force between the pedal and the foot. The driving torques will be optimal if the interface force is perpendicular to the lever.

We are developing a protocol for designing the optimal stimulation-motor assistance profile for the cycling based on the measurements of the interface forces. The setup uses the optimization criterion that maximizes the effect based on the asynchronous activation of synergistic muscles. The protocol is being developed for the therapy performed with Omego bike (Tyromotion GmbH, Graz, Austria) and Motimove FES stimulator (3F-Fit Fabricando Faber Ltd, Belgrade, Serbia). The same principle used for the setup can be used for closed-loop control to correct the original non-optimal temporal pattern.

Keywords*: FES, cycling, force feedback*

Author's Address

Name: Lana Popović-Maneski

Affiliation: Institute of Technical Sciences of the Serbian Academy of Sciences and Arts (ITS-SASA), Belgrade, Serbia

Knez Mihailova 35/IV, 11000 Belgrade, Serbia

e-mail: lanapm13@gmail.com

homepage: http://www.itn.sanu.ac.rs/Lana_Popovic_Maneski-eng.html

Tricycling by FES of quadriceps muscles leads to increased cycling speed over series of trainings of persons with flaccid paraplegia

Mravcsik M[1,2], Klauber A[3], Putz M[3], Kast C[4], Hofer C[4], Mayr W[4], <u>Laczko J</u>[1,2]

[1]University of Pecs, Hungary
[2]Wigner Research Centre for Physics, Budapest Hungary
[3] National Institute for Medical Rehabilitation, Budapest, Hungary
[4] Medical University of Vienna, Wien, Austria

Abstract: *We present that a sequence of FES cycling trainings on a special tricycle for persons with flaccid paraplegia, made them able to drive the tricycle and increase cycling speed during the series of trainings. Participants cycled for 30 minutes, two times a week for six weeks. A custom build 4 channel electrical stimulator for denervated muscles delivered biphasic rectangular pulses for activating synchronously quadriceps muscles of both legs. Thus, bilateral knee extension was actively driving the tricycle. Improvements in cycling speed were observed with progress of trainings. The level of injury was T10 for two and T12 for one participant. Their age was 32, 45 and 67 years. The time since injury was 3, 6, and 29 months.* The cycling speed was measured and the average speed was calculated for each training. The average speed was related to the corresponding sequential number of the training in the sequence of trainings. This relation shows a slope of regression *0.22, 0.23 and 0.12 for the 3 participants. The third participant who showed a lowest slope of improvement was the oldest and his time since injury was the longest. This may explain the slower improvement in cycling speed. The youngest participant reached the highest speed and his improvement of cycling speed was also the highest while he had the same level of injury as the oldest participant. Thus, mainly the age and time since injury may affect the improvement in cycling speed.*

Keywords: *Denervated muscles, tricycle, cycling speed*

Introduction

Functional electrical stimulation (FES) helps to maintain and regenerate denervated muscles [1]. Some FES based training protocols were applied for denervated muscles of persons with paraplegia and relevant improvements were reported in the contractibility and functionality of their muscles. These training generated tetanic contractions in the quadriceps muscles and comprised standing up exercises as well [2]. Our aim is to investigate how FES driven cycling exercises can be performed by denervated muscles. FES cycling is often applied in rehabilitation of Spinal Cord Injured (SCI) individuals with spastic muscles [3,4,5]. However, as far as we know, FES cycling has not been applied for patients with denervated muscles.

We train SCI persons with flaccid paraplegia to perform cycling movements with a special tricycle (Reha-Funtrike, OVG, Munich, Germany) adapted for this purpose and employing a special stimulator device (controller). Participants were very motivated in performing the series of trainings. Earlier we had presented results of 2 young SCI participants who had relatively fresh injuries (they started the training 3 and 6 months after injury) [6]. Here we report the accomplishment of an older participant (P3) who started the trainings much later after the injury than the other 2 persons and we compare his achievement with that of the former participant's. The Ethical Committee of the National Institute for Medical Rehabilitation, Hungary approved the FES trainings.

Material and Methods

Recovery from muscle degeneration after denervation can be reached by FES training and this is the only possibility for denervated muscles to generate force. By this strong motivation participants performed cycling trainings for 30 minutes, two times a week during six weeks. The basic data of participants are given in Table 1.

A custom build 4 channel electrical stimulator for denervated muscles can deliver biphasic rectangular pulses (15 - 100 ms per phase, +/- 80 V), for activating synchronously quadriceps muscles of both legs. Thus, bilateral knee extension was actively driving the tricycle equipped with the stimulator device (Figure 1). In both legs, pairs of conductive rubber electrodes (Schuhfried Inc., Vienna Austria) with wetted foam pads were used to stimulate the quadriceps and induce knee extension. In this "cycling mode" the muscle contractions move the trunk backwards in the longitudinally sliding seat, with the cycle chain coupled to the seat and thus driving the cycle. The size of each electrode was 200 cm^2, they were placed above the quadriceps muscles, centered to the rectus femoris. Interelectrode distance was approximately 10 cm.

In "rowing mode", passive knee flexion is generated by pulling the body forward, towards the firm steering bar by active arm flexion, and moving the sliding, but now decoupled from the chain, seat forward. There was no stimulation during forward movement phase in rowing mode.

In each training the average cycling speed was computed for three equal phases (10 minutes long intervals at the starting, middle and finishing) of the training and for the whole training as well. The means of these speed values were then computed across trainings. The across trainings standard deviation of the speed for each particular phase (starting, middle and finishing) was investigated to reveal whether the speed changed within the trainings consistently comparing different trainings.

The average speed in a particular training was related to the corresponding sequential number of that training.
The slope of the regression line of this relation characterized the improvement of the participant's performance in terms of cycling speed.

Figure 1. The special tricycle equipped with a stimulator (controller) that delivers signals to the quadriceps muscles through surface electrodes. Bilateral knee extension starts and actively drives the tricycle as the quadriceps muscles are stimulated.

Table 1: Basic data of participants

	P1	P2	P3
Gender	male	male	Male
Age	32	45	67
Level of injury	T10	T12	T10
Time since injury	3 months	6 months	29 months
Average speed during the training (mean and SD across trainings)	5 km/h SD=0.87	4 km/h SD=0.86	4.38 km/h SD=0.52

Results

Regarding P3 the improvement in speed across trials is presented at Fig 2. The slope of regression was 0.12.
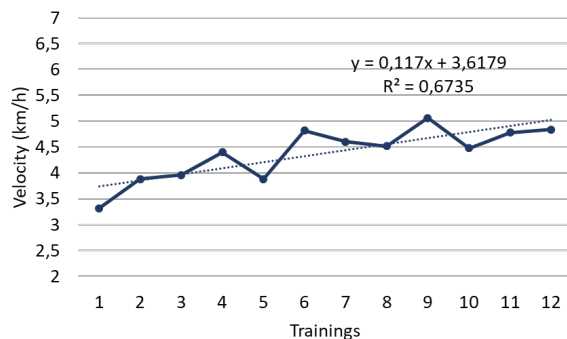
Figure 2: The average (within training) speed in each 12 consecutive trainings for a 67 years old SCI person. Dotted line represents linear regression corresponding to the given regression equation.

Interestingly, the mean speed (across trainings) in the first second and third phases were almost equal (4.44, 4.34, 4.36 km/h (Fig 3.). Standard deviation was 0.57, 0.65, and 0.56 for the 1st, 2nd and 3rd phases respectively.
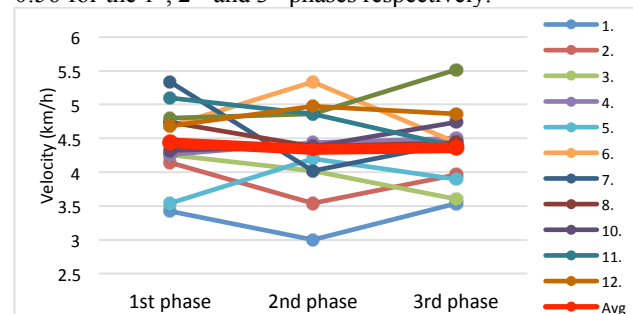
Figure 3: The average (across trainings) speed in the 1st 2nd and 3rd phases of the trainings (dots connected by thick lines). Small dots (connected by thin lines) represent speed values for 12 separate trainings for the older (P3) participant.
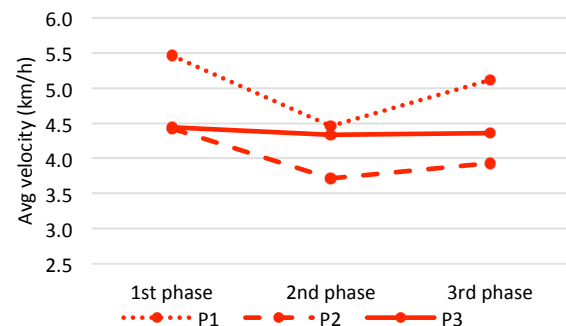
Figure 4: The average (across trainings) speed in the three phases of the trainings for 3 participants.

Discussion

The tricycling speed increased during the series of trainings in the case of two participants (P1 and P2), whose results have been presented earlier [6]. The slope of regression (that characterized he improvement in speed) for P1 and P2 (0.22, 0.23 respectively) was larger than that of the third participant whose results are presented here. In this latter case the slope of regression was 0.12.

The third participant who showed a lowest slope of improvement in speed, was the oldest and the time since his injury was the longest compared to the other two participants. This may explain the slower improvement in his cycling speed. The youngest participant reached the highest speed and his improvement of cycling speed was also the highest, while his level of injury (T10) was the same as that of the oldest person.

It was presented earlier [6], that in the case of the first two participants (P1 and P2) the speed was lower in the middle phase of the training than at the beginning and at the end of it, in almost all of the trainings (in 10 and out of 12 trainings) for both participants. This is reflected in the average (across trainings) speeds in the three phases of the trainings: dotted and dashed lines at Fig 4.

For the older participant (P3) this was not the case, instead the mean (across trainings) speed was almost constant regarding the 3 phases of the trainings (Fig 3 and Fig 4). Only in 4 trainings was the speed the lowest in the middle phase of the training and in 3 of the 12 trainings the speed was even the highest in the middle of the training.

The analysis of the observed variation of speed across trainings is subject of further research. We can only speculate that at the beginning of the trainings the first two participants tended to start with a high speed and could not keep that speed, but approaching the end of trainings they tried to achieve as long cycling distance within the training as possible and additional use of upper body helped them to increase speed. The third participant started with a lower speed and his change of speed was less consequent, but he may have used less upper body movement during the whole training.

It has been reported that during series of FES cycling trainings on cycle ergometers, SCI participants with spastic muscles improved in cycling distance [7]. Our study suggests, that such improvement may also happen in persons with flaccid paraplegia. However, the reason may be different and it is a question of further research.

Our study has limitation regarding the number of participants as well. The number of participants is not sufficient to make statistical conclusions but it supports the assumptions that age and time since injury affect the improvement and performance during the series of trainings. On the other hand P3, who is clearly out of the acute and far in the chronic phase of SCI gives evidence, that beneficial training is possible also in persons with longer-term flaccid paralysis.

References

[1] Mayr W, Hofer C, Bijak M, Rafolt D, Unger E, Sauermann S, Lanmueller H, Kern H. Functional electrical stimulation (FES) of denervated muscles: existing and prospective technological solutions. *Basic Appl. Myol* vol. 12, pp. 287-290, 2002

[2] Kern H, Carraro U, Adami N, Hofer C, Loefler S, Vogelauer M, Mayr W, Rupp R. Zampieri S. One year of home-based daily FES in complete lower motorneuron paraplegia: recovery of tetanic contractility drives the structural improvements of denervated muscle. *Neurological Res.*, v.32, pp.5-12, 2010

[3] Mravcsik M, Klauber A and Laczko J (2016): FES driven lower limb cycling by four and eight channel stimulations – a comparison in a case study. *In: the 12th Vienna International Workshop on Functional Electrical Stimulation. 2016. September 08-09, Wien, Austria, Proceedings Book* pp.89-93, ISBN: 978-3-900928-12-4

[4] Popovic-Maneski L, Aleksic A, Metani A, Bergeron V, Cobeljic R, and Popovic D: Assessment of Spasticity by a Pendulum Test in SCI Patients Who Exercise FES Cycling or Receive Only Conventional Therapy, *IEEE Transactions on Neural Systems and Rehabilitation Engineering,* vol. 26/1, pp. 181-187, 2018

[5] Szecsi J, Straube A, Fornusek C.: A biomechanical cause of low power production during FES cycling of subjects with SCI, *Journal of NeuroEngineering and Rehabilitation*, vol. 11pp. 123, 2014

[6] Mravcsik M, Kast C, Vargas Luna JL, Aramphianlert W, Hofer C, Malik Sz, Putz M, Mayr W, Laczko J. FES driven cycling by denervated muscles. *22th Anual Conference of the Functional Electrical Stimulation Society.* Nottwil, Switzerland, Program Book, pp. 134-136, 2018

[7] Kuhn D, Leichtfried V, Schobersberger W.: Four weeks of functional electrical stimulated cycling after spinal cord injury: a clinical cohort study, *International Journal of Rehabilitation Research*, vol. 37, pp. 243-250, 2014

Author's Address

Jozsef Laczko,
University of Pécs, Pécs, and
Wigner Research Centre for Physics, Budapest, Hungary
e-mail: laczko.jozsef@wigner.mta.hu

Winfried Mayr,
Medical University of Vienna, Austria
Center for Medical Physics and Biomedical Engineering
e-mail: winfried.mayr@meduniwien.ac.at

Mariann Mravcsik
University of Pécs, Pécs, and
Wigner Research Centre for Physics, Budapest, Hungary
e-mail: percze-mravcsik.mariann@wigner.mta.hu

Authors Index

Authors Index

SCHUHFRIED
MEDIZINTECHNIK

STIMULETTE edition 5 S2x

TAKING ELECTROTHERAPY A STEP FURTHER

- 28 current forms of proven effectiveness
- two independent channels – intensity can be individually selected
- 6 freely programmable current forms
- intuitive operation – one touch to start
- expanded range of indications

The STIMULETTE edition5 S2x is notable for its wide range of parameters, such as broad impulses, high output capacity, brief pauses. It is the best choice for practical applications, science and research.

QUALITY – DEVELOPED AND MANUFACTURED IN AUSTRIA
www.schuhfriedmed.at

www.pelvipower.com

PELVIPOWER™
KRAFT AUS DER MITTE

STANDORT-PARTNER

EXKLUSIVE VORTEILE

ÄRZTE KLINIKEN

PHYSIOTHERAPIE SPORT-REHA

FITNESS-STUDIOS

PELVIPOWER™-PARTNER WERDEN

WERDEN SIE JETZT PARTNER UND GENIESSEN SIE DIE VORTEILE.

BECKENBODENTRAINING FÜR DIE BEDÜRFNISSE IHRER PATIENTEN
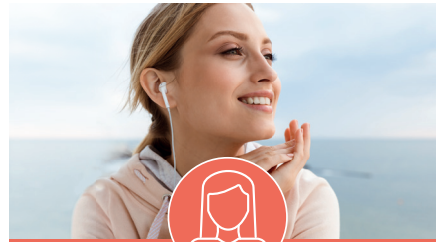
Inkontinenz

Blasenschwäche, Darmschwäche, Tröpfeln, Vorbeugung

Rückbildung nach Geburt

Geburtsvorbereitung, Rückbildung nach der Geburt

Frauen

Wechseljahre, Regelschmerzen, Gewebestraffung, Libidosteigerung

Männer

Vitalität, Potenzstärkung, Prostatektomie, Rehabilitation

Rückenschmerzen

Rückenschmerzenschmerzen, Entspannung, Kräftigung, Haltung

Sport

Kräftigung, Leistung steigern, Fitness, Stabilität, Bodyforming

Sie möchten mehr über die Vorteile als Standort-Partner wissen?
Wir sind gerne für Sie da!
Phone: +41 71 333 60 77

www.pelvipower.com

PELVIPOWER™
KRAFT AUS DER MITTE

Official Journal of the Vienna FES Workshop:
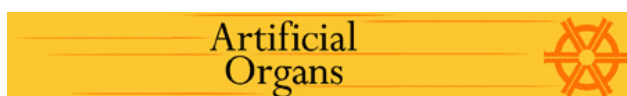
Sponsors and Exhibitors (in alphabetic order):

DR. SCHUHFRIED
MEDIZINTECHNIK GMBH

Dr. Schuhfried
Medizintechnik GmbH
Van Swieten-Gasse 10
A-1090 Wien
Austria

bständig

Bständig GmbH
Strohbogasse 8
1210 Wien
Austria

INERVENTIONS

Inerventions AB
Ankdammsgatan 35
171 67 Solna
Sweden

MED EL

MED-EL
Fürstenweg 77a
6020 Innsbruck
Austria

PonteMed

PonteMed GmbH Austria
Biberstraße 3
1010 Wien
Austria